

THE EFFECT OF SOLUTE ATOMS ON THE PHASE  
TRANSFORMATION KINETICS OF PURE THALLIUM

by

Covilur B. Sampathkumar

Arvind N. Patel

Submitted in Partial Fulfillment of the Requirements

for the Degree of

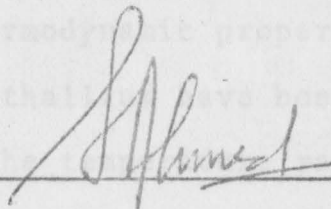
Master of Science in Engineering

in the

Metallurgical Engineering

Program

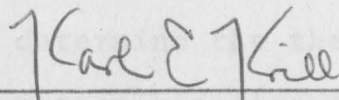
Adviser



Aug 15, 1972

Date

Dean of the Graduate School



August 18, 1972

Date

YOUNGSTOWN STATE UNIVERSITY

August, 1972

284312

## ABSTRACT

THE EFFECT OF SOLUTE ATOMS ON THE PHASE  
TRANSFORMATION KINETICS OF PURE THALLIUM.

Covilur B. Sampathkumar

Arvind N. Patel.

Master of Science in Engineering

Youngstown State University, 1972.

Pure thallium exhibits  $\beta$  to  $\alpha$  transformation on cooling at 508°K. The high temperature modification is face centered cubic structure in contrast to low temperature modification which is hexagonal close-packed structure. The thermodynamic properties and crystal structure of pure thallium have been determined by several investigators in the temperature range of 334°K to 773°K.

In the present investigation, attempts have been made to determine the thermodynamic properties and phase transformation kinetics of pure thallium and the effect of solute atoms on the phase transformation characteristics and thermodynamic parameters of pure thallium. This study includes detailed investigations on the thermodynamic properties of the dilute Tl-Ag, Tl-Au, Tl-Zn, Tl-Cd, and Tl-Sn alloys in the thallium rich end. This investigation directly results in the determination of enthalpy, entropy, free energy, enthalpy of mixing, entropy of mixing and

284342

free energy of mixing for all alloy composition thereof.

The enthalpy and temperature of phase transformation of pure thallium are considerably changed by the addition of solute atoms. The alloying elements belonging to the same group in the periodic table affect the phase transformation kinetics in a similar manner. However, the element having a higher atomic number in a group of element seems to make the most outstanding contribution.

The free energy of mixing shows significant change due to the additions of solute atoms. This is due to the tendency of attractive interactions between unlike atoms. The conduction electrons from the solute atoms make important contributions to determine the nature of primary bonds.

## ACKNOWLEDGEMENT

We wish to express our sincere thanks to Dr. S. Ahmed, for his kind help, patient advice, and valuable guidance, throughout the course of this work.

TABLE OF CONTENTS	
LIST OF SYMBOLS	vi
LIST OF FIGURES	viii
LIST OF TABLES	x
CHAPTER	
I. INTRODUCTION	1
II. Experimental Procedure	2
Experimental Results	4
Discussion	9
III. CONCLUSION	15
APPENDIX A	167
BIBLIOGRAPHY	168

## TABLE OF CONTENTS

	PAGE
ABSTRACT	ii
ACKNOWLEDGEMENT	iv
TABLE OF CONTENTS	v
LIST OF SYMBOLS	vi
LIST OF FIGURES	viii
LIST OF TABLES	x
CHAPTER	
I    INTRODUCTION	1
II   Experimental Procedure	4
Experimental Results	6
Discussion	9
III  CONCLUSION	18
APPENDIX A	167
BIBLIOGRAPHY	168

## LIST OF SYMBOLS

SYMBOL	DEFINITION	UNITS
$\%$	Atom percent	
$\text{\AA}$	Angstrom	$\text{\AA} = 10^{-8} \text{ cm.}$
$a$	Lattice parameter	
$c/a$	Axial ratio of crystal structure	
$H_T$	Enthalpy at temperature T	Calories per mole
$H_{550}$	Enthalpy at temperature $550^\circ\text{K}$	Calories per mole
Tl	Thallium	
Ag	Silver	
Au	Gold	
Cd	Cadmium	
Sn	Tin	
Zn	Zinc	
$F_T$	Free energy at temperature T	Calories per mole
$F_{550}$	Free energy at temperature $550^\circ\text{K}$	Calories per mole
$\neq$	Not equal to	
$\int$	Integral sign	
$\Delta F_m$	Change in free energy of mixing	Calories per mole
$\Delta H_m$	Change in enthalpy of mixing	Calories per mole
$\Delta S_m$	Change in entropy of mixing	Calories per mole per $^\circ\text{K}$ .

SYMBOL	DEFINITION	UNITS
$\Delta H_T^m$	Enthalpy of mixing at temperature T	
$\Delta H_T^A$	Enthalpy of the alloying element A at T°K	
$N_{T1}$	The mole fraction of T1	
$N_A$	The mole fraction of alloying element A	
$\Delta H_T^{T1}$	Enthalpy of T1 at T°K	

## LIST OF FIGURES

FIGURE		PAGE
1.	Olsen calorimeter	23
23 to 36	Enthalpy as a function of temperature for Tl, group A, B, C, D, and E alloys.	24 to 38
37 to 71	Free energy as a function of temperature for Tl, group A, B, C, D, and E alloys.	59 to 93
72 to 105	Free energy of mixing as a function of temperature for group A, B, C, D, and E alloys.	94 to 127
106 to 111	The combined curves of free energy of mixing as a function of temperature for group A, B, C, D, and E alloys.	128 to 133
112 to 121	Enthalpy of mixing as a function of atom percents of alloying element, for group A, B, C, D, and E alloys.	134 to 143
122 to 126	Entropy of mixing as a function of atom percents of alloying elements, for all groups A, B, C, D, and E alloys.	144 to 148
127 to 131	Transformation temperature as a function of concentration of alloying element for group A, B, C, D, and E alloys.	149 to 153
132	The combined curves of transformation ion temperature Vs Concentration of alloying elements for group A, B, C, D, and E alloys.	154



FIGURE		PAGE
133 to 137	Enthalpy of transformation as a function of concentrations of alloying element for group A,B,C,D, and E alloys.	155 to 159
138	Enthalpy of transformation as a function of concentrations of alloying elements for Tl-Ag, and Tl-Au alloys.	160
139	Enthalpy of transformation as a function of concentrations of alloying elements, for Tl-Zn, and Tl-Cd alloys.	161
140 to 144	Free energy of mixing as a function of concentrations of alloying elements, for group A,B,C,D, and E alloys.	162 to 166.

## LIST OF TABLES

TABLE	PAGE
1. Table of enthalpy values.	19
2. Table of ionic radii	21
3. Table of electronic structures of elements	22

## CHAPTER I

Introduction

Pure thallium undergoes a martensitic phase transformation from  $\alpha$  thallium to  $\beta$  thallium at 507°K on heating<sup>1</sup>. This allotropic transformation was first reported by Levin<sup>2</sup> in 1905 and subsequently confirmed by Werner<sup>3</sup> and Nishikawa and Ashara<sup>4</sup>. The crystal structure of both phases were determined by Sinkiti Sekito<sup>5</sup>. The crystal structure of  $\alpha$  thallium was determined to be hexagonal close-packed with lattice parameter of  $a=3.40 \text{ \AA}$  and  $c/a=1.60$ . The crystal structure of  $\beta$  thallium is face centered cubic with  $a=4.841 \text{ \AA}$ .

1

Ralph Hultgren, Raymond L. Orr, Philip D. Anderson, Kenneth K. Kelly, Selected values of thermodynamic properties of metals and alloys (New York: John Wiley & Sons, 1963), p.289.

2

Levin, M, Z.anorg.Chem., (1905), 45, p. 31-8.

3

Werner, M, Z.anorg.Chem., (1913), 83, p. 275.

4

Nishikawa & Ashara, Physic.Rev., (1920), 15, p.38.

5

Sinkiti Sekito, Z.Krist., (1930), 74, p.189-95.  
Crystal structure.

The thermodynamic properties of pure thallium has been studied by several investigators in various temperature ranges<sup>6-12</sup>. The heat content measurement of Roth, Meyer, and Zeumer<sup>13</sup> in the temperature range of 378°K to 628°K has been confirmed by the unpublished work of Orr, Warner, and Hultgren<sup>14</sup>. The heat content data of Umino<sup>15</sup> and Roeskamp<sup>16</sup> is higher than those of Hultgren's data by about 5 to 7%.

6

Ewald, R., Ann. Physik, (1914), 44, 1213. Heat content.

7

Oelsen, W., O. Oelson, and D. Thiel, Z. Metallkunde, (1955), 46, 555-60. Heats of transition and fusion.

8

Oelsen, W., K. Rieskamp, and O. Oelsen, Arch. Eisen huttenw., (1955), 26, 253-266. Heats of fusion and transition.

9

Orr, R.L., L.P. Warner, and Hultgren, R., To be published, Heat content (334 K - 562 K).

10

Roth, W.A., I. Meyer, and H. Zeumer, Z. anorg. Chem., (1933), 214, 309, Z. anorg. Chem., (1934), 216, 303, Heat content (373°K - 628°K).

11

Umino, S., Science reports. Tohoku Imperial Univ. series I, (1927), 16, 775. Heat content (373°K - 773°K).

12

Schneider, A., and O. Hilmer, Z. anorg. u. allegem. chem., (1956), 286, 97-117.  $H_T - H_{st}$ .

13

Roth, W.A., I. Meyer, and H. Zeumer, Z. anorg. Chem., 1933), 214, 309, and 1934, 216, 303.

14

Orr, R.L., L.P. Warner, and R. Hultgren, to be published.

The heat content data of Umino<sup>15</sup> and Seekamp<sup>16</sup> is higher than those of Hultgren's data by about 3 to 7%. Oelsen's<sup>17</sup> measurement at 480°K is 12% higher than those of Hultgren. The latent heat of  $\alpha$  to  $\beta$  transition-range from 94 to 98  $\frac{\text{cal}}{\text{mole}}$ <sup>18</sup>.

In the present investigation attempts have been made to determine the thermodynamic properties - enthalpy, free energy, specific heat, and entropy data including the enthalpy and entropy of phase transformation - of pure thallium, and also to study the effect of Silver, Gold (group I elements), Cadmium, Zinc (group II elements), and Tin (group IV elements) on the thermodynamic properties and the phase transformation kinetics of pure thallium.

---

<sup>15</sup>Umino, S. Science Reports, Heat Content (373°K - 773°K), Tohoku Imperial University, 1927, Series I, 16, 775.

<sup>16</sup>Seekamp, H., 1931, Z. anorg. u. allegemchem., 195 345.

<sup>17</sup>Oelsen, W., Arch. Eisenhüttenw., H<sub>480</sub> H<sub>315</sub>, 1955, 26, 519 - 22

<sup>18</sup>R. Hultgren, Selected Values of Thermo properties of metals and alloys, 1963, 290.

## CHAPTER II

Experimental Procedure

Pure thallium sample was obtained by melting high purity thallium (99.999%) in quartz tube under vacuum. Care was taken to prepare the sample since pure thallium is readily oxidised. Proper amounts of clean thallium and solute elements were capsuled under vacuum in a quartz tube, homogenized and then annealed at 200°C for 24 hours. The sample was removed from quartz tube and plated with Nickel and Chromium. The thickness of coating was 0.0002". The weights of the samples range from 28.86 gms to 58 gms. The alloys of the following compositions were prepared following the above procedure.

Group A

Tl-Ag (0.05 atom Percent Ag)  
 Tl-Ag (0.10 atom Percent Ag)  
 Tl-Ag (0.20 atom Percent Ag)  
 Tl-Ag (0.40 atom Percent Ag)  
 Tl-Ag (0.4971 atom Percent Ag)  
 Tl-Ag (0.60 atom Percent Ag)  
 Tl-Ag (0.80 atom Percent Ag)  
 Tl-Ag (1.00 atom Percent Ag)  
 Tl-Ag (2.00 atom Percent Ag)

Group B

Tl-Au (0.05 atom Percent Au)  
 Tl-Au (0.10 atom Percent Au)  
 Tl-Au (0.20 atom Percent Au)  
 Tl-Au (0.40 atom Percent Au)  
 Tl-Au (0.60 atom Percent Au)  
 Tl-Au (1.00 atom Percent Au)

Group C

Tl-Cd (0.044 atom Percent Cd)

Tl-Cd (0.18 atom Percent Cd)

Tl-Cd (0.44 atom Percent Cd)

Tl-Cd (0.50 atom Percent Cd)

Tl-Cd (0.60 atom Percent Cd)

Tl-Cd (0.88 atom Percent Cd)

Tl-Cd (1.00 atom percent Cd)

Group D

Tl-Zn (0.10 atom Percent Zn)

Tl-Zn (0.20 atom Percent Zn)

Tl-Zn (0.40 atom Percent Zn)

Tl-Zn (0.60 atom Percent Zn)

Tl-Zn (0.80 atom Percent Zn)

Tl-Zn (1.00 atom Percent Zn)

Tl-Zn (1.20 atom Percent Zn)

Group E

Tl-Sn (0.05 atom Percent Sn)

Tl-Sn (0.20 atom Percent Sn)

Tl-Sn (0.40 atom Percent Sn)

Tl-Sn (0.60 atom Percent Sn)

Tl-Sn (1.00 atom Percent Sn)

A modified Olsen calorimeter (Figure 1) having an adiabatic jacket was used with nanovolt amplifiers and other electronic devices. The temperature measurement was carried out by thermopile and a quartz thermometer having a precision of  $1/10,000^{\circ}\text{C}$ . The experimental procedure consisted of heating the sample to a temperature of about  $550^{\circ}\text{K}$  and subsequently cooling it in the calorimeter. The increase in temperature of the calorimeter media was recorded as a function of sample temperature by an X-Y recorder. The media was spectro quality isopropyl alcohol for which the specific heats are known for given temperature ranges.

## Experimental Results

The experimental results then consist of changes in temperature of calorimeter media as a function of sample temperature. From this data the enthalpy values were calculated using the following expression,

$$\Delta H = H_T - H_R = w \cdot C_p \cdot \Delta T \quad (1)$$

where,  $\Delta H$  = the enthalpy change with respect to reference state R,

$H_T$  = enthalpy at temperature T,

$H_R$  = enthalpy at reference state R,

w = weight of calorimeter media,

$C_p$  = specific heat of isopropyl alcohol, at  $T^\circ\text{K}$ ,

$\Delta T$  = temperature change of the calorimeter media.

The reference state was initially chosen to be the temperature of the sample at the beginning of the experimental run. This was then later normalised at  $550^\circ\text{K}$ . In other words the reference state is at  $550^\circ\text{K}$ . Thus, we obtained the enthalpy values for given samples as a function of temperature with respect to reference state at  $550^\circ\text{K}$ .

The experimental results were then corrected for heat exchanged between the system and surrounding following



The experimental results were then corrected for heat exchanged between the system and surrounding following the procedure outlined in Appendix A. The corrected values for each sample as a function of temperature are shown in figures(2) to (36). From the experimental results the enthalpy and entropy of phase transformation for each alloy composition was determined (Table 1). The transformation temperature  $T_c$  was taken to be the mean of the temperature at which the transformation starts ( $T_s$ ) and the temperature at which the transformation ends ( $T_f$ ). Additional independent experiments were carried out to find the transformation temperature on heating ( $T_h$ ). The equilibrium temperature  $T_o$  was taken to be the mean of  $T_h$  and  $T_c$ .

The free energy values for each alloy composition was then calculated by using the Gibbs Helmholtz equation:

$$\frac{\partial(\Delta F/T)}{\partial(1/T)} = \Delta H \quad (2)$$

we get then,

$$\Delta F^T_{\text{alloy}} = T \left[ \int_{550}^T \Delta H_{\text{alloy}} \partial(1/T) \right] \quad (3)$$

The right hand side of the above equation can be obtained by integrating the experimental results after plotting the enthalpy change ( $\Delta H = H_T - H_{550}$ ) as a function of  $1/T$ . The enthalpy curves were adjusted at  $T_o$  by extrapolating

284342

the low temperature curve to  $T_0$ . Then the integration was carried out. The free energy curves of pure thallium and of all alloys are shown in figures (37) to (71).

The free energy of mixing was calculated for each alloy composition by using the following equation:

$$\Delta F_T^m = \Delta F_T^{\text{alloy}} - \left[ N_{\text{Tl}} \cdot \Delta F_{\text{Tl}}^{\text{Tl}} + N_A \cdot \Delta F_T^A \right] \quad (4)$$

where,

$\Delta F_T^m$  = the free energy of

mixing at temperature T,

$\Delta F_T^{\text{alloy}}$  = the free energy of the

alloy (Tl-A) at temperature T,

$\Delta F_{\text{Tl}}^{\text{Tl}}$  = the free energy of thallium  
at  $T^\circ\text{K}$ ,

$\Delta F_T^A$  = the free energy of the alloying  
element A at  $T^\circ\text{K}$ ,

$N_{\text{Tl}}$  = the mole fraction of thallium

$N_A$  = the mole fraction of alloying  
element A.

These free energy of mixing curves for all alloy composition are shown as a function of temperature in figures (72) to (105). The free energy of mixing curves of all alloys in a given group (group A, B, C, D, and E) are shown in figures (106) to (111).

The enthalpy of mixing was calculated at given temperatures in the high and low temperature phases using the following equation:

$$\Delta H_T^m = \Delta H_T^A - \left( N_{T1} \cdot \Delta H_T^{T1} + N_A \cdot \Delta H_T^A \right) \quad (5)$$

The entropy of mixing was obtained from the free energy of mixing curves of alloys. The results are shown in figures (112) to (121) and (122) to (126).

### Discussion

Pure thallium undergoes  $\beta$  to  $\alpha$  transformation on cooling at 508°K. The enthalpy and entropy change associated with the transformation are 100 calories/mole and 0.197 calories/mole/°K. The transformation temperature on cooling  $T_c$  and the enthalpy of phase transformation  $\Delta H_R$  are drastically changed by the addition of small amounts of solute atoms - Ag, Au, Zn, Cd, and Sn. The transformation temperature in all cases decreases monotonically with increasing alloying additions - figures (127) to (131). The combined curves of  $T_c$  Vs alloy composition for all the alloy groups is shown in figure 132. The decrease in  $T_c$  follows a definite pattern in that for the elements, belonging to the same group in the periodic table, the transformation temperature decreases differently. The element that has lower atomic number seems to have less effect than elements having larger atomic number, thereby

indicating possible

indicating possible electronic contribution. This is true for both group I and group II alloying elements.

The enthalpy of phase transformation in pure thallium is changed considerably with the addition of alloying elements (figures 133 to 137). The group I elements seem to affect the transformation temperature in a similar manner although the effects are different (figure 138). The effect on the transformation temperature, due to Au is considerably more than that due to Ag. Similar effects are also seen with Cd and Zn. It is significant to note that the larger changes in enthalpy of phase transformation are observed with elements having lower atomic number in the same group of elements in the periodic table. There are certain variations in the enthalpy of phase transformation with increasing amounts of alloying elements, the minimum and maximum values for a group of elements occur almost at identical compositions. However, the temperature and the enthalpy of phase transformation decreases monotonically with the additions of Sn (figure 137). This result appear to be significantly different from those of group I and group II elements (figure 138 and 139).

The gradual decrease in the transformation temperature with the addition of alloying elements, obviously indicate larger degree of undercooling is required with increasing alloying additions. It is important to note that degree of undercooling required for phase transformation is determined by the non chemical free energy changes associated with the phase transformation. The chemical free energy change should overcome this non chemical free energy changes associated with the phase transformation. The chemical free energy change should overcome this non chemical free energy change in order for the transformation to take place. The non chemical free energy change include the interface energy and the strain free energy contributions. Therefore, when the non chemical free energy term assumes a higher value for reasons discussed below, the amount of undercooling is to be increased for the phase transformation to take place such that the chemical free energy change becomes equal to or greater than the non chemical free energy change. One of the possible sources for increase in free energy contribution is the increase in strain free energy. The ionic radii of all the alloying elements is different from that of pure thallium. The ionic radii (Table 2 ) of group I elements Ag and Au are quite similar to each other, so it is reasonable to believe that the strain introduced by the substitutional occupation of thallium lattice sites, will be equal. Nevertheless, this will introduce strain in the thallium lattice. The non chemical free energy will therefore increase, thereby demanding a larger degree of undercooling. This is also the observed

result. However, there exists significant difference in the degree of undercooling by Ag and Au. These differences are possibly due to electronic contributions. The electronic contributions from Ag and Au will be different since the valence electron in Au is from 6S whereas valence electron of Ag is from 5S (Table 3 ). The interaction between 6S, (from gold) and 6P (of Tl) electrons will be greater than that between 5S and 5P electrons. This is why the effect due to Au appears to be more drastic than that due to Ag.

The difference in the transformation temperature in Tl-Cd series of alloys and Tl-Zn series of alloys are essentially due to the strain energy contribution arising from differences in ionic radii between Tl and Zn and Tl and Cd. Difference in ionic radii between Tl and Cd is small compared to the difference in ionic radii between Zn and Tl. The larger differences that exist in the Tl-Zn series of alloys contribute to the strain energy term which include the non chemical free energy change. One then needs a larger degree of undercooling for phase transformation for these alloys. The electronic configuration of Zn and Cd are shown in Table 3. Cd has 2 electrons in 5S level and Zn has 2 electrons in 4S level. The valence level of Cd and Zn are full with the number of electrons they can have. The interactions of these electrons in these elements, with the valence electron of pure thallium will be rather negligible. Therefore the degree of undercooling required is a direct consequence of changes in non chemical free energy

in non chemical free energy contribution due to increase in strain free energy term.

The enthalpy and temperature of phase transformation of thallium is affected by Sn and Cd in a similar way. There is a gradual decrease in transformation temperature with the addition of Sn and Cd. The changes in enthalpy of phase transformation of thallium due to the addition of Sn and Cd are also qualitatively alike. However, there exists some difference in the relative order of magnitude on the above parameter. This effect cannot be due to ionic radii since Cd and Sn have radii close to each other and within 15% of that of thallium. This means then, that these differences are due to the electronic contributions from Sn and Cd. The differences in the electronic structure of Sn and Cd is that Cd has completely filled 5S level and Sn has incompletely filled 5P level. These P electrons of Sn are more likely to interact with 6S electrons of Tl.

It has been reported<sup>19</sup> that thallium-Silver and thallium-gold phase diagrams are simple eutectic types with features of retrograde solidus. On the thallium rich

---

19

M.Hansen, Constitution of binary alloys, (New York: McGraw-Hill book company, Inc., 1958), 61.

end of these diagrams the solubilities of Ag and Au in Tl are quite small. The eutectic composition in thallium-gold and thallium-silver are approximately 74 atom percent and 96 atom percent Tl, respectively. The alloy compositions under investigations are well within this eutectic range.

The free energy of mixing for the dilute Tl-Au and Tl-Ag systems are shown in figures (72) to (105). From these data the free energy of mixing as a function of the concentration of alloying elements were drawn (figures 140 to 144). Furthermore, the enthalpy of mixing  $\Delta H_m$  were calculated at various temperatures and concentrations (figures 112 to 121). The entropy of mixing for the  $\beta$  phase at 515°K is shown together with that of  $\alpha$  phase at 480°K (figures 122 to 126). The free energy of mixing curve in both of these alloy groups has similar shapes. The solubility of Au and Ag in pure thallium is very small. The initial small additions of Ag and Au will form a primary solid solution. When the primary solid solution limit is exceeded, then there exist a phase mixture. It is important to note that at higher temperatures the tendency to form phase mixture becomes less. This is suggested by the concave upward shape of the  $\Delta F_m$  curve.



In the Heitler and Herzfeld treatment of solid solution it has been shown that,

$$\Delta F^m = \Delta H^m - T \cdot \Delta S^m = -x_1 \cdot x_2 \cdot \Omega + RT(x_1 \ln x_1 + x_2 \ln x_2) \quad (6)$$

Where,  $x_1$  = Mole fraction of element 1

$x_2$  = Mole fraction of element 2

$$\Omega = Z N_0 [V_{AB} - \frac{1}{2}(V_{AA} + V_{BB})]$$

$Z$  = Co-ordination number

$N_0$  = Avogadro's number

$V_{AB}$  = Bond energies of AB bond

$V_{AA}$  = Bond energies of AA bond

$V_{BB}$  = Bond energies of BB bond

$R$  = Gas constant

$T$  = Temperature

$\Delta F^m$  = Free energy of mixing

$\Delta H^m$  = Enthalpy of mixing

$\Delta S^m$  = Entropy of mixing

The first term can be negative or positive depending on the value of  $\Omega$ ,  $\Omega$  is negative in case of attractive interactions and this makes this term positive. This positive value will eventually result in the concave downward section of the  $\Delta F_m$  curve. It is important to

note that

in the high temperature region, the second term becomes more predominant term, whereas at lower temperature the first term plays an important role. The gradual decrease in  $\Delta H_m$  values for Tl-Au alloys upto a composition 0.6 % Tl, simply reflect the tendency of attractive interactions between unlike atoms (ie increase in number of AB bonds). This in turn means presence of short range order in the system. Similar trends are also seen in Tl-Ag alloys upto a composition of 0.2 % Tl.

Tl-Cd phase diagram is a simple eutectic diagram where the solubilities of Cd in Tl is not definitely established. It has been reported that there is a phase in Tl rich end with solubility of 2.0 atomic percent Cd in thallium at 400°K. The alloys under investigation are within this solubility range. The Tl-Zn system exhibits a large miscibility gap in the liquid state and Zn has very little solubilities in Tl. The free energy of mixing of Tl-Cd and Tl-Zn system exhibit trend similar to those observed in dilute Tl-Au Tl-Ag alloys.

The alloys under investigation exhibit non regular behavior as much as  $\Delta H_m \neq 0$  and  $\Delta S_m$  is also not equal to zero. In these alloys the free energy of mixing curve indicate a tendency to gradual increase in the degree of order at lower temperatures. There also exist a tendency to maximise the contribution due to  $\Delta H_m$  by changing the number of AB bonds in either attractive or repulsive interactions. The number of AB bonds can be changed by the contribution of conduction electrons which is primarily responsible for bonds between

positive ions. Furthermore, changes in concentration of valence electrons in the alloying additions will also affect the solubility limit of an element in thallium. Pure thallium atoms have one valence electron per atom. When pure thallium is alloyed with metals having higher valencies Zn, Cd, Sn, the concentration of valence electron per atom will be greater than one. This will increase the fermi energy of the electrons effectively. On the other hand the addition of Ag and Au in thallium will not change the effective electron concentration of pure thallium. Such differences will also be reflected in the  $\Delta F_m$ ,  $\Delta H_m$  and  $\Delta S_m$  curves, to generate the characteristic shape observed in the experimental results. Thus, in these alloys the thermodynamic properties are a direct consequence of the contributions from the valence electrons, the size of the metallic ions, and also the tendency to form AB bonds.

## CHAPTER III

## CONCLUSION

From the experimental results it can be concluded that,

1. The temperature of transformation of thallium from  $\beta$  phase to  $\alpha$  phase, was observed to  $508^{\circ}\text{K}$ , on cooling. The enthalpy and entropy change associated with the transformation of Tl are calculated to be 100 calories/mole/ $^{\circ}\text{K}$ , and  $0.197$  cal/mole/ $^{\circ}\text{K}$  respectively.

2. The small additions of solute atoms of elements viz. Ag, Au, Zn, Cd, and Sn, changed the phase transformation characteristics of Tl. The alloying elements belonging to the same group in the periodic table affect the phase transformation kinetics of Tl in a similar way. However, the elements having a higher atomic number in a group of elements seems to make the most outstanding contribution.

3. The differences in ionic radii and the electronic structure between the solute elements, and their electronic interactions with pure Tl, considerably changed the enthalpy and temperature of phase transformation of pure Tl.

4. The additions of solute elements changed the free energy of mixing, significantly. This is due to the tendency of attractive interaction between the unlike atoms, due to the electronic contribution.

TABLE 1

Alloy Composition	$T_s$ °K	$T_f$ °K	$T_c$ °K	$T_h$ °K	$T_o$ °K	$\Delta H_R$ cal/mole
Thallium	508.2	508.2	508.2	510.5	509.35	100
Tl-Au(0.05 atom% Au)	501.00	500.00	500.5	502.00	501.00	140
Tl-Au(0.1 atom% Au)	497.00	495.75	496.425	499.50	497.963	70
Tl-Au(0.2 atom% Au)	494.50	490.500	492.50	497.00	494.75	91
Tl-Au(0.4 atom% Au)	497.75	487.75	487.75	489.500	488.625	115
Tl-Au(0.6 atom% Au)	487.00	487.00	487.00	489.50	488.25	70
Tl-Au(1.0 atom% Au)	485.75	485.75	485.75	489.00	487.625	90
Tl-Sn(0.05 atom% Sn)	508.25	508.25	508.25	509.25	508.750	150
Tl-Sn(0.2 atom% Sn)	500.700	498.25	499.475	504.00	400.510	120
Tl-Sn(0.4 atom% Sn)	493.30	492.00	492.650	497.00	494.825	85
Tl-Sn(0.6 atom% Sn)	489.70	488.00	488.85	494.00	491.425	72
Tl-Sn(1.0 atom% Sn)	474.50	466.00	470.25	475.00	472.62	47
Tl-Zn(0.1 atom% Zn)	504.50	504.50	504.50	506.00	505.25	50
Tl-Zn(0.2 atom% Zn)	502.00	502.00	502.00	505.00	503.50	64
Tl-Zn(0.4 atom% Zn)	503.25	503.25	503.25	504.00	503.625	78
Tl-Zn(0.6 atom% Zn)	503.25	503.25	503.25	504.00	503.625	94
Tl-Zn(0.8 atom% Zn)	502.00	502.00	502.00	505.00	503.500	85
Tl-Zn(1.0 atom% Zn)	503.10	513.10	503.10	505.00	504.050	132

TABLE 1 (Contd)

Tl-Ag(0.05	atom% Ag)	502.00	500.75	501.38	507.75	504.06	81
Tl-Ag(0.1	atom% Ag)	503.25	499.50	501.375	501.75	501.56	86
Tl-Ag(0.2	atom% Ag)	509.25	598.25	508.75	509.25	509.00	270
Tl-Ag(0.4	atom% Ag)	492.00	488.00	490.00	495.00	492.50	120
Tl-Ag(0.4971	atom% Ag)	503.25	502.25	502.75	508.25	505.50	100
Tl-Ag(0.6	atom% Ag)	503.25	502.00	502.63	505.00	503.81	92
Tl-Ag(0.8	atom% Ag)	503.00	502.00	502.50	506.25	504.38	110
Tl-Ag(1.0	atom% Ag)	503.25	502.00	502.63	506.75	504.09	120
Tl-Ag(2.0	atom% Ag)	503.25	502.00	502.63	504.50	503.56	110
Tl-Cd(0.44	atom% Cd)	509.25	508.25	508.75	513.00	510.88	130
Tl-Cd(0.18	atom% Cd)	508.25	507.00	507.63	508.75	508.19	130
Tl-Cd(0.44	atom% Cd)	503.50	504.50	505.00	507.00	506.00	110
Tl-Cd(0.5	atom% Cd)	510.00	499.50	500.25	505.00	502.63	90
Tl-Cd(0.6	atom% Cd)	508.20	507.00	507.60	509.25	508.43	127
Tl-Cd(0.88	atom% Cd)	511.00	509.00	510.00	512.00	511.00	28
Tl-Cd(1.0	atom% Cd)	588.25	485.50	486.88	490.00	488.44	50

TABLE 2

## Table of ionic radii

Element	Goldshmidt's radii. (Kx units)
Tl	3.42
Cd	3.042
Sn	3.160
Zn	2.748
Ag	2.883
Au	2.878

TABLE 3

Table of electronic structure of  
elements

Element	atomic No.	Electronic structure
Zn	30	$1s^2 2s^2 2p^6 3s^2 3p^6 3d^{10} 4s^2$
Cd	48	$1s^2 2s^2 2p^6 3s^2 3p^6 3d^{10} 4s^2 4p^6 4d^{10} 5s^2$
Ag	47	$1s^2 2s^2 2p^6 3s^2 3p^6 3d^{10} 4s^2 4p^6 4d^{10} 5s^1$
Au	79	$1s^2 2s^2 2p^6 3s^2 3p^6 3d^{10} 4s^2 4p^6 4d^{10} 4f^{14} 5s^2$ $5p^6 5d^{10} 6s^1$
Sn	50	$1s^2 2s^2 2p^6 3s^2 3p^6 3d^{10} 4s^2 4p^6 4d^{10} 5s^2 5p^2$
Tl	81	$1s^2 2s^2 2p^6 3s^2 3p^6 3d^{10} 4s^2 4p^6 4d^{10} 4f^{14}$ $5s^2 5p^6 5d^{10} 6s^2 6p^1$



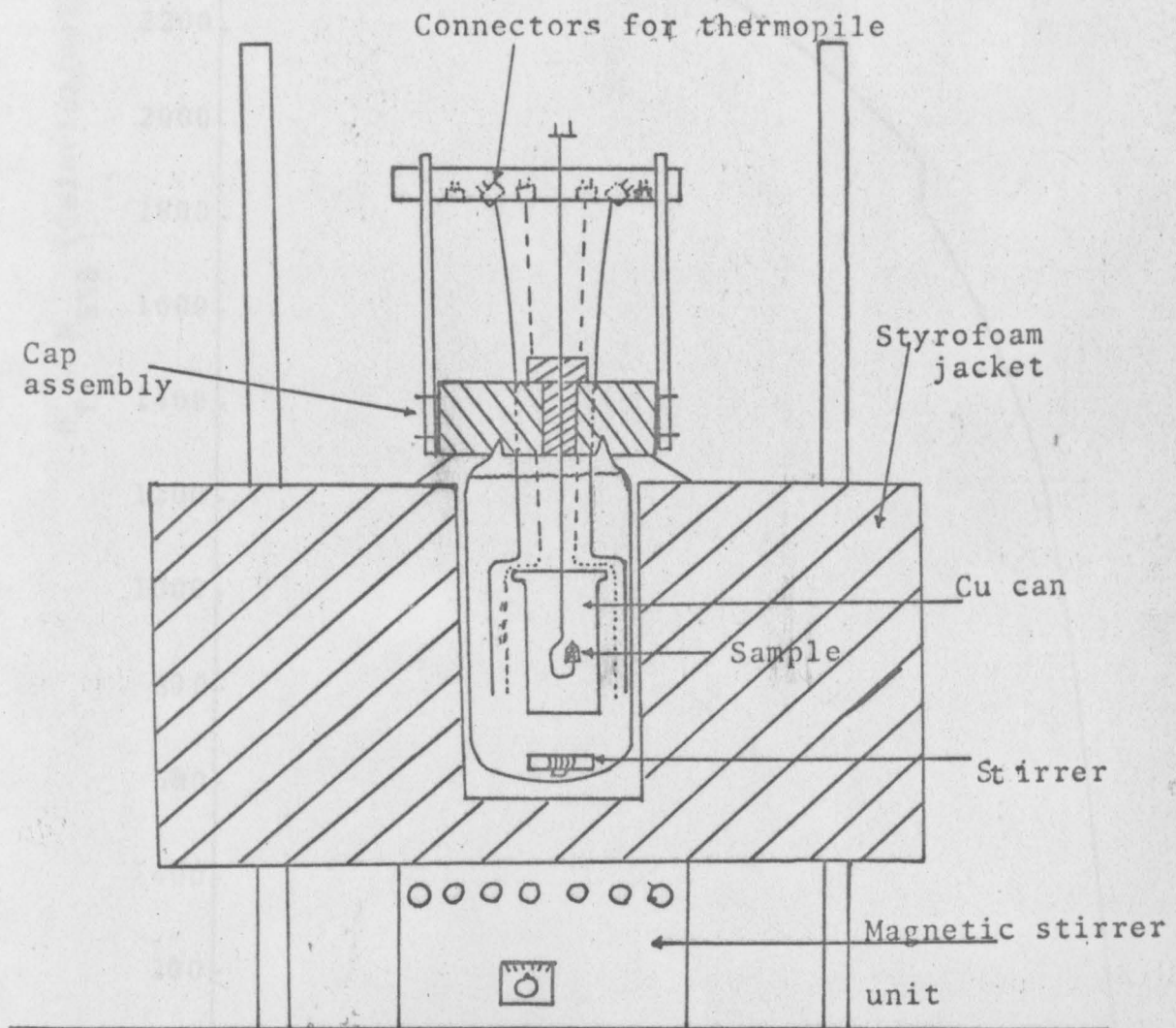


Fig. 1. Olsen Calorimeter.

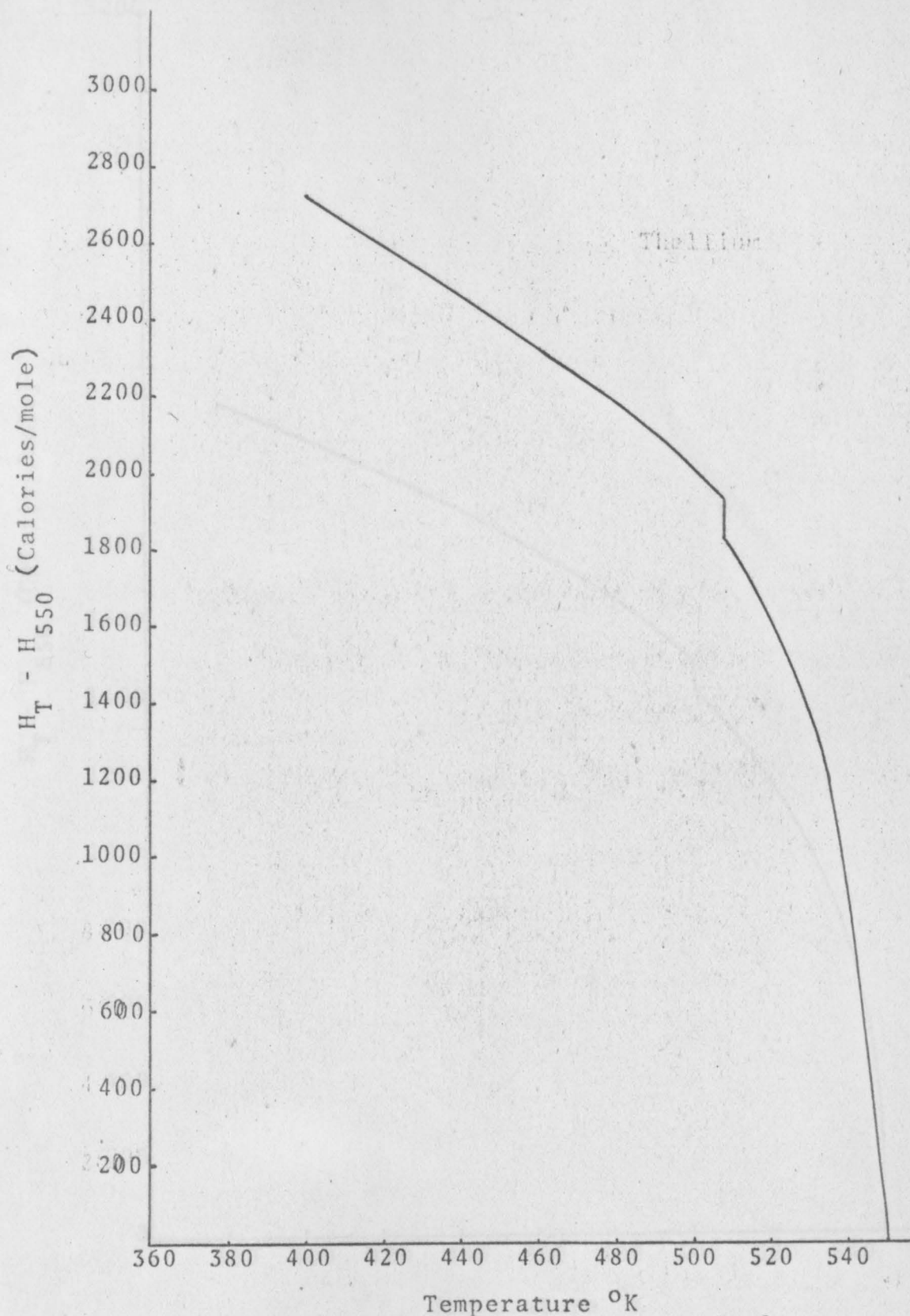


Fig. 2.--Enthalpy as a function of temperature of Tl.

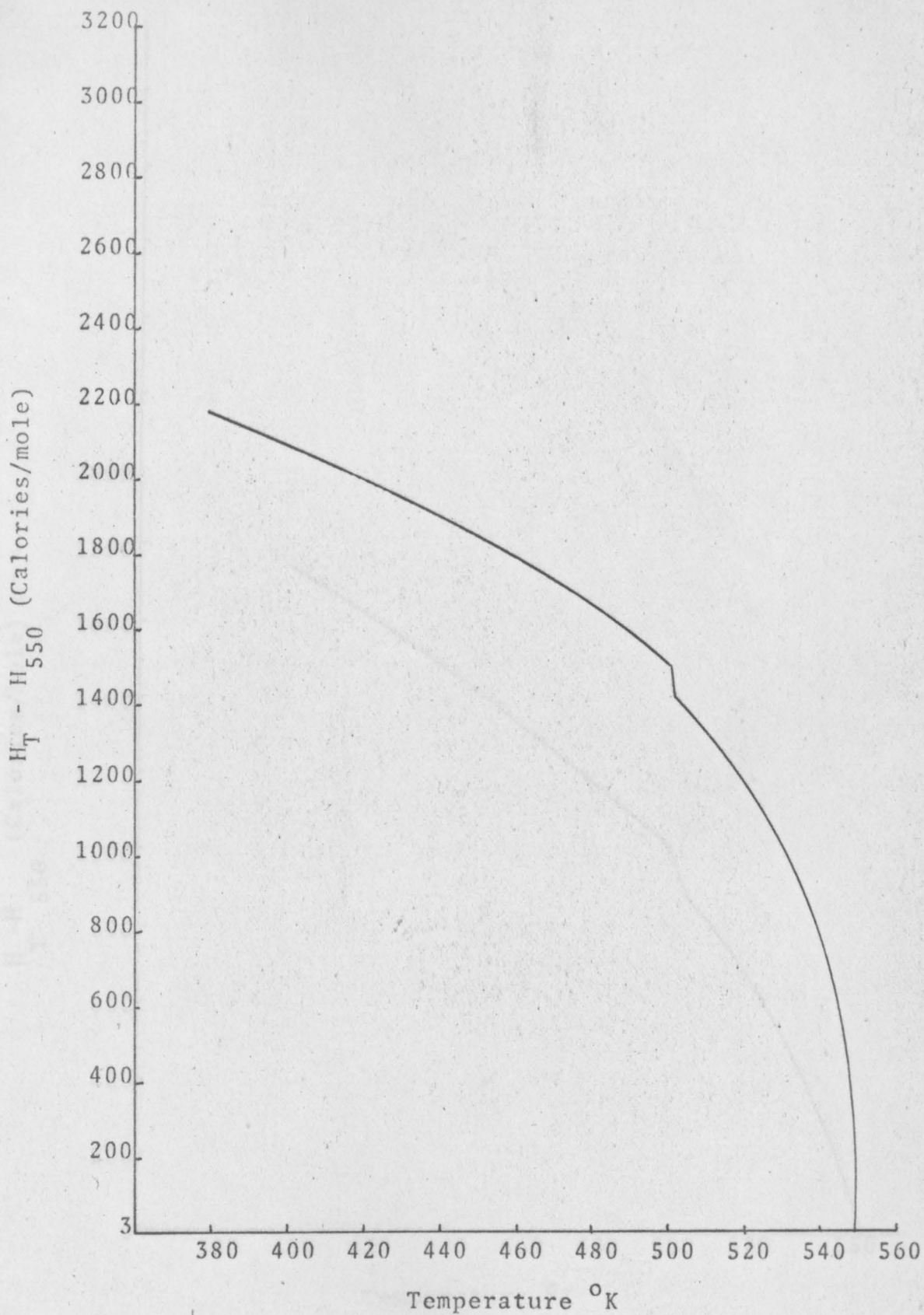


Fig. 3. Enthalpy as a function of temperature for thallium-silver (0.05 atom percent).

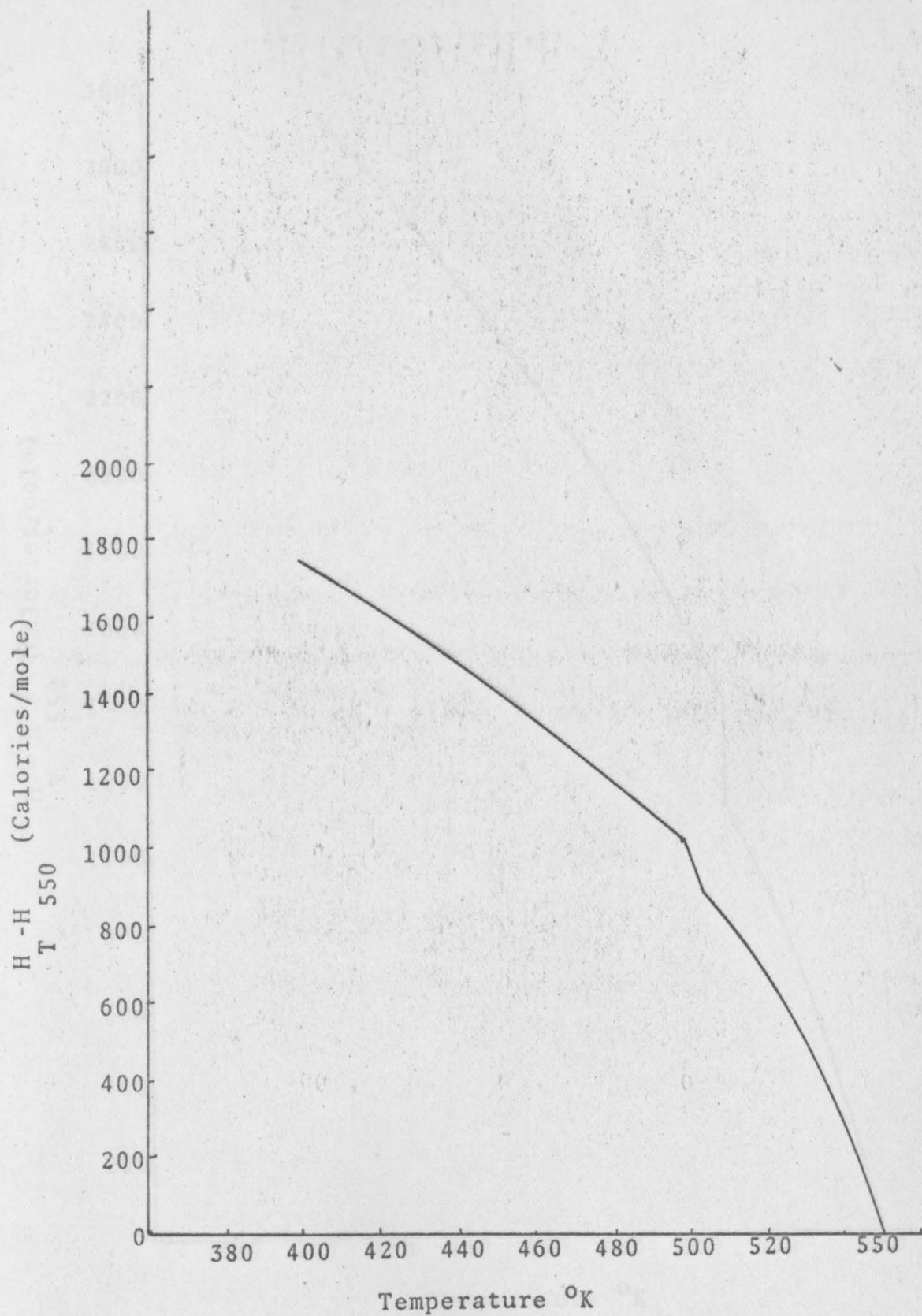


Fig. 4. Enthalpy as a function of temperature for Tl-Ag alloy (0.10 atom percent Ag)

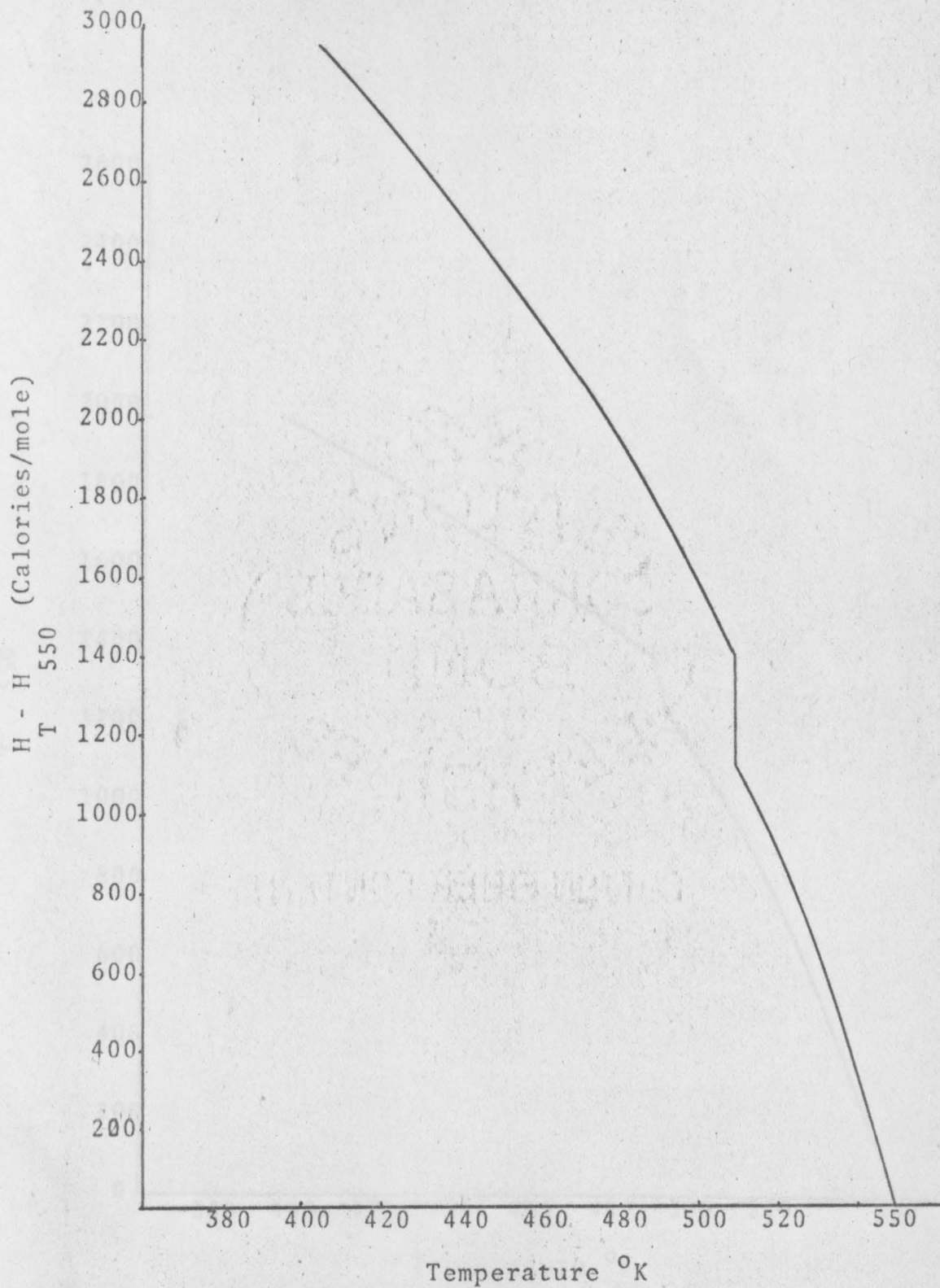


Fig. 5. Enthalpy as a function of temperature for Tl-Ag alloy ( 0.2 atom percent Ag).

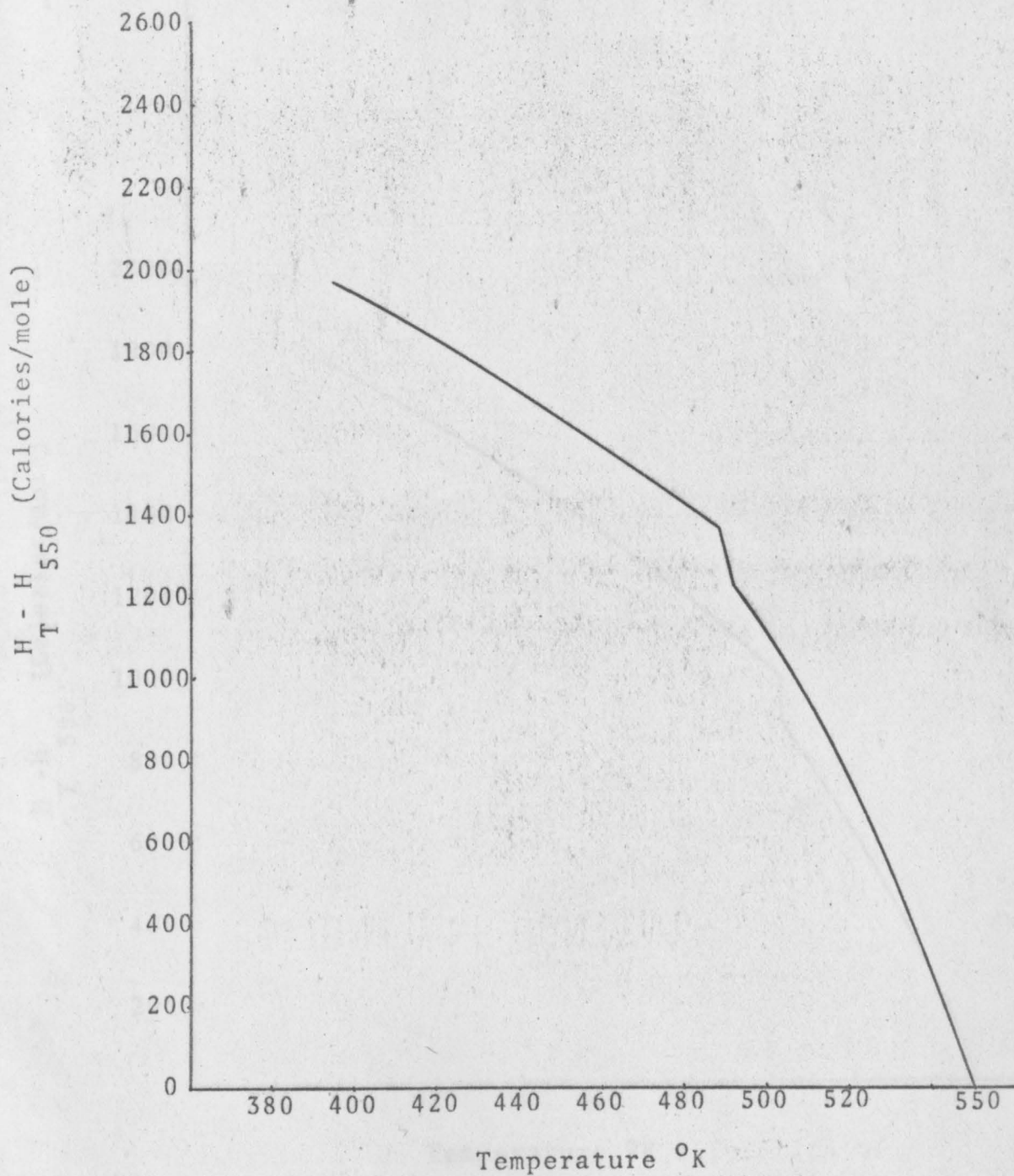


Fig. 6. Enthalpy as a function of temperature for Tl-Ag alloy (0.4 atom percent Ag).

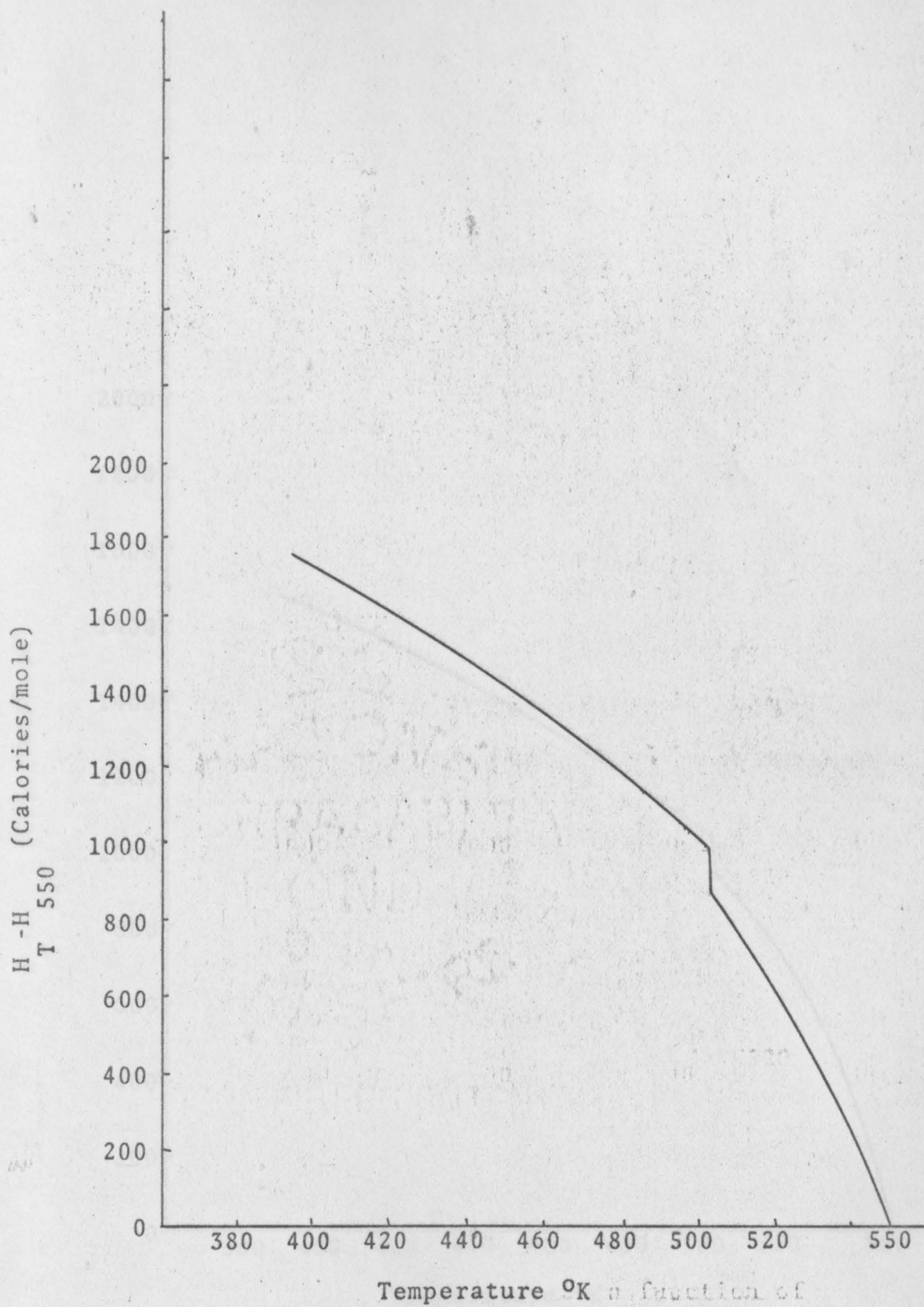


Fig. 7. Enthalpy as a function of temperature for Tl-Ag alloy (0.4971 atom percent Ag)

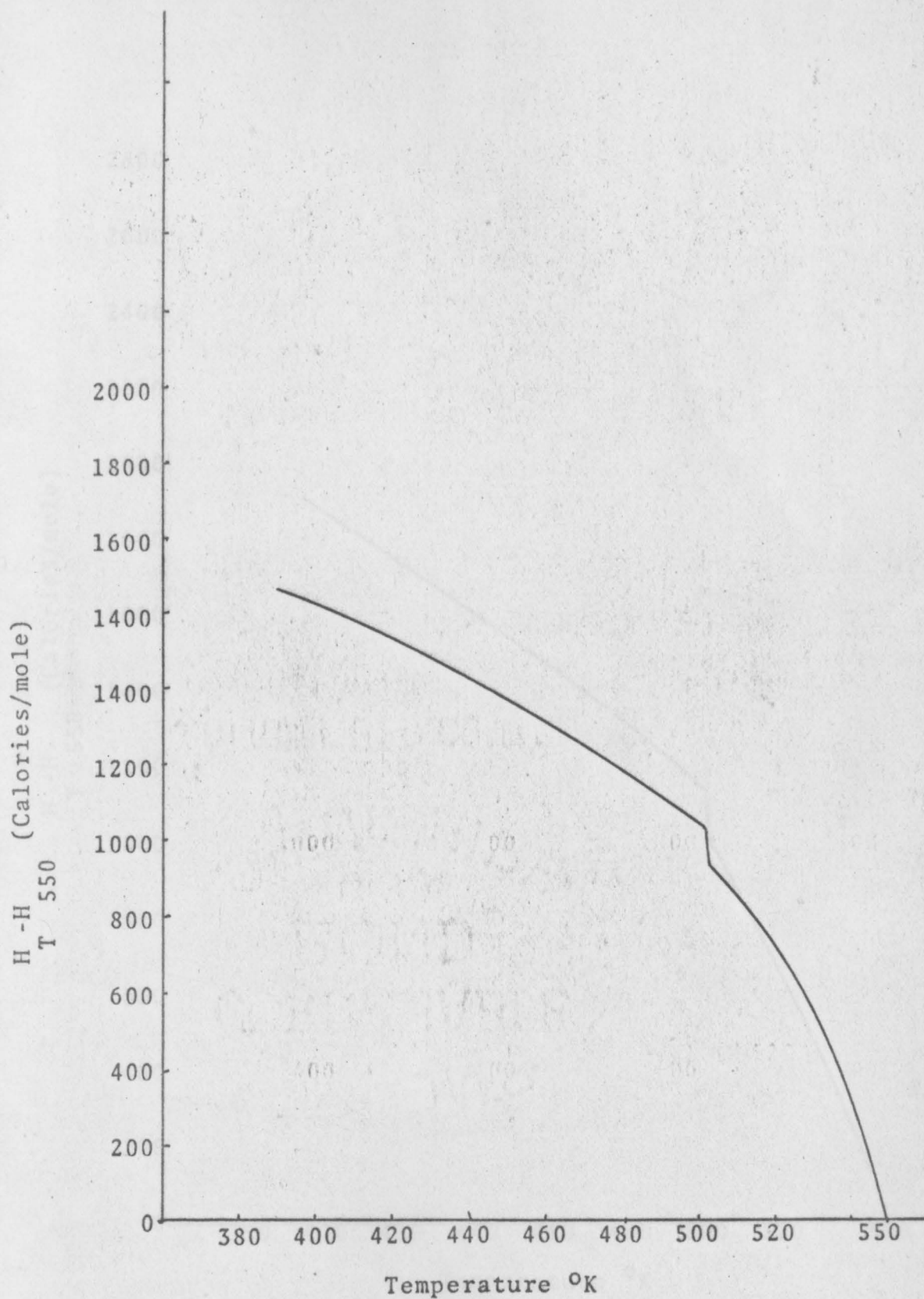


Fig. 8. Enthalpy as a function of temperature for Tl-Ag alloy (0.60 atom percent Ag)



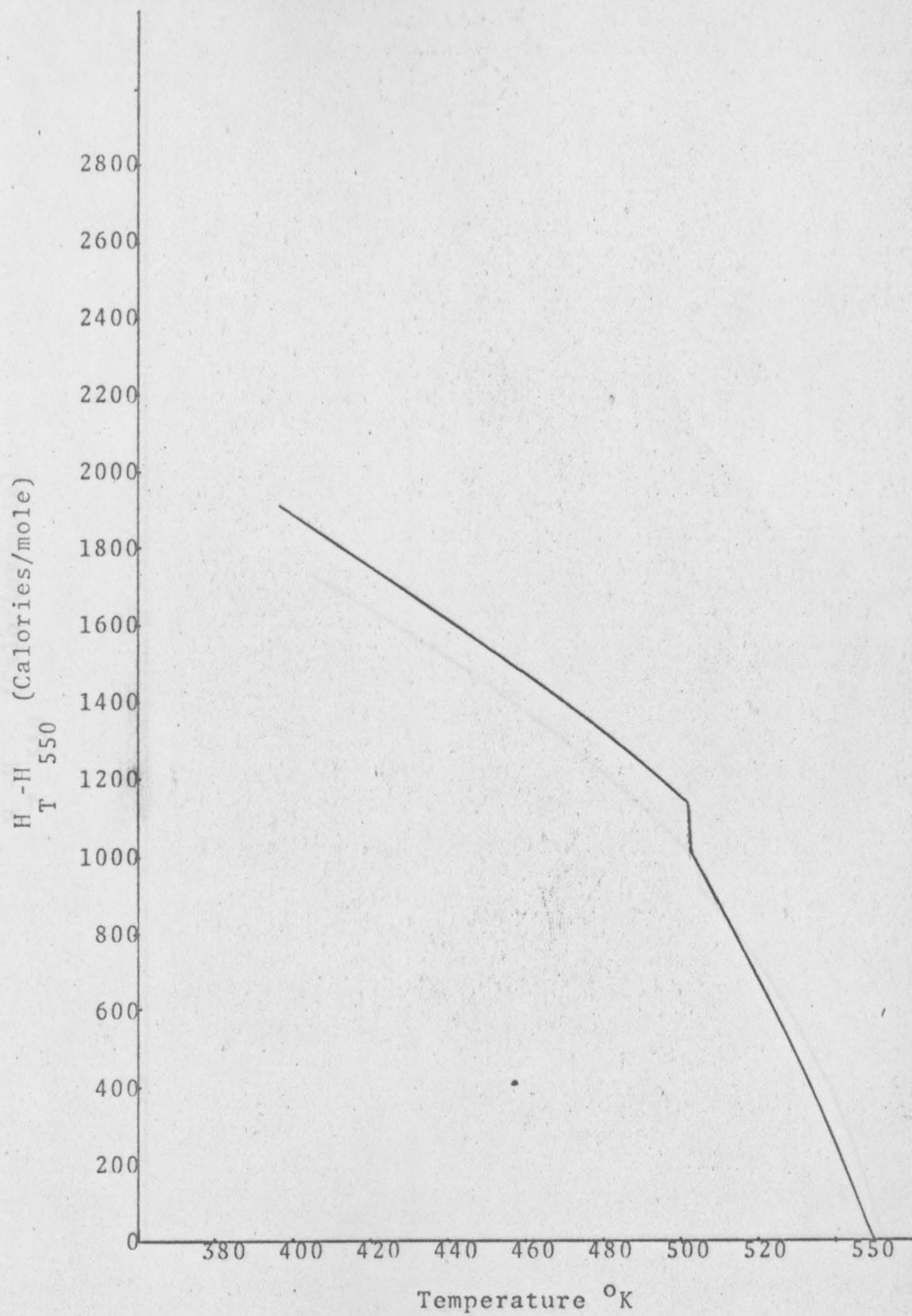


Fig. 9. Enthalpy as a function of temperature for Tl-Ag alloy (0.80 atom percent Ag)

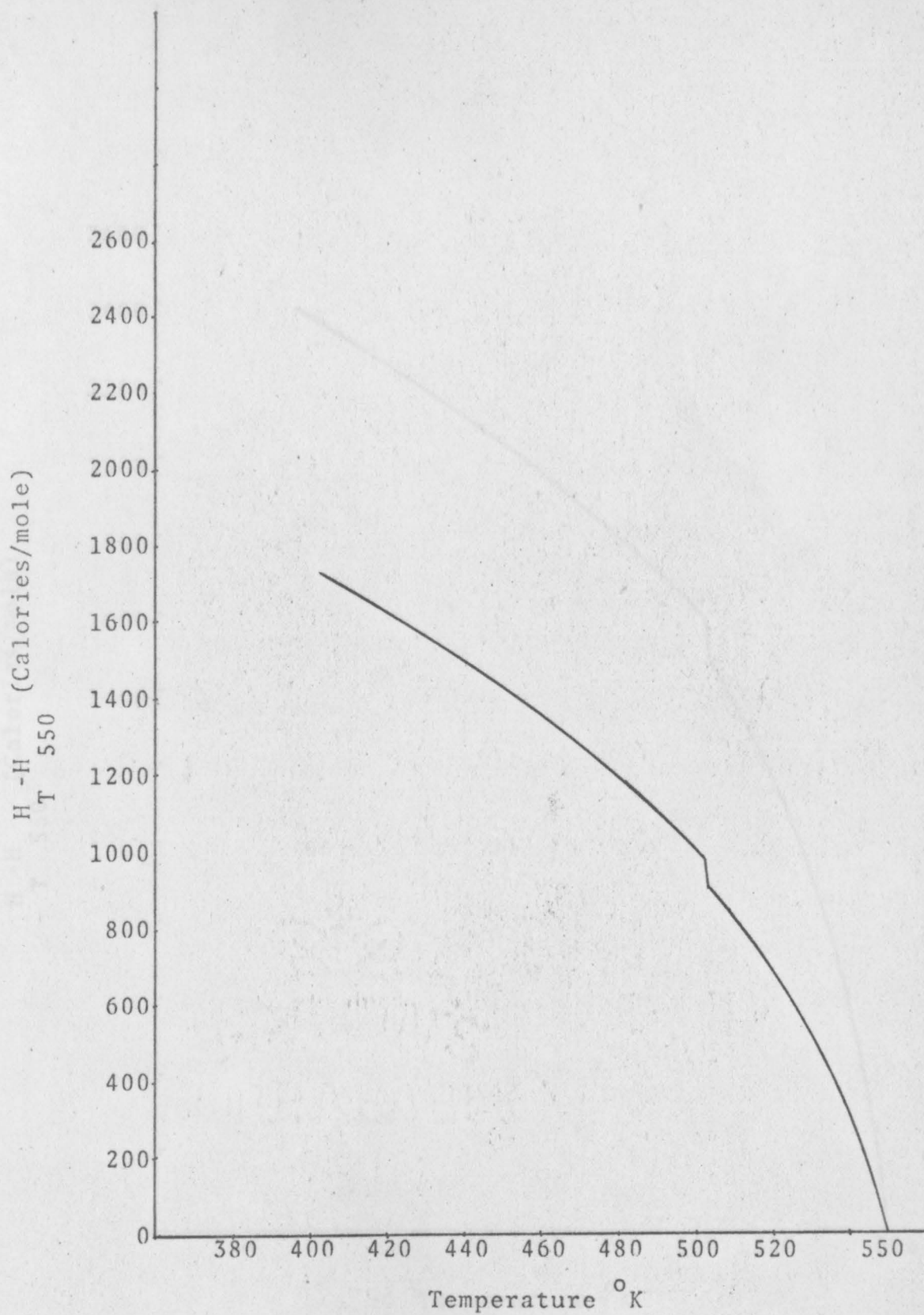


Fig. 10. Enthalpy as a function of temperature for Tl-Ag alloy (1.00 atom percent Ag).

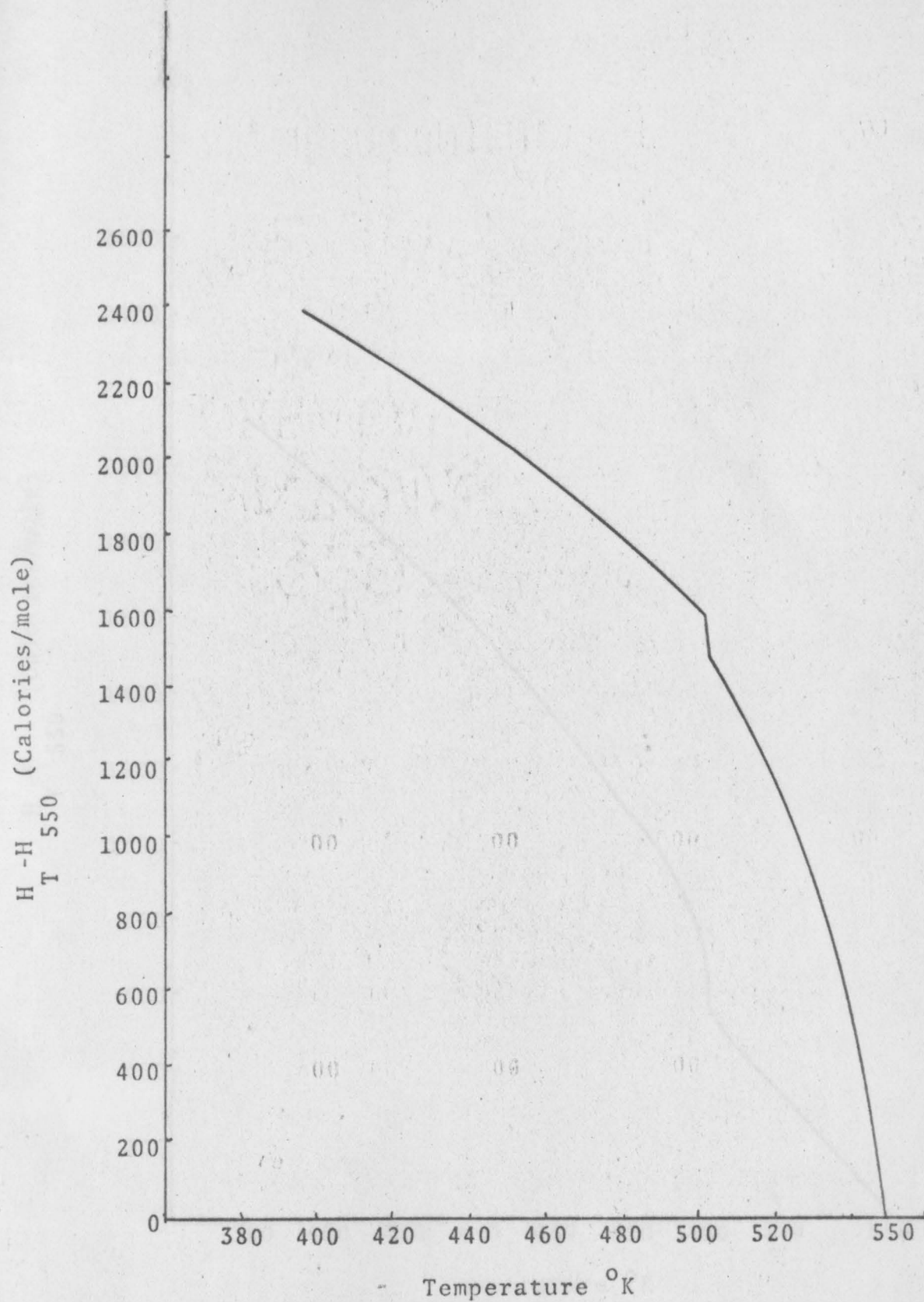


Fig. 11. Enthalpy as a function of temperature for Tl-Ag alloy (2.00 atom percent Ag).

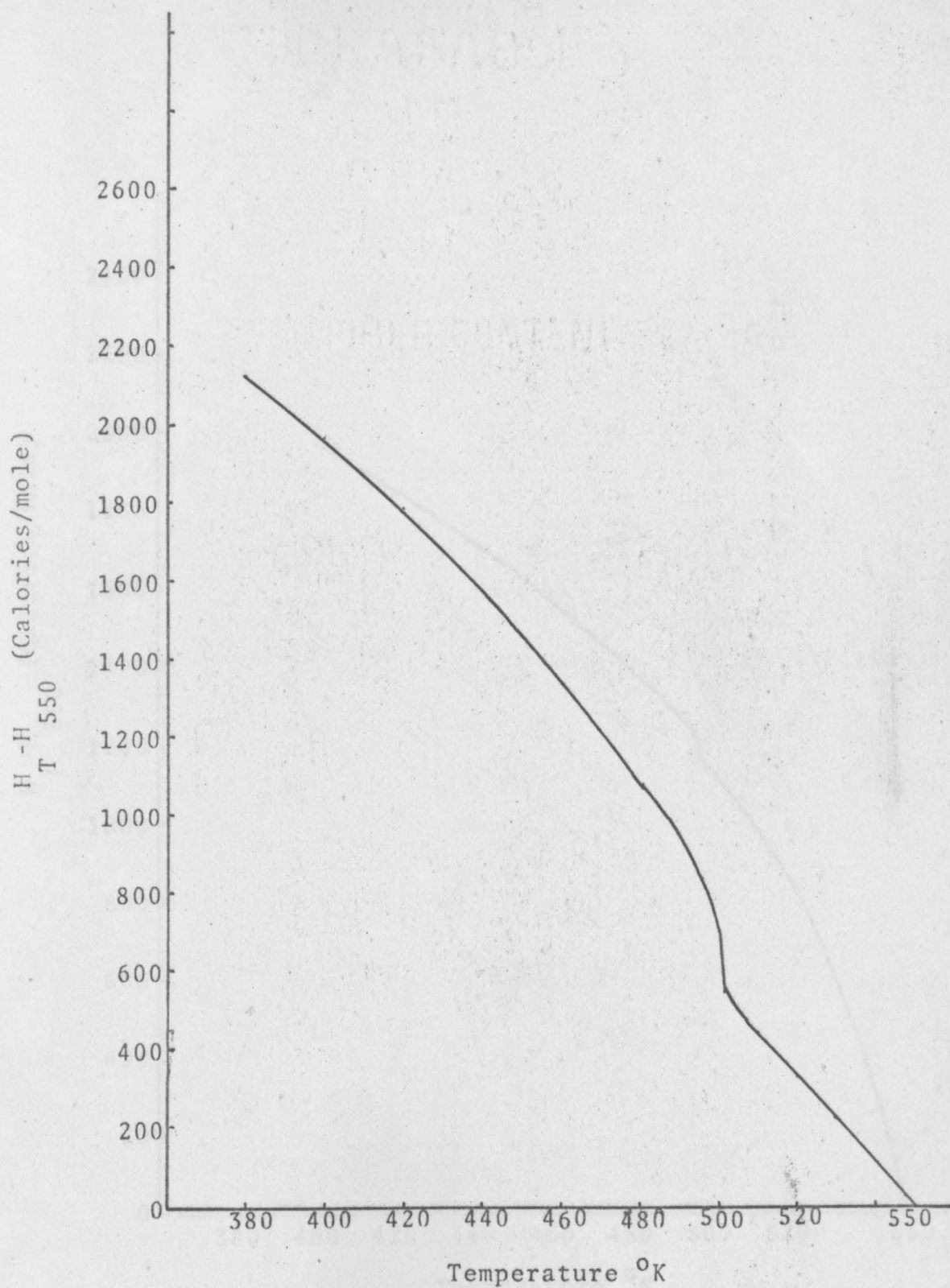


Fig. 12. Enthalpy as a function of temperature for Tl-Au alloy (0.05 atom percent Au).

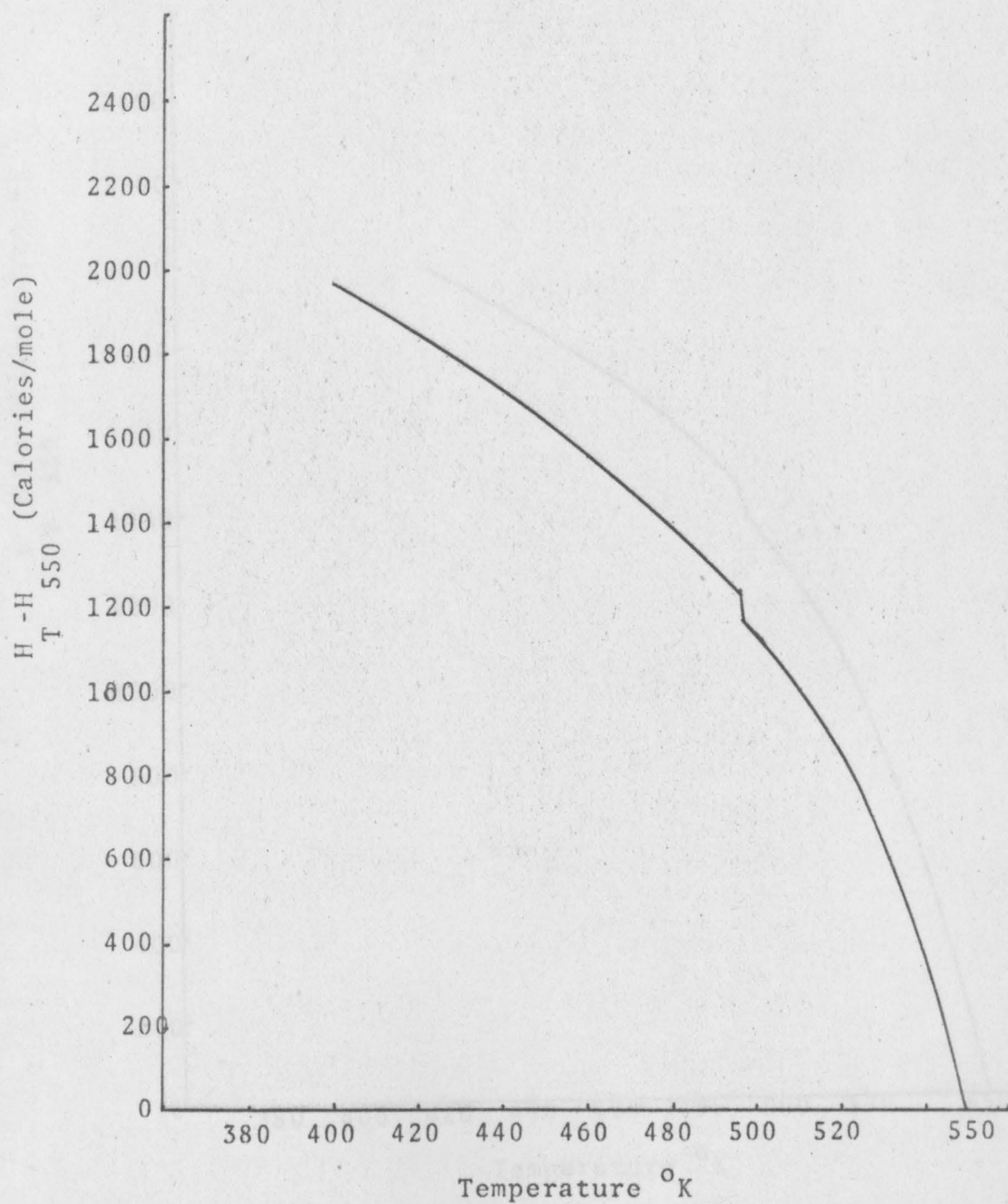


Fig. 13. Enthalpy as a function of temperature for Tl-Au alloy (0.10 atom percent Au).

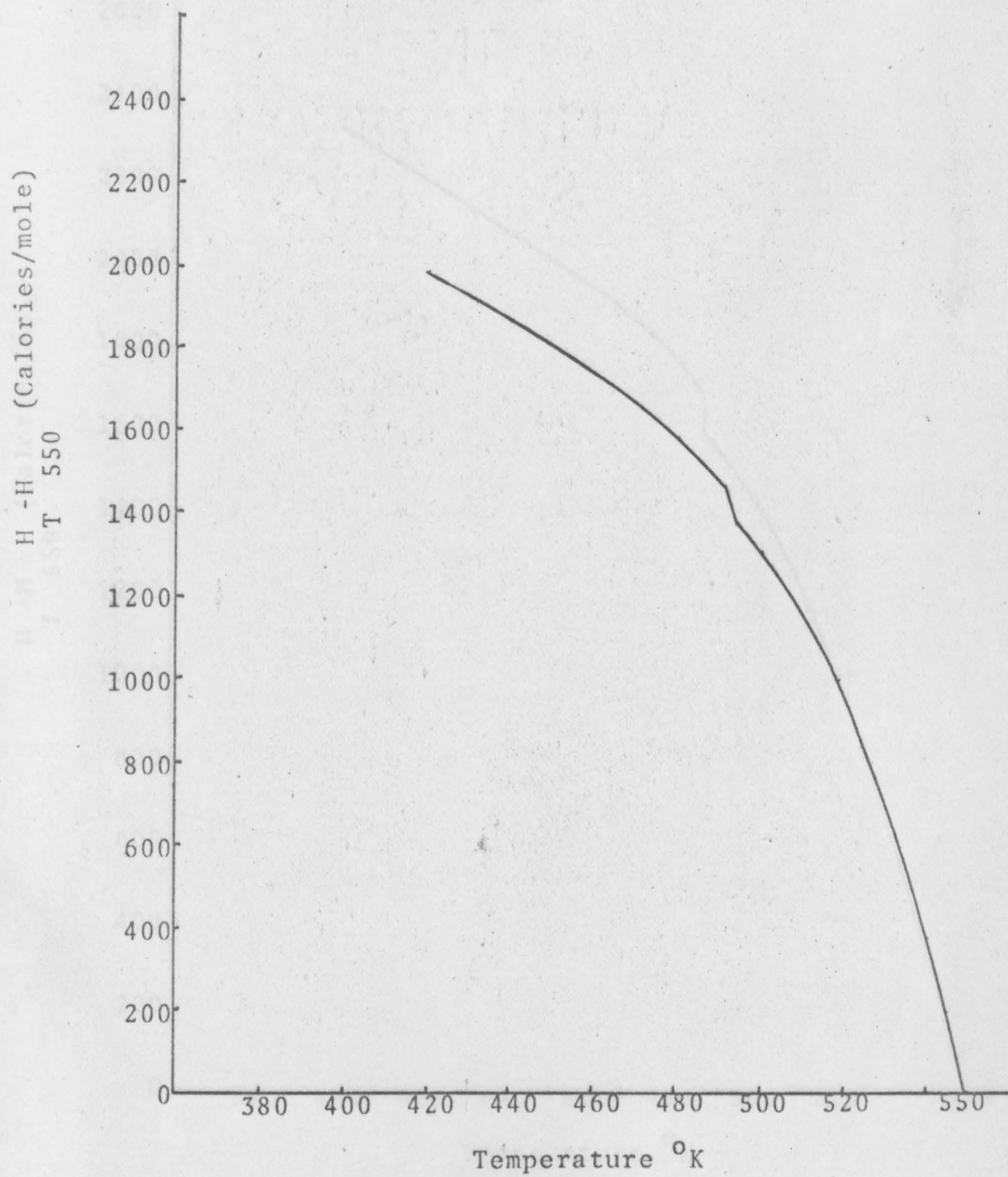


Fig. 14. Enthalpy as a function of temperature for Tl-Au alloy (0.2 atom percent Au).

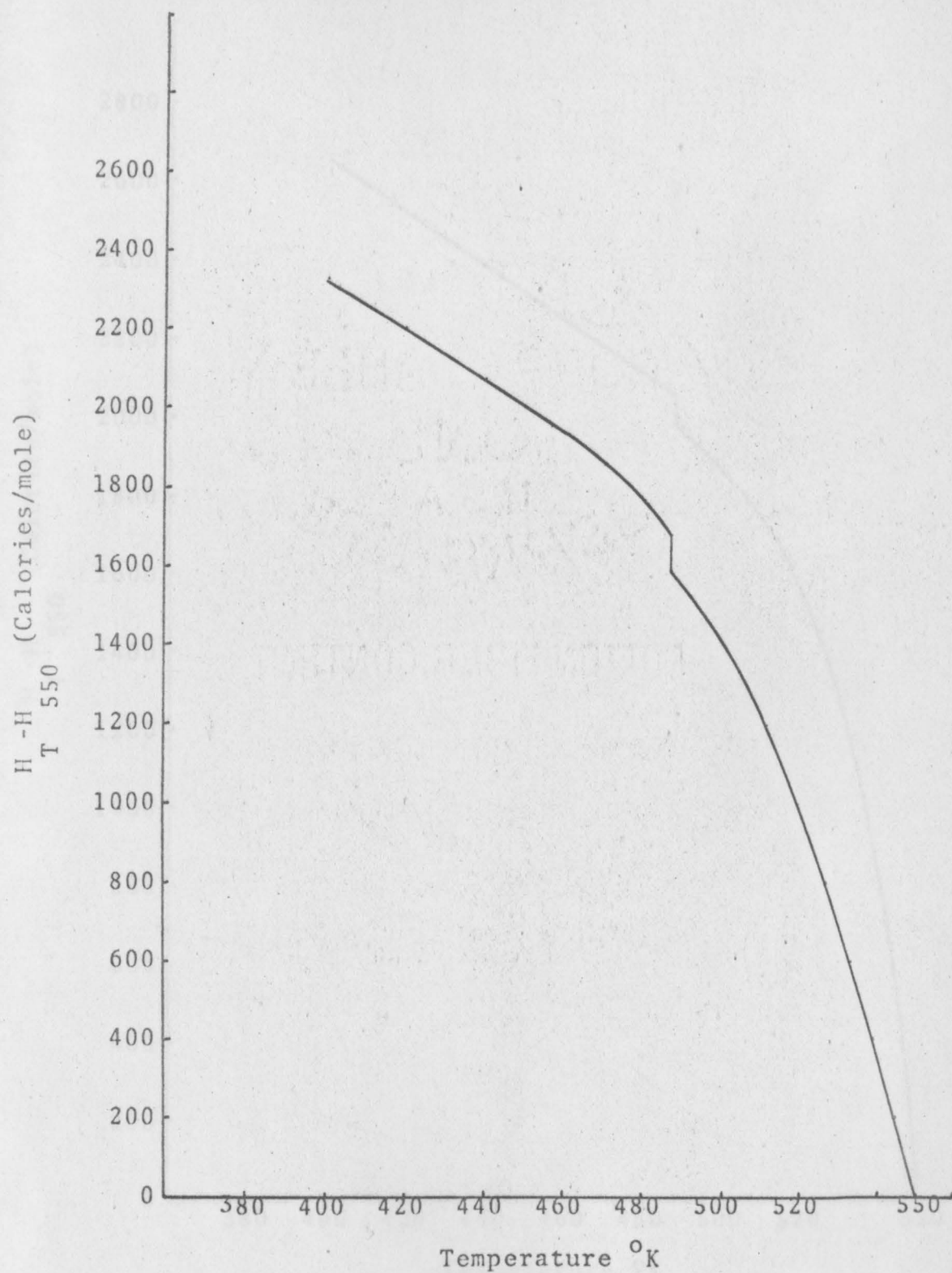


Fig. 15. Enthalpy as a function of temperature for Tl-Au alloy (0.40 atom percent Au)

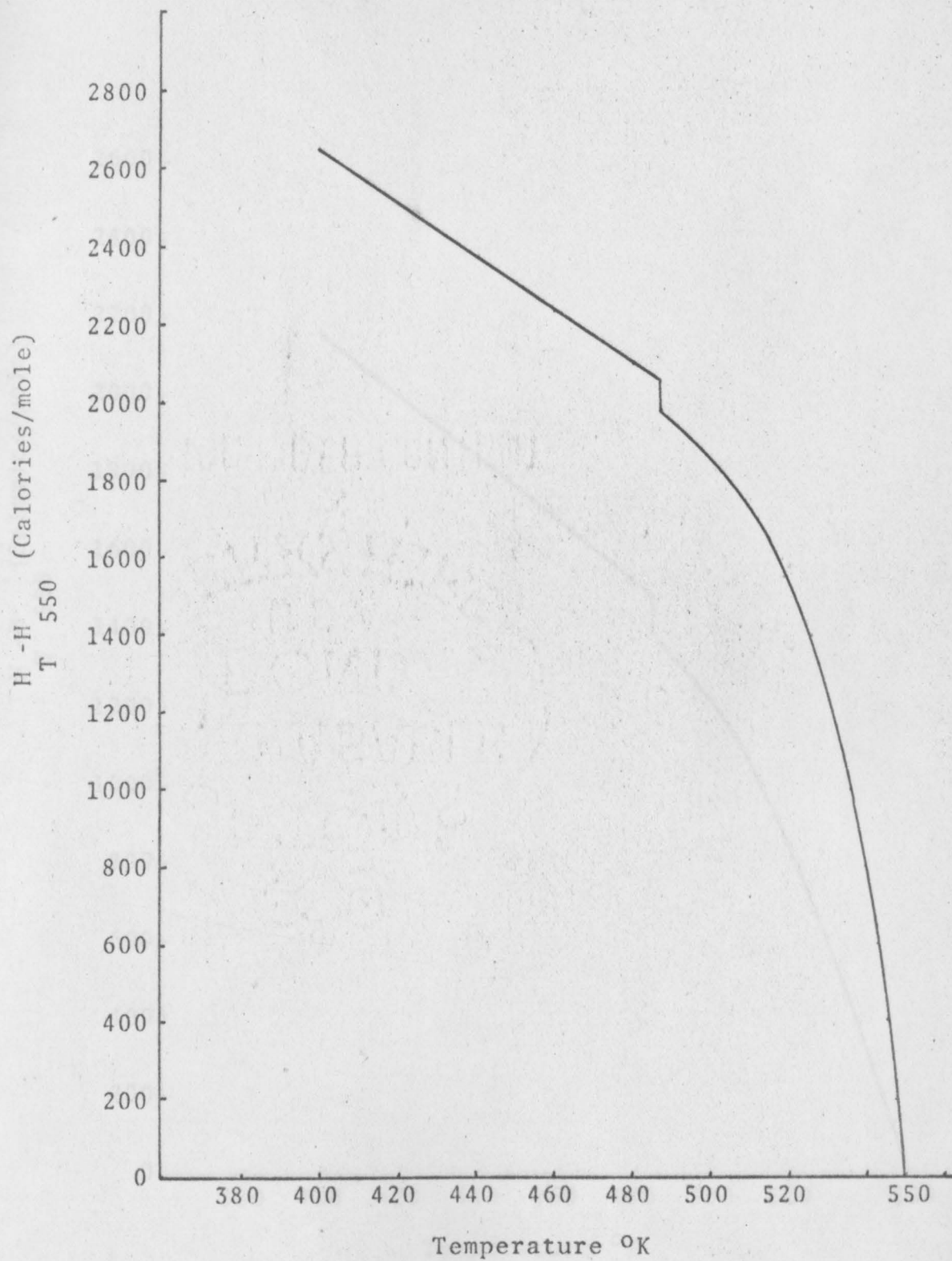


Fig.16. Enthalpy as a function of temperature for Tl-Au alloy (0.60 atom percent Au).



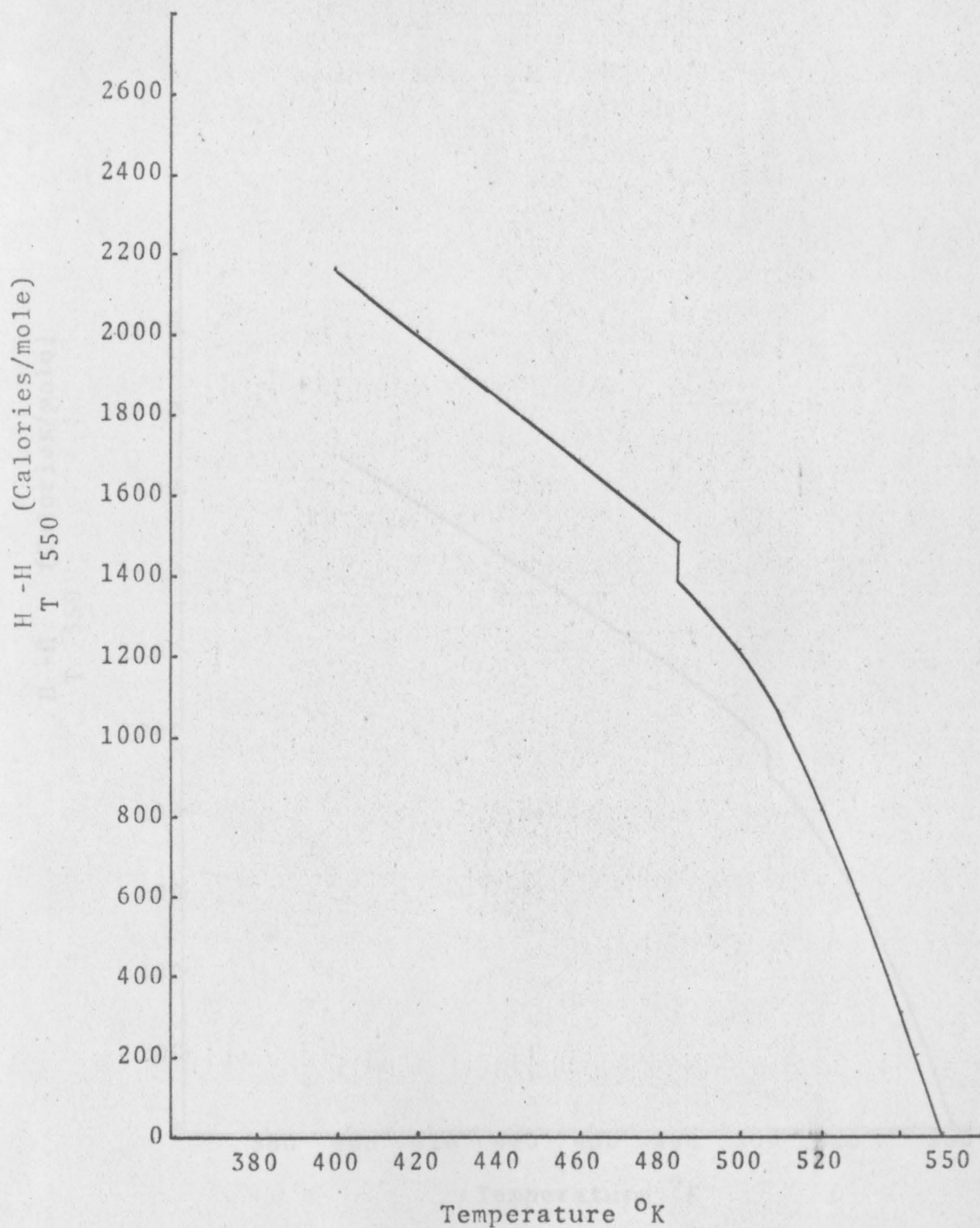


Fig. 17. Enthalpy as a function of temperature for Tl-Au alloy (1.0 atom percent Au).

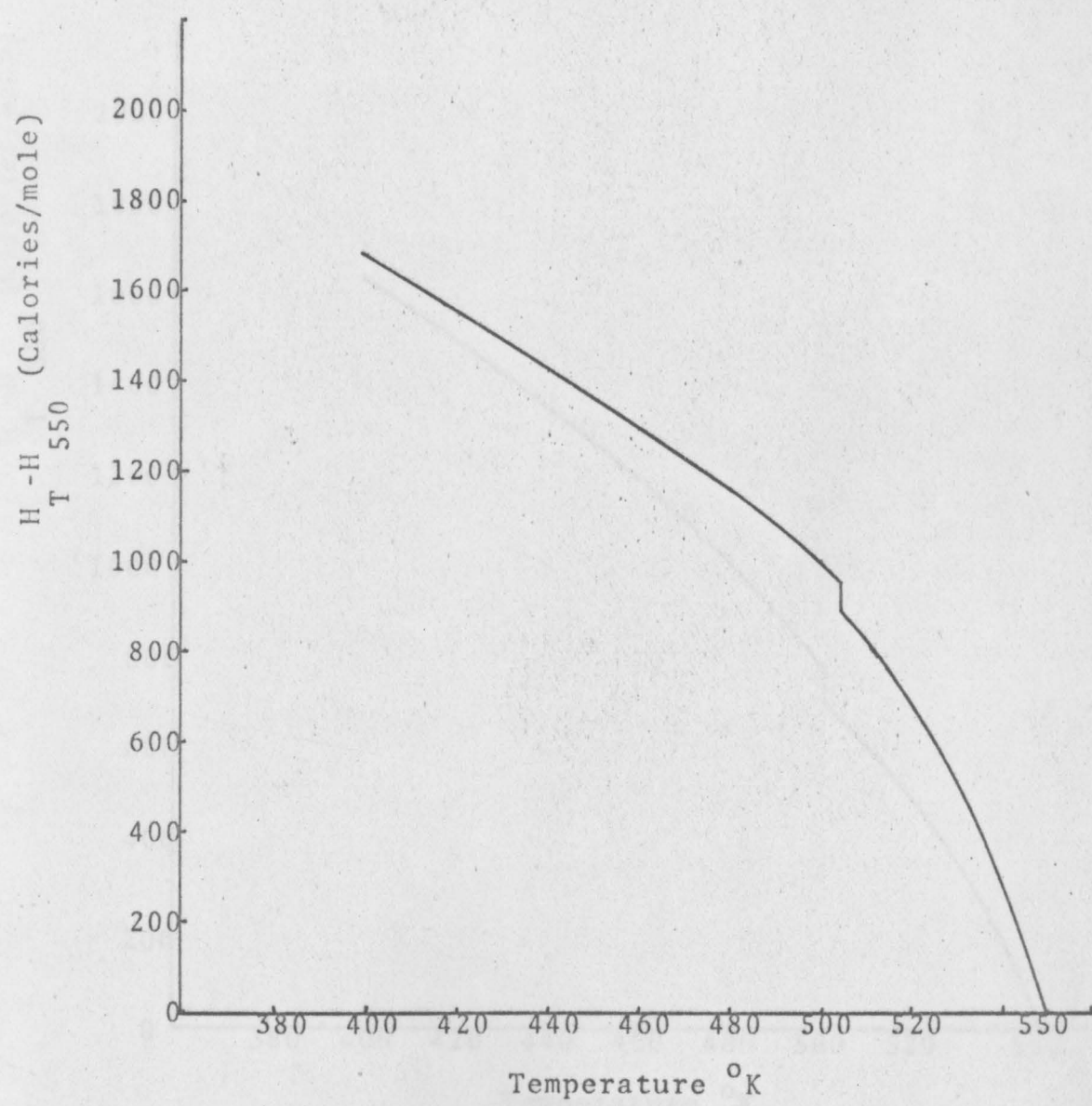


Fig. 18. Enthalpy as a function of temperature for Tl-Zn alloy (0.10 atom percent Zn)

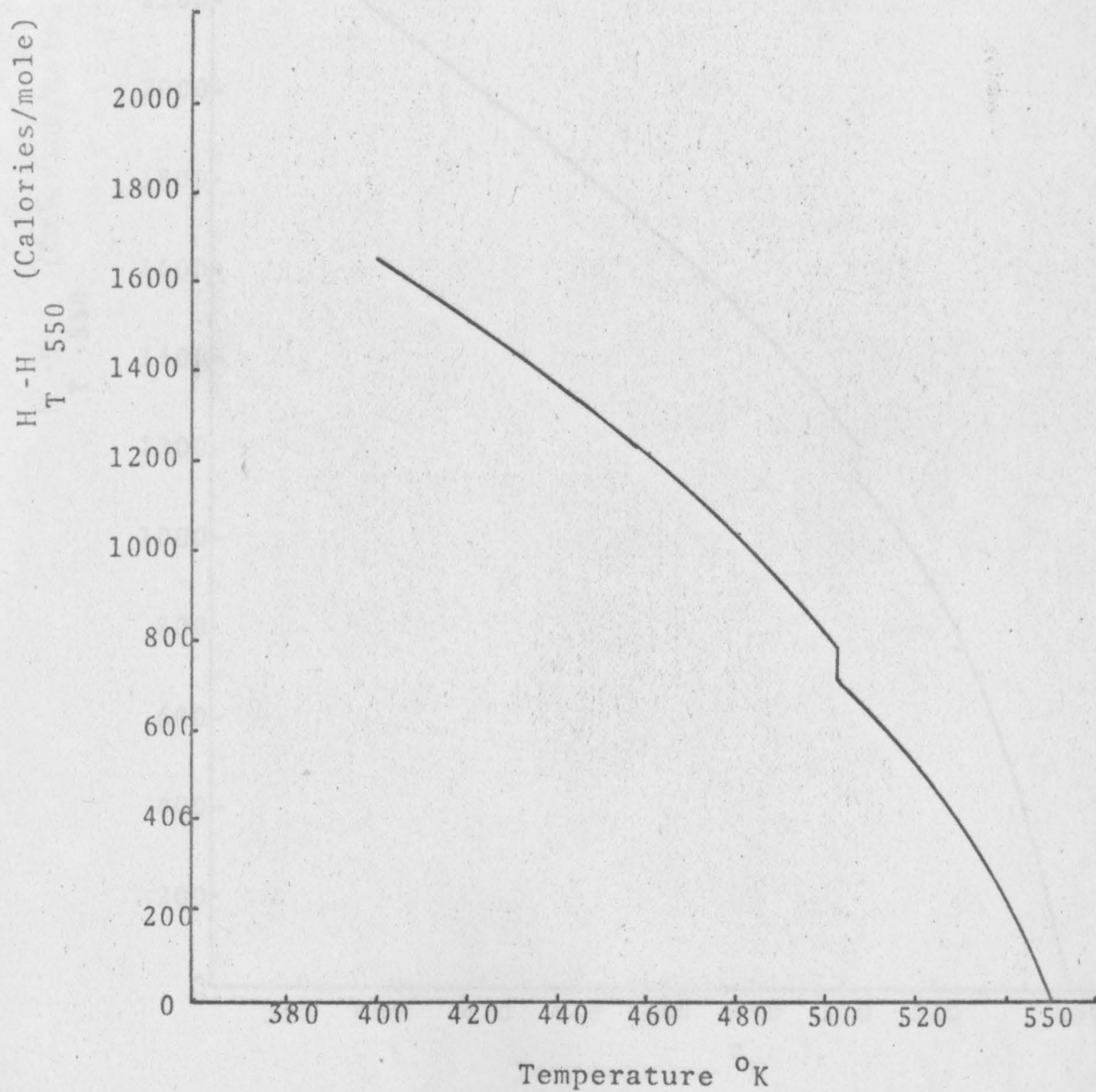


Fig. 19. Enthalpy as a function of temperature for Tl-Zn alloy (0.20 atom percent Zn)

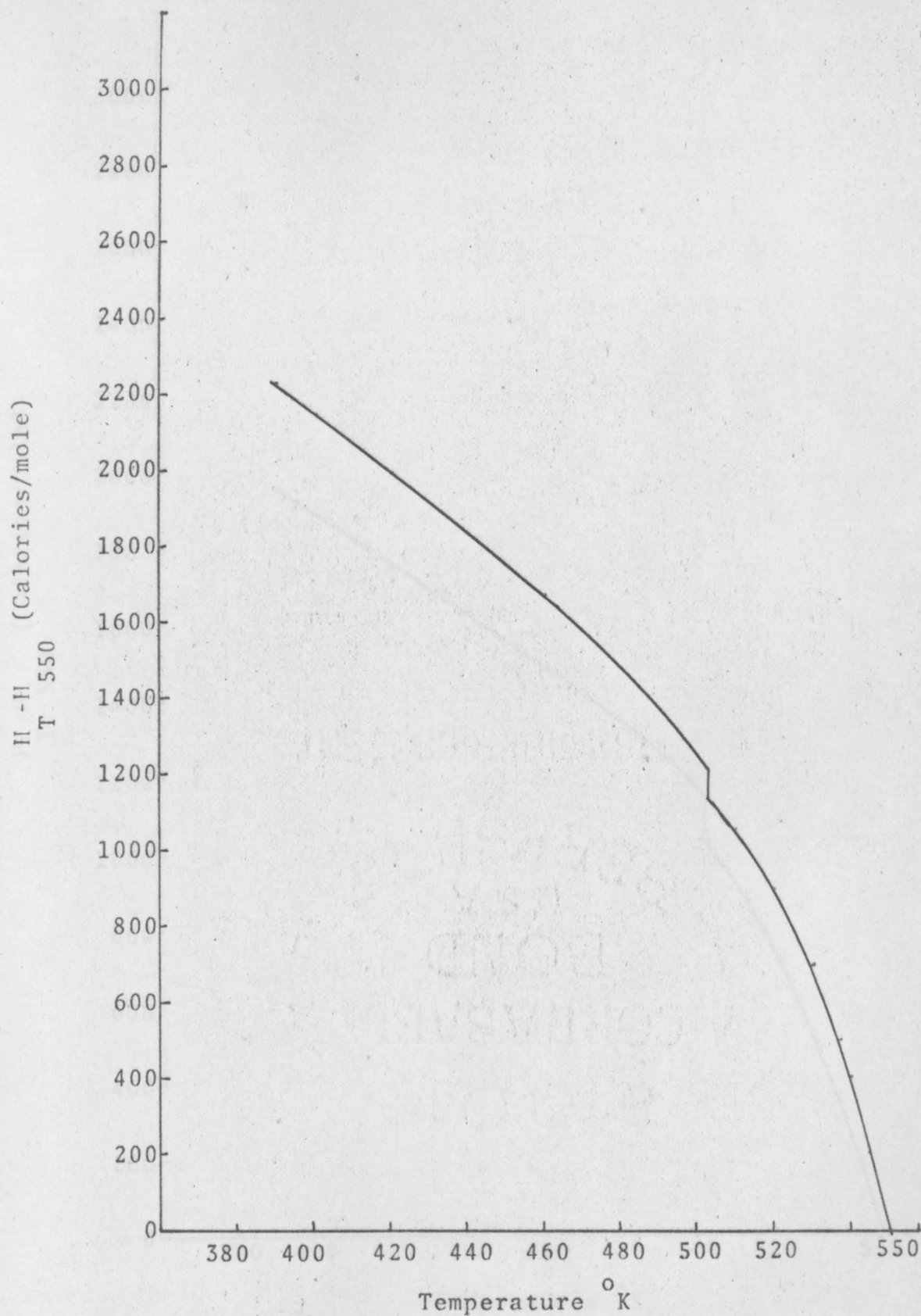


Fig. 20. Enthalpy as a function of temperature for Tl-Zn alloy (0.40 atom percent Zn)

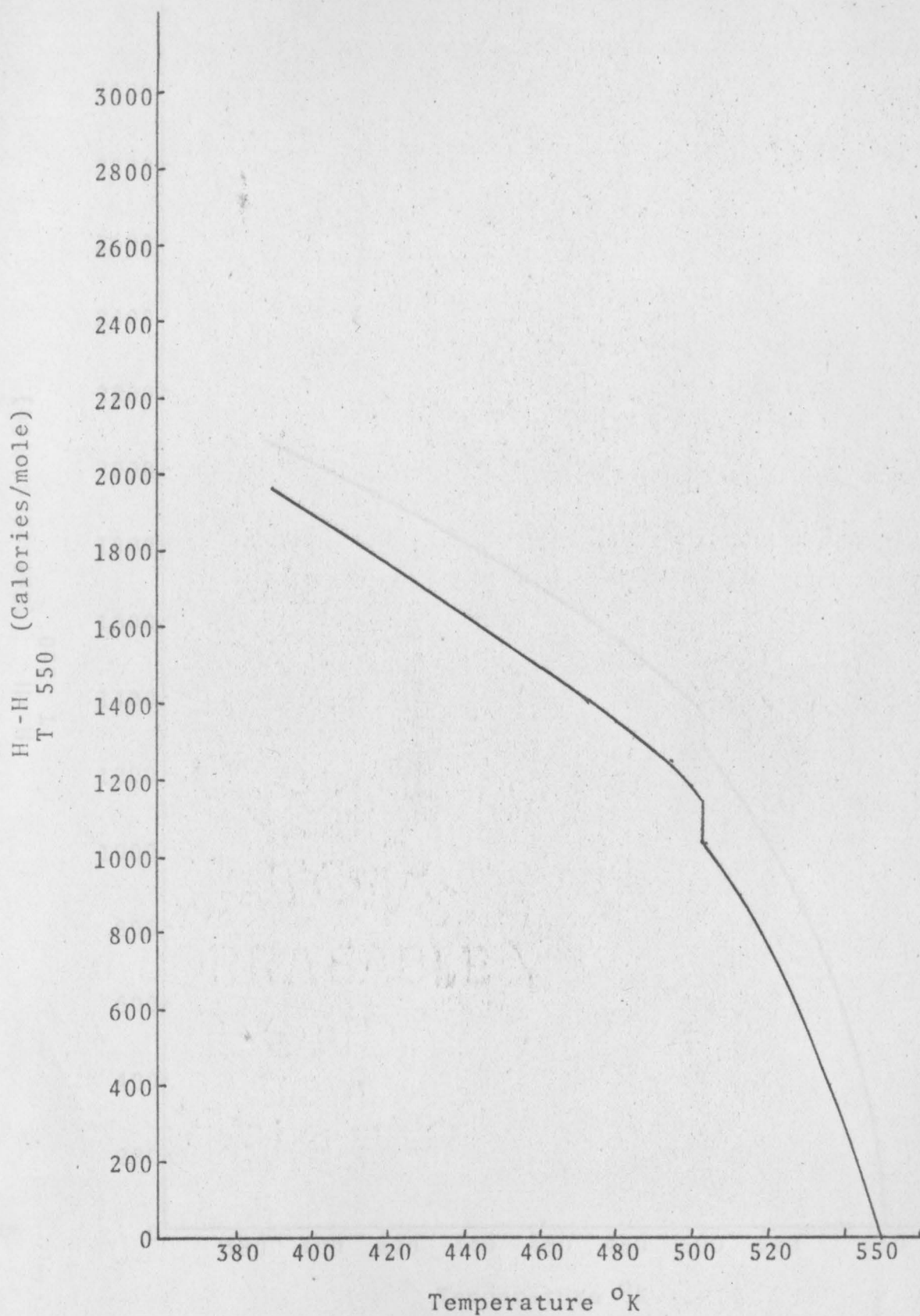


Fig. 21. Enthalpy as a function of temperature for Tl-Zn alloy (0.60 atom percent Zn).

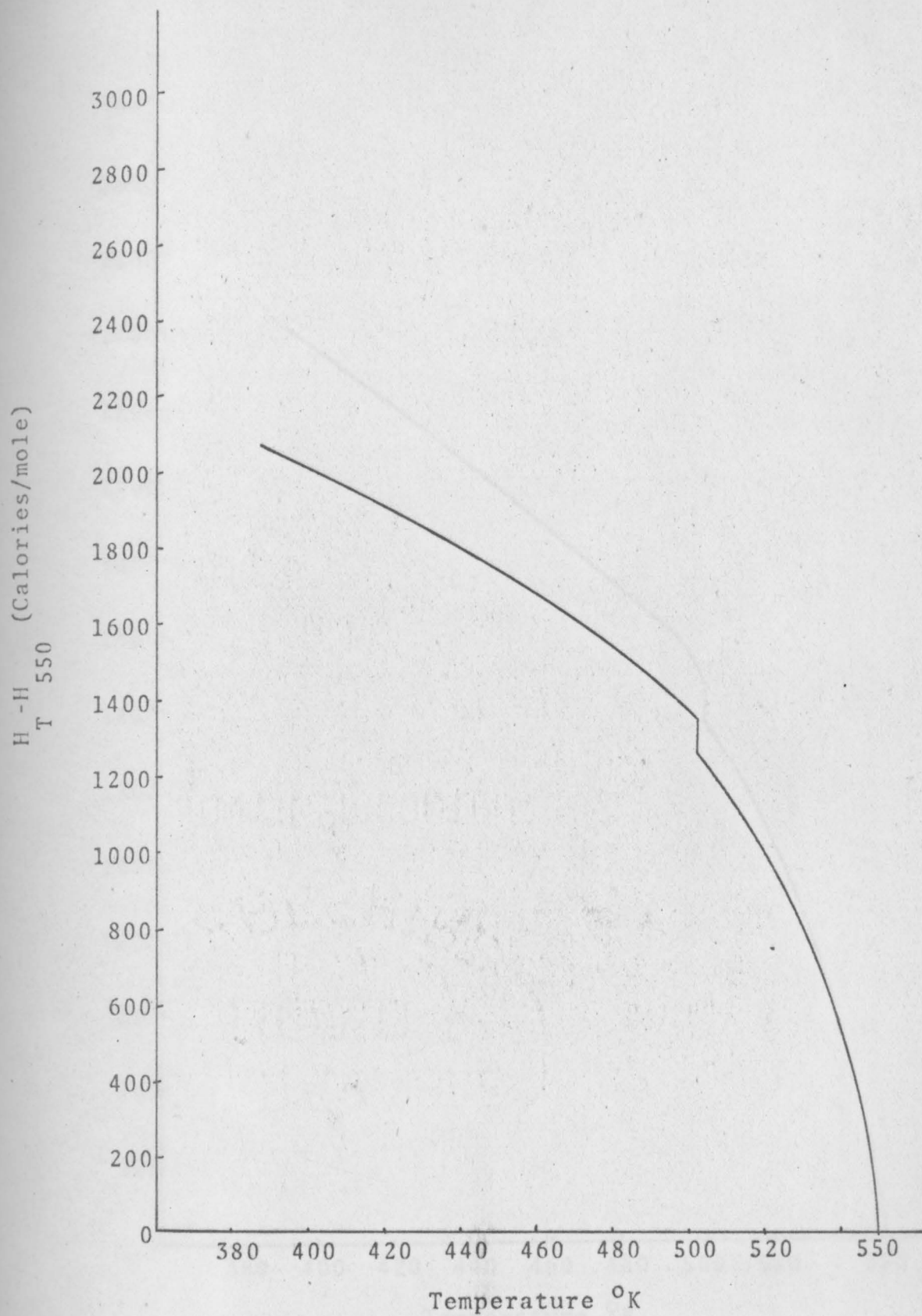


Fig. 22. Enthalpy as a function of temperature for Tl-Zn alloy (0.80 atom percent Zn)

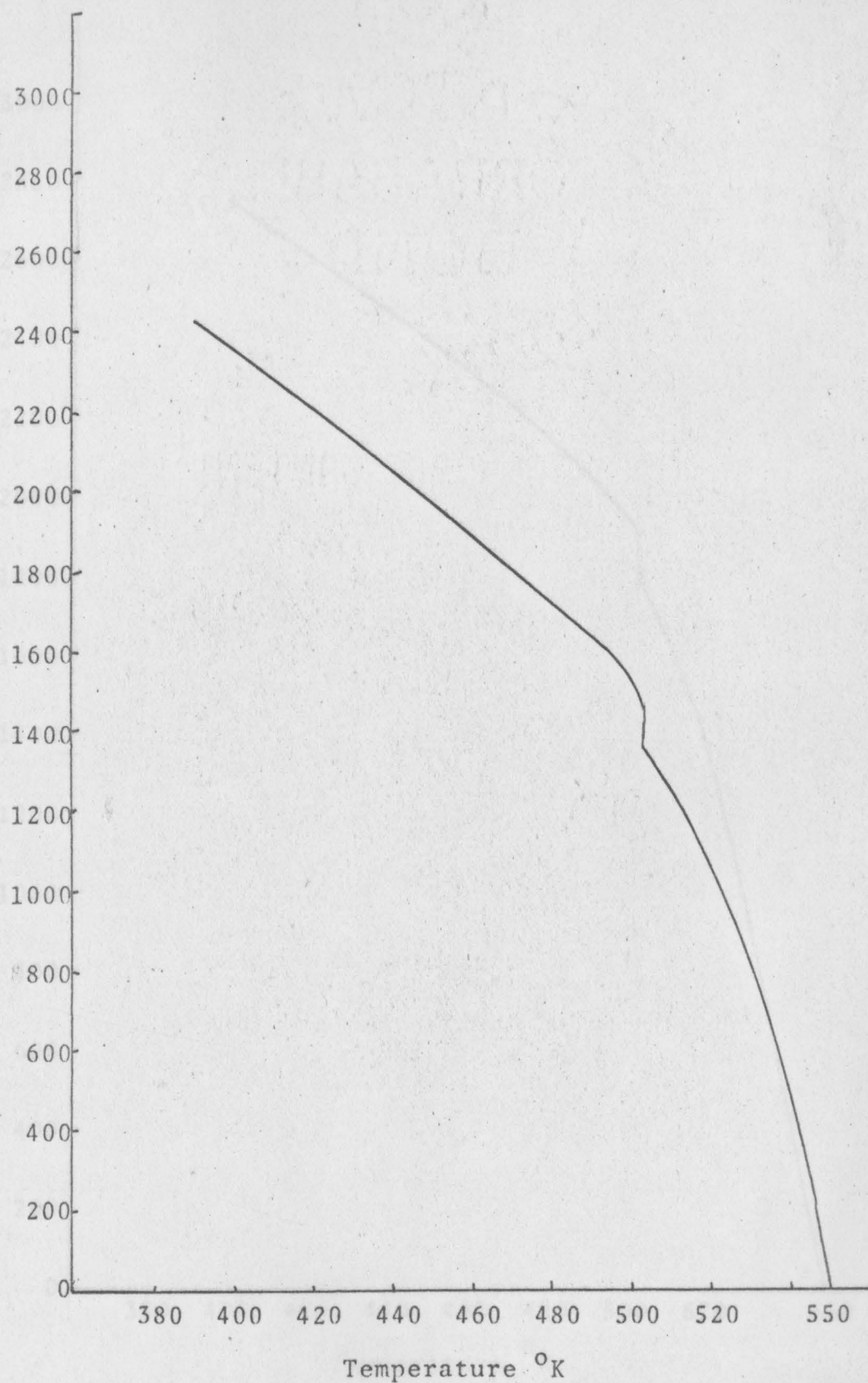


Fig. 23. Enthalpy as a function of temperature for Tl-Zn alloy (1.0 atom percent Zn)

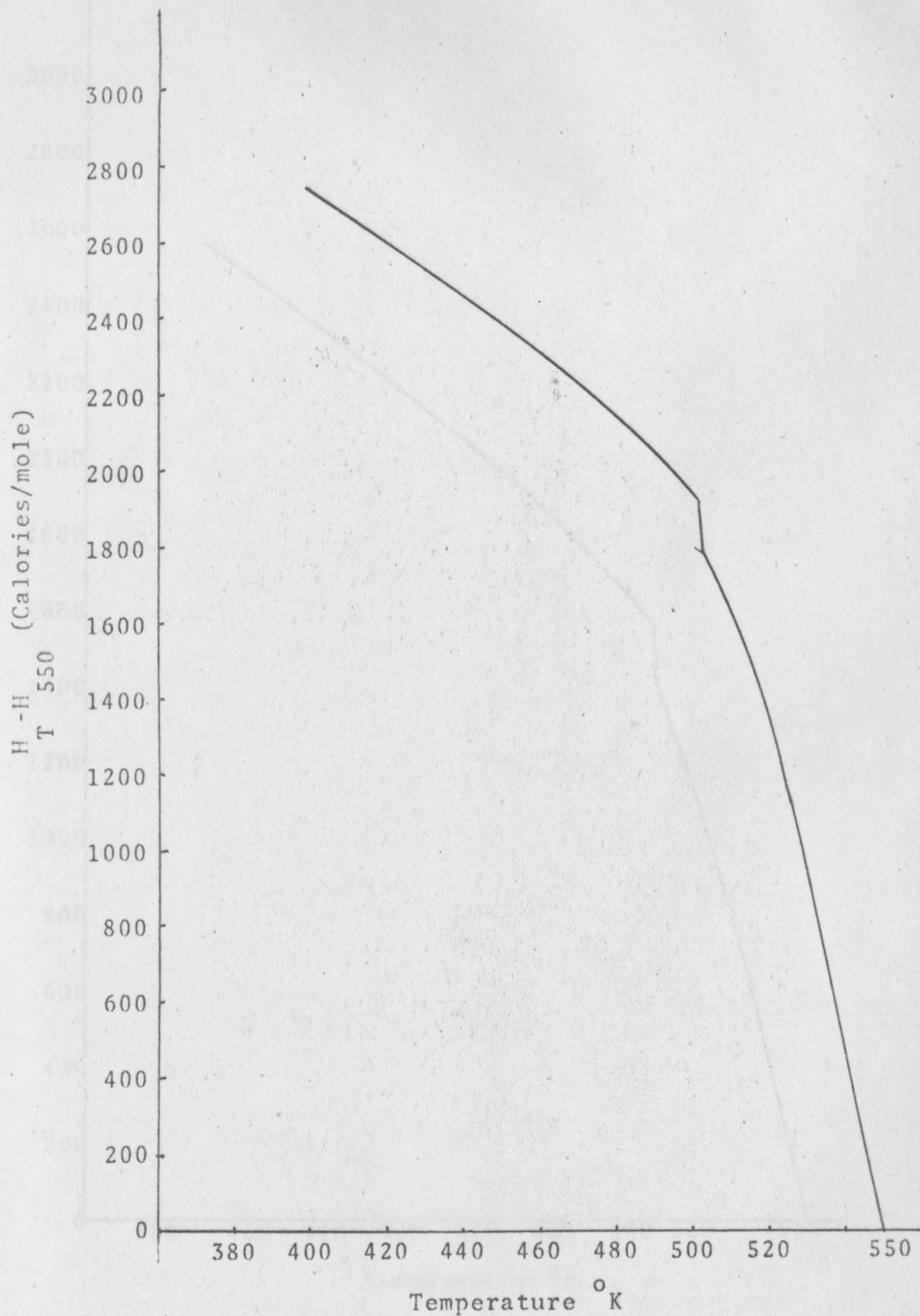


Fig. 24. Enthalpy as a function of temperature for Tl-Zn alloy (1.20 atom percent Zn)



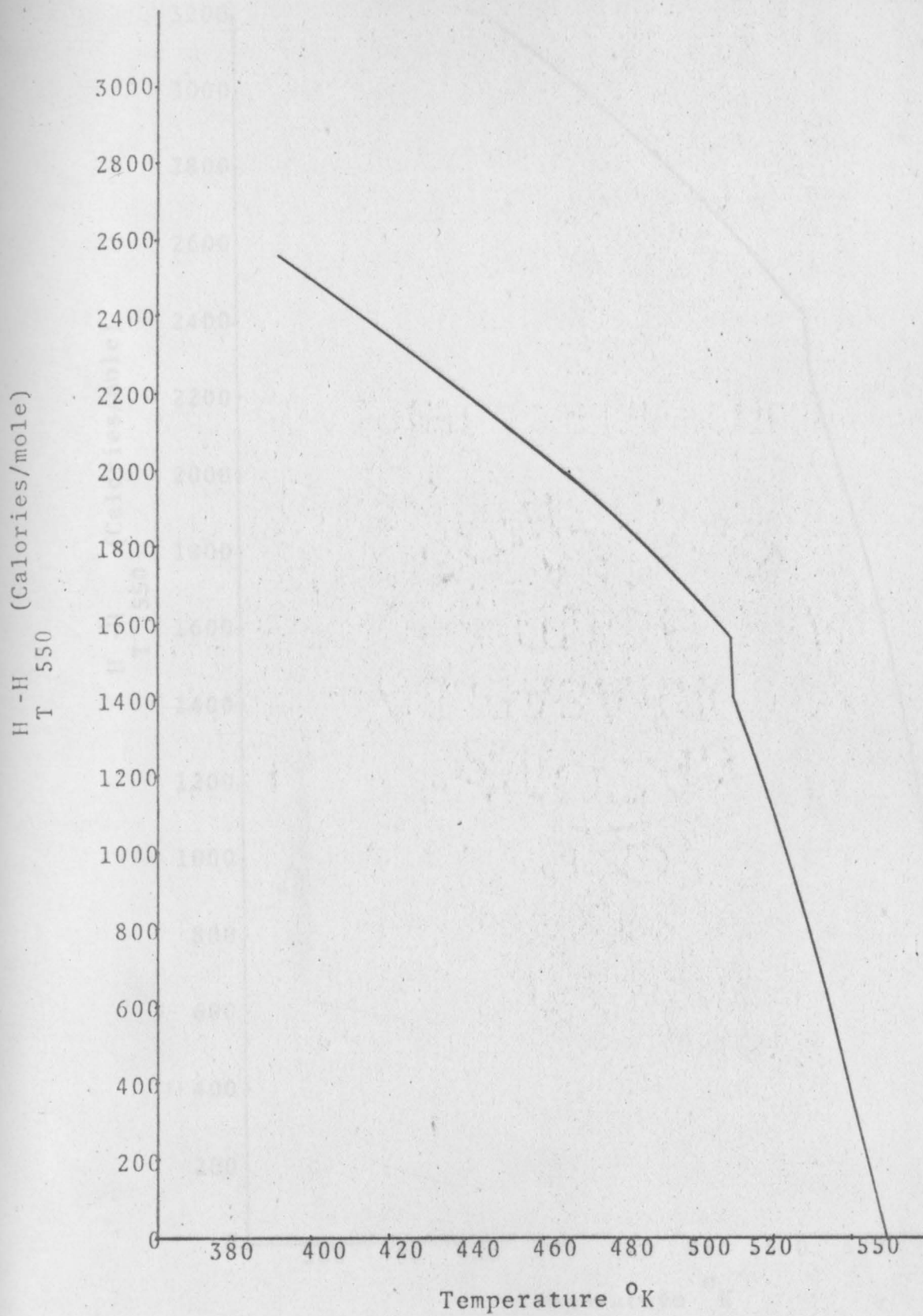


Fig. 25. Enthalpy as a function of temperature for Tl-Cd alloy (0.044 atom percent Cd)

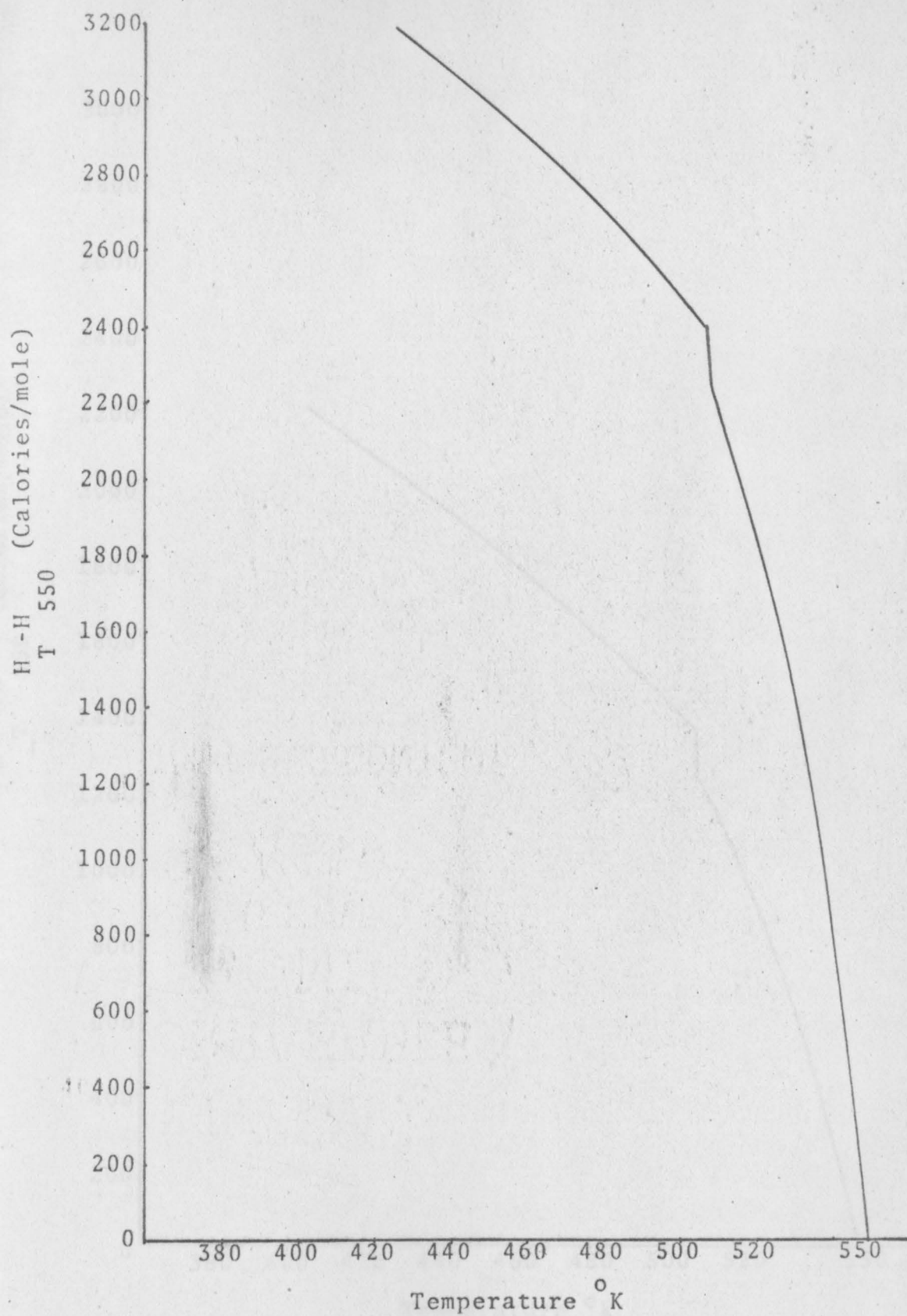


Fig. 26. Enthalpy as a function of temperature for Tl-Cd alloy (0.18 atom percent Cd)

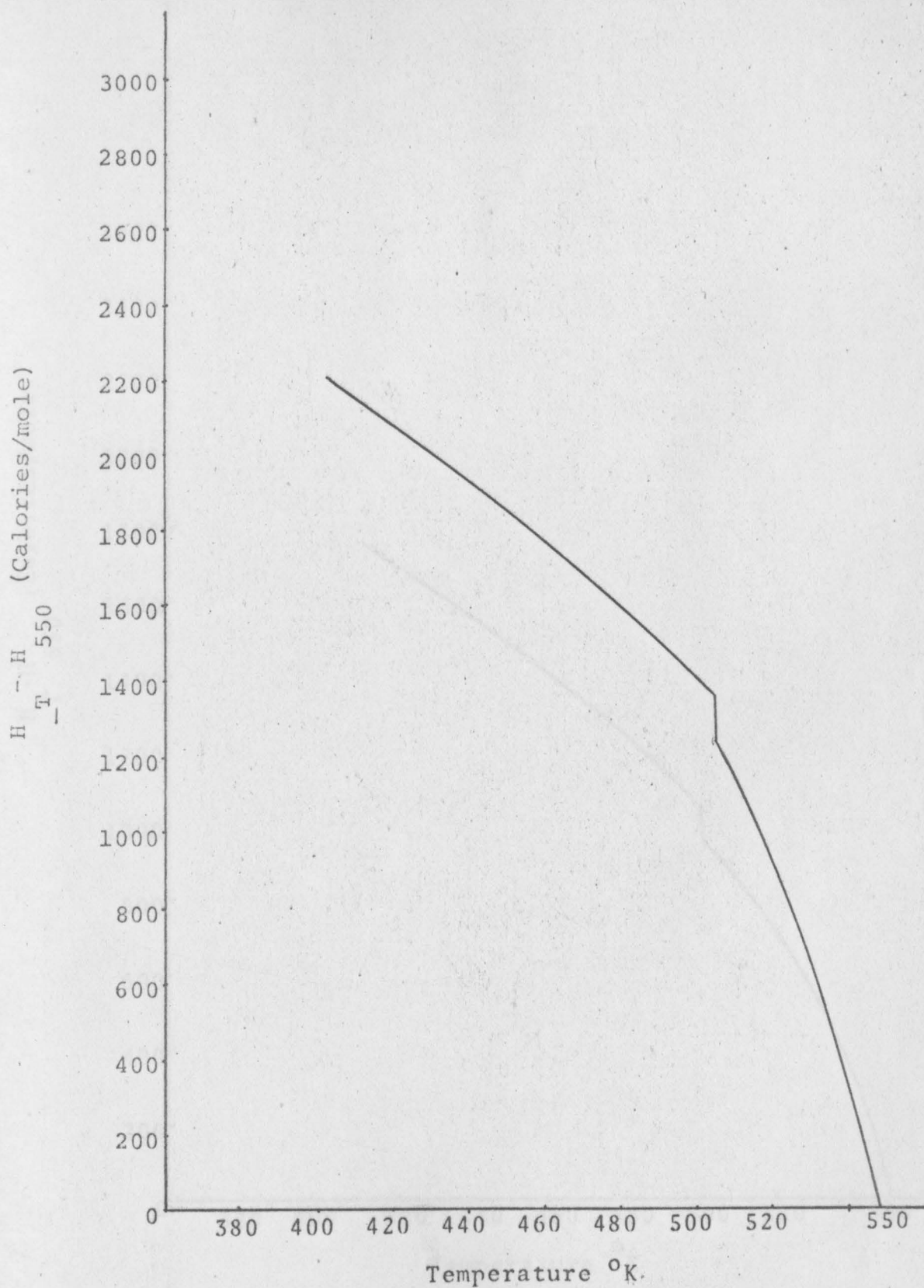


Fig.27. Enthalpy as a function of temperature for Tl-Cd alloy (0.44 atom percent Cd)

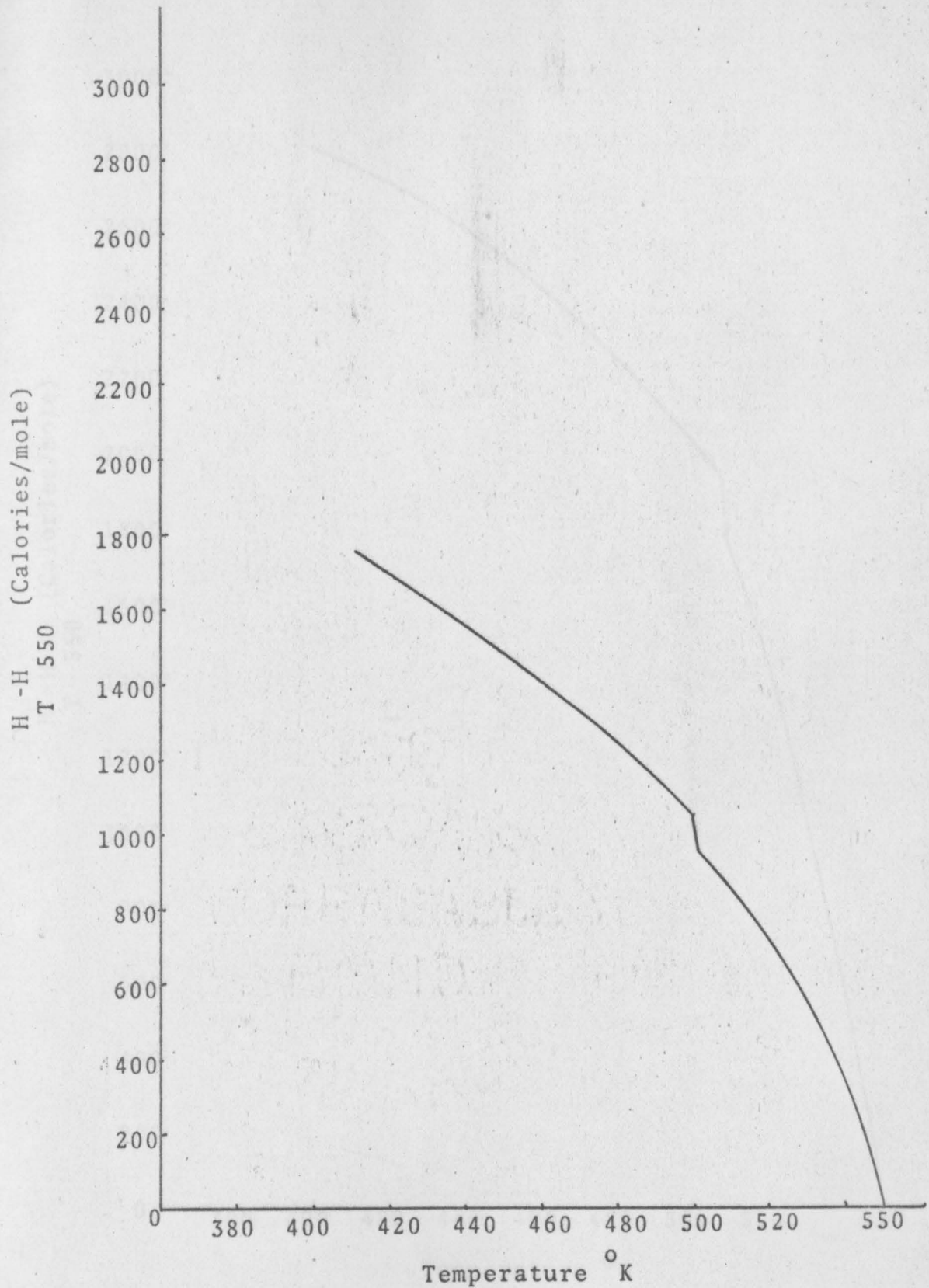


Fig. 28. Enthalpy as a function of temperature for Tl-Cd alloy (0.5 atom percent Cd).

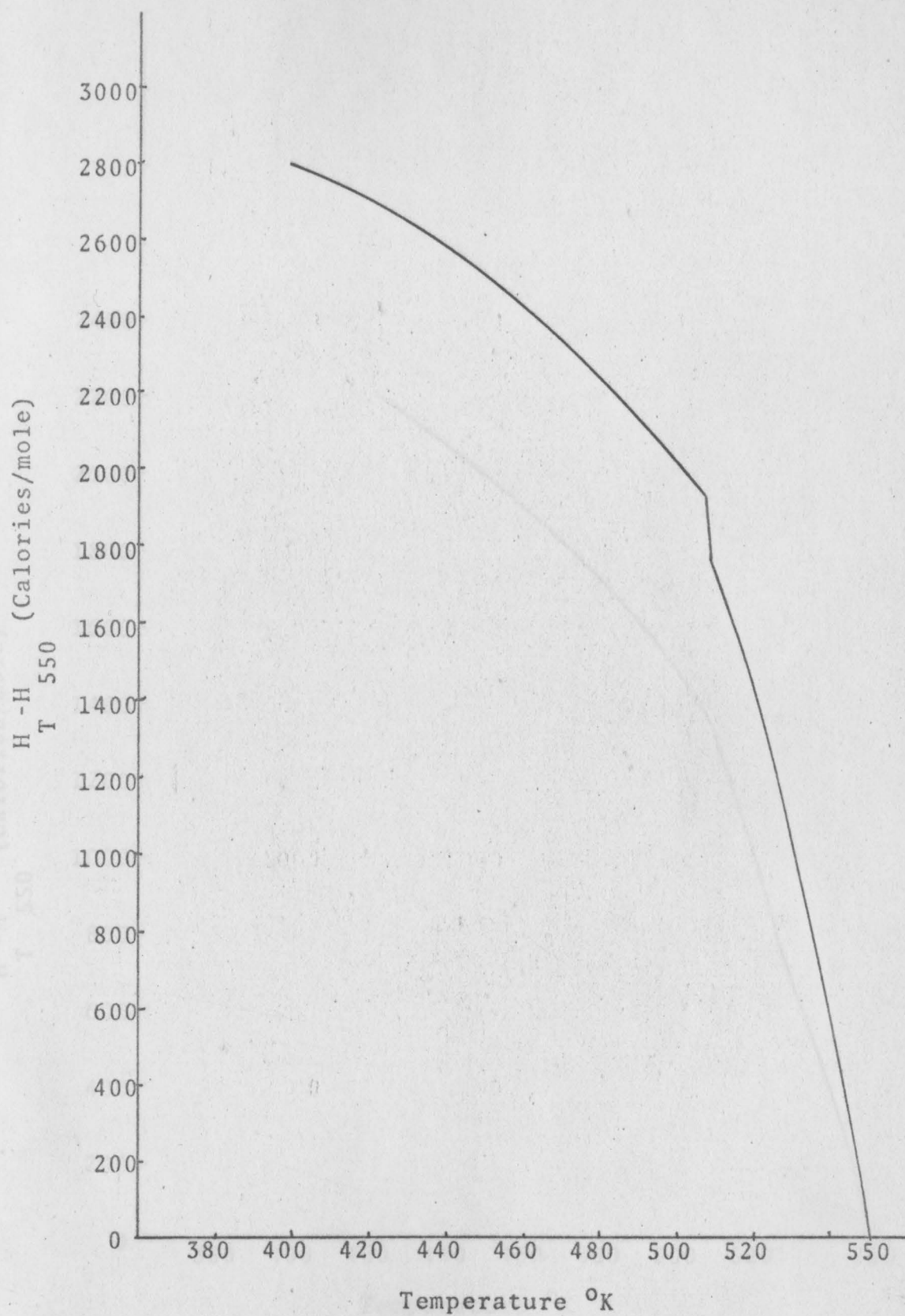


Fig. 29. Enthalpy as a function of temperature for Tl-Cd alloy (0.60 atom percent Cd).

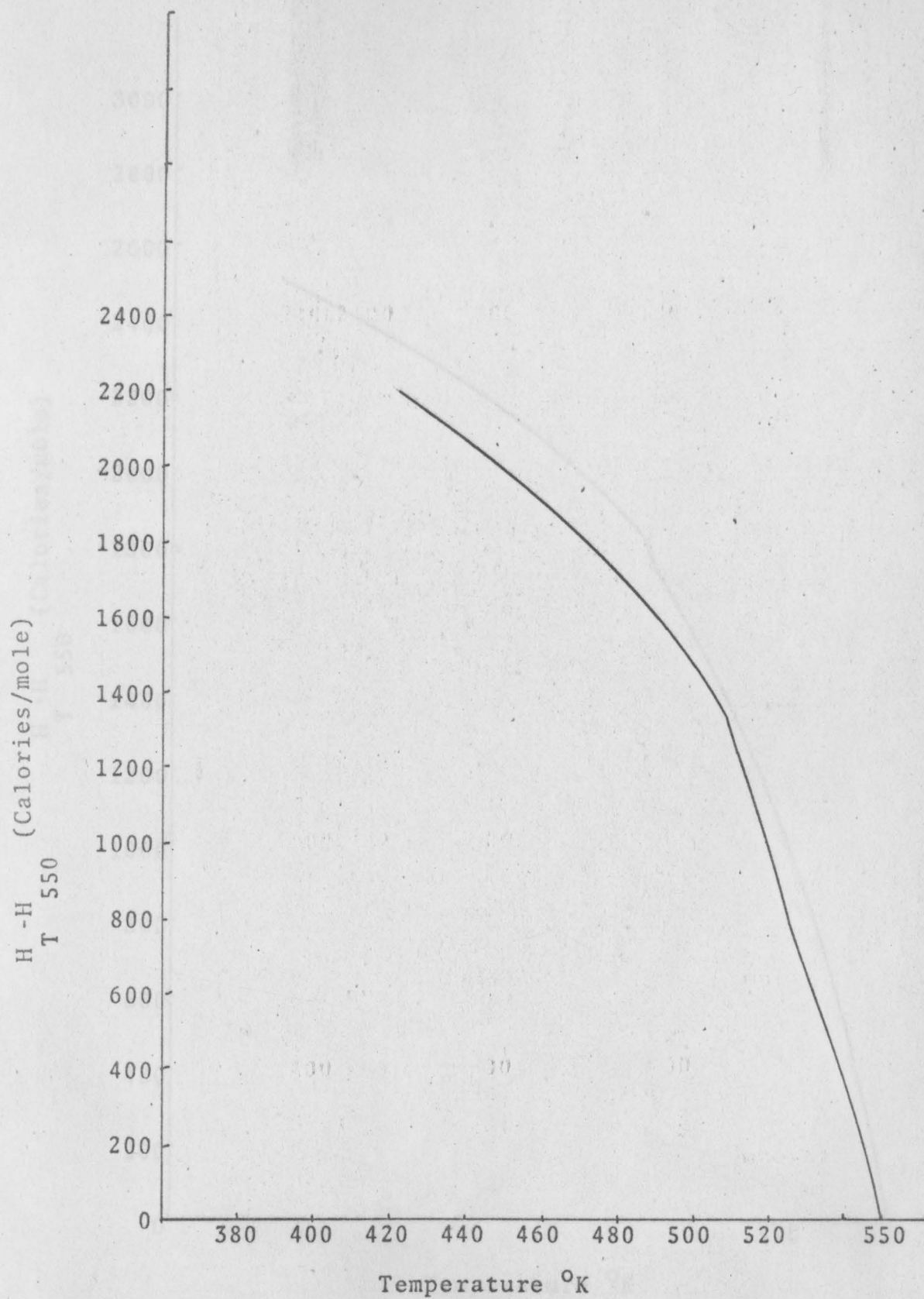


Fig. 30. Enthalpy as a function of temperature for Tl-Cd alloy (0.88 atom percent Cd)

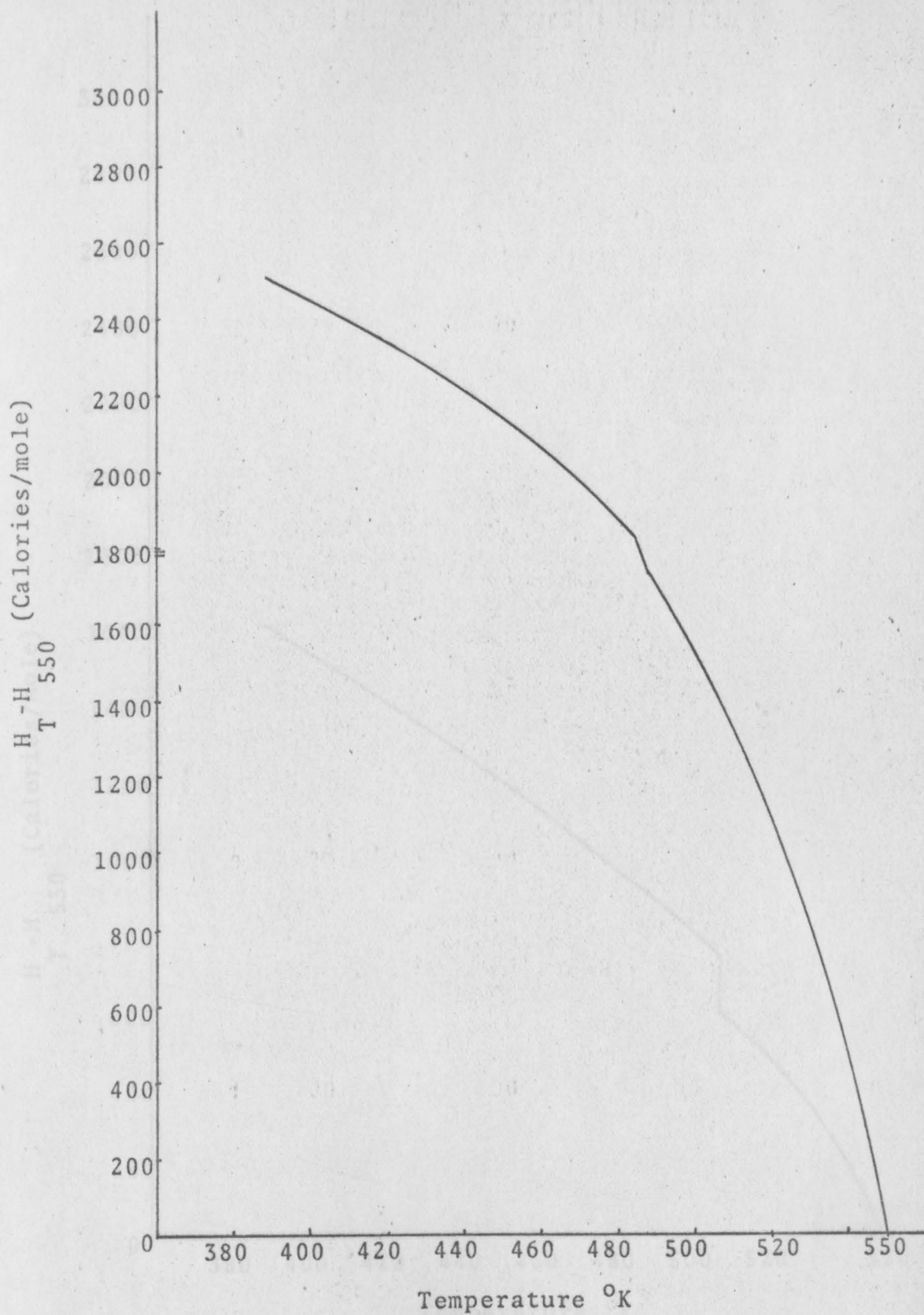


Fig. 31. Enthalpy as a function of temperature for Tl-Cd alloy (1.0 atom percent Cd)

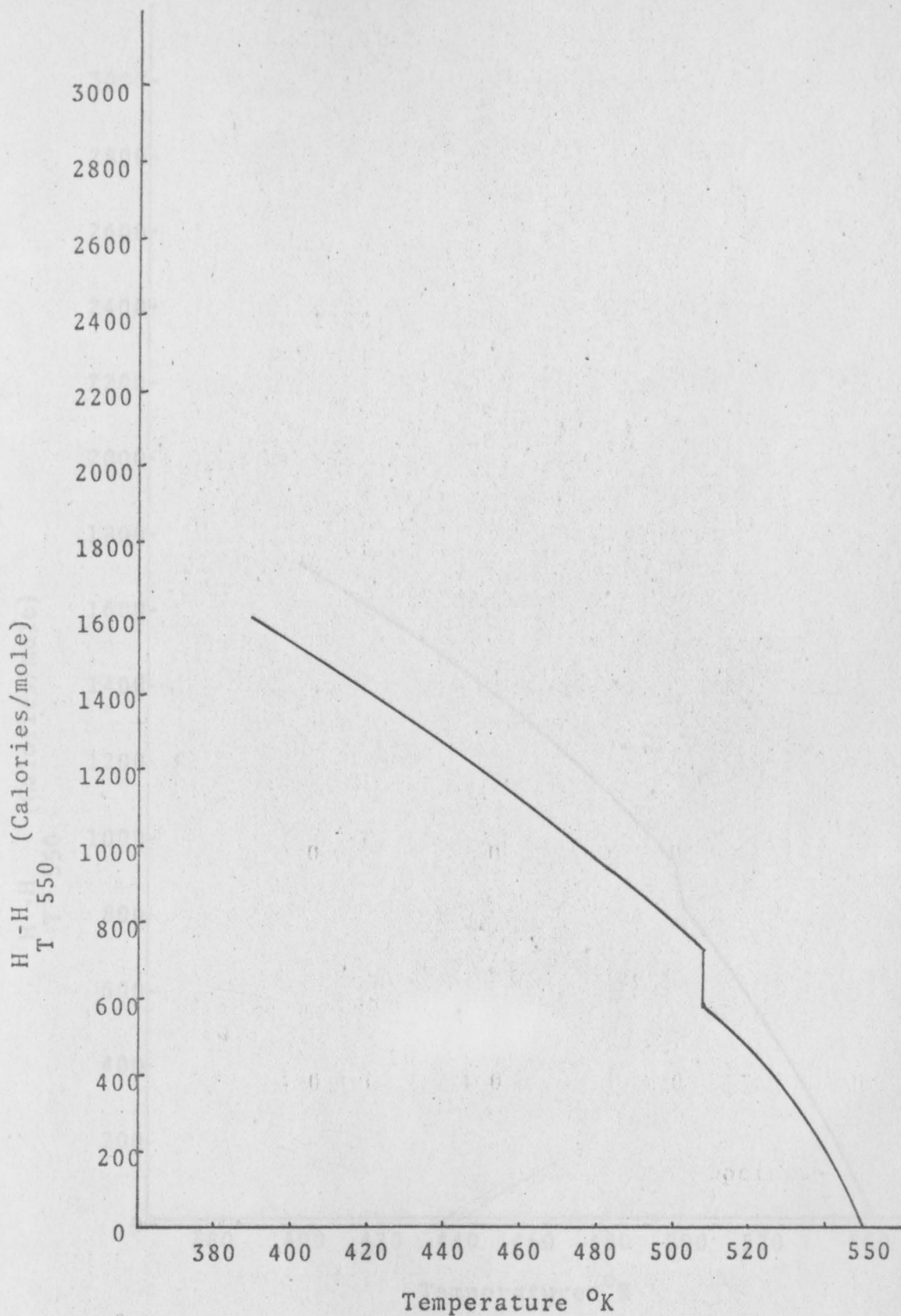


Fig. 32. Enthalpy as a function of temperature for Tl-Sn alloy ( 0.05 atom percent Sn)



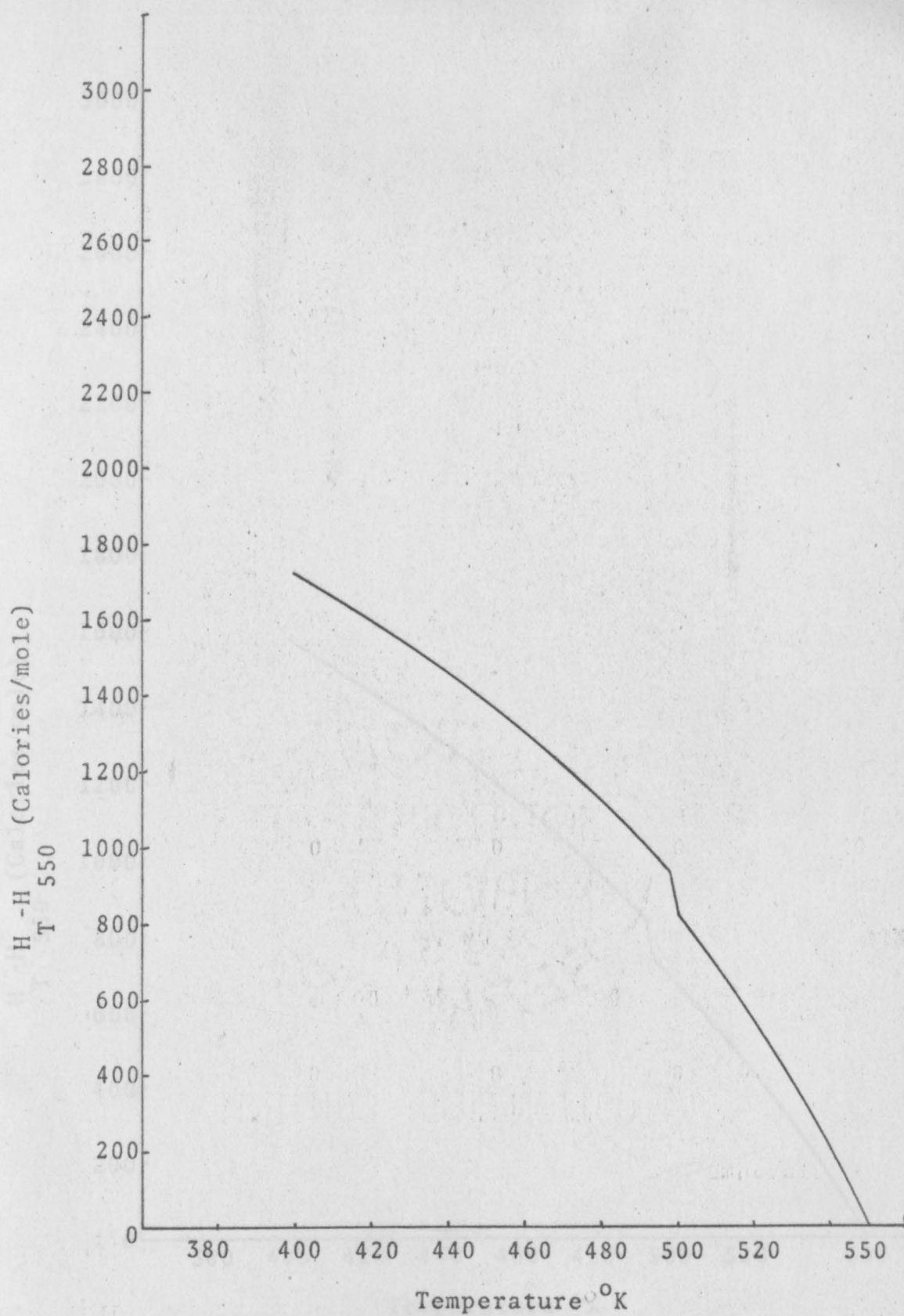


Fig. 33. Enthalpy as a function of temperature for Tl-Sn alloy (0.2 atom percent Sn)

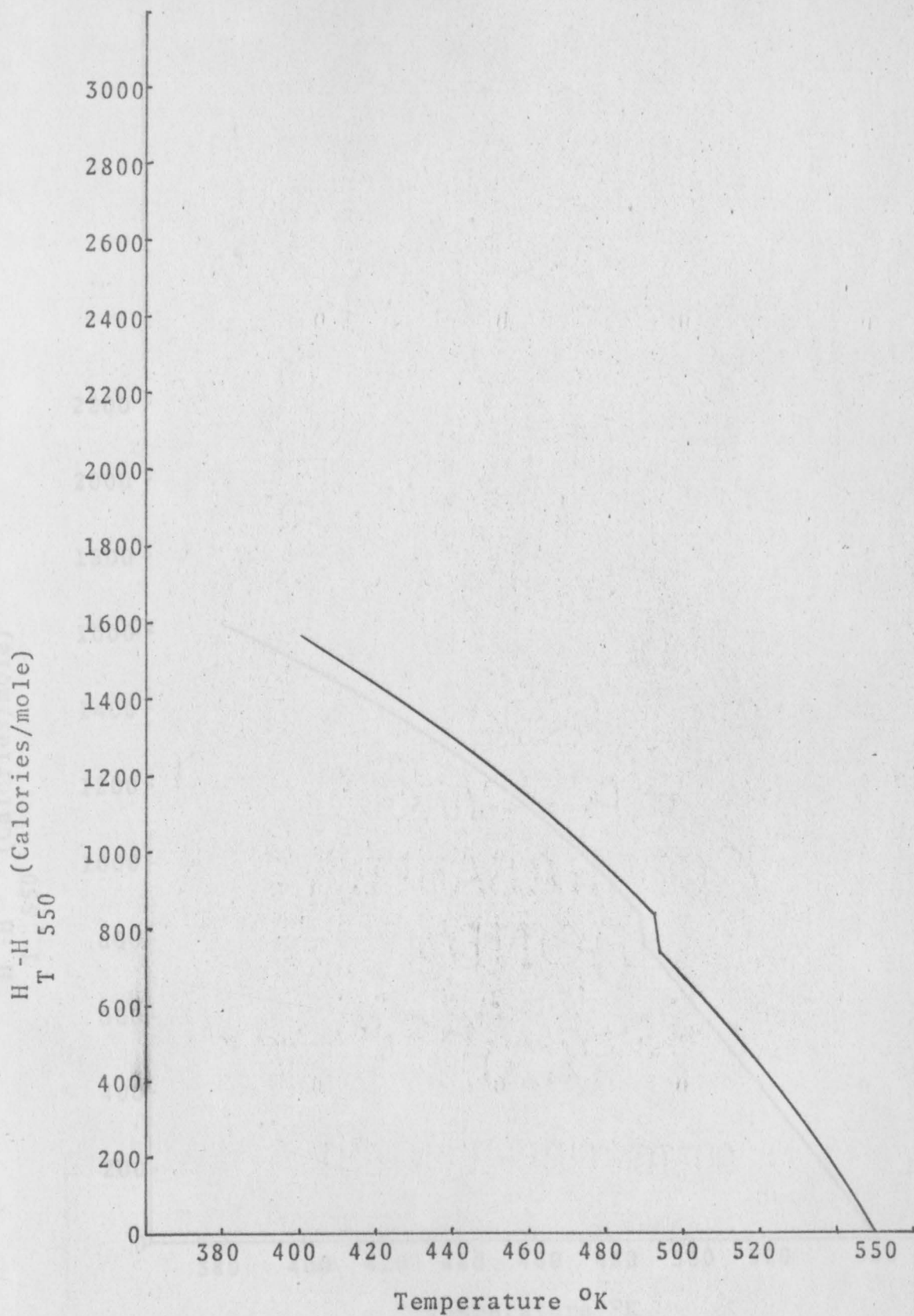


Fig. 34. Enthalpy as a function of temperature for Tl-Sn alloy (0.40 atom percent Sn)

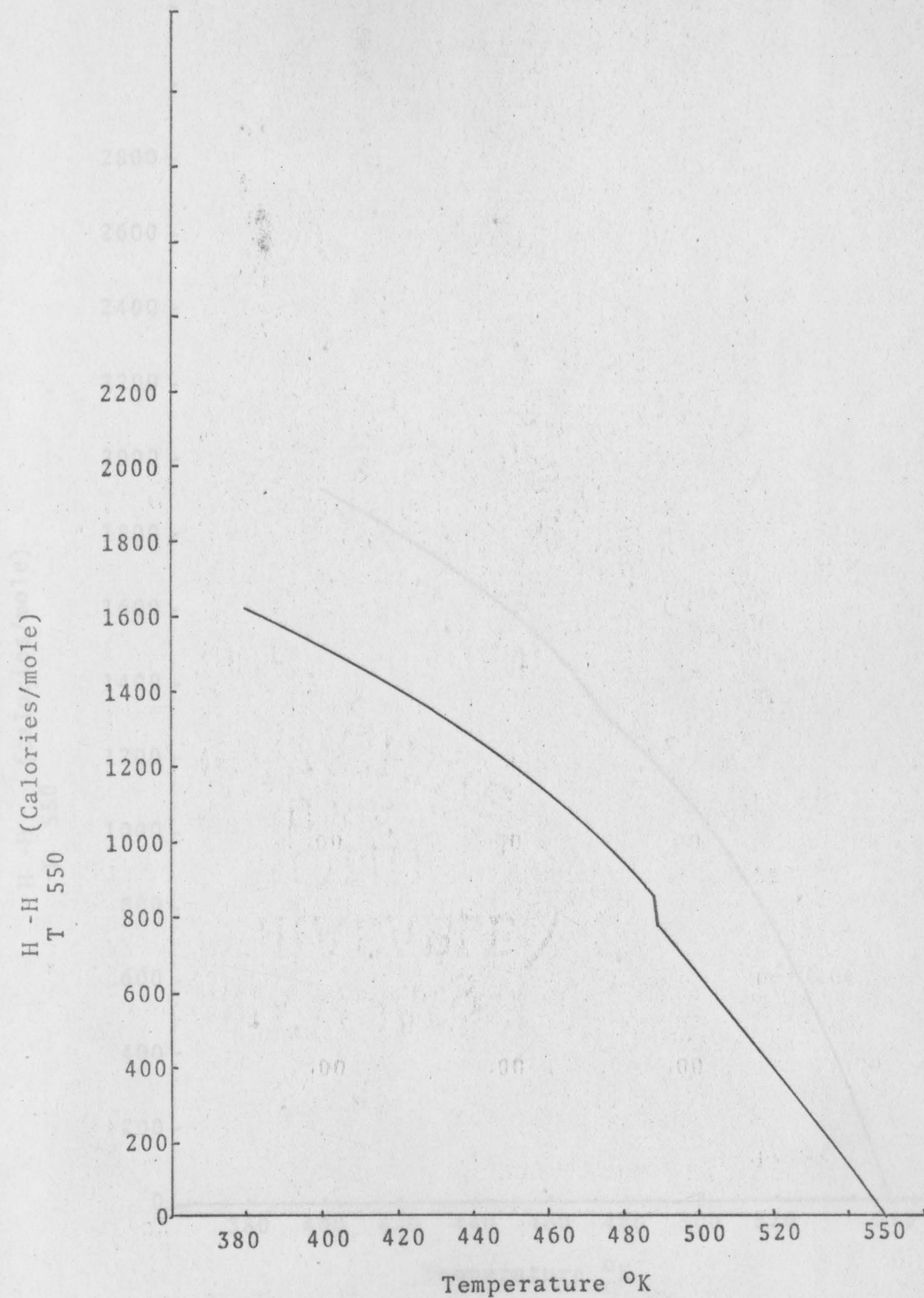


Fig. 35. Enthalpy as a function of temperature for Tl-Sn alloy (0.60 atom percent Sn)

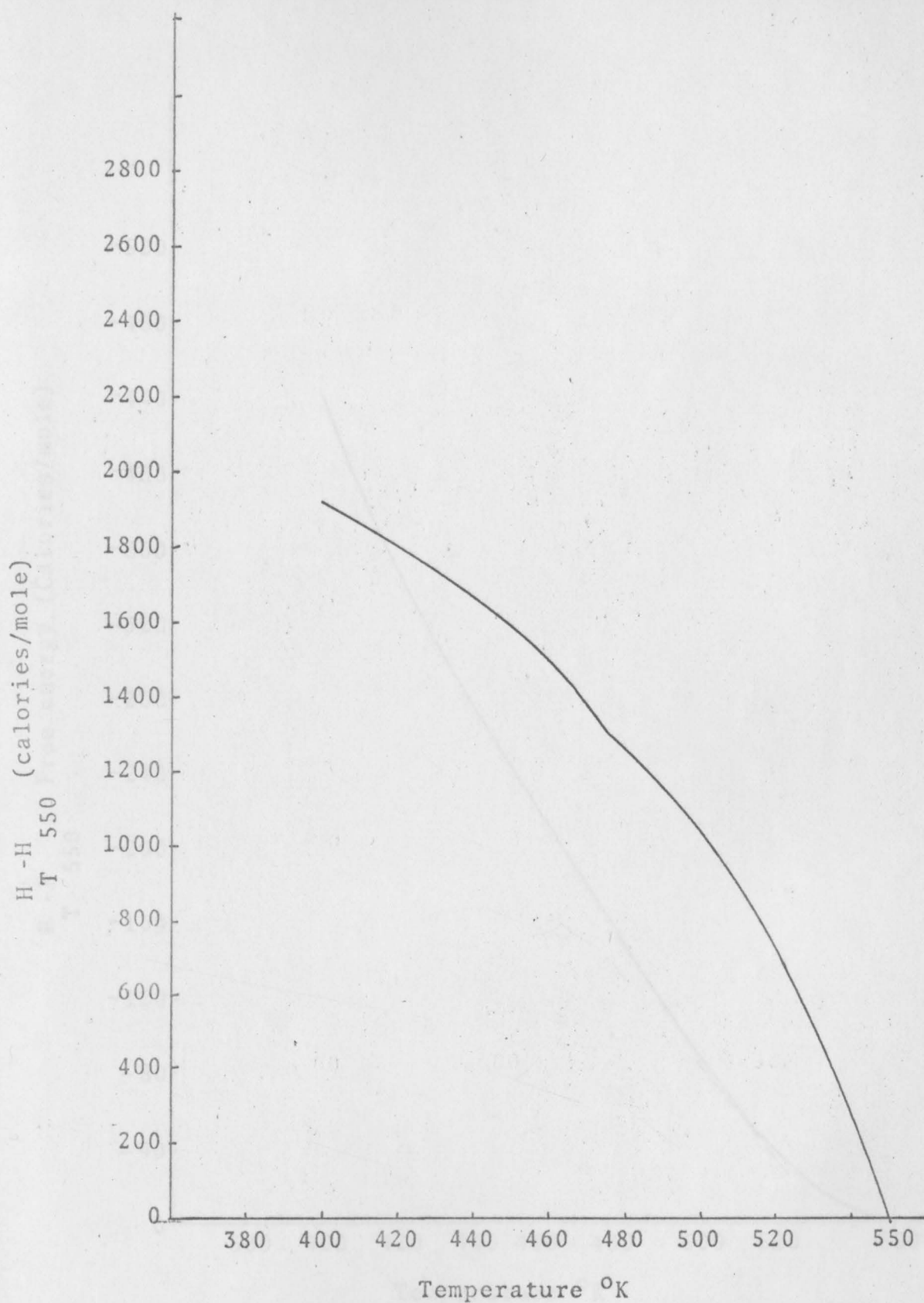


Fig.36. Enthalpy as a function of temperature for Tl-Sn alloy (1.0 atom percent Sn)

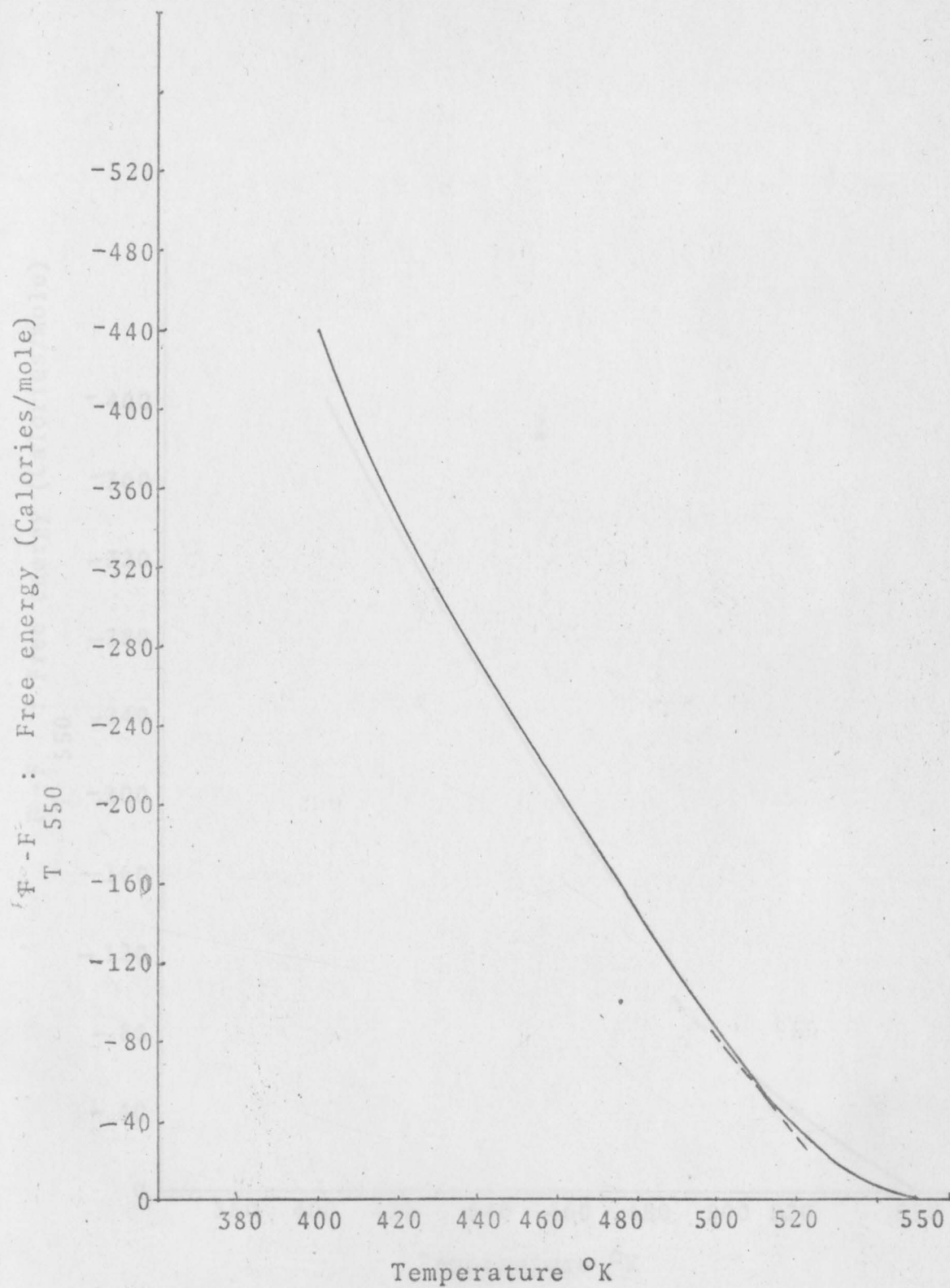


Fig. 37. Free energy as a function of temperature for pure thallium.

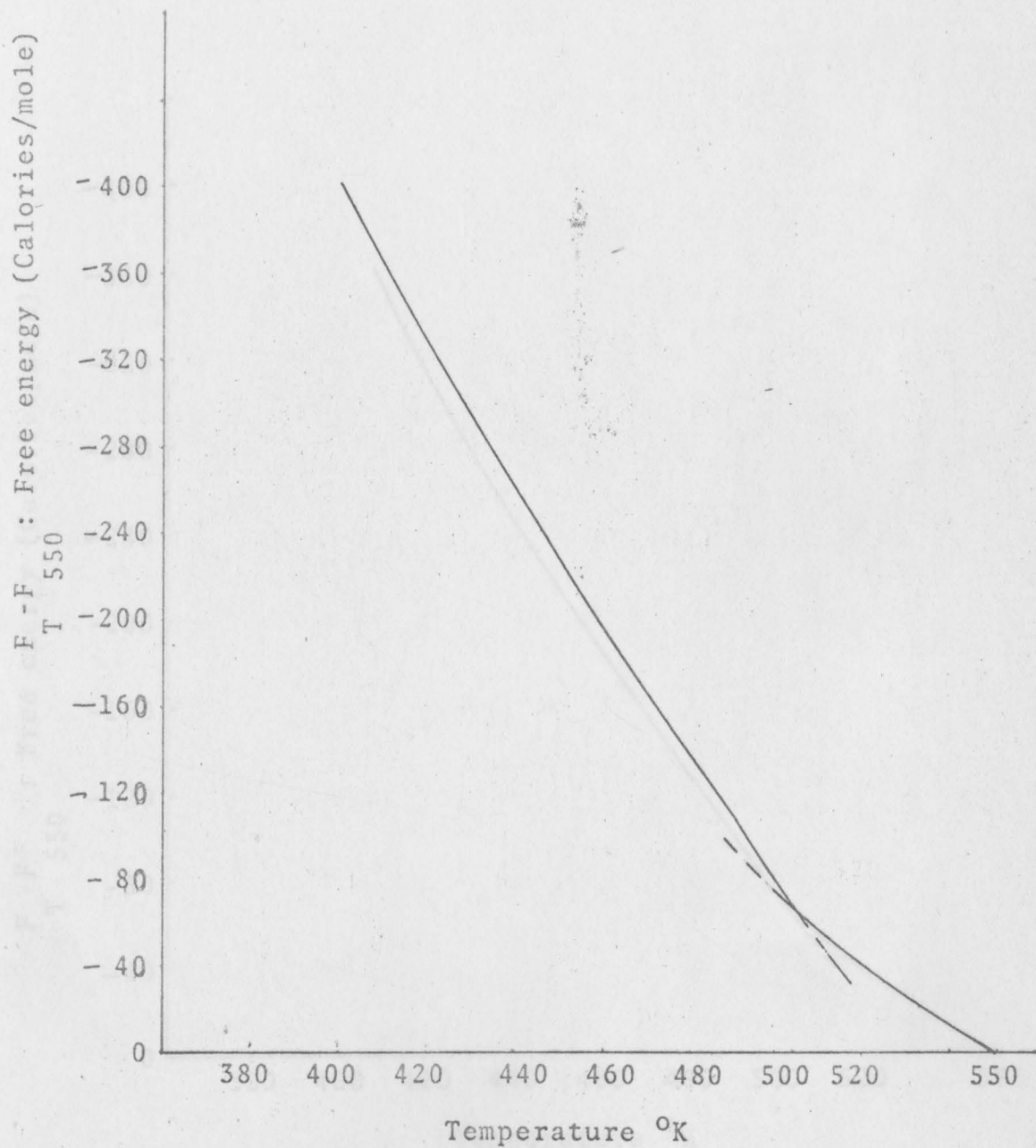


Fig. 38. Free energy as a function of temperature for Tl-Ag alloy (0.05 atom percent Ag)

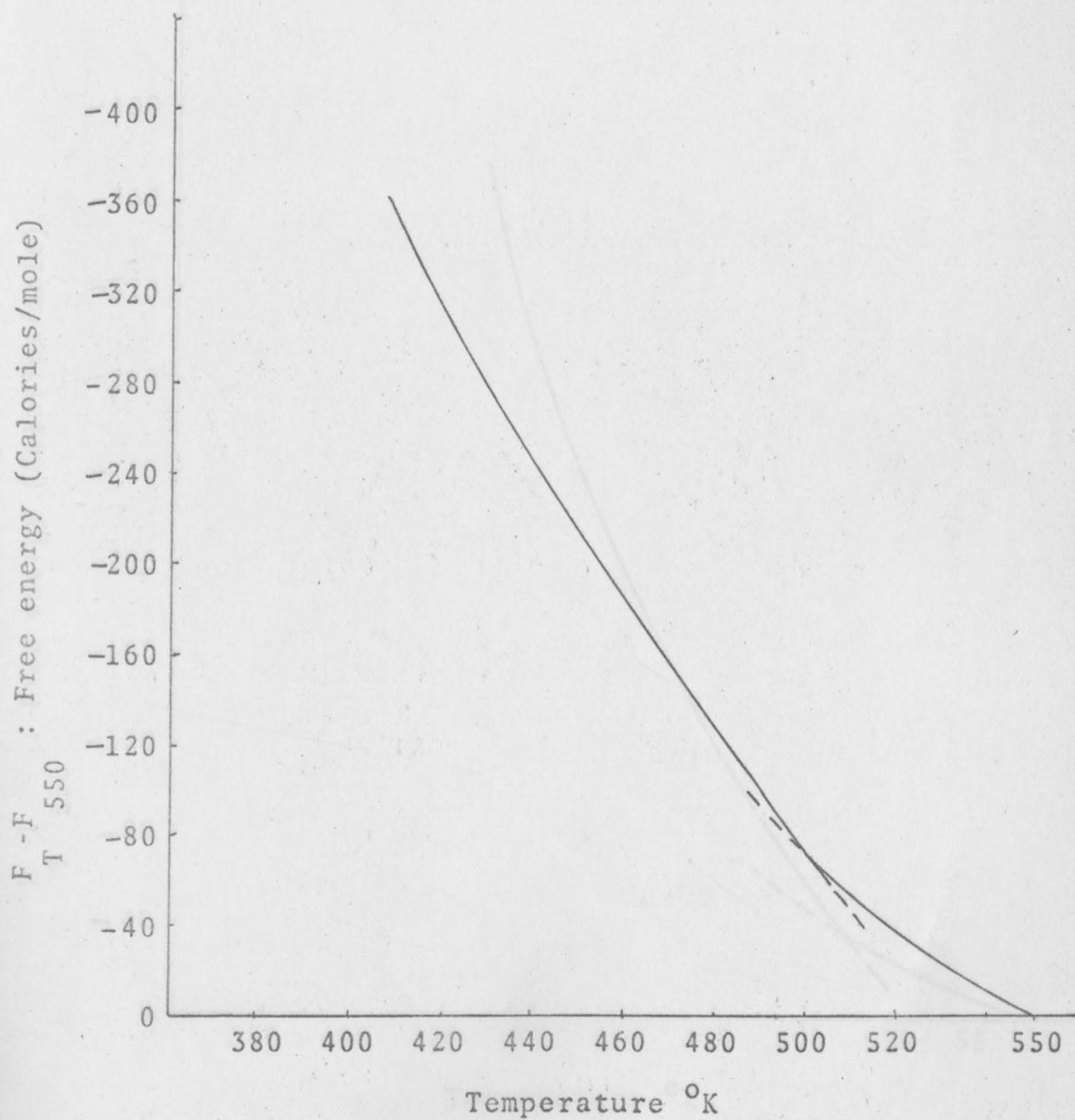


Fig. 39. Free energy as a function of temperature for Tl-Ag alloy (0.10 atom percent Ag)

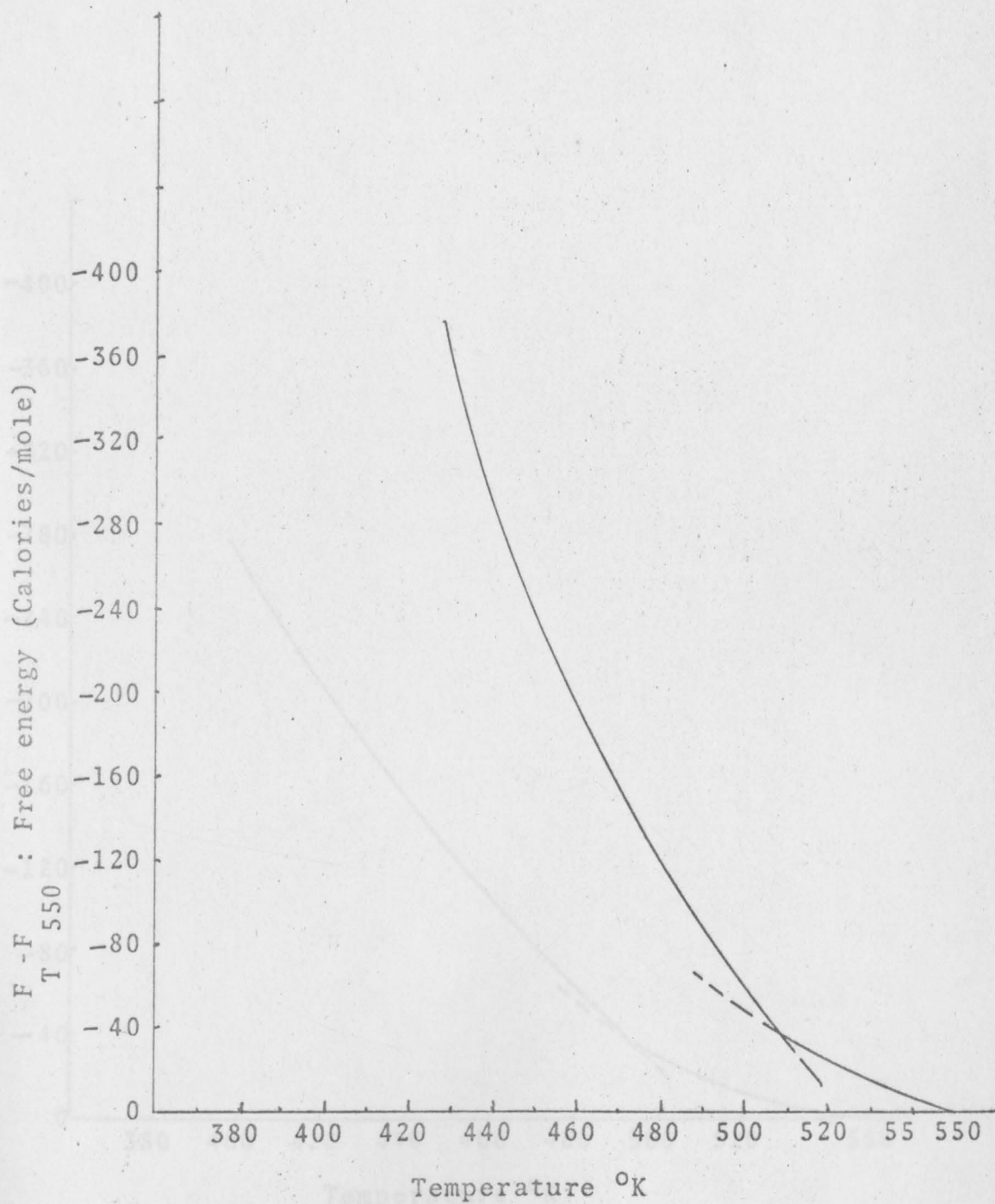


Fig. 40. Free energy as a function of temperature for Tl-Ag alloy (0.20 atom percent Ag)



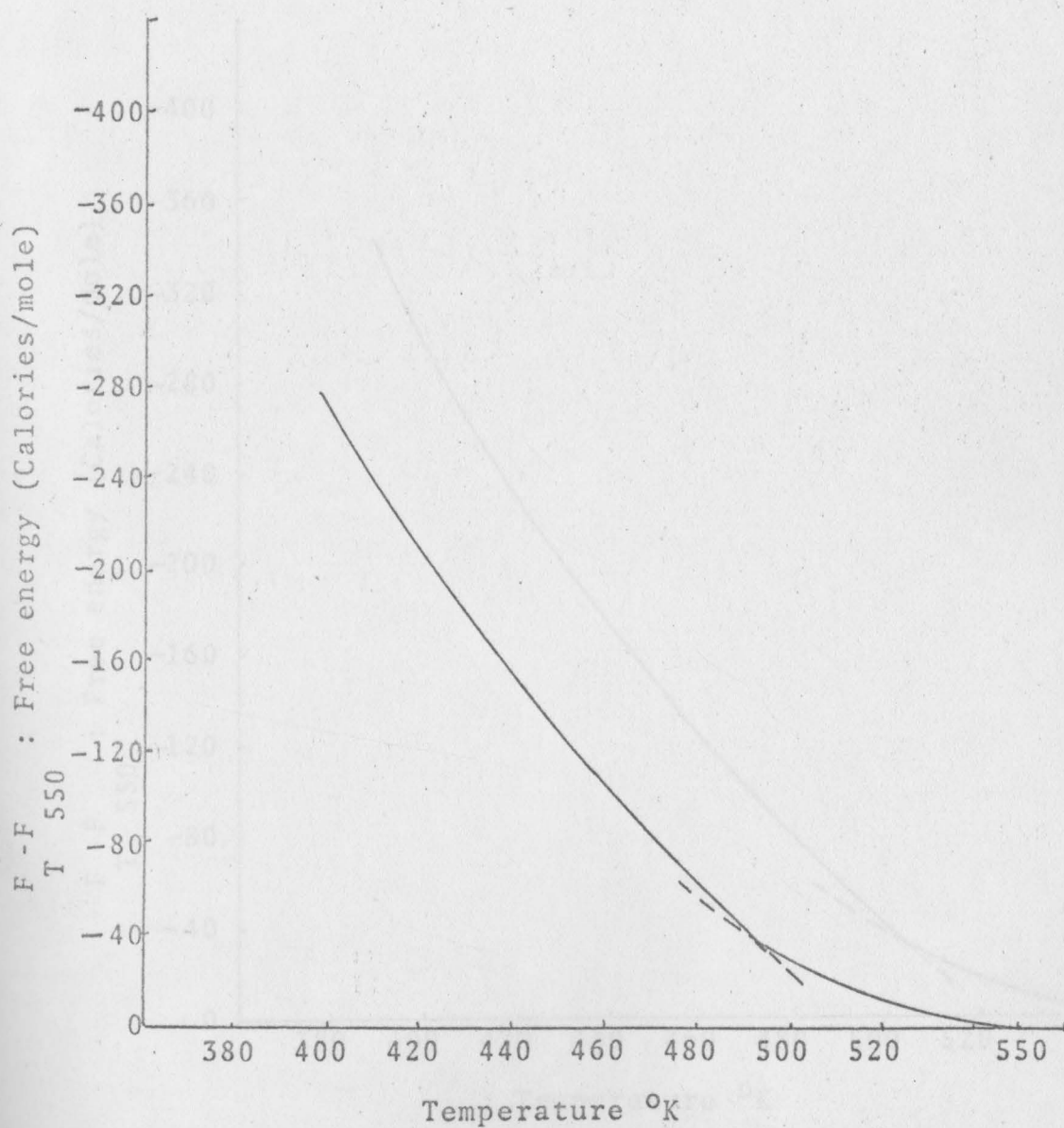


Fig. 41. Free energy as a function of temperature for Tl-Ag alloy (0.40 atom percent Ag)

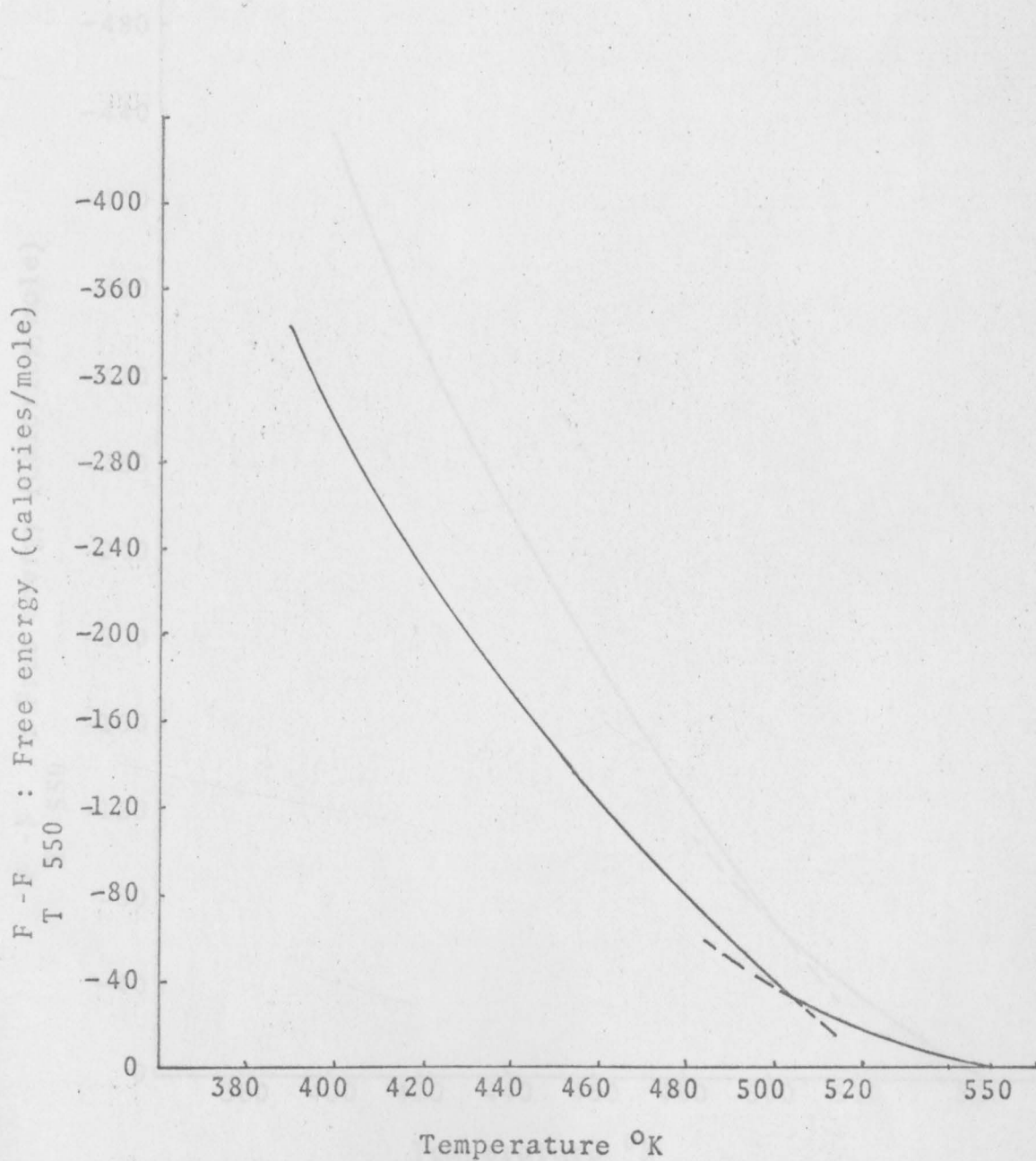


Fig. 42. Free energy as a function of temperature for Tl-Ag alloy (0.4971 atom percent Ag).

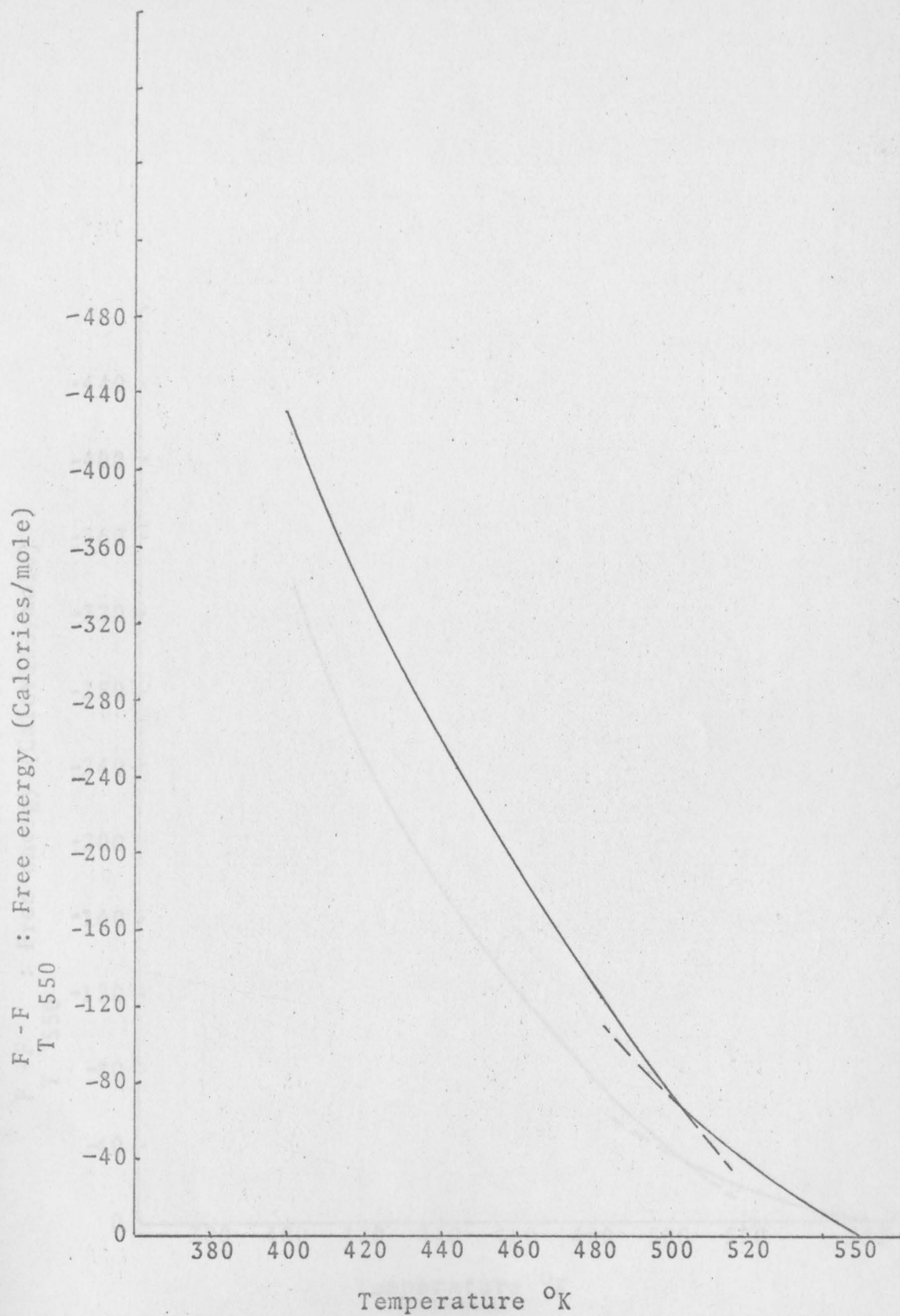


Fig. 43. Free energy as a function of temperature for Tl-Ag alloy (0.60 atom percent Ag)

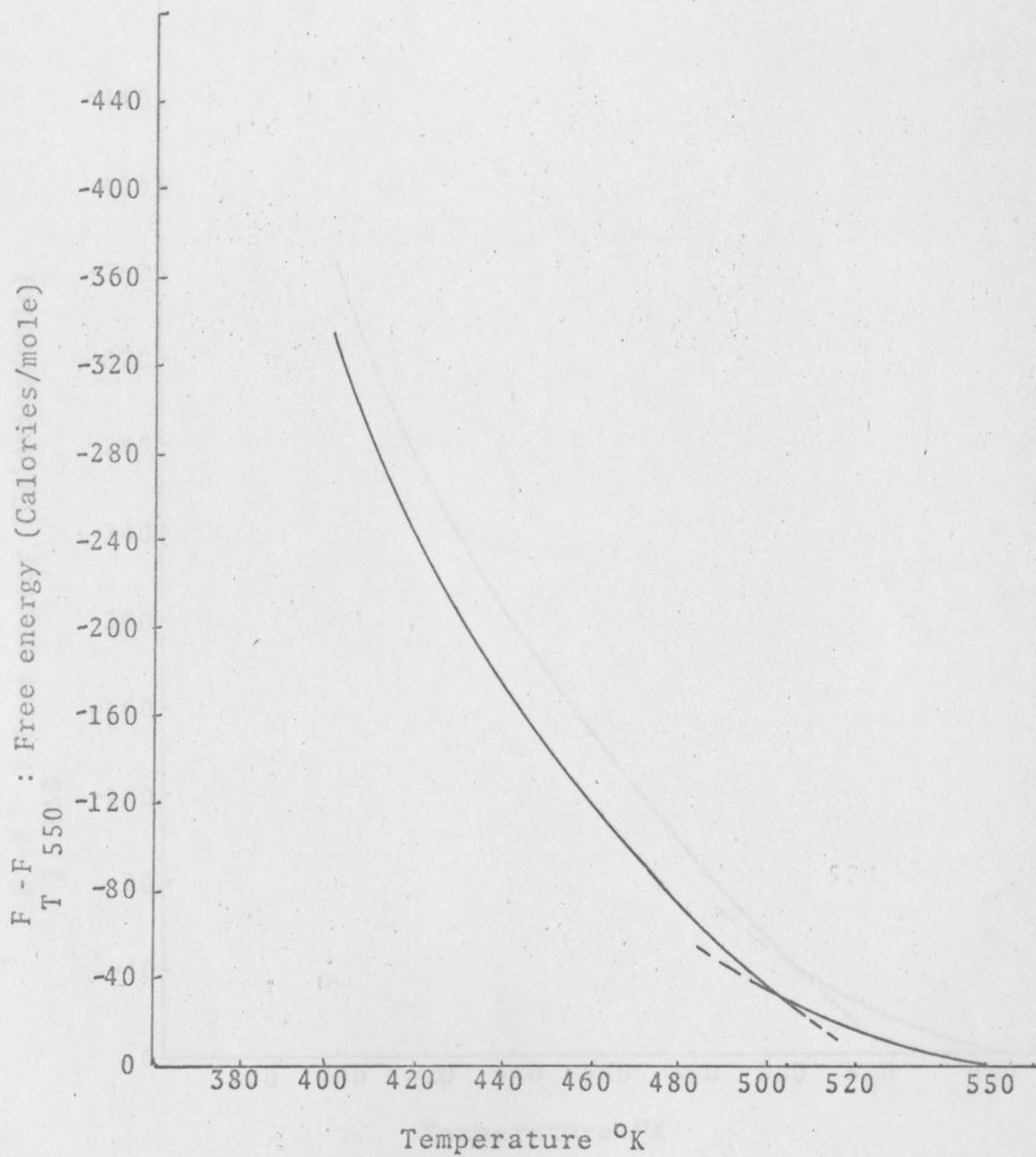


Fig. 44. Free energy as a function of temperature for Tl-Ag alloy (0.80 atom percent Ag)

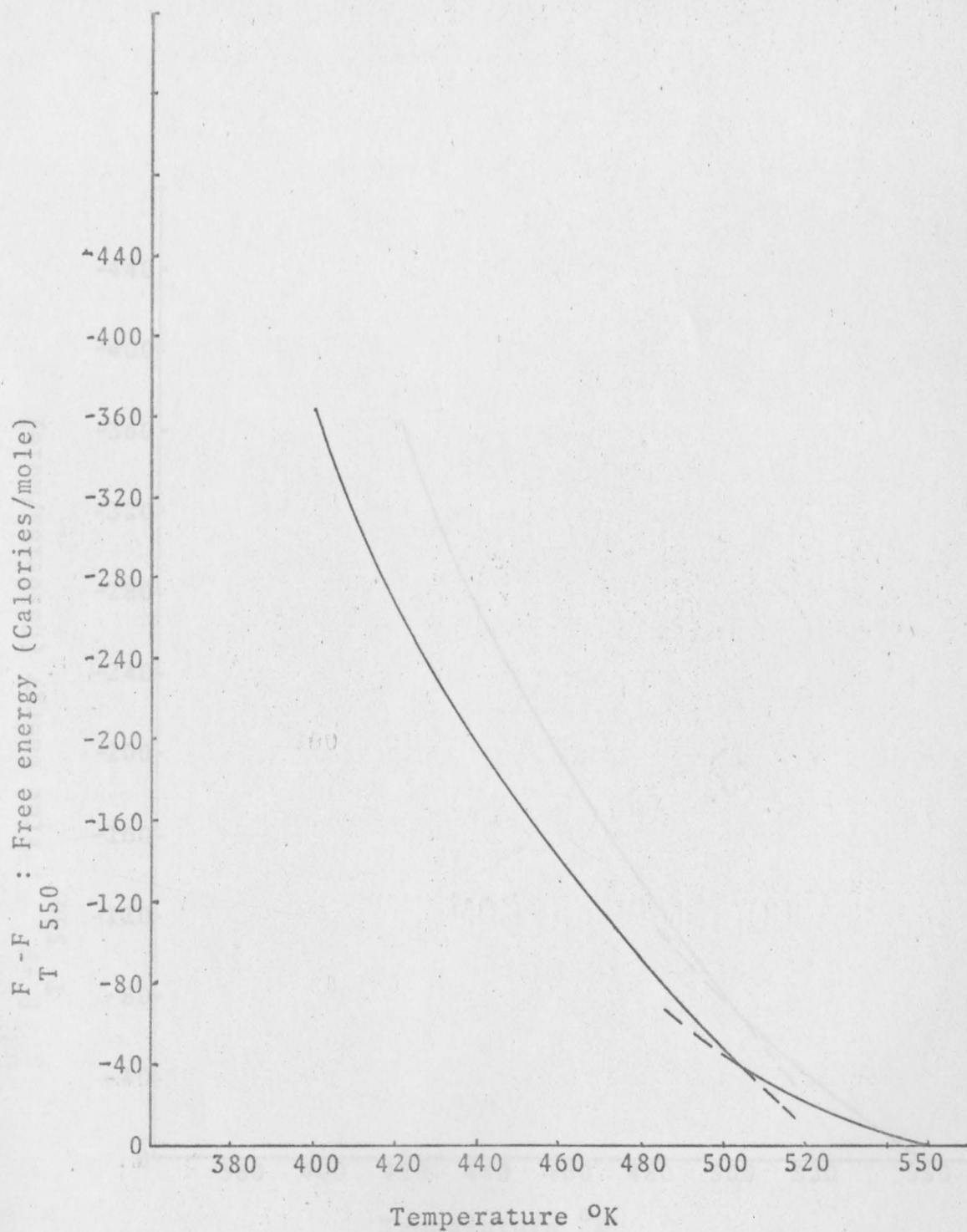


Fig. 45. Free energy as a function of temperature for Tl-Ag alloy (1.0 atom percent Ag)

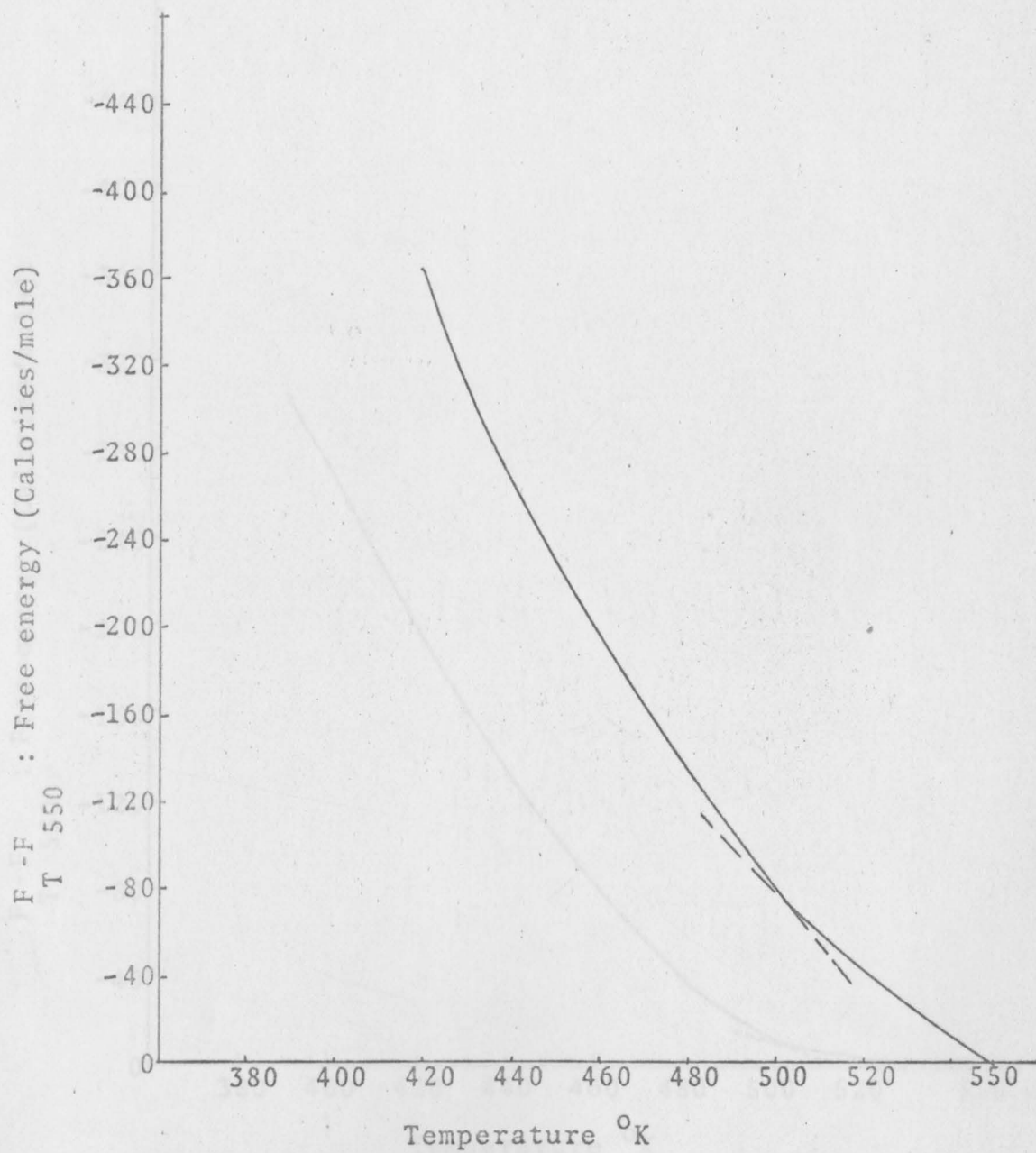


Fig.46. Free energy as a function of temperature for Tl-Ag alloy (2.0 atom percent Ag)

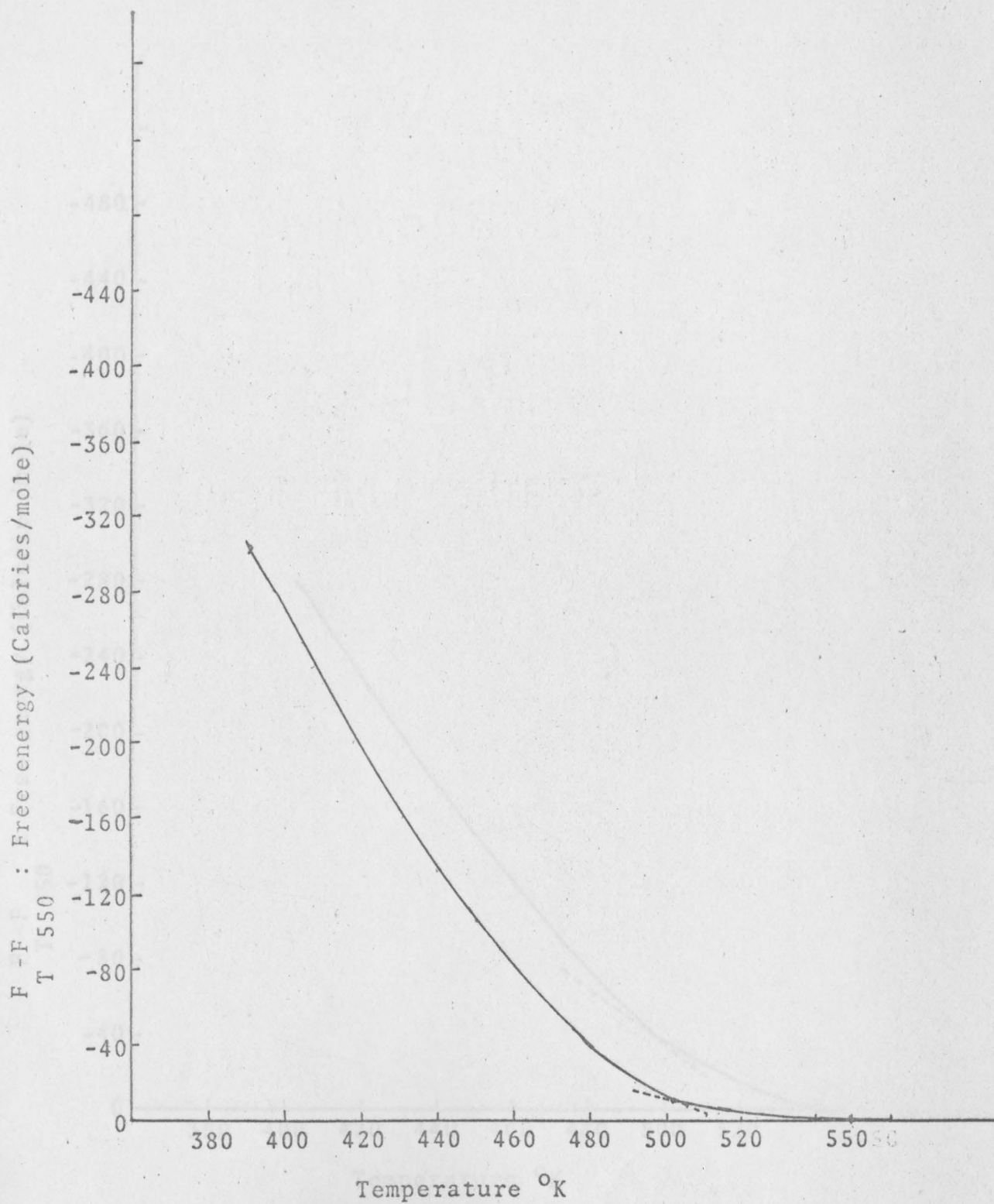


Fig. 47. Free energy as a function of temperature for Tl-Au alloy (0.05 atom percent Au)

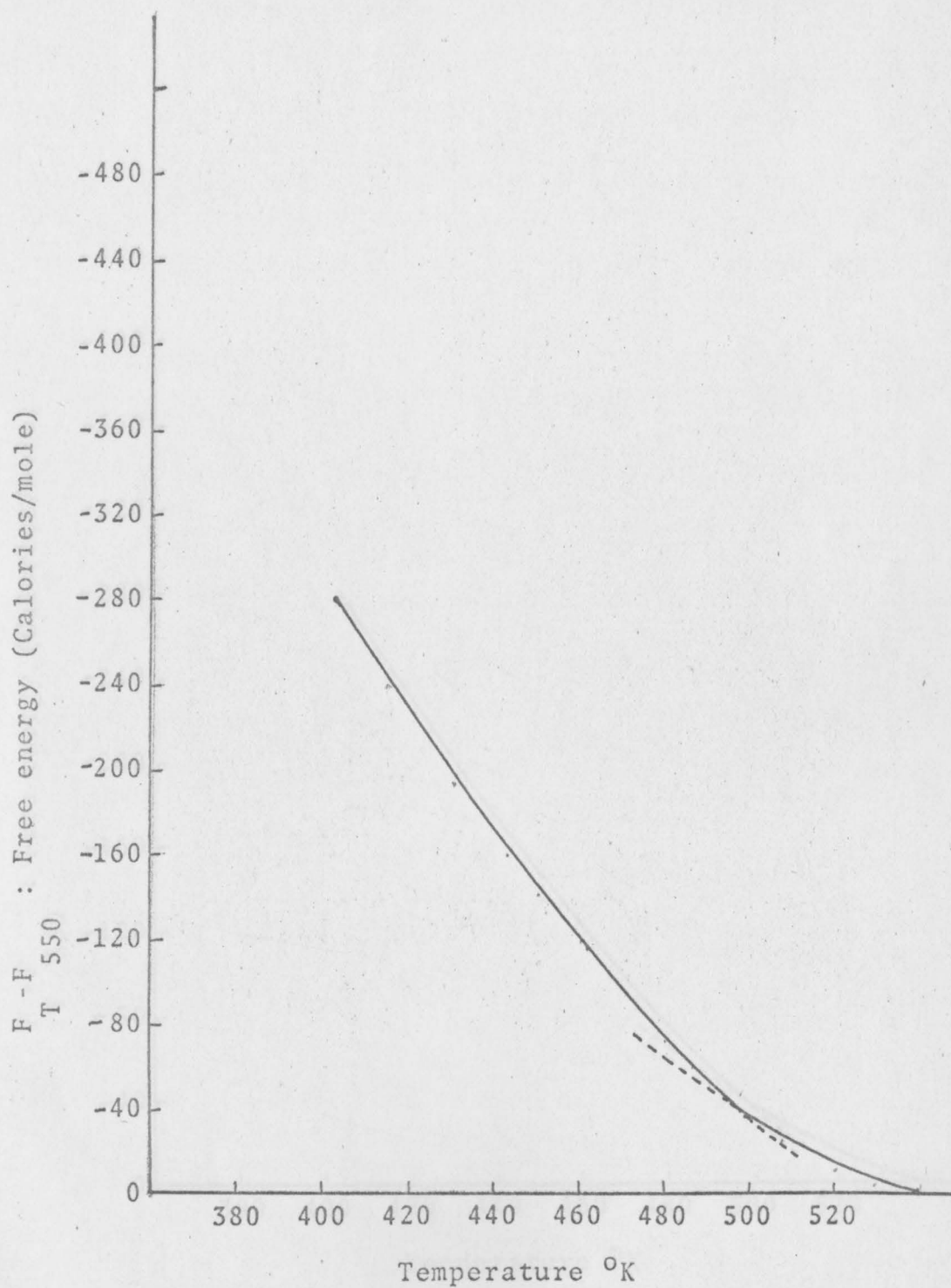


Fig. 48. Free energy as a function of temperature for Tl-Au alloy (0.10 atom percent Au)



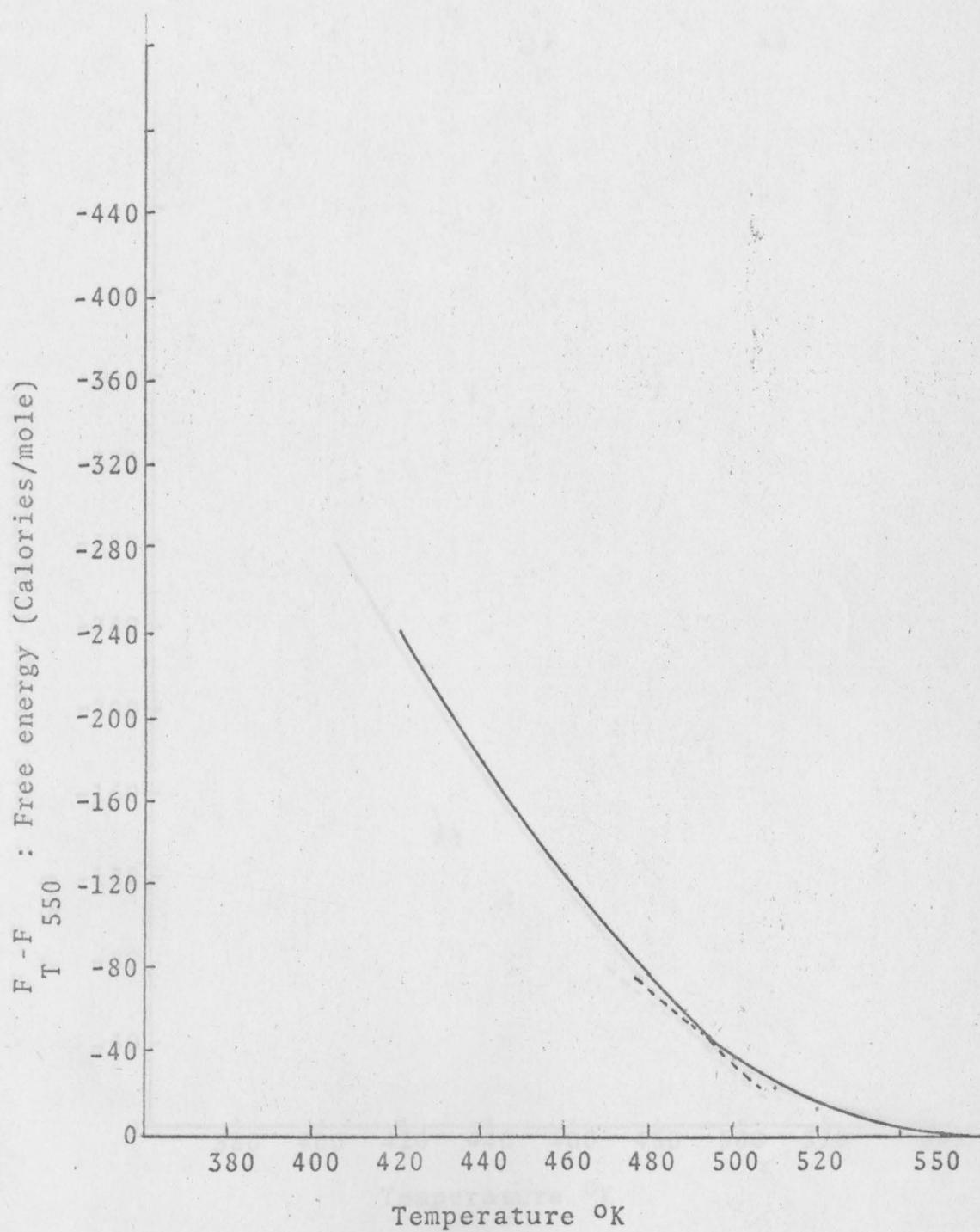


Fig. 49. Free energy as a function of temperature for Tl-Au alloy (0.20 atom percent Au)

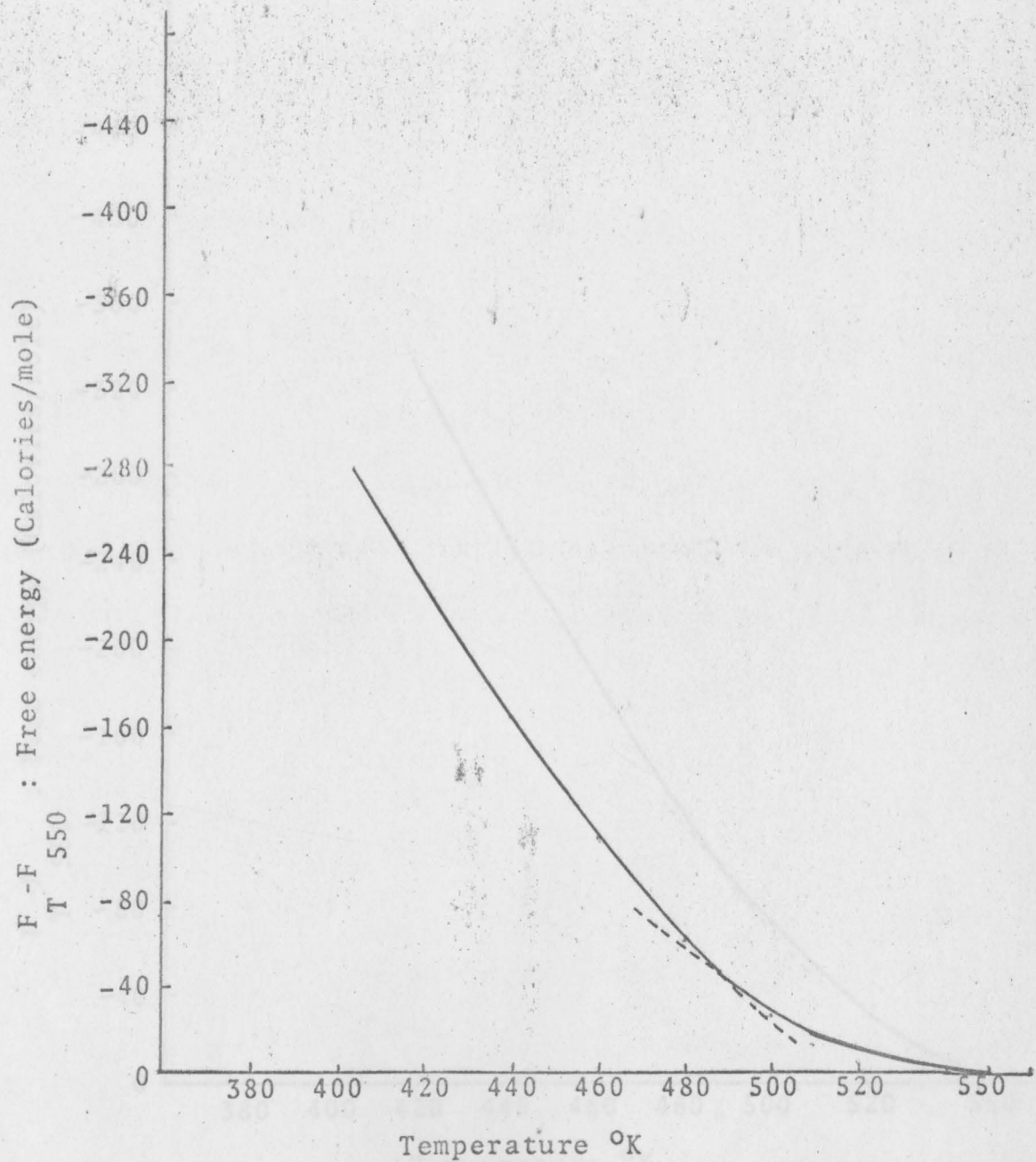


Fig. 50. Free energy as a function of temperature for Tl-Au alloy (0.40 atom percent Au)

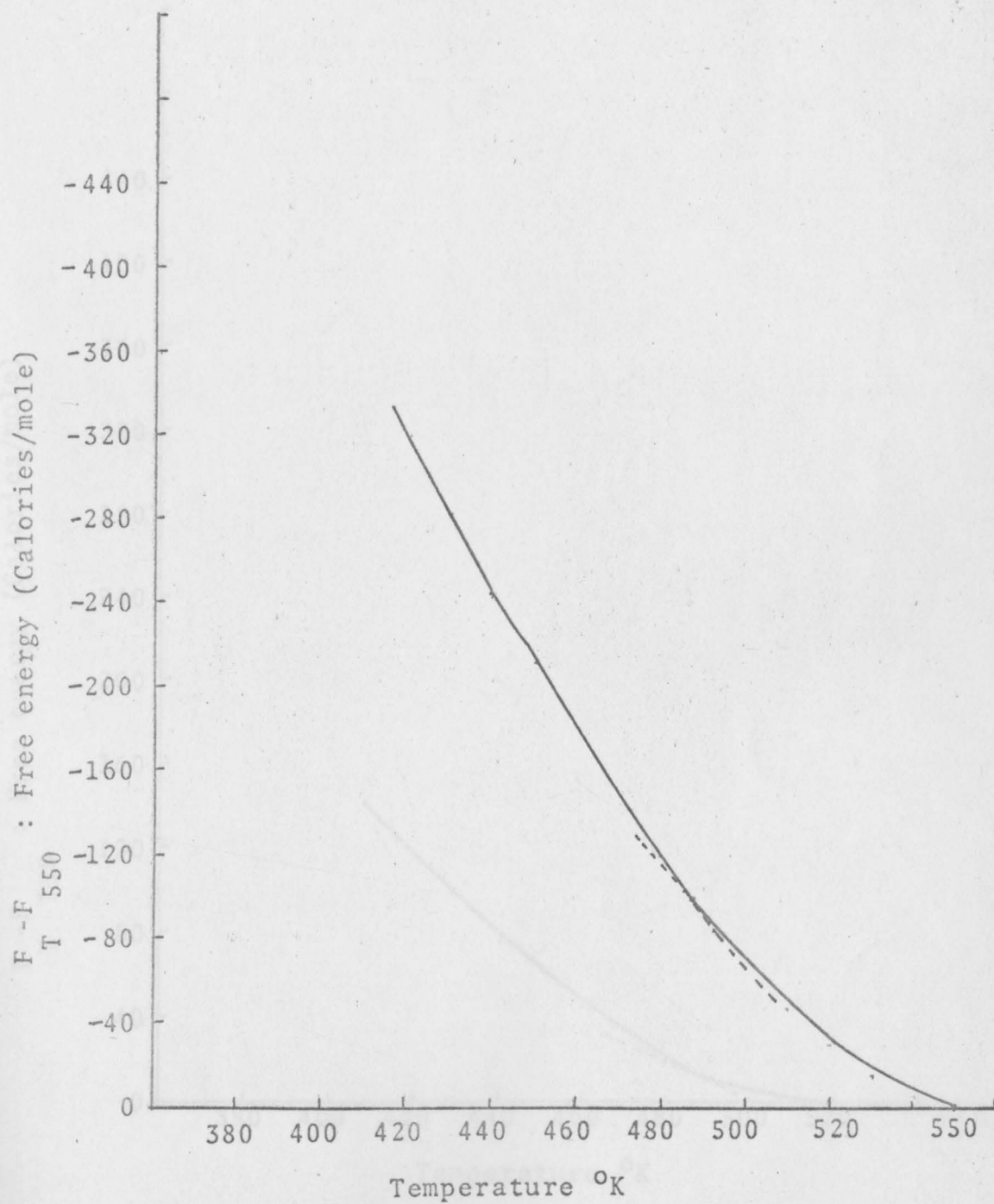


Fig. 51. Free energy as a function of temperature for Tl-Au alloy (0.60 atom percent Au)

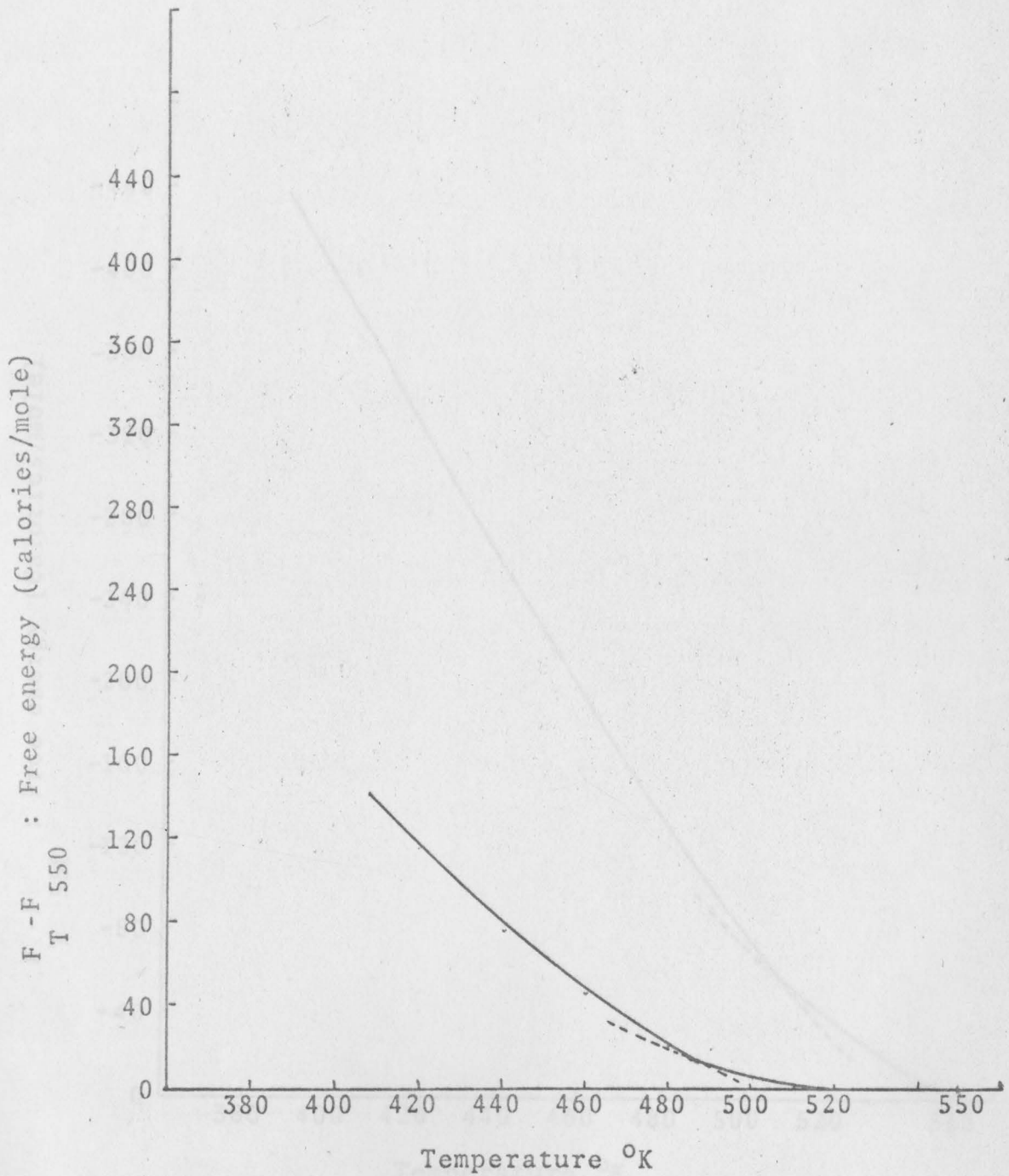


Fig. 52. Free energy as a function of temperature for Tl-Au alloy (1.0 atom percent Au)

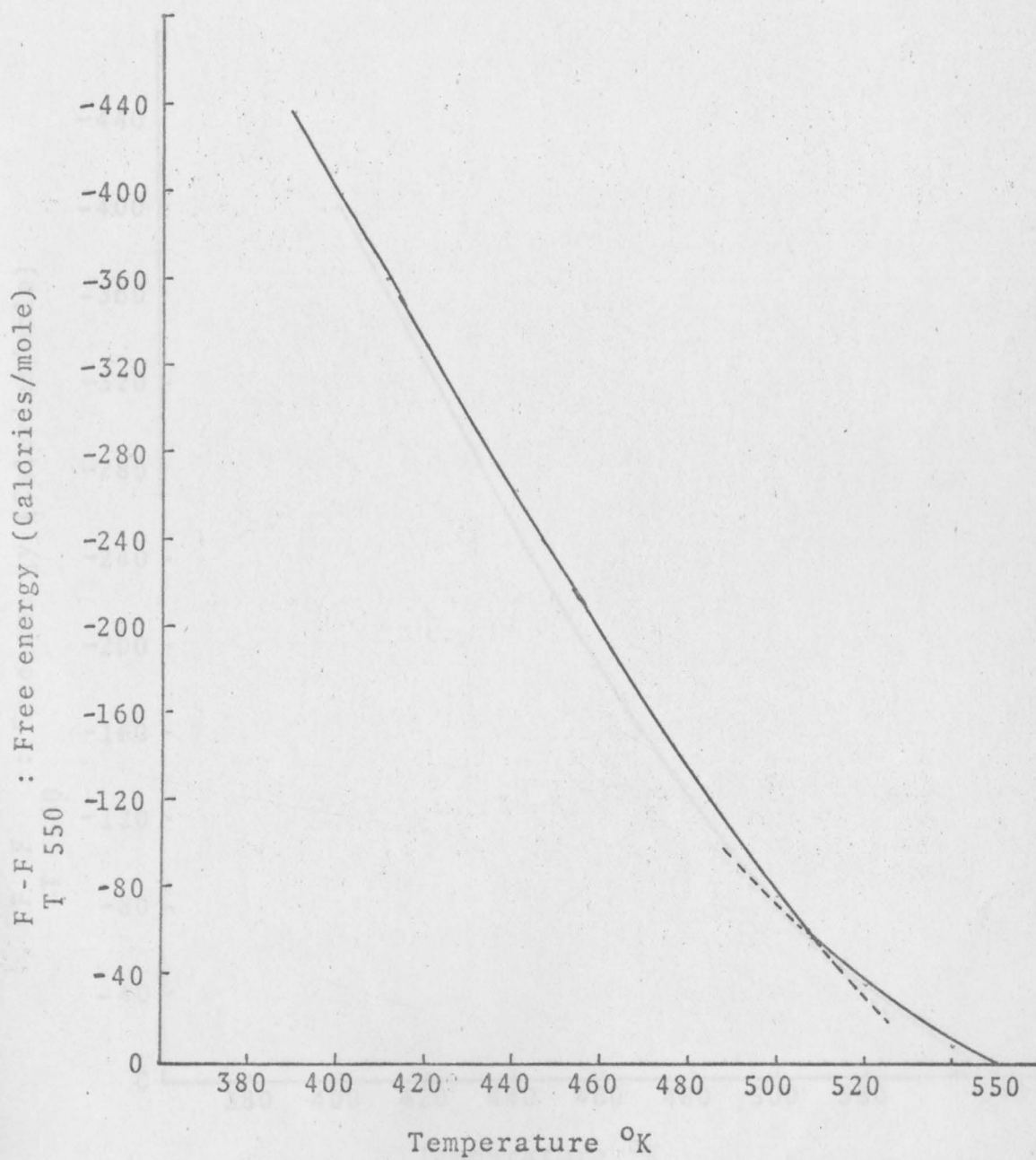


Fig. 53. Free energy as a function of temperature for Tl-Zn alloy (0.10 atom percent Zn)

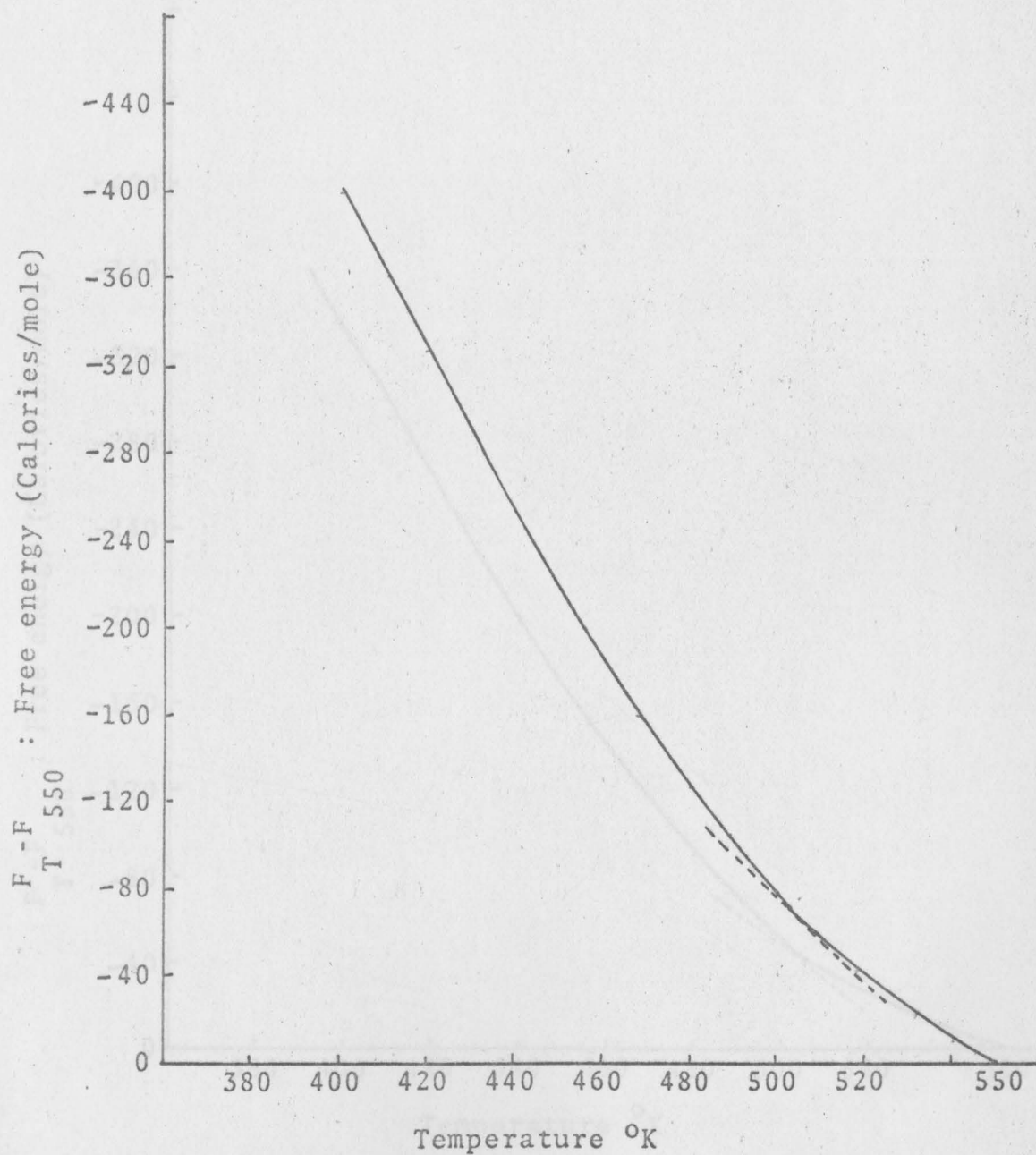


Fig.54. Free energy as a function of temperature for Tl-Zn alloy (0.20 atom percent Zn)

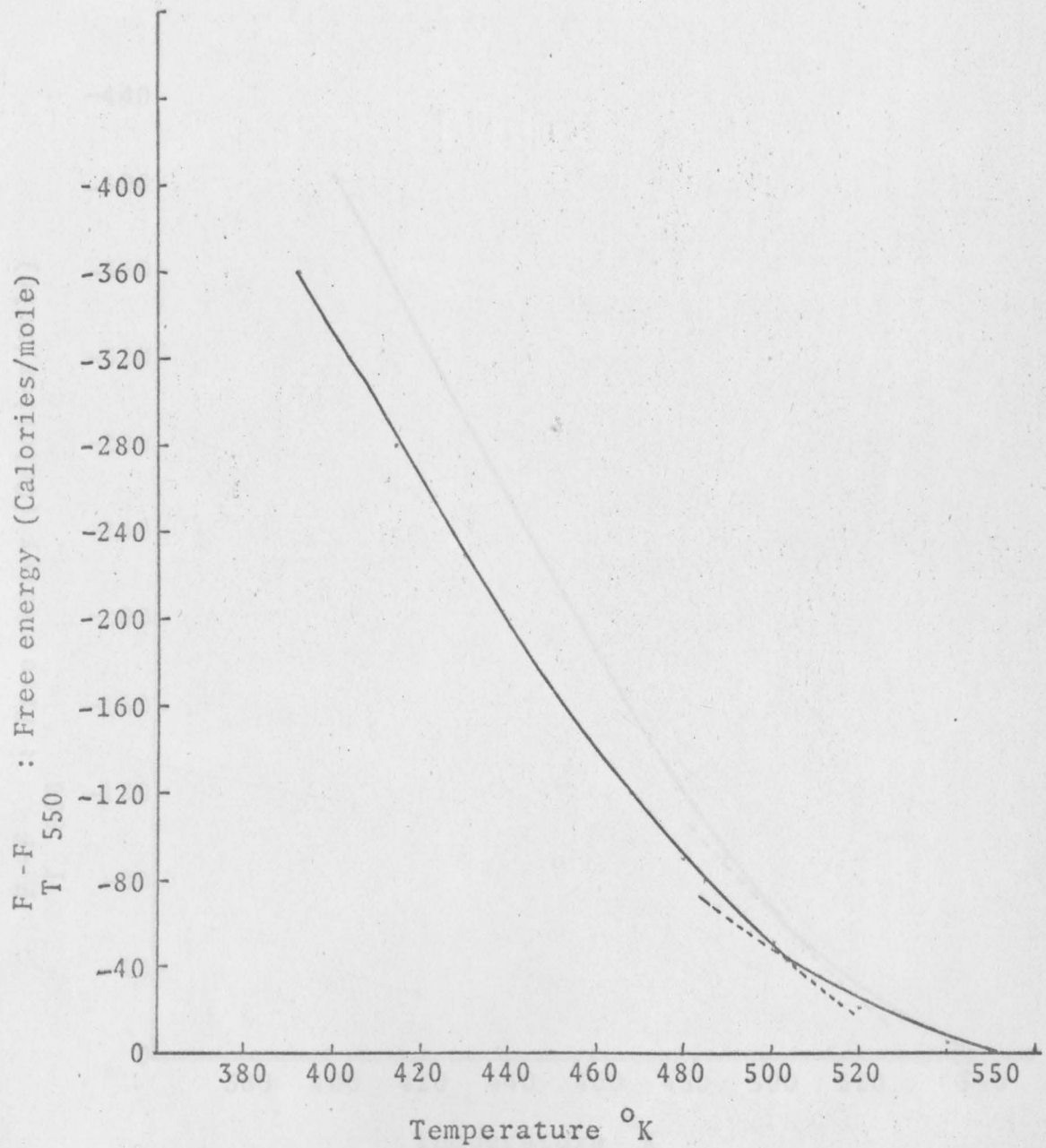


Fig.55. Free energy as a function of temperature for Tl-Zn alloy (0.40 atom percent Zn)

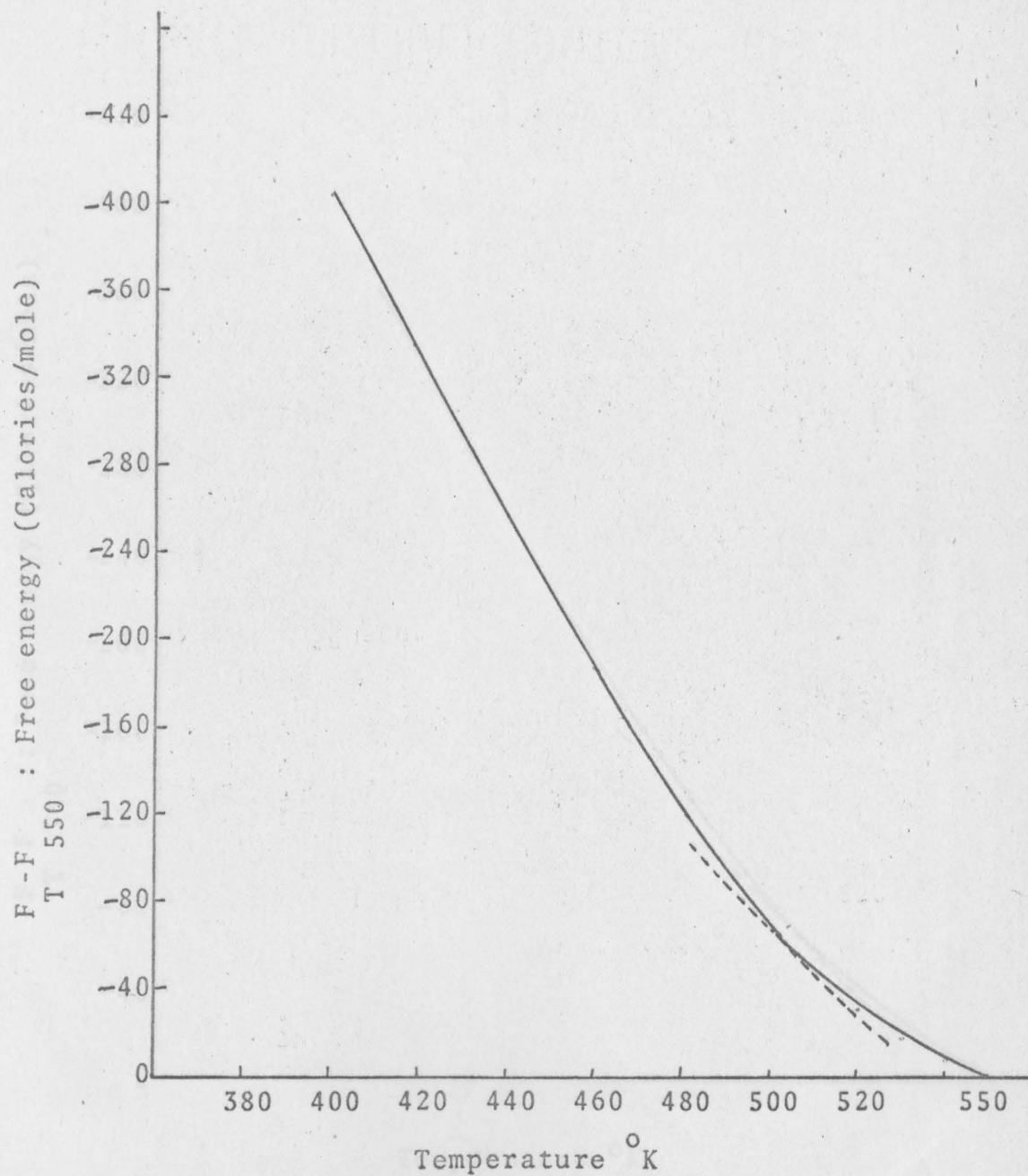


Fig. 56. Free energy as a function of temperature for Ti-Zn(0.60 atom percent Zn)



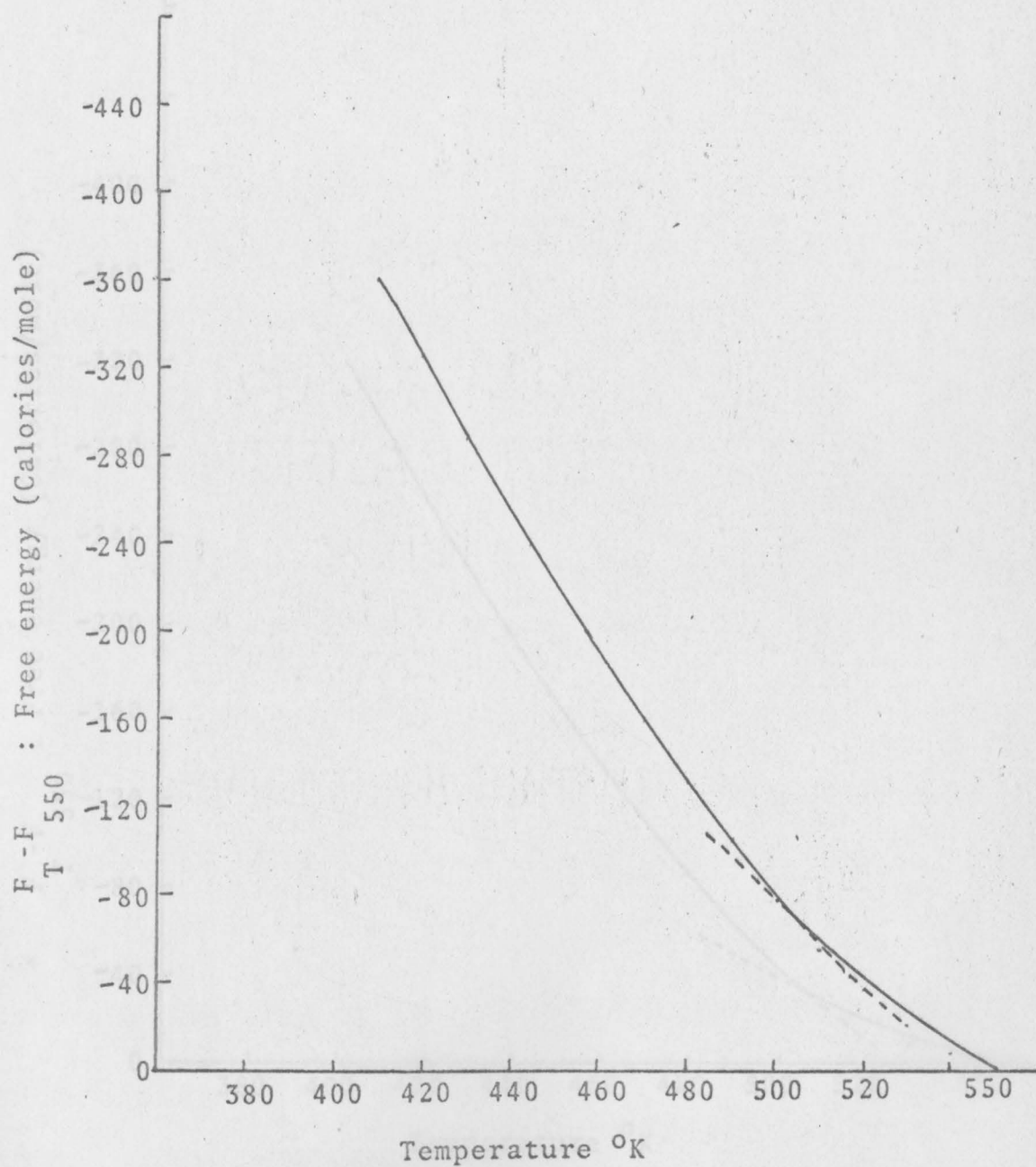


Fig. 57. Free energy as a function of temperature for Tl-Zn (0.80 atom percent Zn)

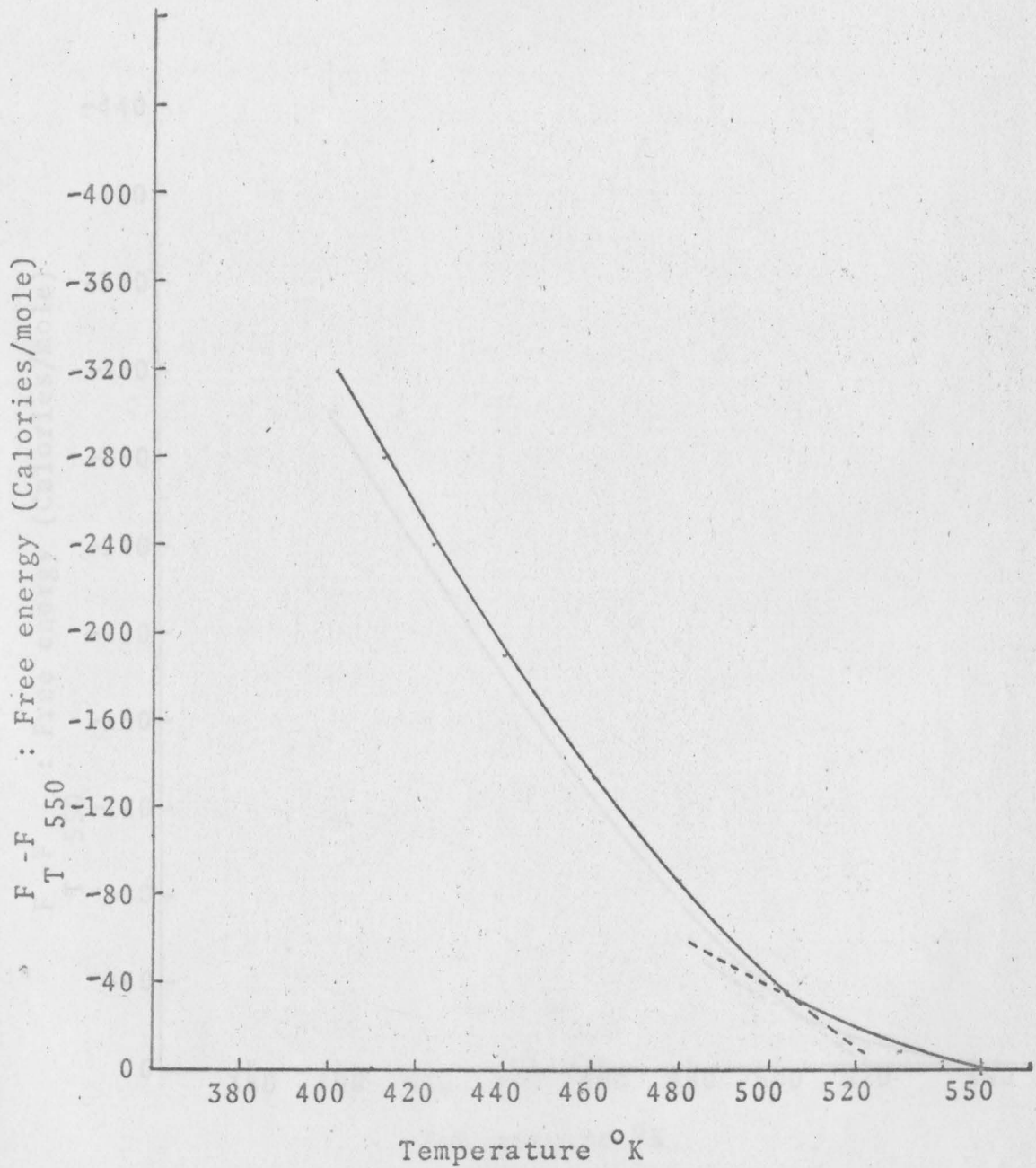


Fig. 58. Free energy as a function of temperature for Tl-Zn alloy (1.0 atom percent Zn)

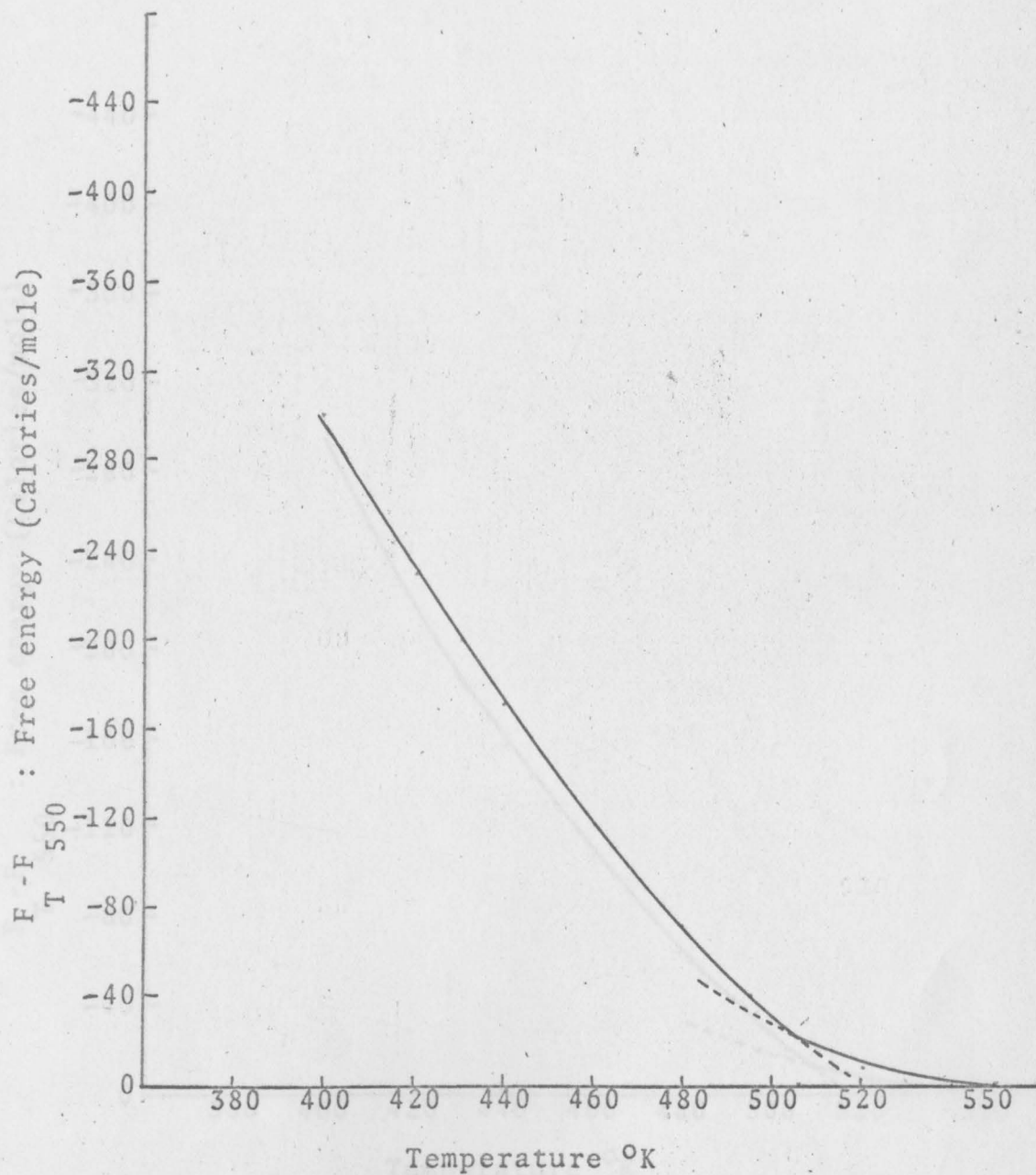


Fig. 59. Free energy as a function of temperature for Tl-Zn alloy (1.20 atom percent Zn)

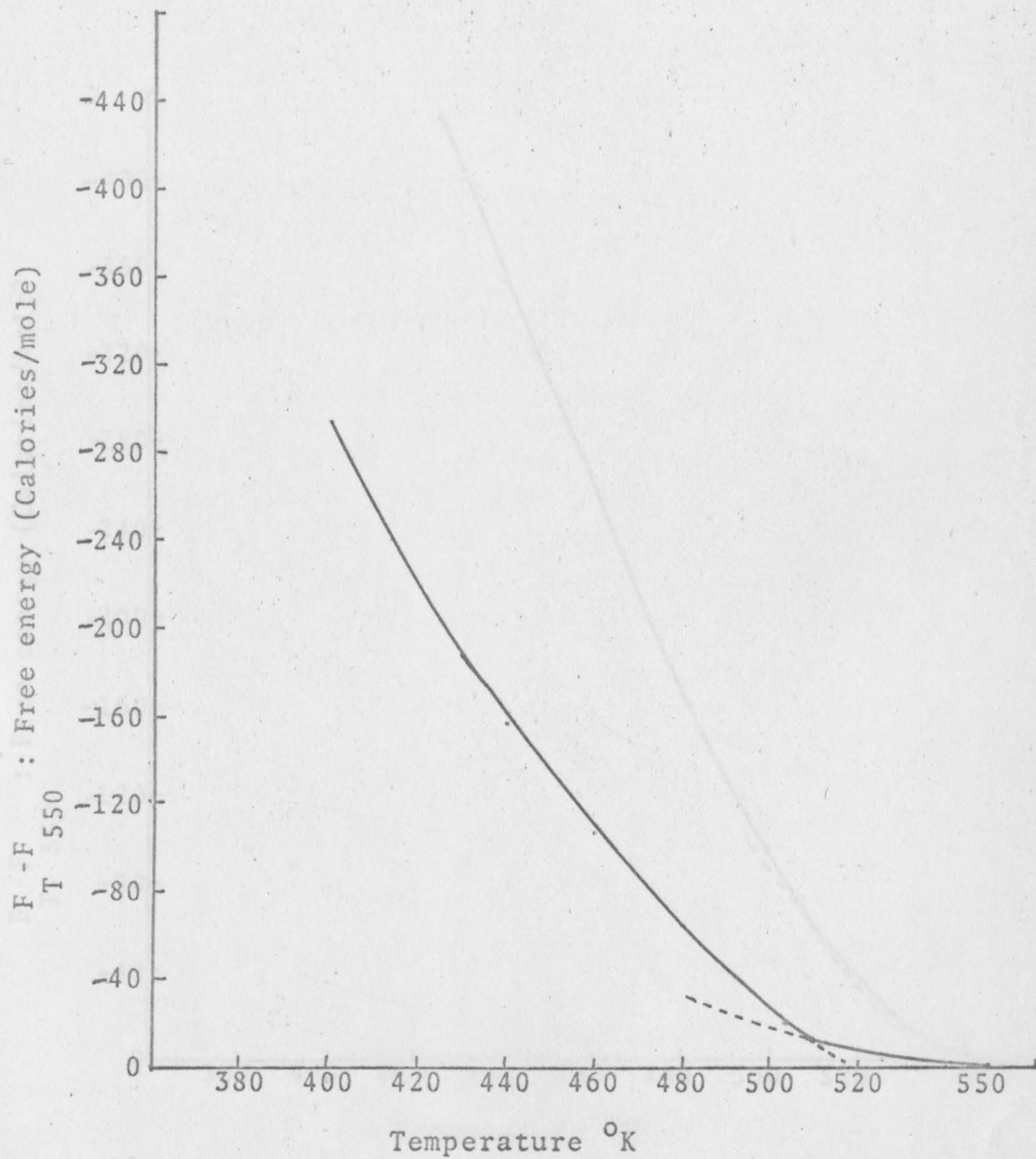


Fig. 60. Free energy as a function of temperature for Tl-Cd alloy (0.044 atom percent Cd)

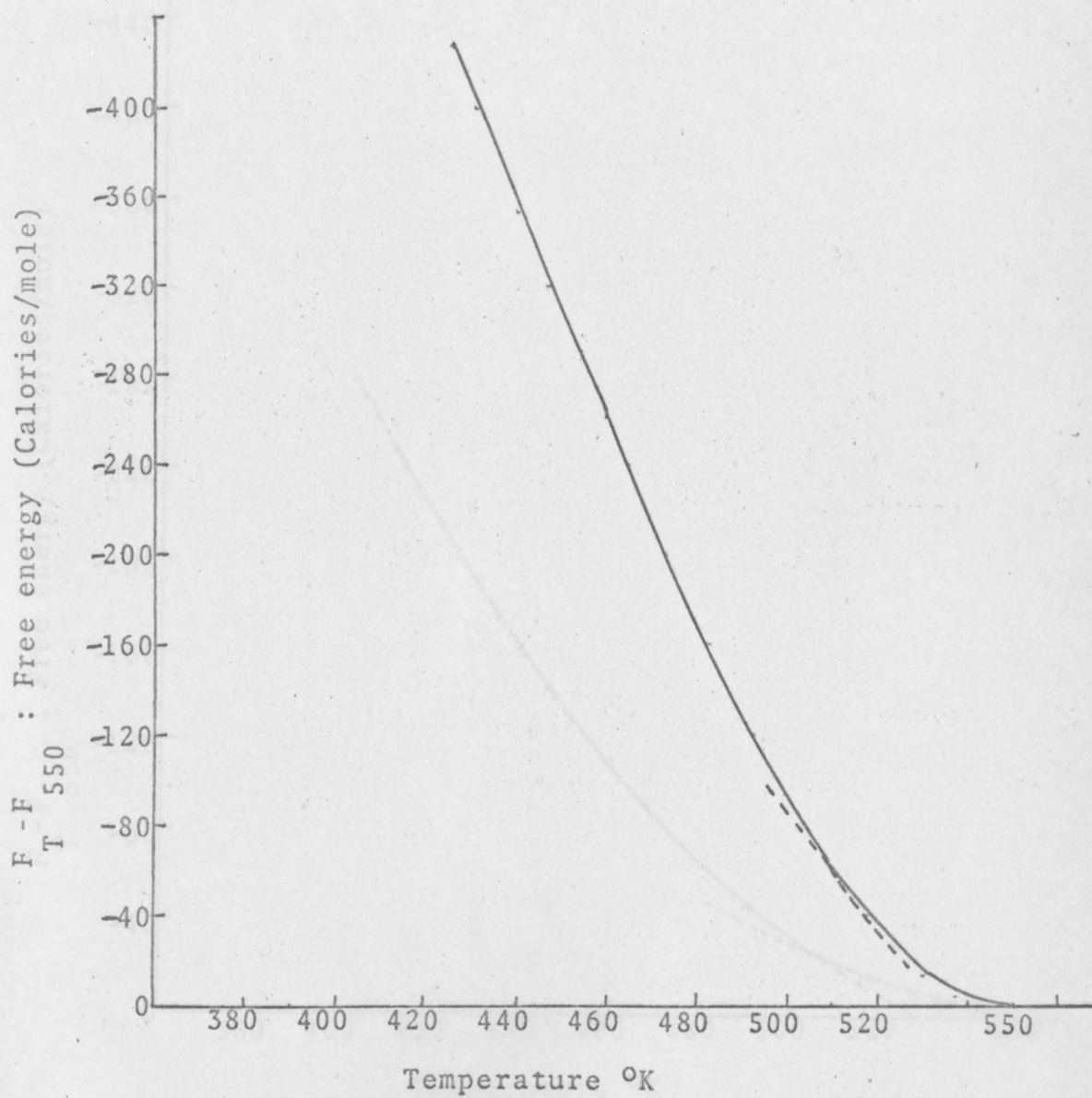


Fig. 61. Free energy as a function of temperature for Tl-Cd alloy (0.18 atom percent Cd)

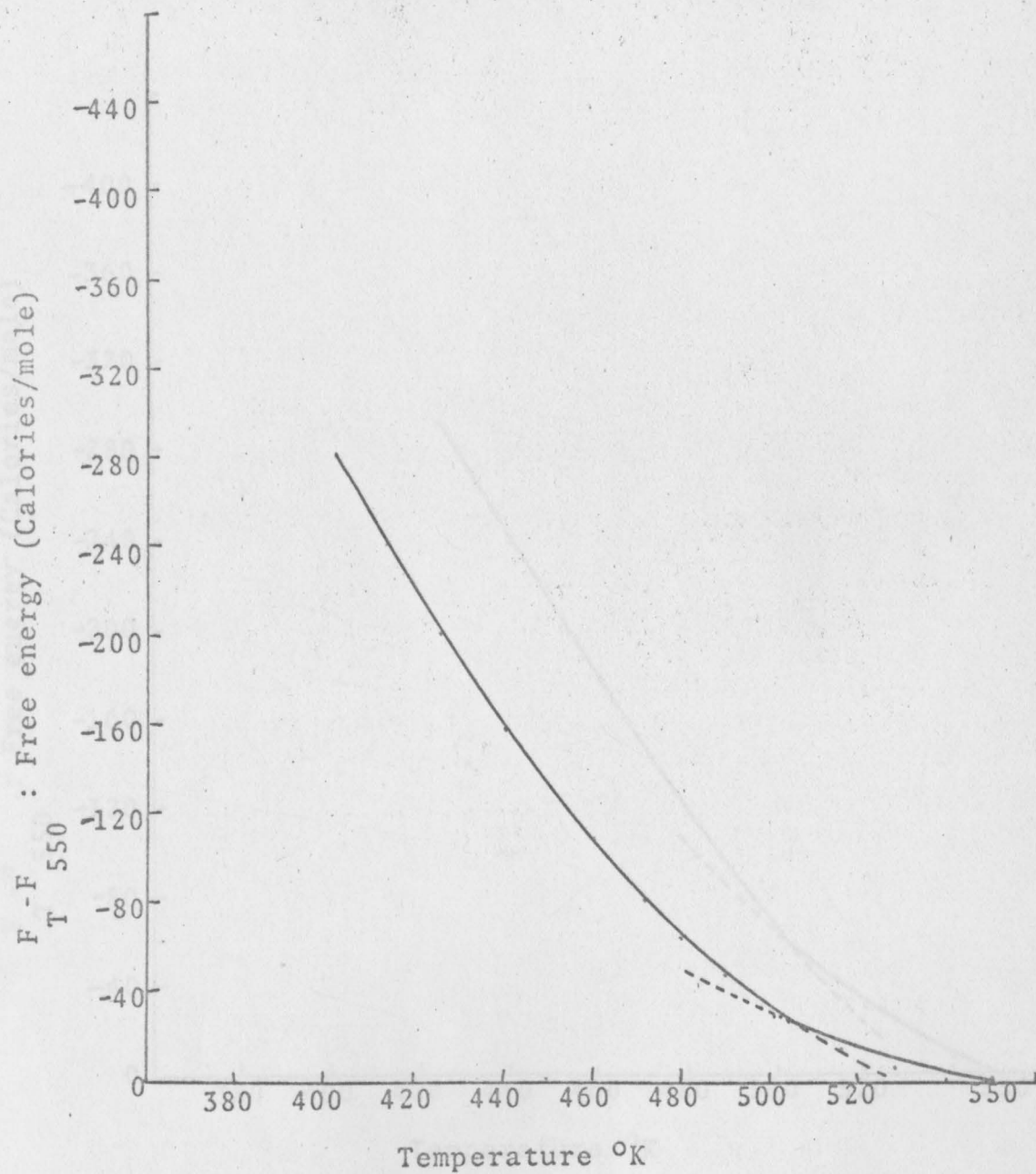


Fig. 62. Free energy as a function of temperature for Tl-Cd alloy (0.44 atom percent Cd)

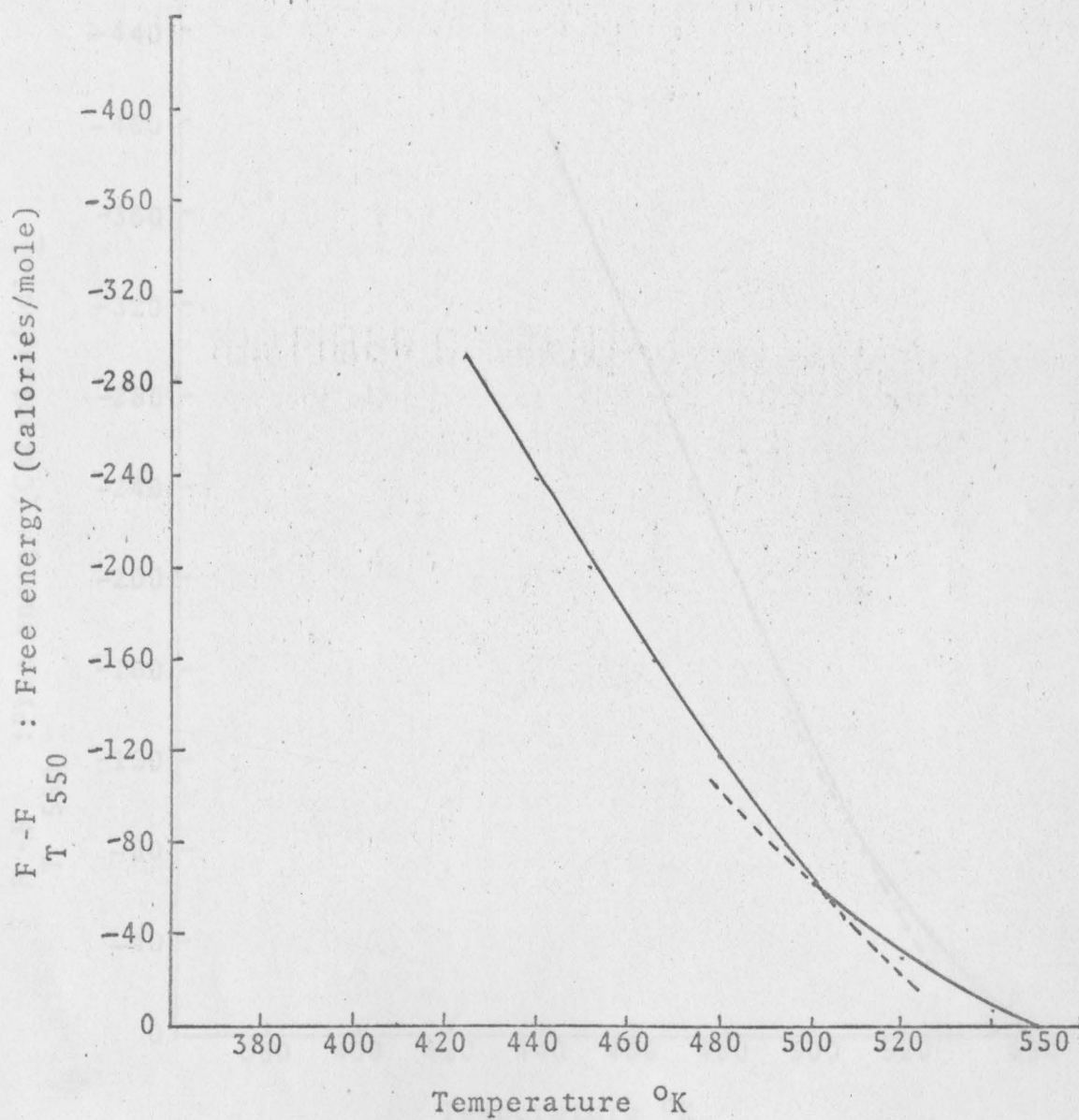


Fig.63. Free energy as a function of temperature for Tl-Cd alloy (0.50 atom percent Cd)

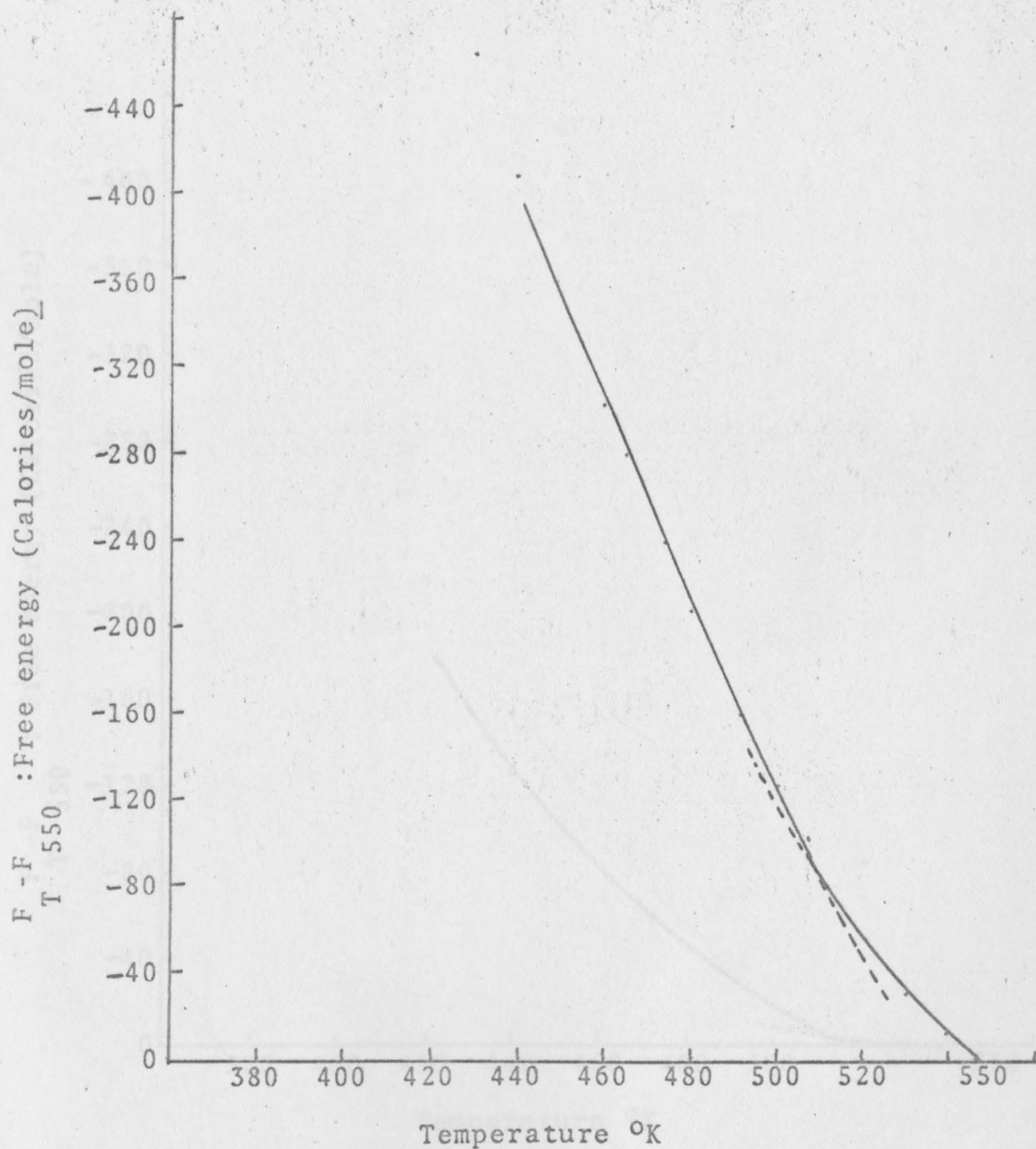


Fig. 64. Free energy as a function of temperature for Tl-Cd alloy (0.60 atom percent Cd)



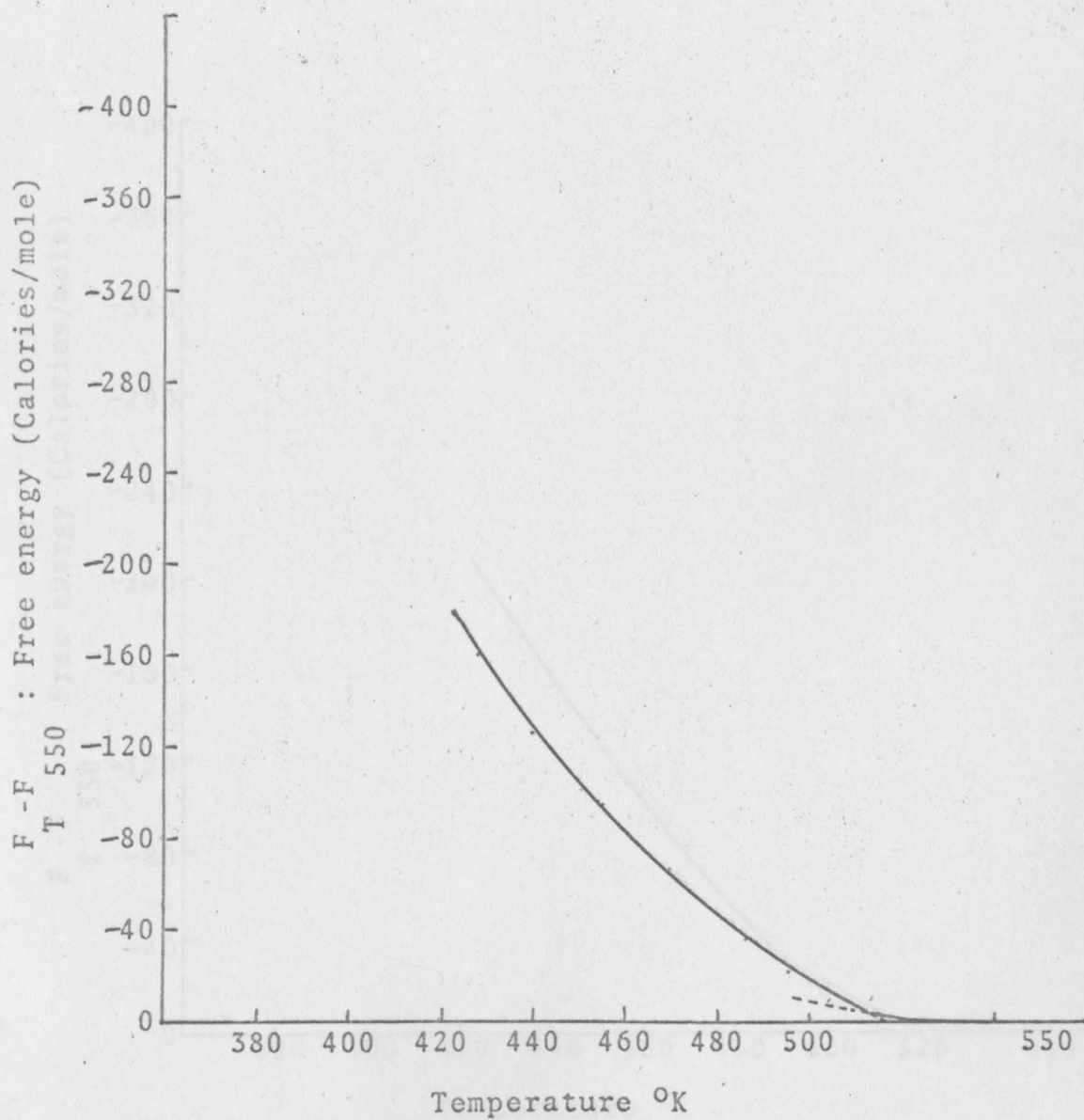


Fig. 65. Free energy as a function of temperature for Tl-Cd alloy (0.88 atom percent Cd)

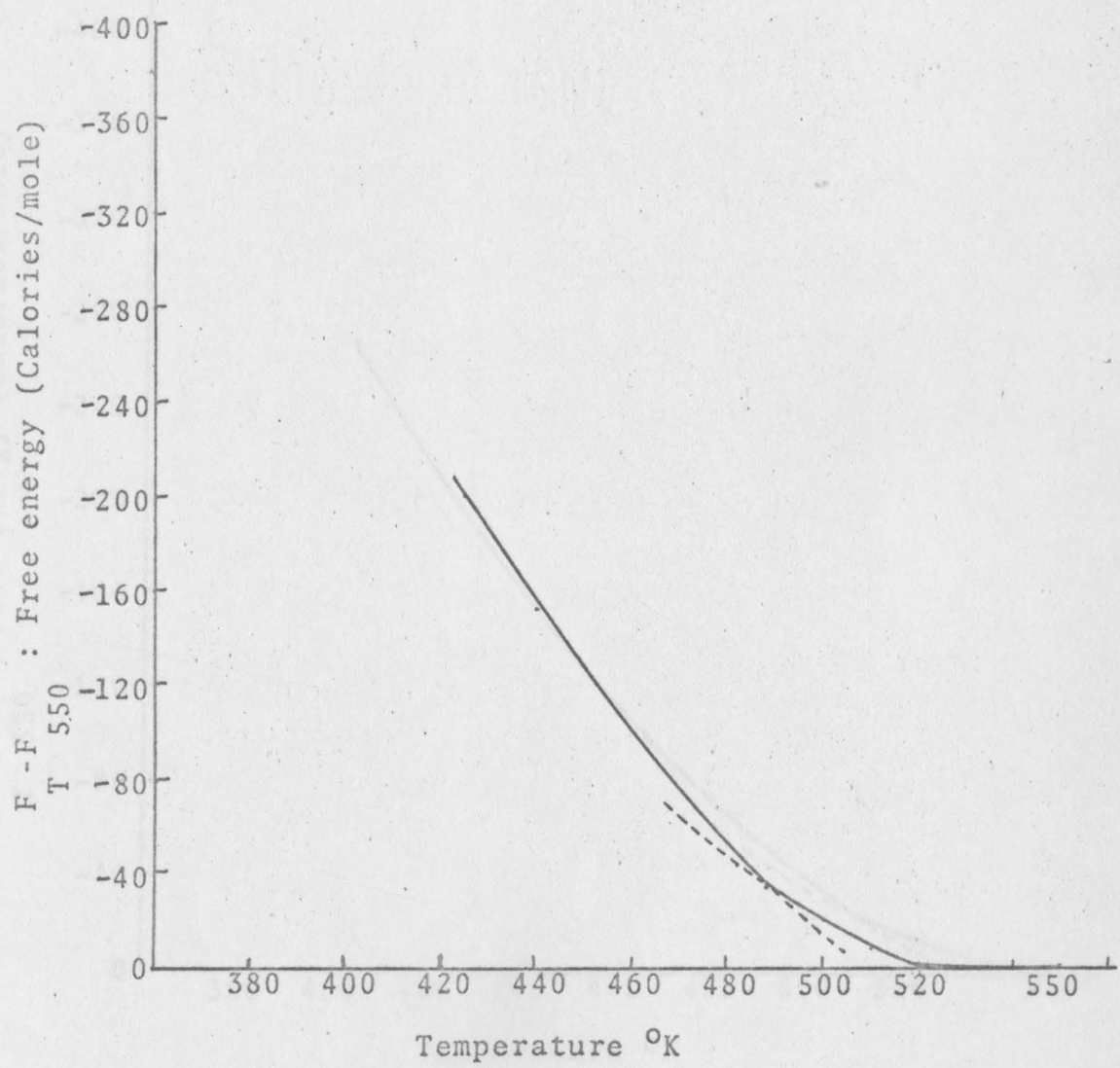


Fig. 66. Free energy as a function of temperature for Tl-Cd alloy (1.0 atom percent Cd)

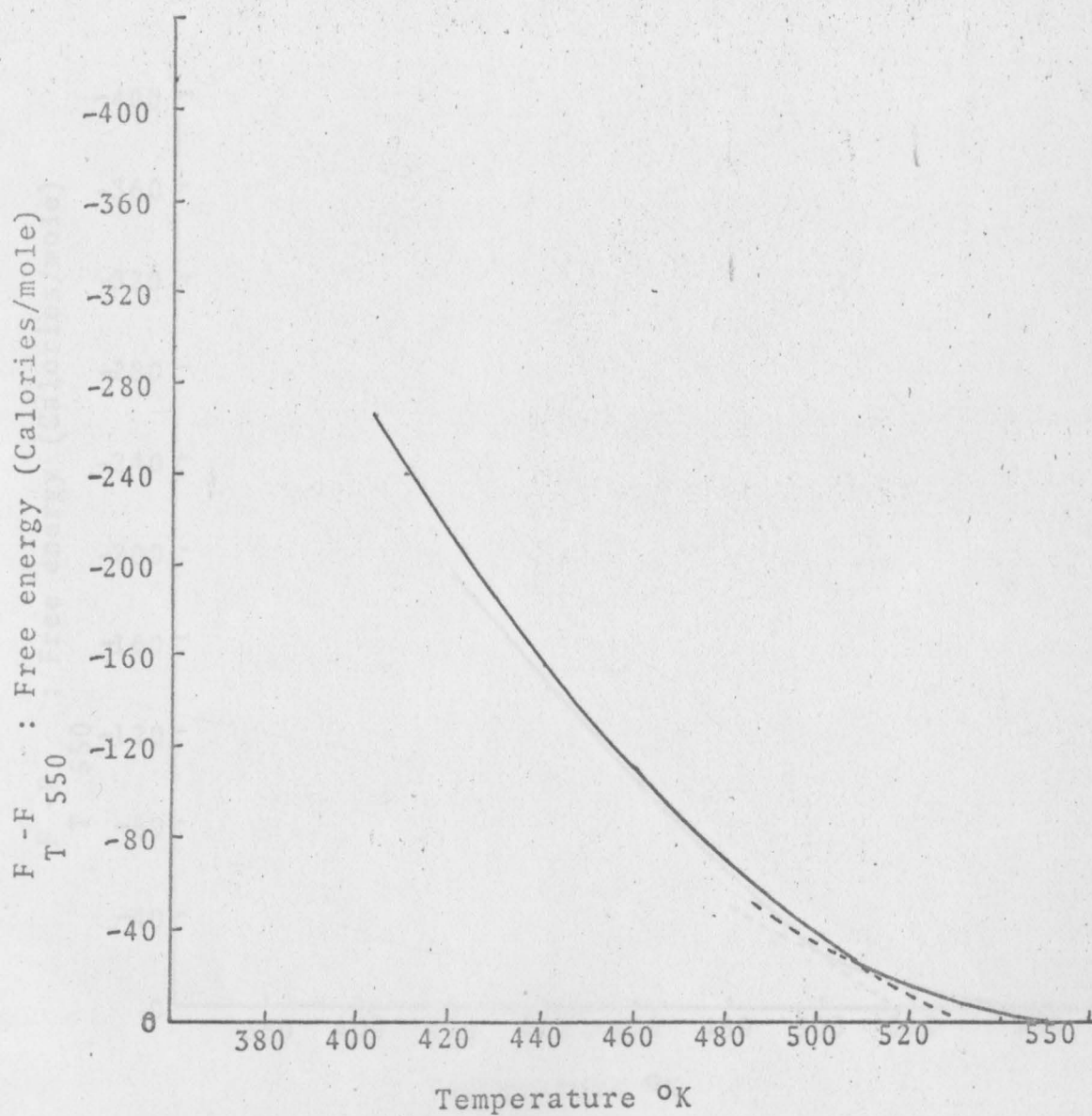


Fig. 67. Free energy as a function of temperature for Tl-Sn alloy (0.05 atom percent Sn)

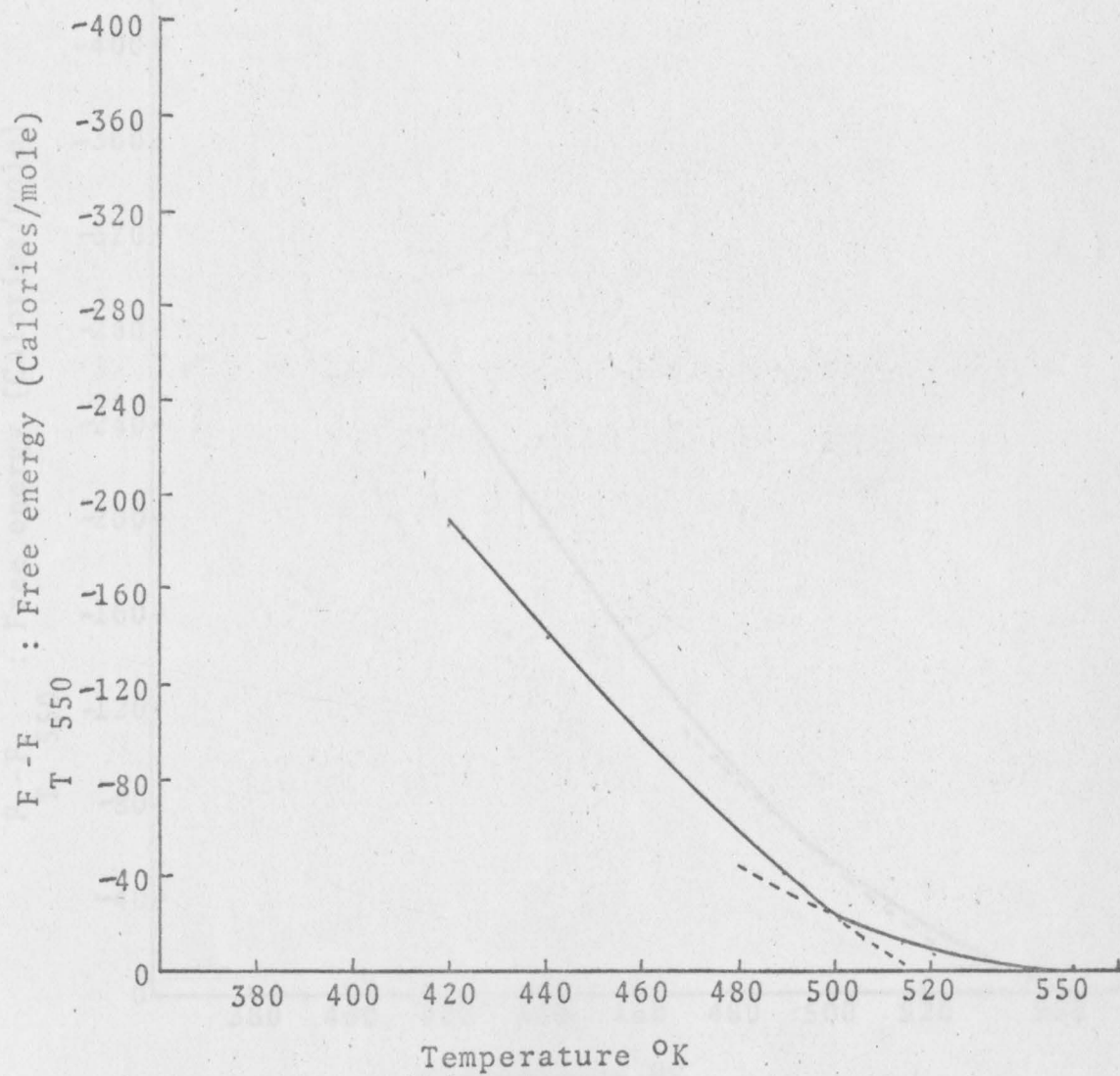


Fig. 68. Free energy as a function of temperature for Tl-Sn alloy (0.20 atom percent Sn)

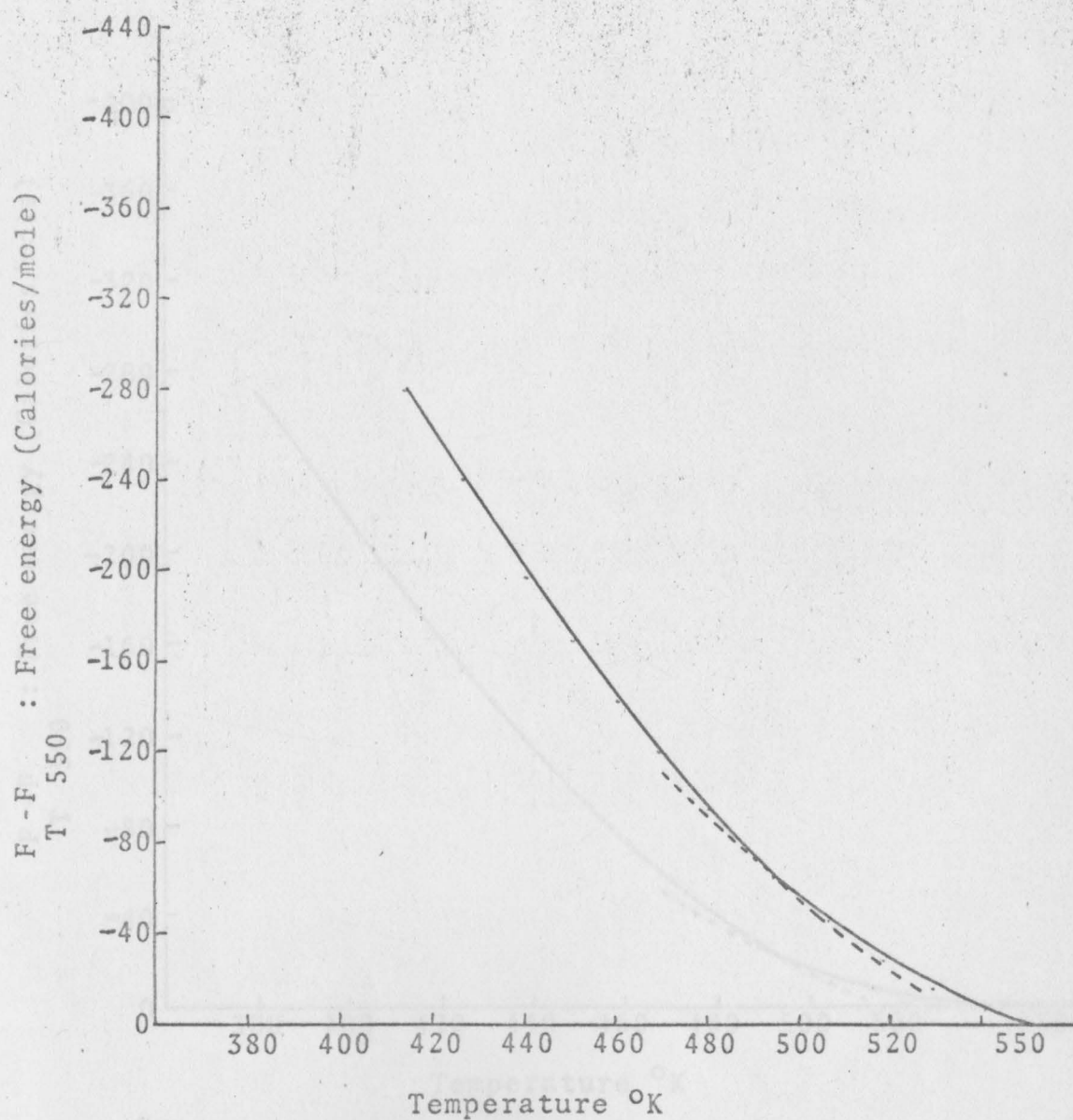


Fig. 69. Free energy as a function of temperature for Tl-Sn alloy (0.40 atom percent Sn)

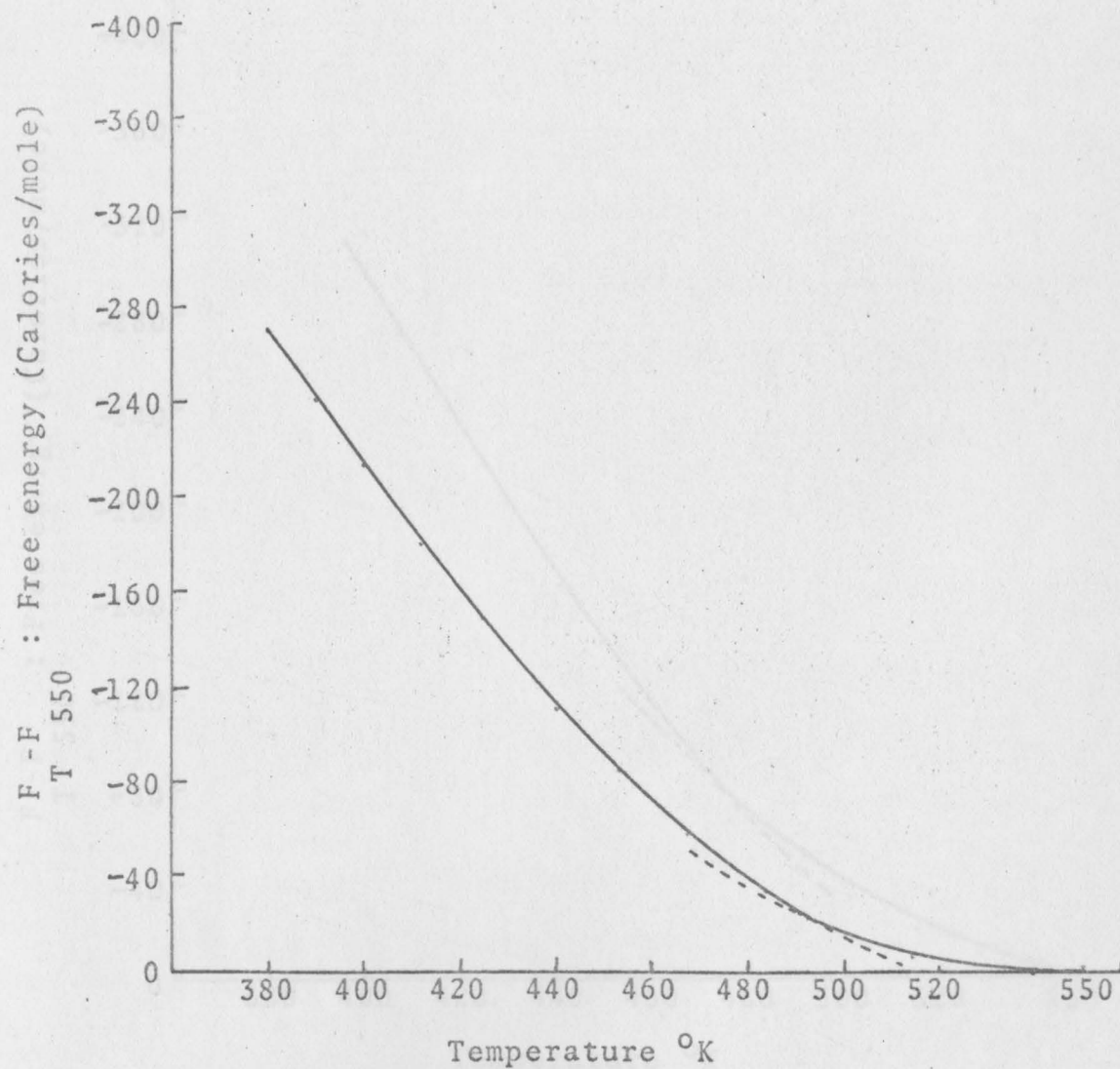


Fig. 70. Free energy as a function of temperature for Tl-Sn alloy (0.60 atom percent Sn)

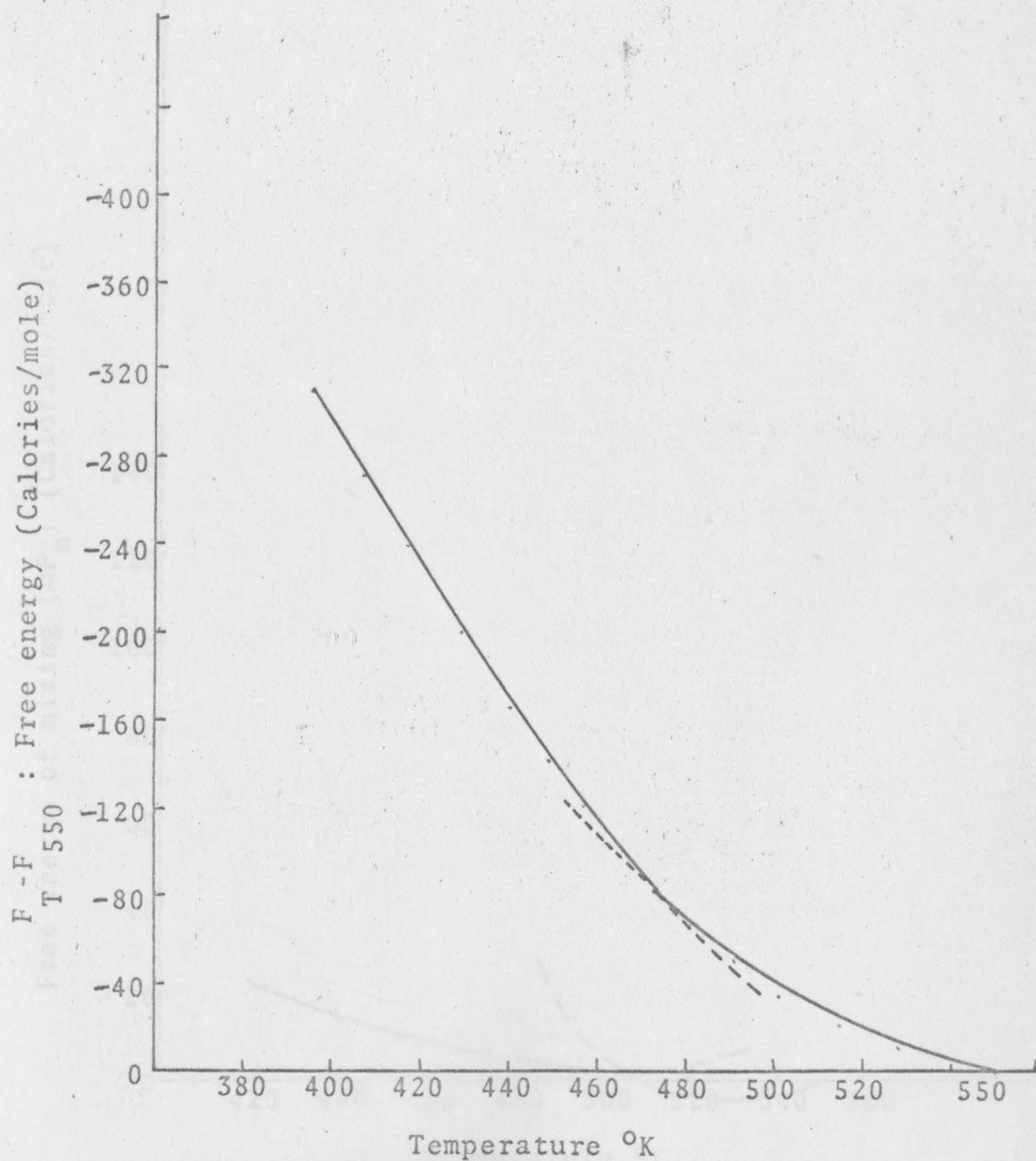


Fig. 71. Free energy as a function of temperature for Tl-Sn alloy (1.0 atom percent Sn)

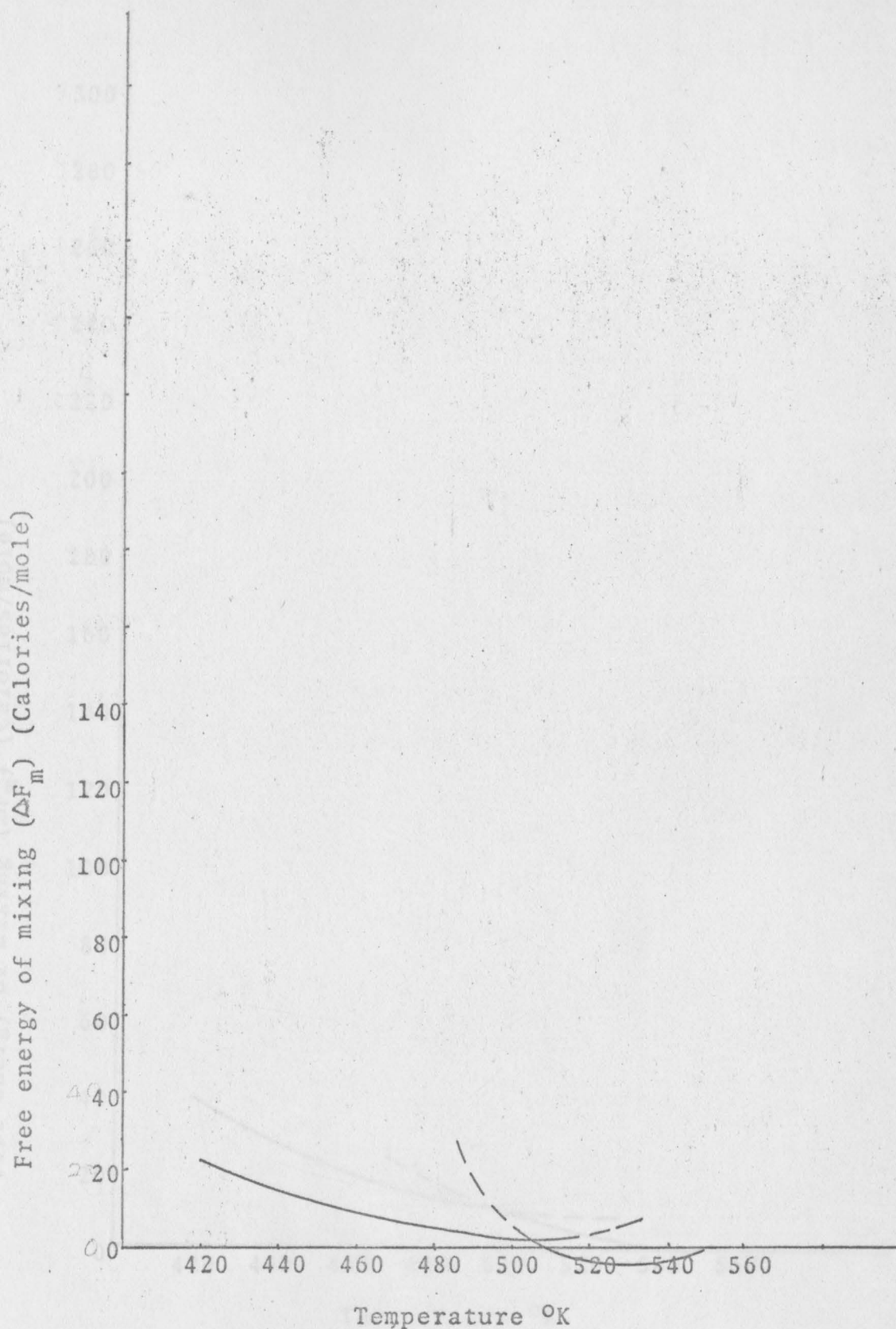


Fig. 72. Free energy of mixing as a function of temperature for Tl-Ag alloy (0.05 atom percent Ag)



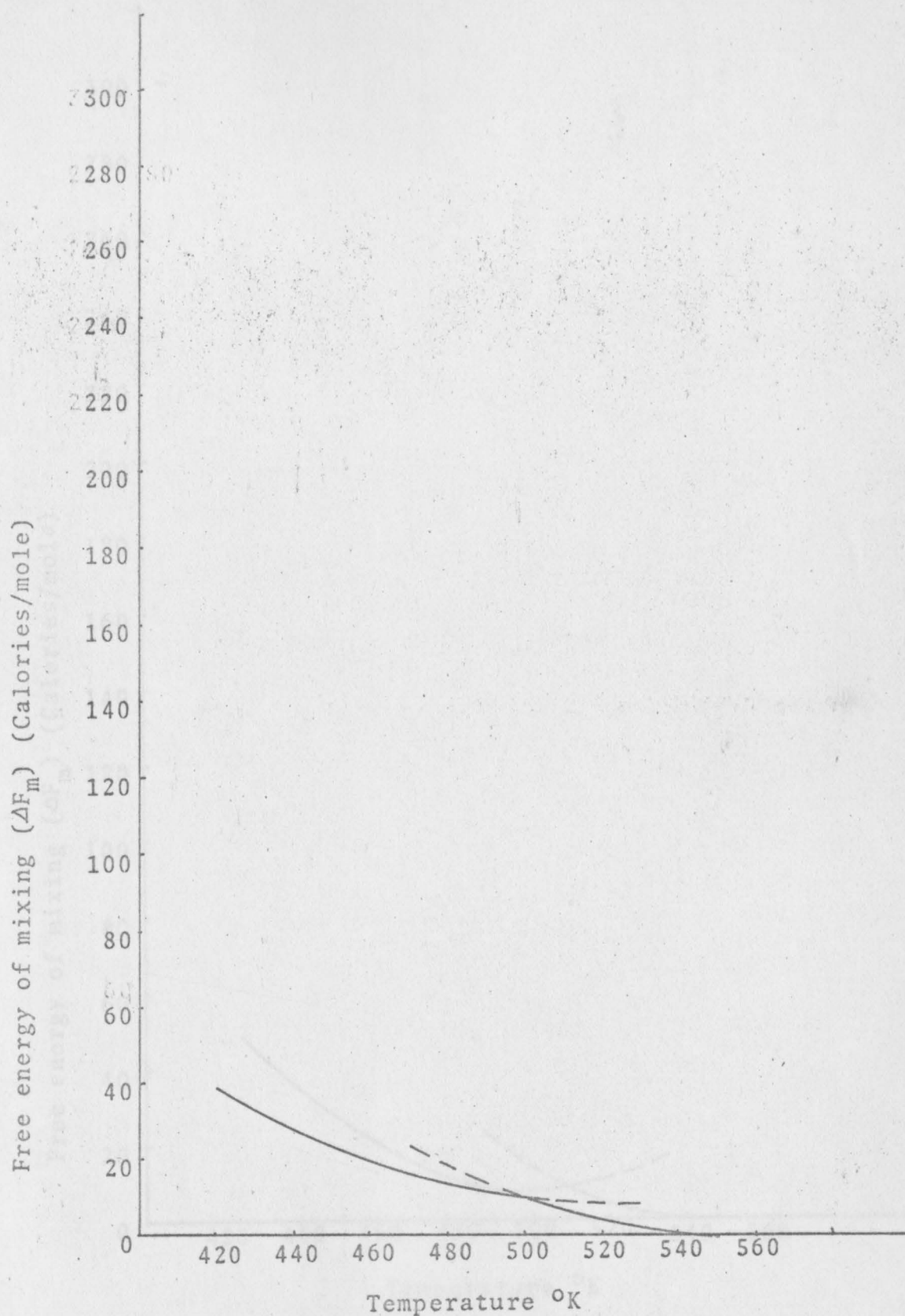


Fig. 73. Free energy of mixing as a function of temperature for Tl-Ag alloy (0.10 atom percent Ag)

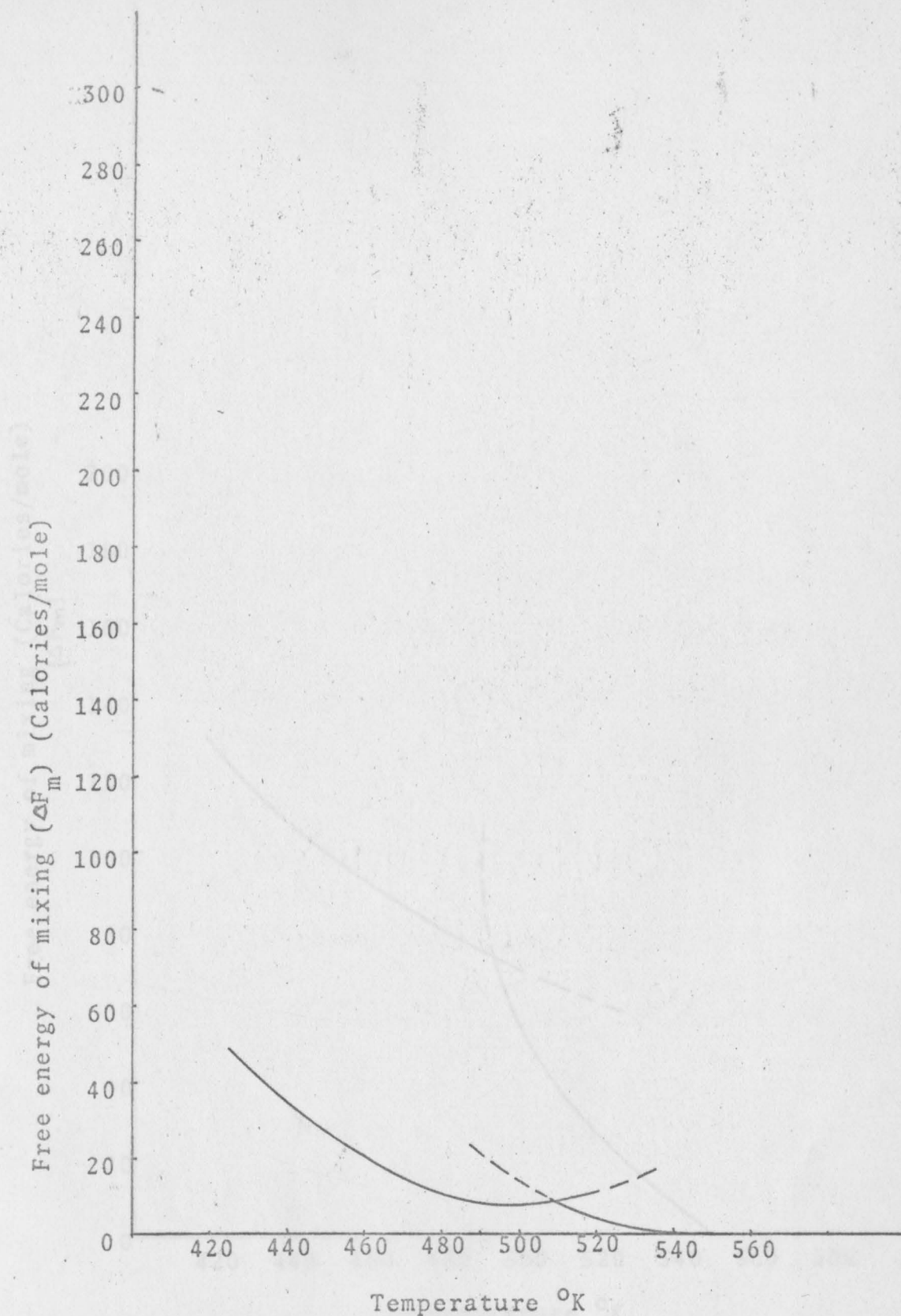


Fig. 74. Free energy of mixing as a function of temperature for Tl-Ag alloy (0.20 atom percent Ag)

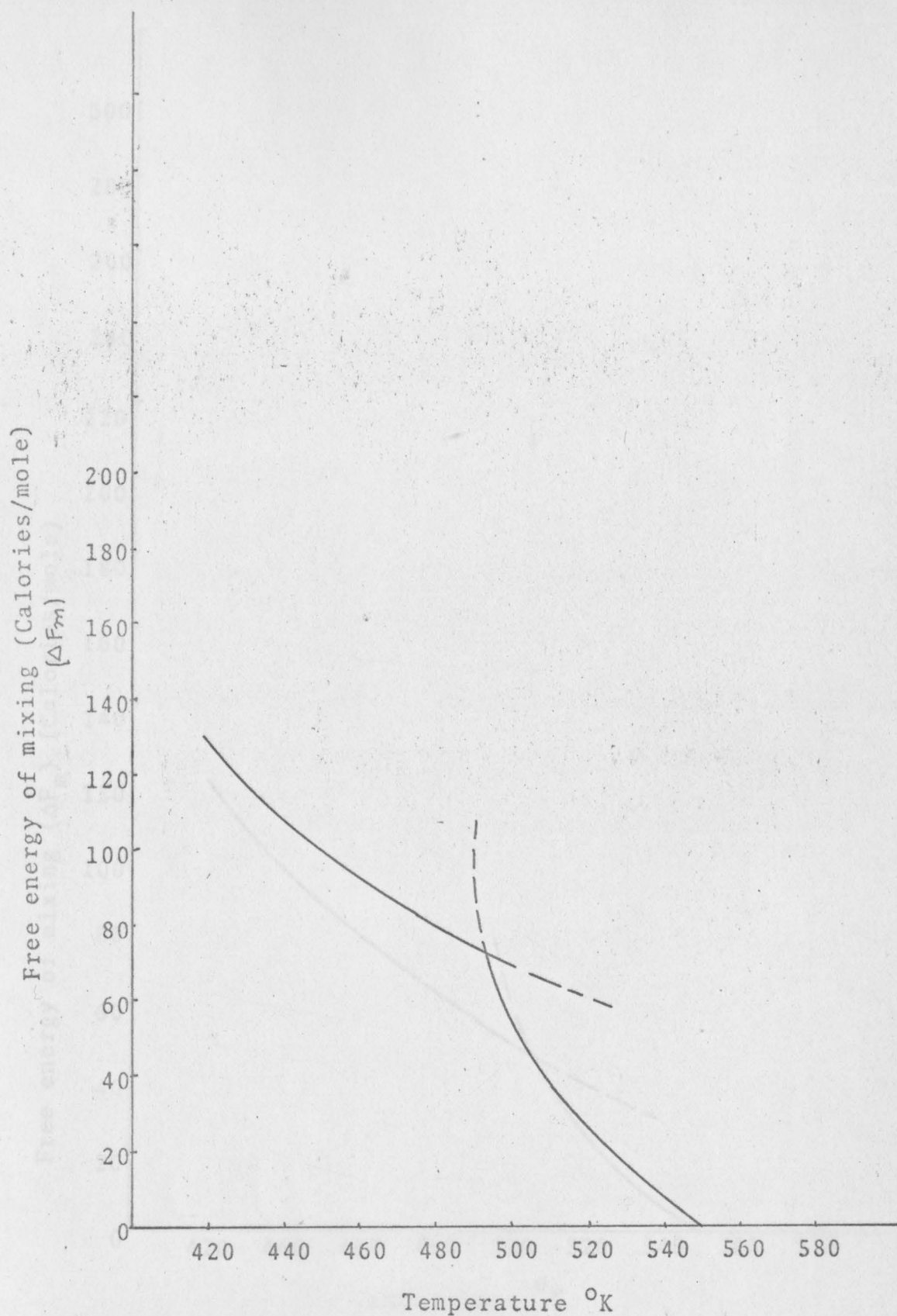


Fig. 75. Free energy as a function of temperature for Tl-Ag alloy (0.40 atom percent Ag)

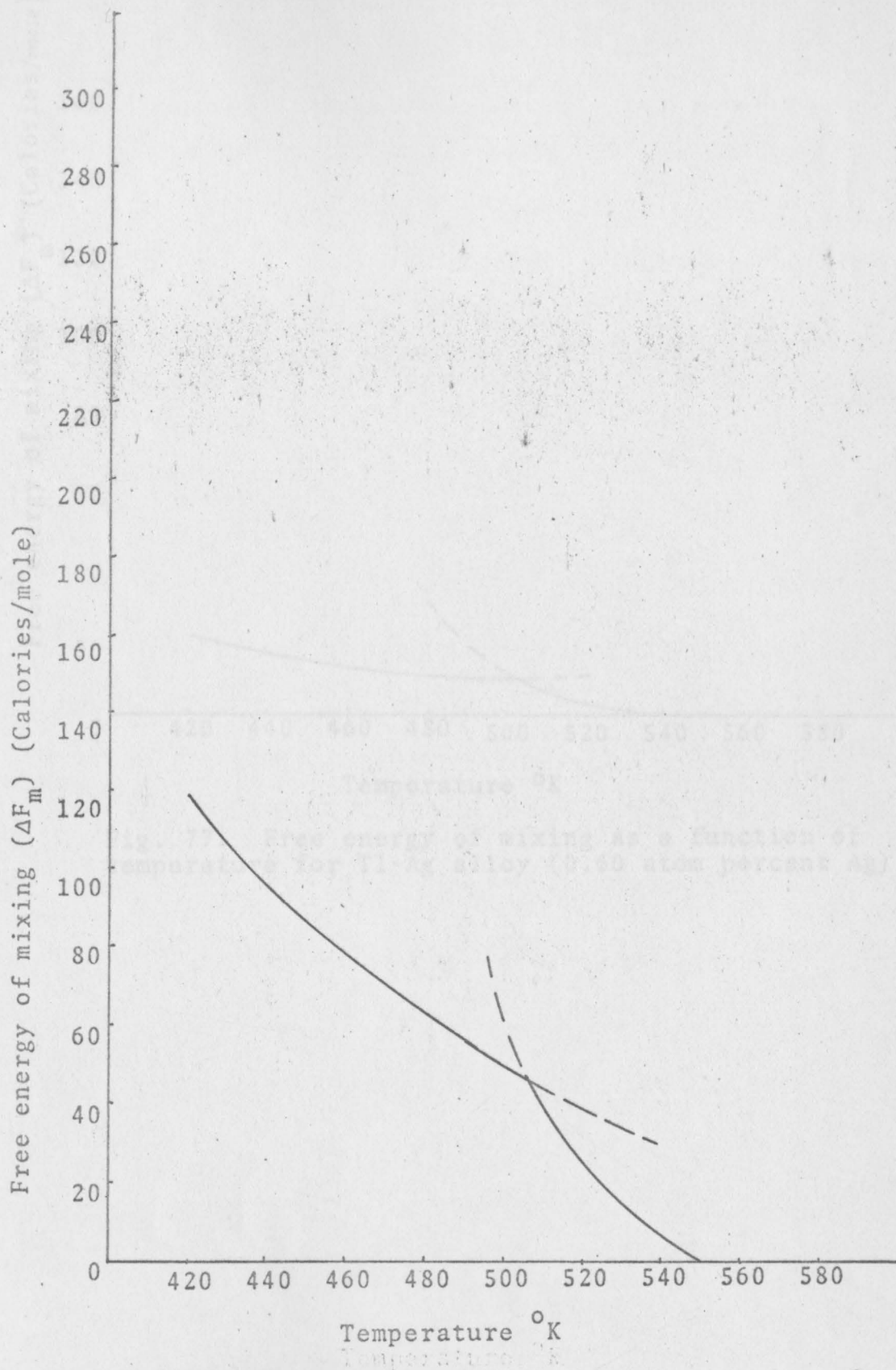


Fig. 76. Free energy of mixing as a function of temperature for Tl-Ag alloy (0.4971 atom percent Ag)

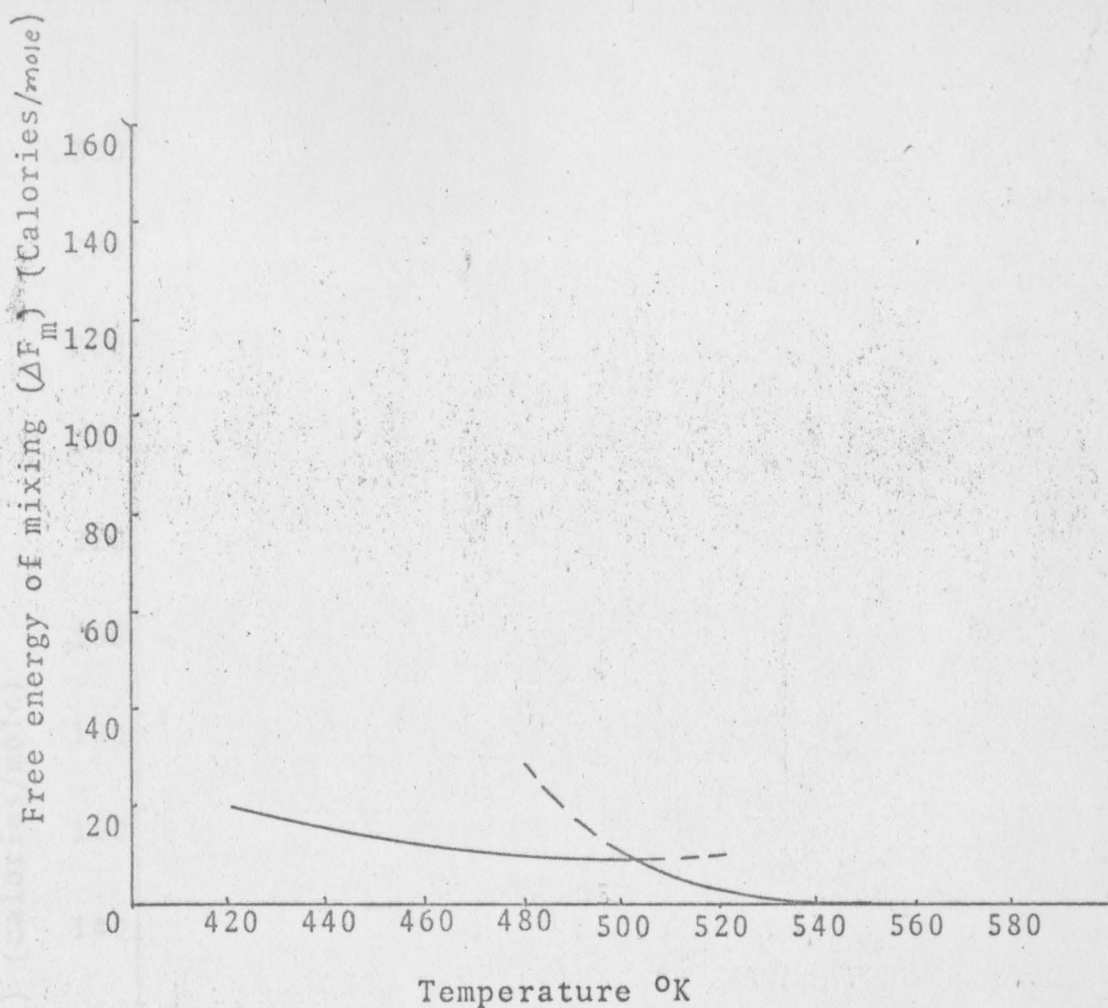


Fig. 77. Free energy of mixing as a function of temperature for Tl-Ag alloy (0.60 atom percent Ag)

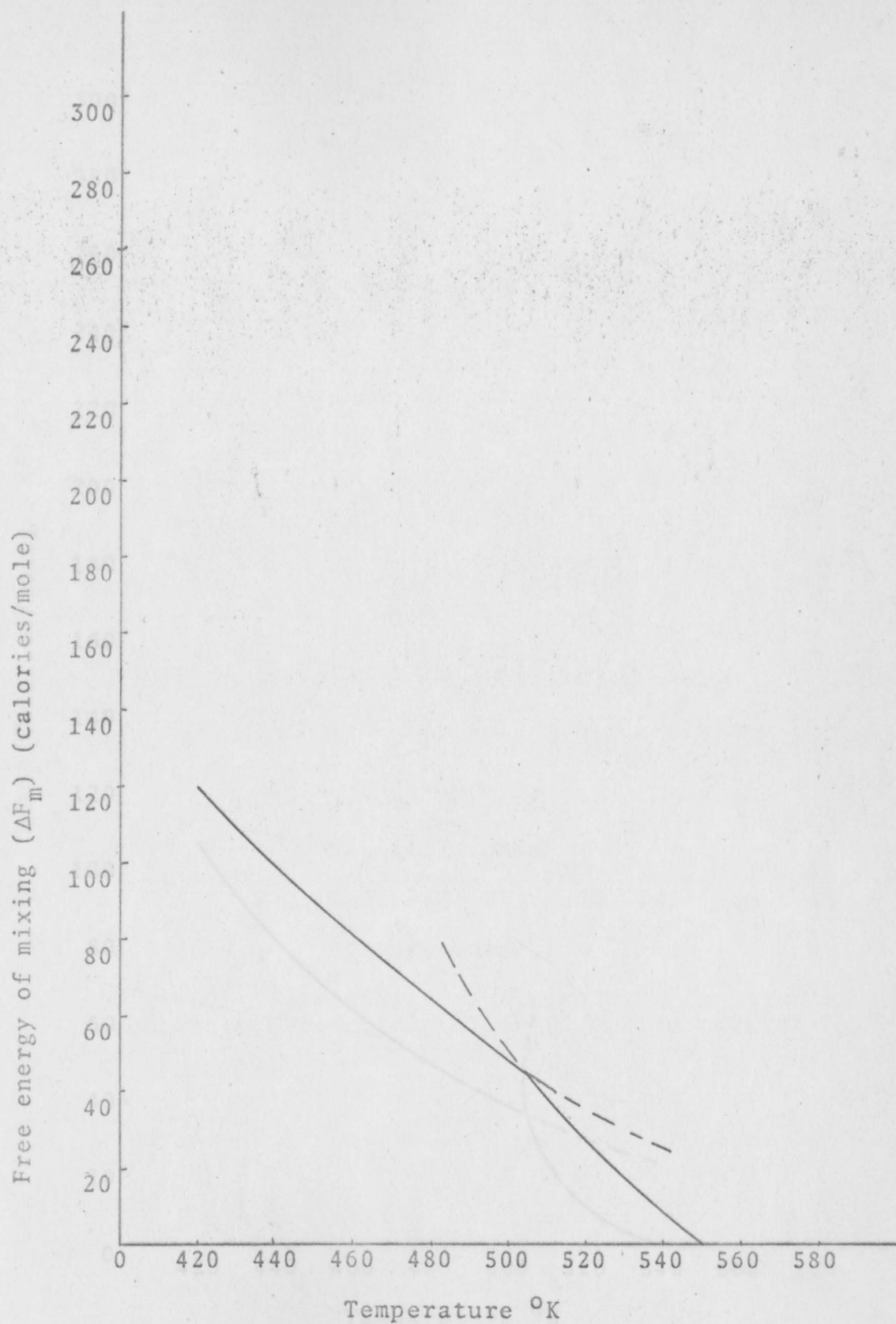


Fig. 78. Free energy of mixing as a function of temperature for Tl-Ag alloy (0.80 atom percent Ag)

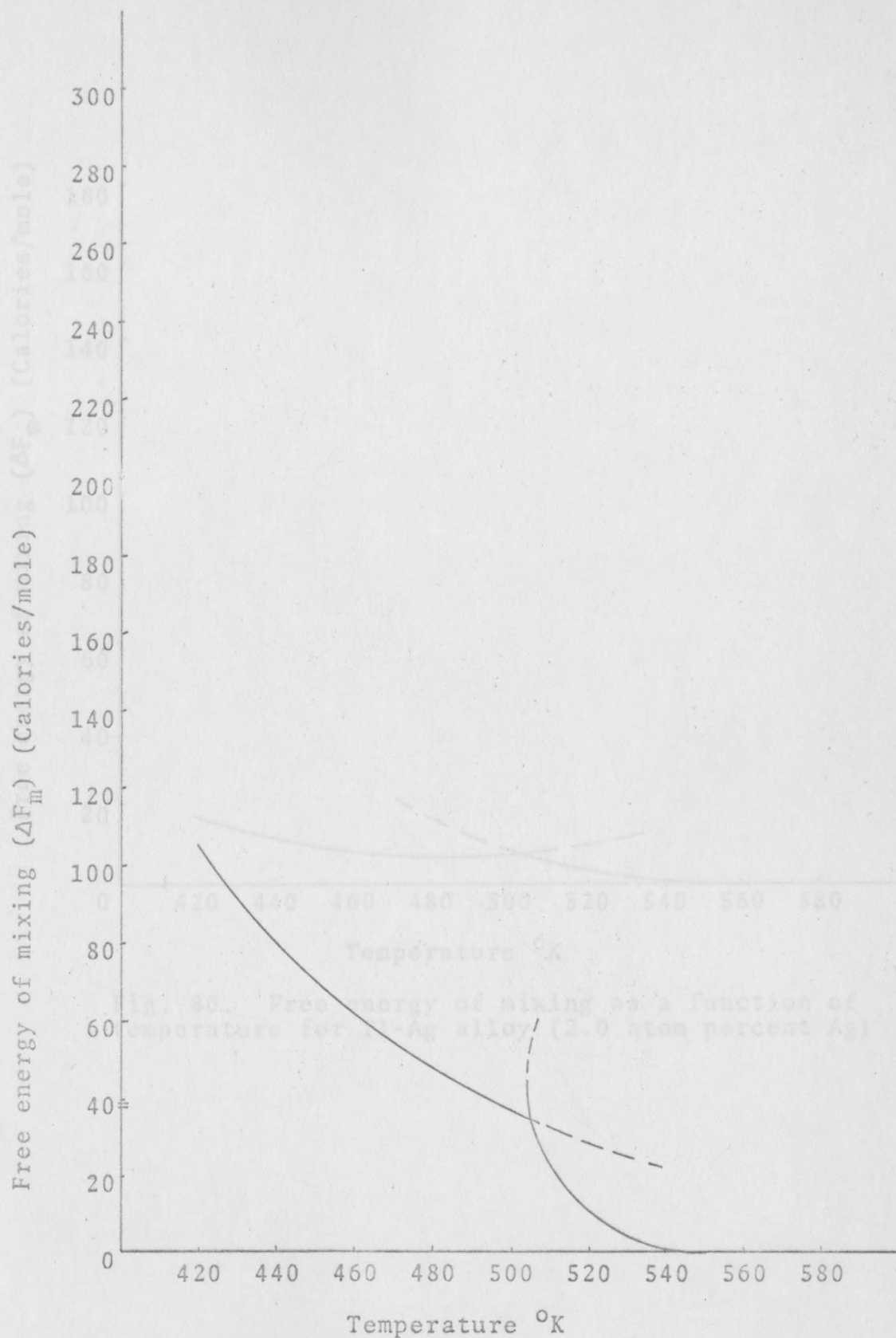


Fig. 79. Free energy of mixing as a function of temperature for Tl-Ag alloy (1.0 atom percent Ag)

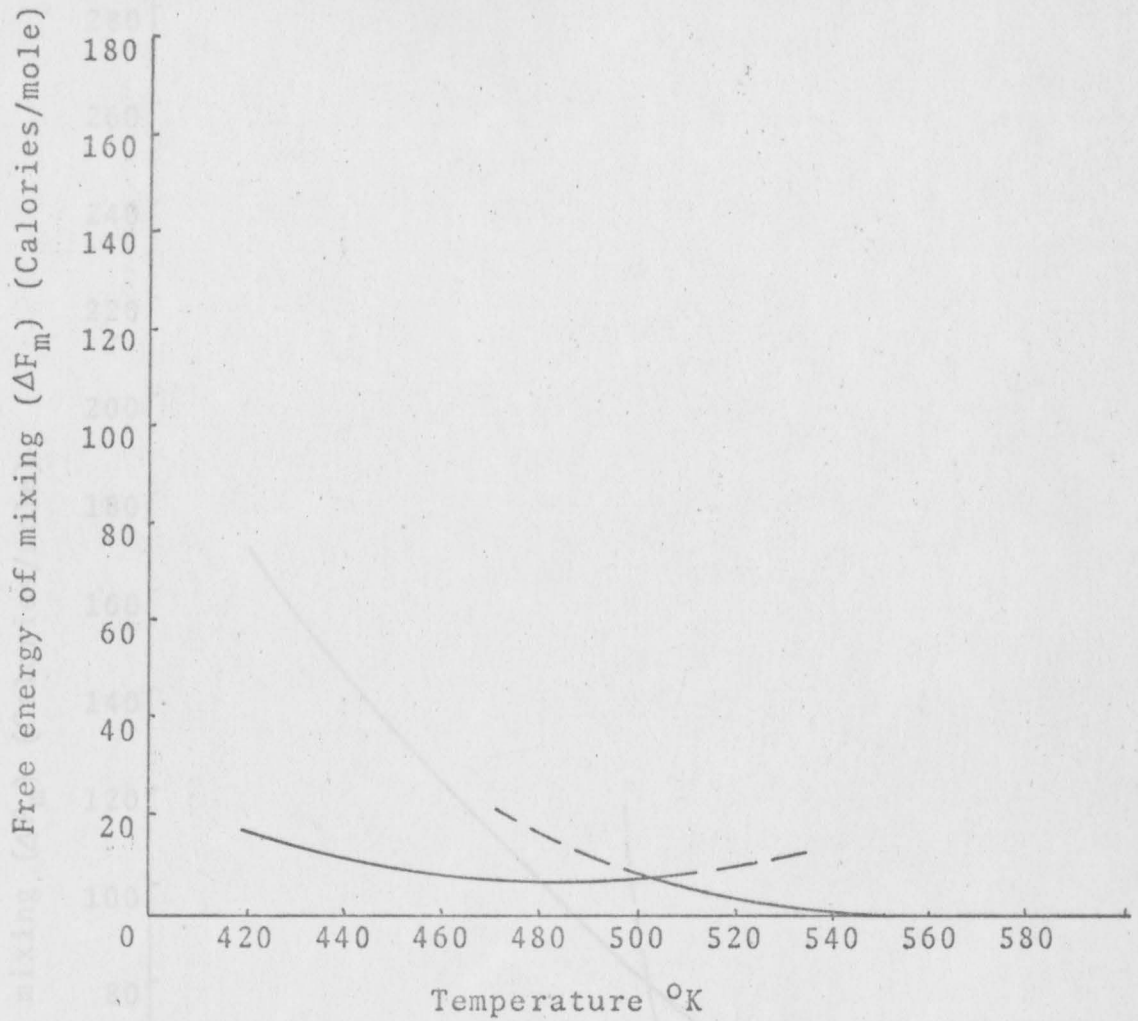


Fig. 80. Free energy of mixing as a function of temperature for Tl-Ag alloy (2.0 atom percent Ag)



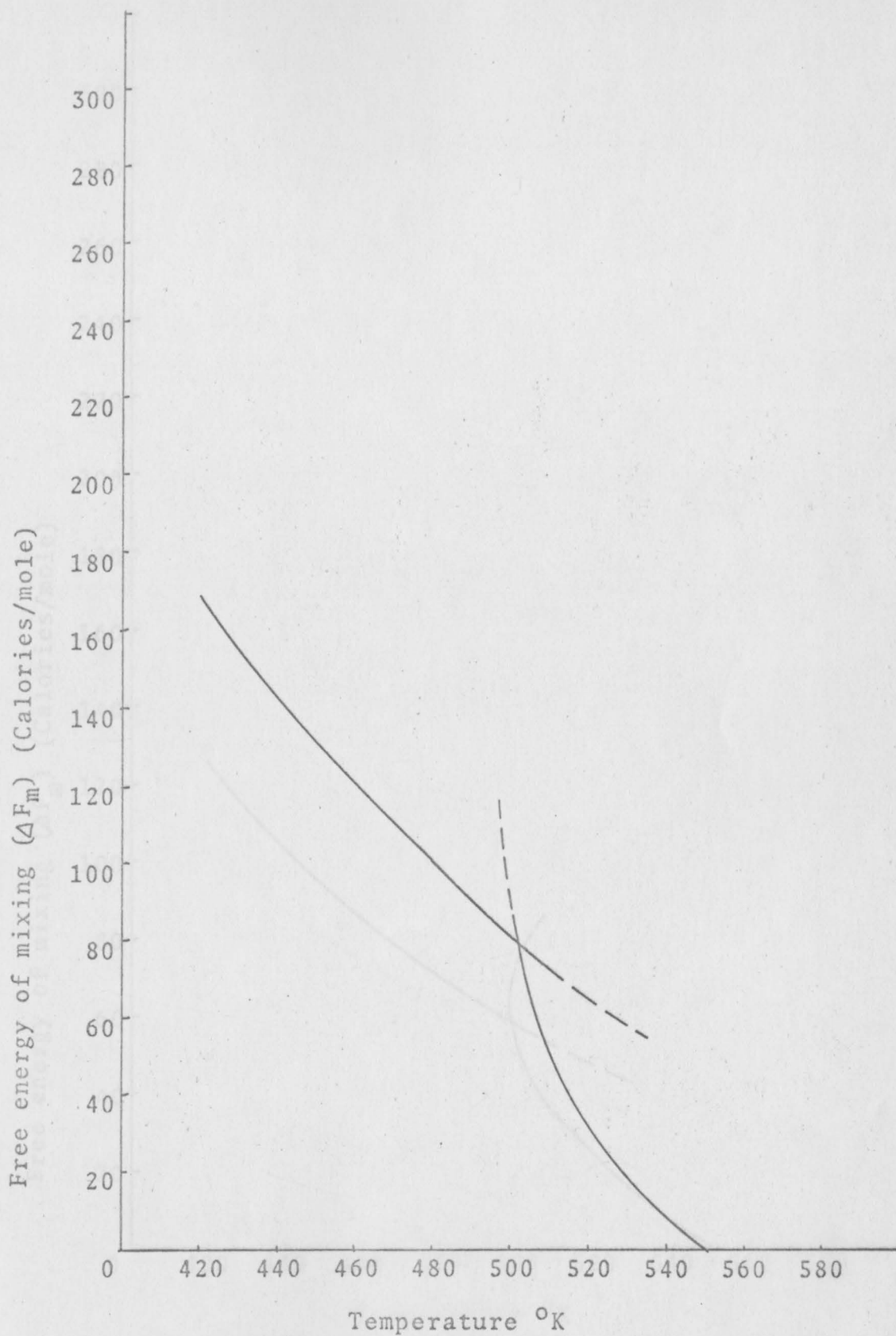


Fig. 81. Free energy of mixing as a function of temperature for Tl-Au alloy (0.05 atom percent Au)

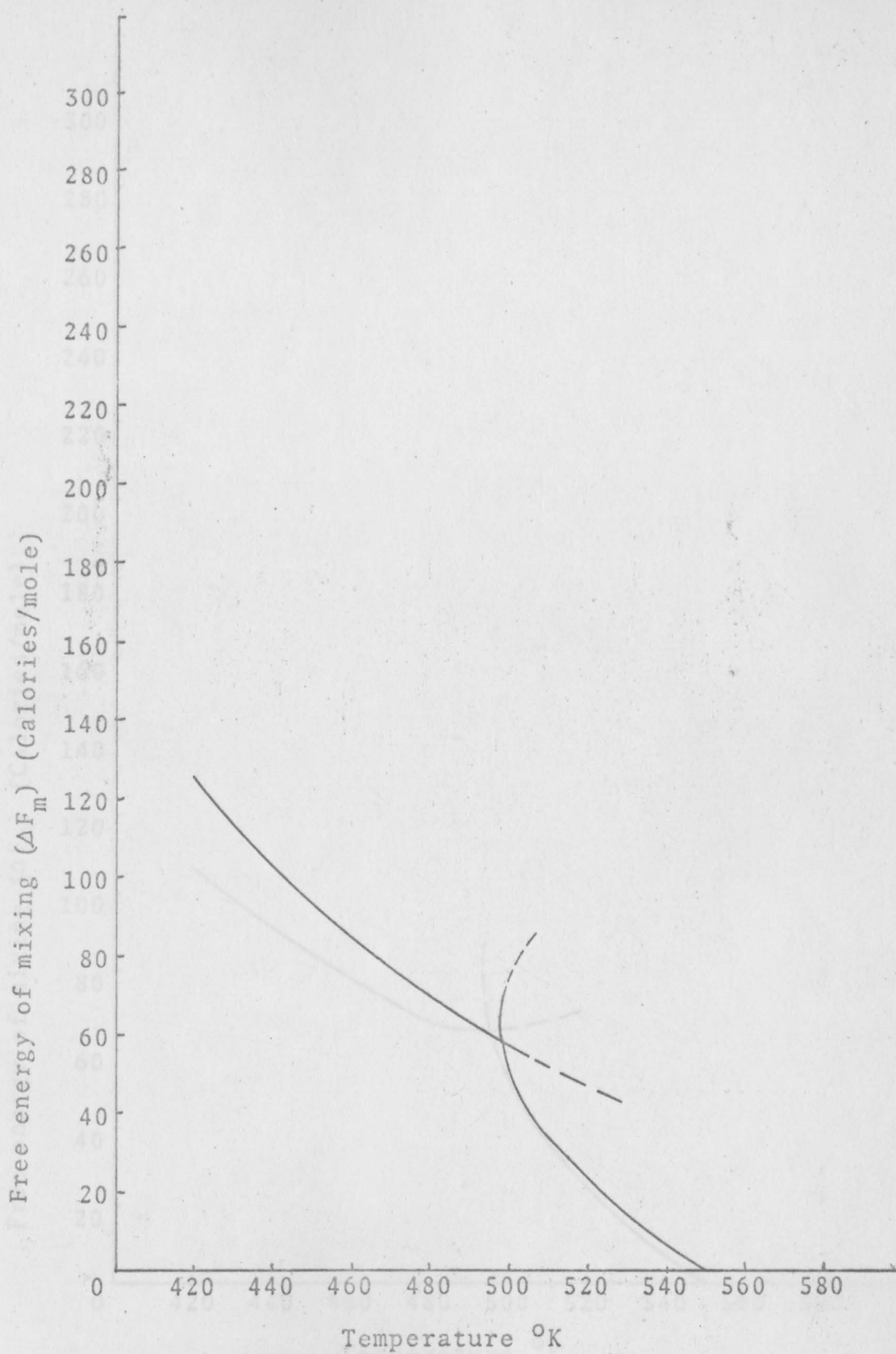


Fig. 82. Free energy of mixing as a function of temperature for Tl-Au alloy (0.10 atom percent Au)

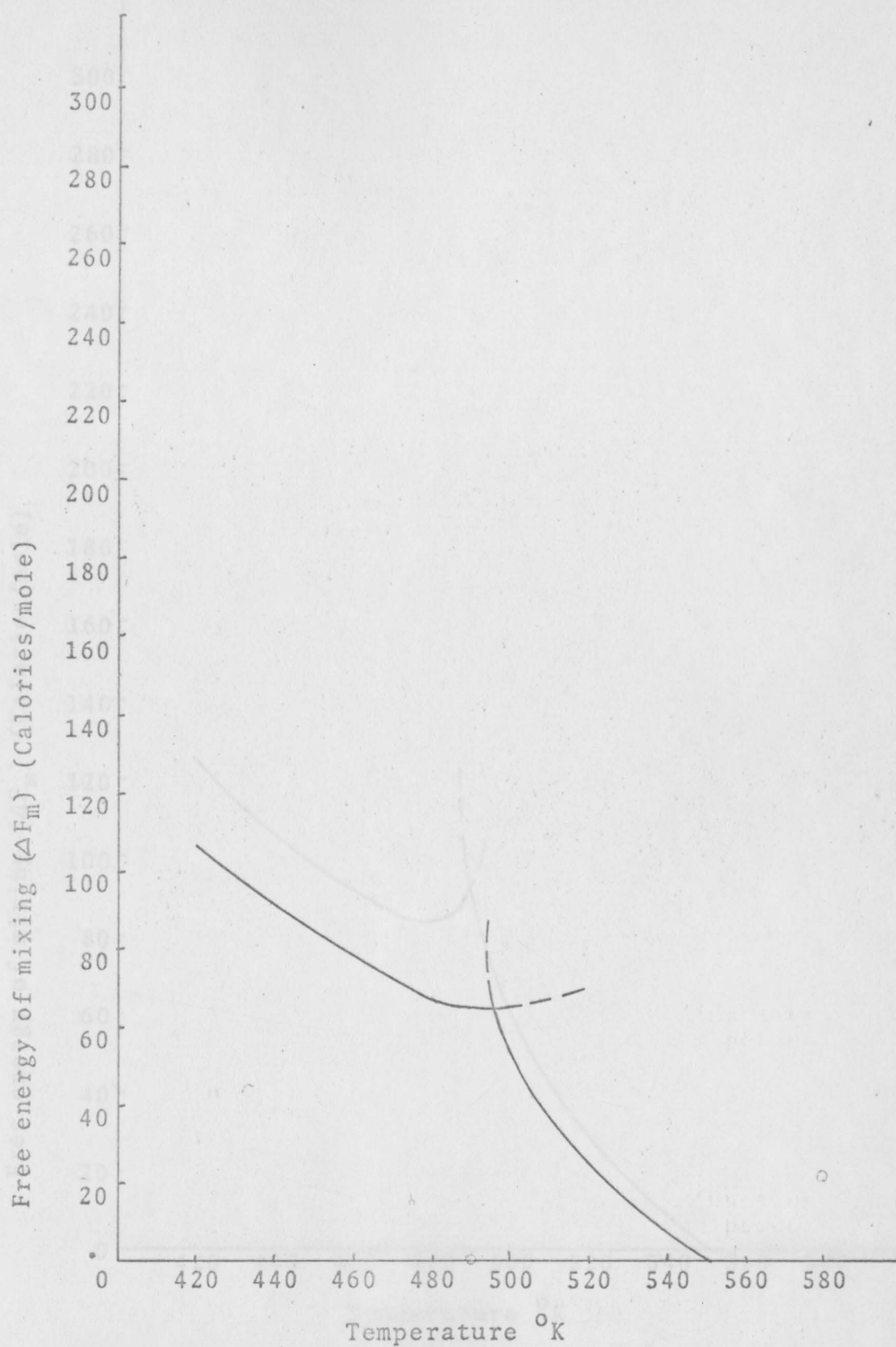


Fig. 83. Free energy of mixing as a function of temperature for Tl-Au alloy (0.20 atom percent Au)

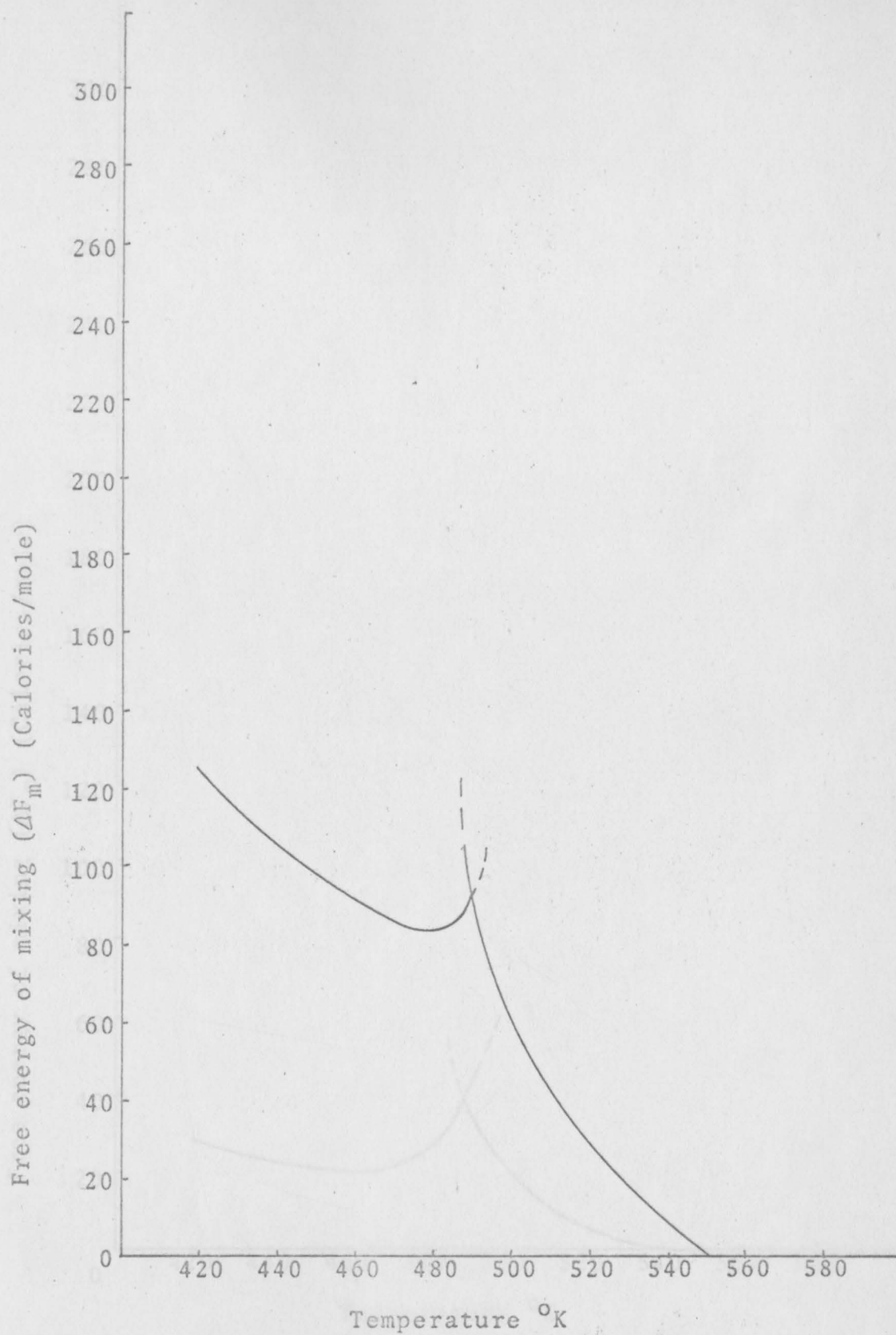


Fig. 84. Free energy of mixing as a function of temperature for Tl-Au alloy (0.40 atom percent Au)

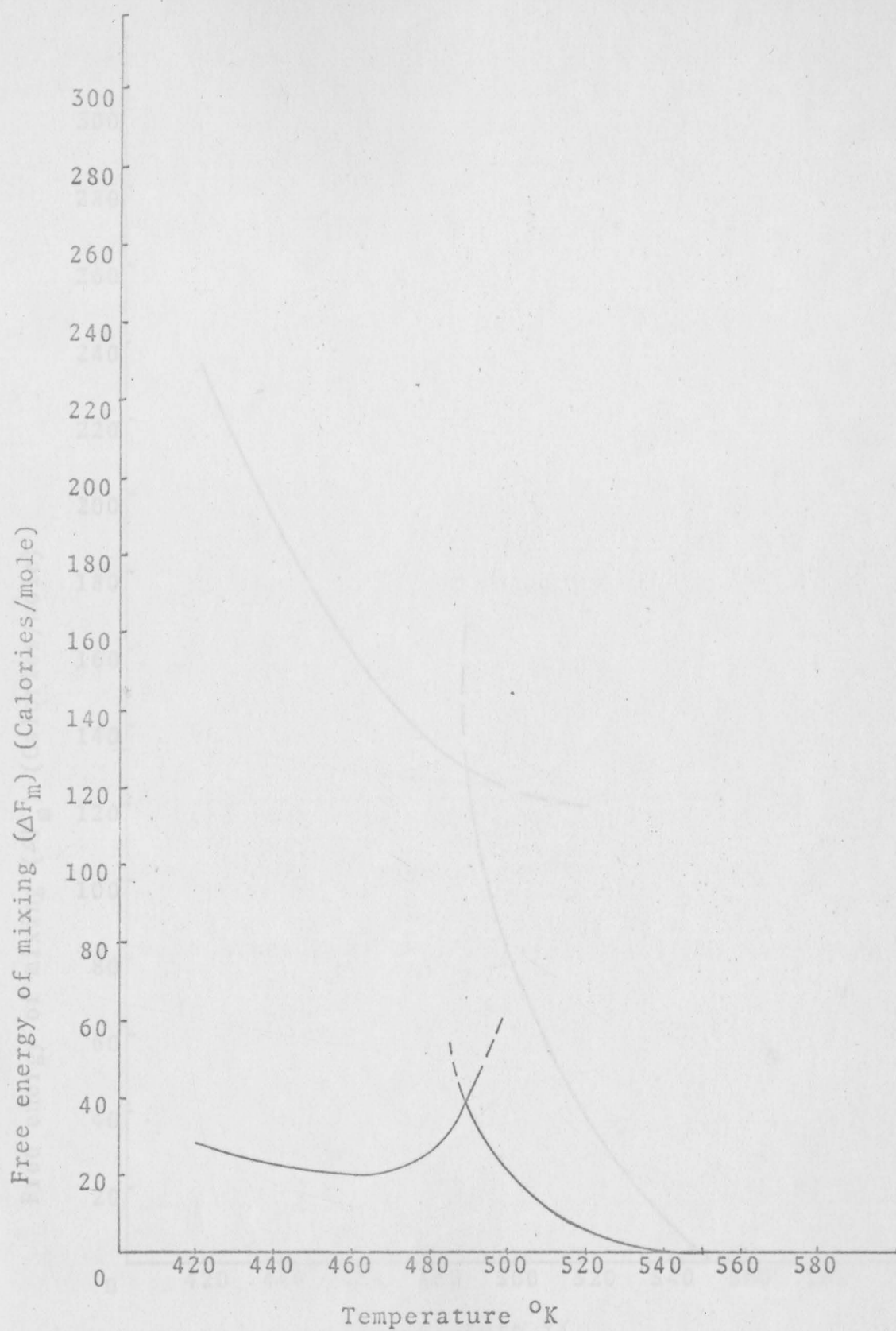


Fig. 85. Free energy of mixing as a function of temperature for Tl-Au alloy (0.60 atom percent Au)

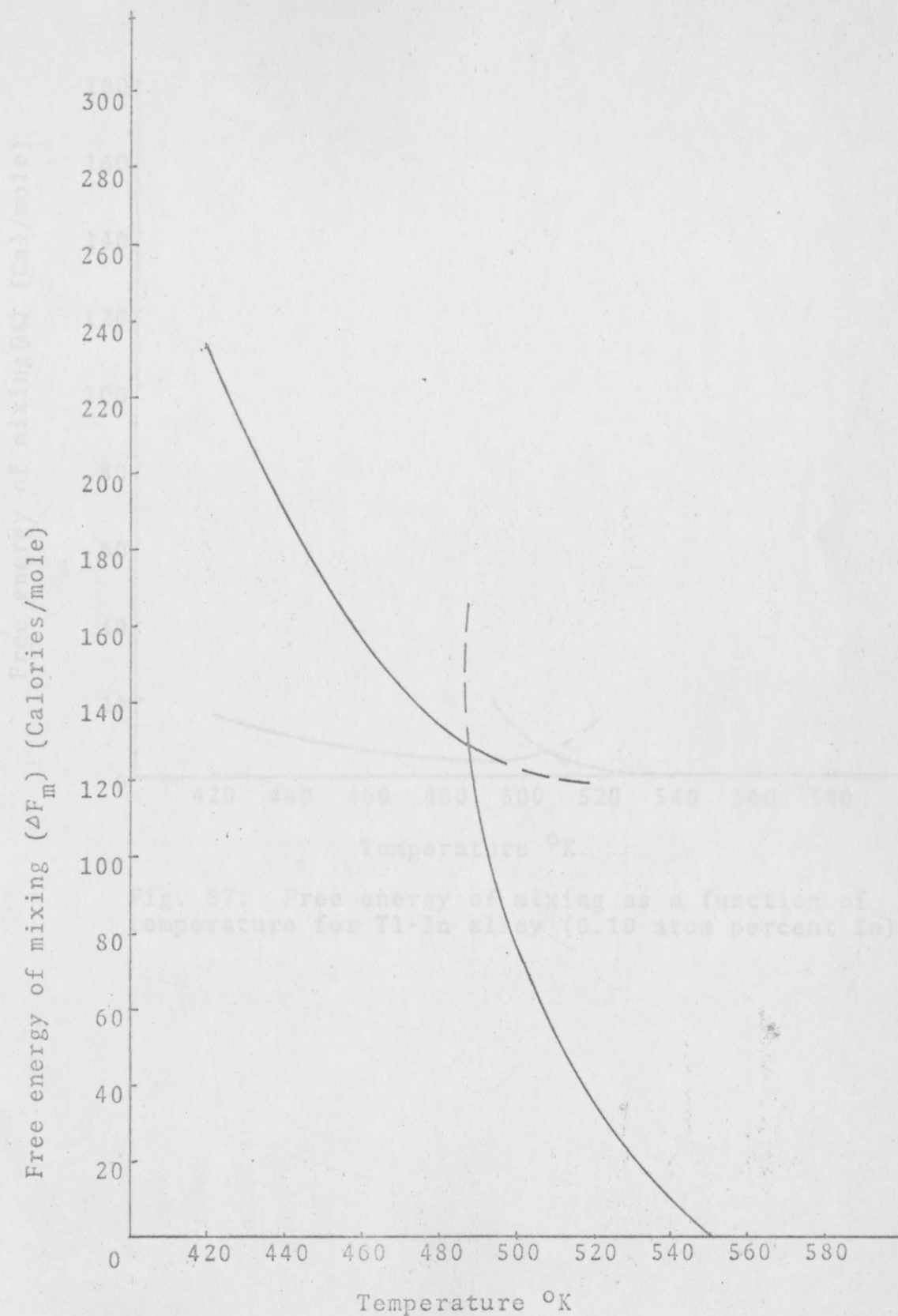


Fig. 86. Free energy of mixing as a function of temperature for Tl-Au alloy (1.0 atom percent Au)

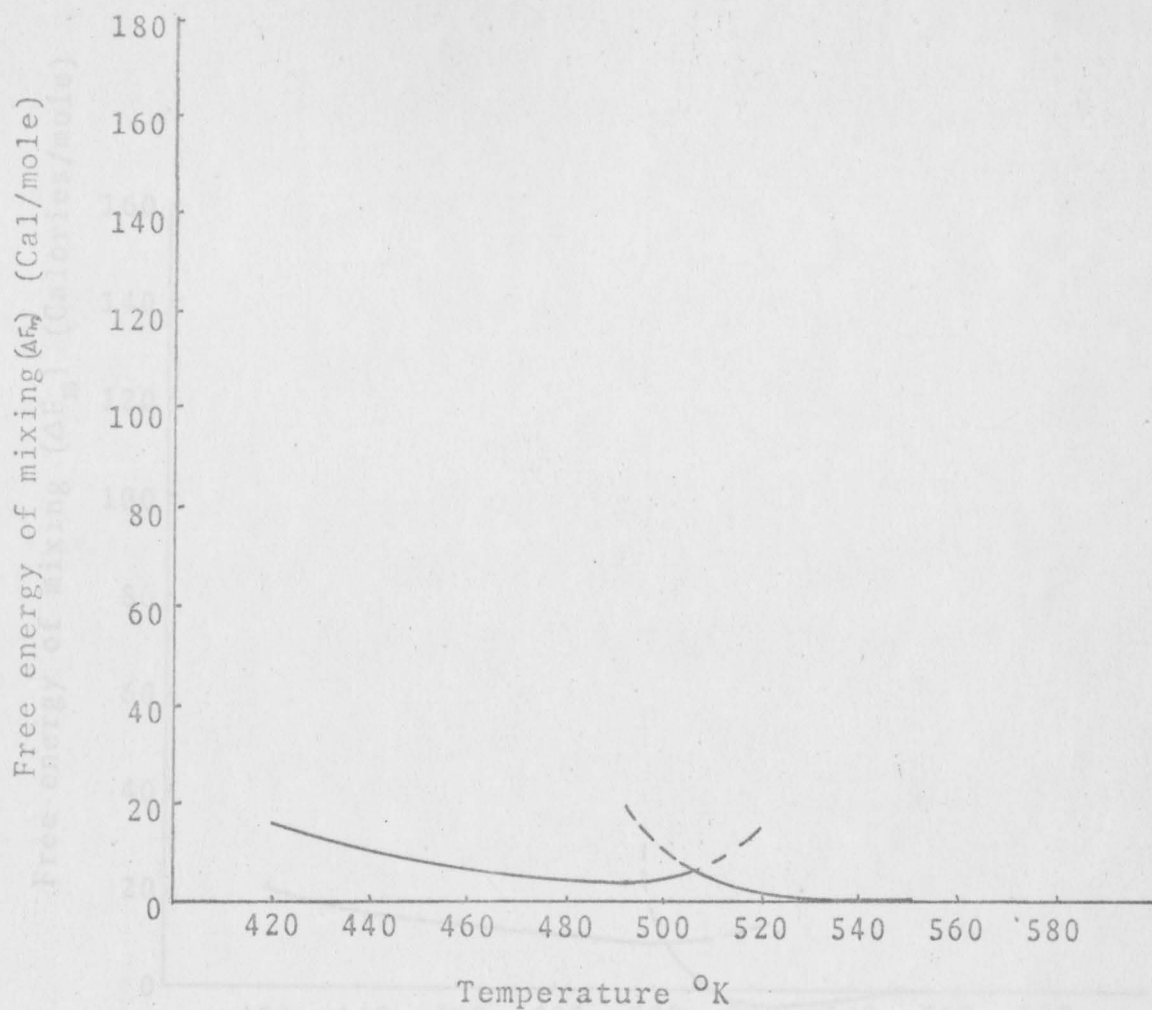


Fig. 87. Free energy of mixing as a function of temperature for Tl-Zn alloy (0.10 atom percent Zn)

Fig. 88. Free energy of mixing as a function of temperature for Tl-Zn alloy (0.10 atom percent Zn)

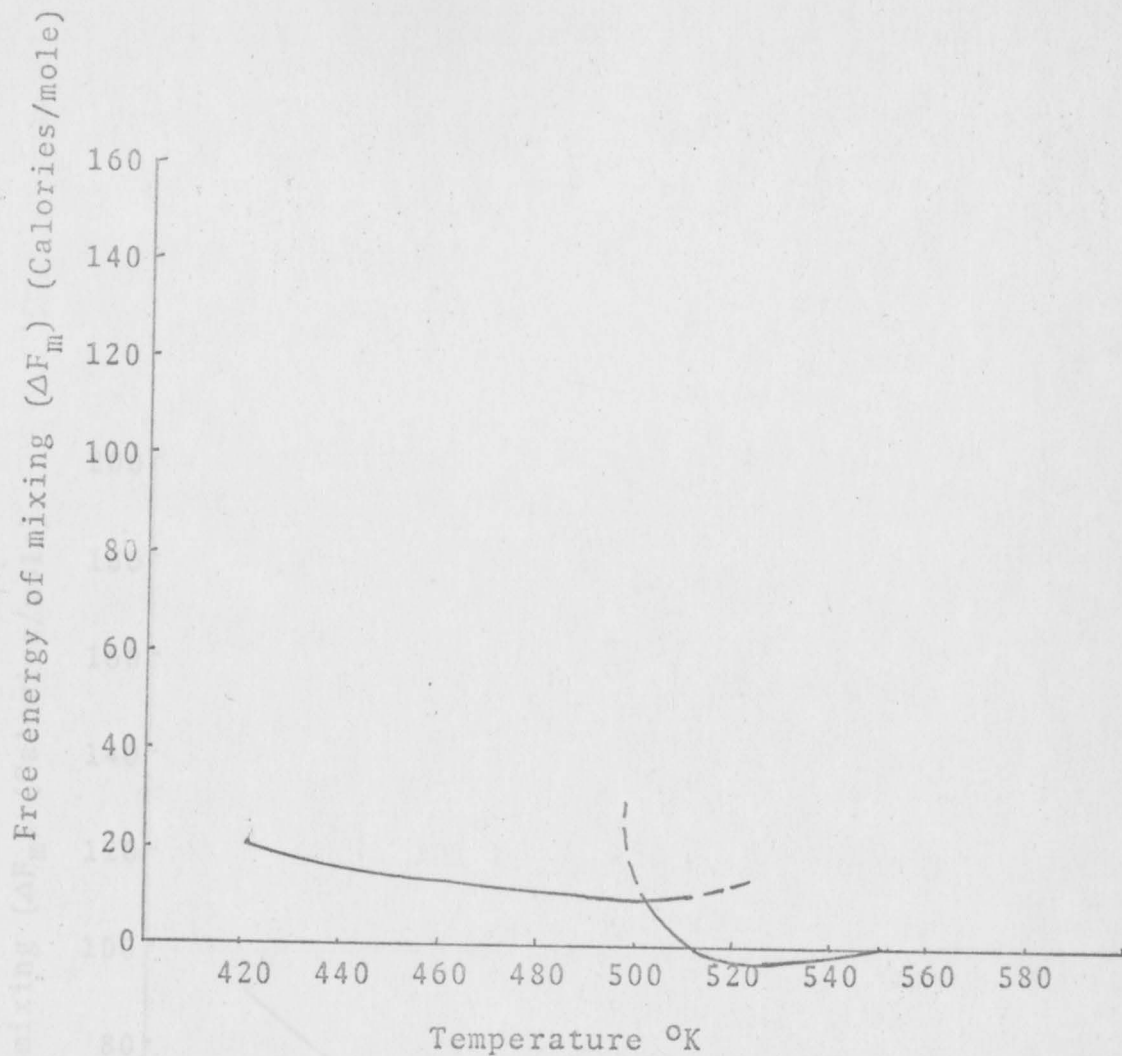


Fig. 88. Free energy of mixing as a function of temperature for Tl-Zn alloy (0.20 atom percent Zn)



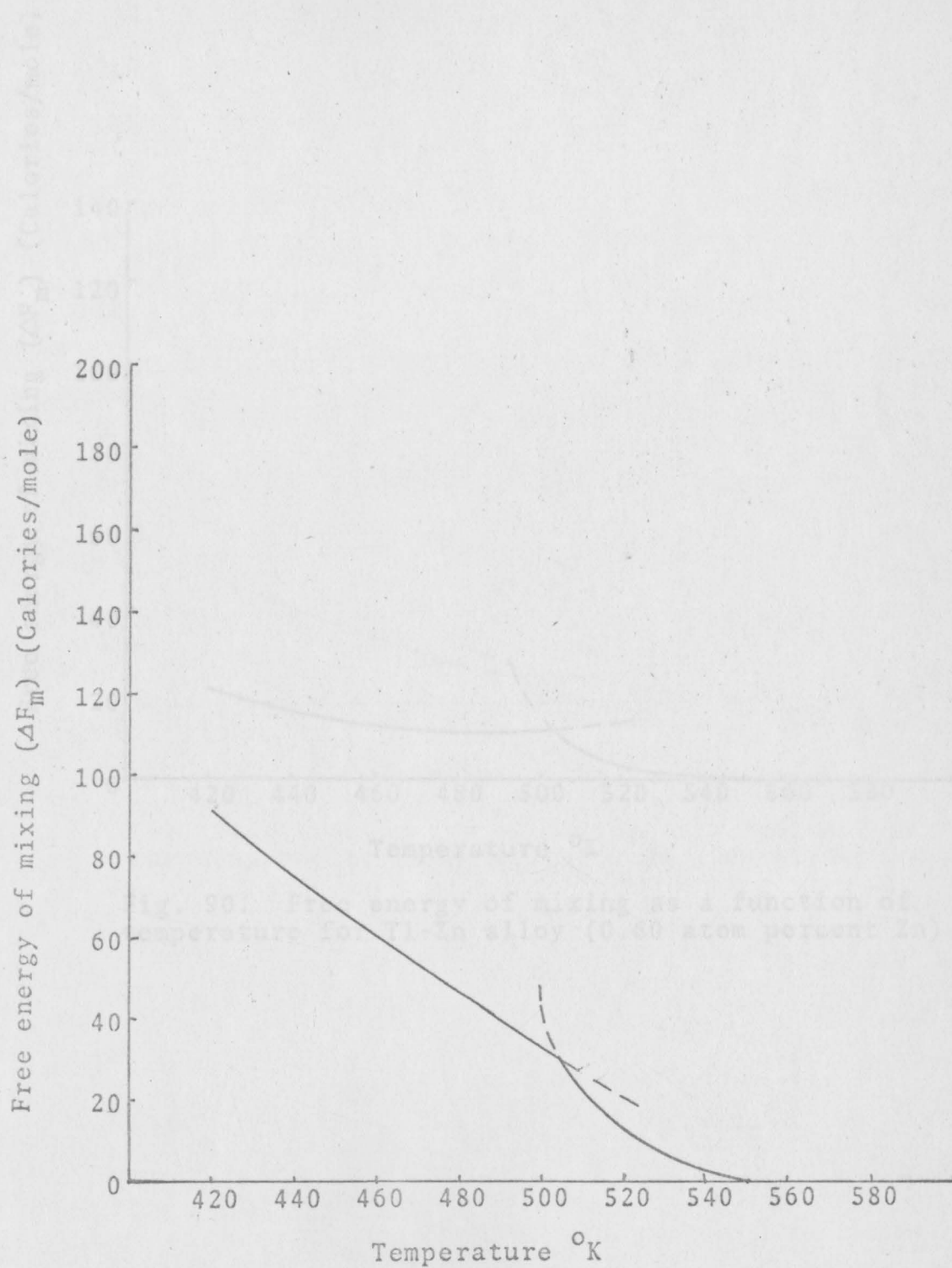


Fig. 89. Free energy of mixing as a function of temperature for Tl-Zn alloy (0.40 atom percent Zn)

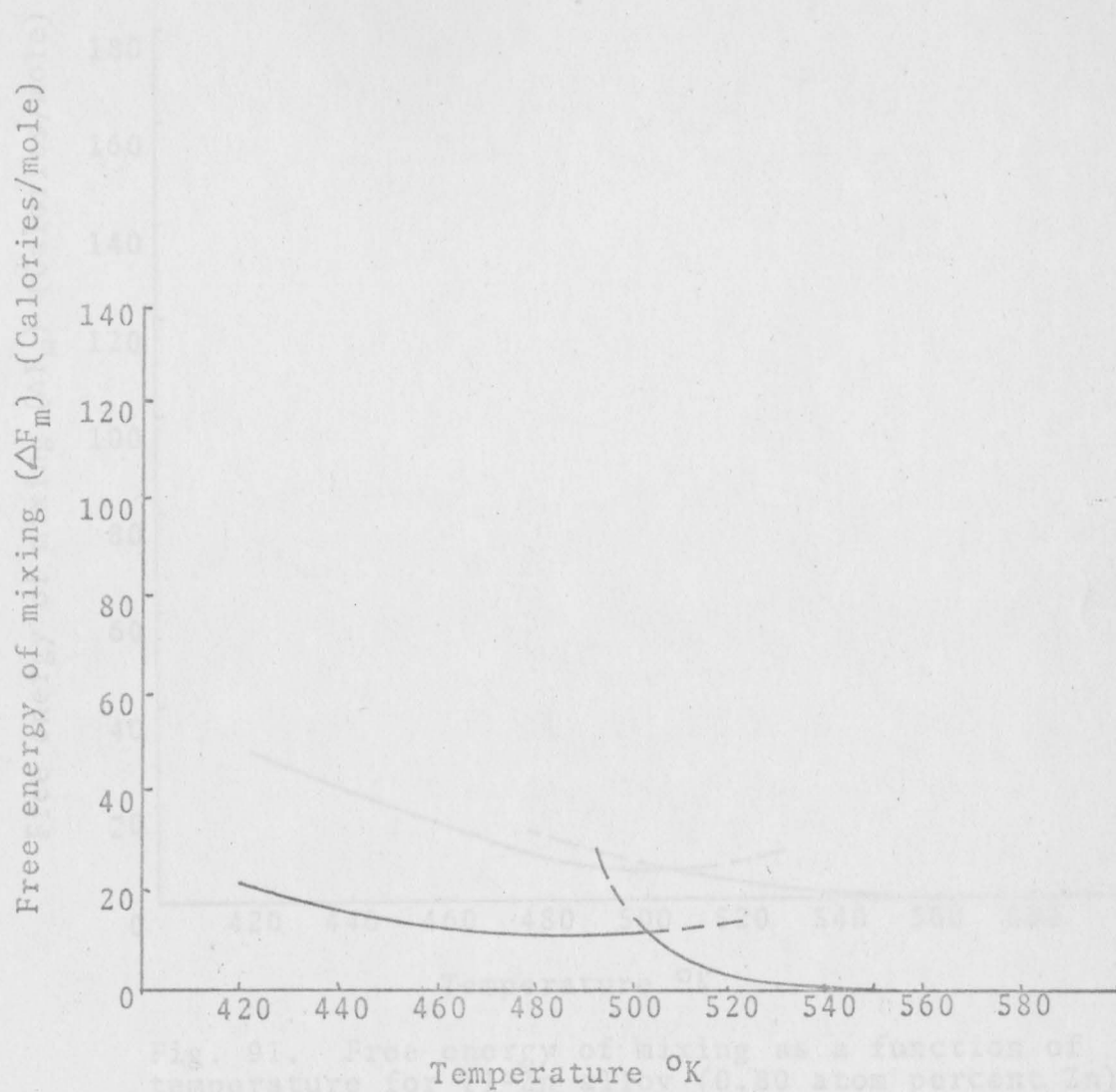


Fig. 90. Free energy of mixing as a function of temperature for Tl-Zn alloy (0.60 atom percent Zn)

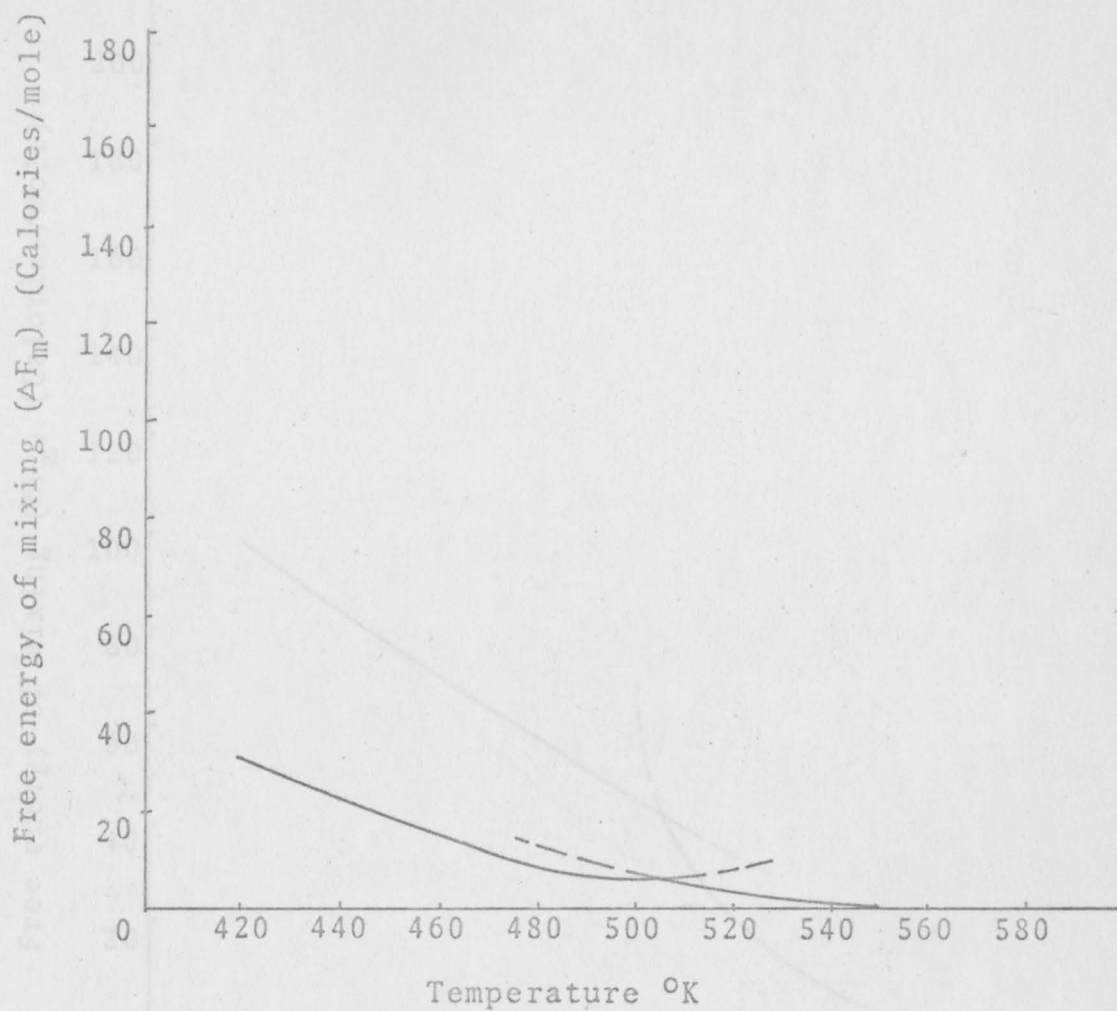


Fig. 91. Free energy of mixing as a function of temperature for Tl-Zn alloy (0.80 atom percent Zn)

Fig. 92. Free energy of mixing as a function of temperature for Tl-Zn alloy (1.0 atom percent Zn)

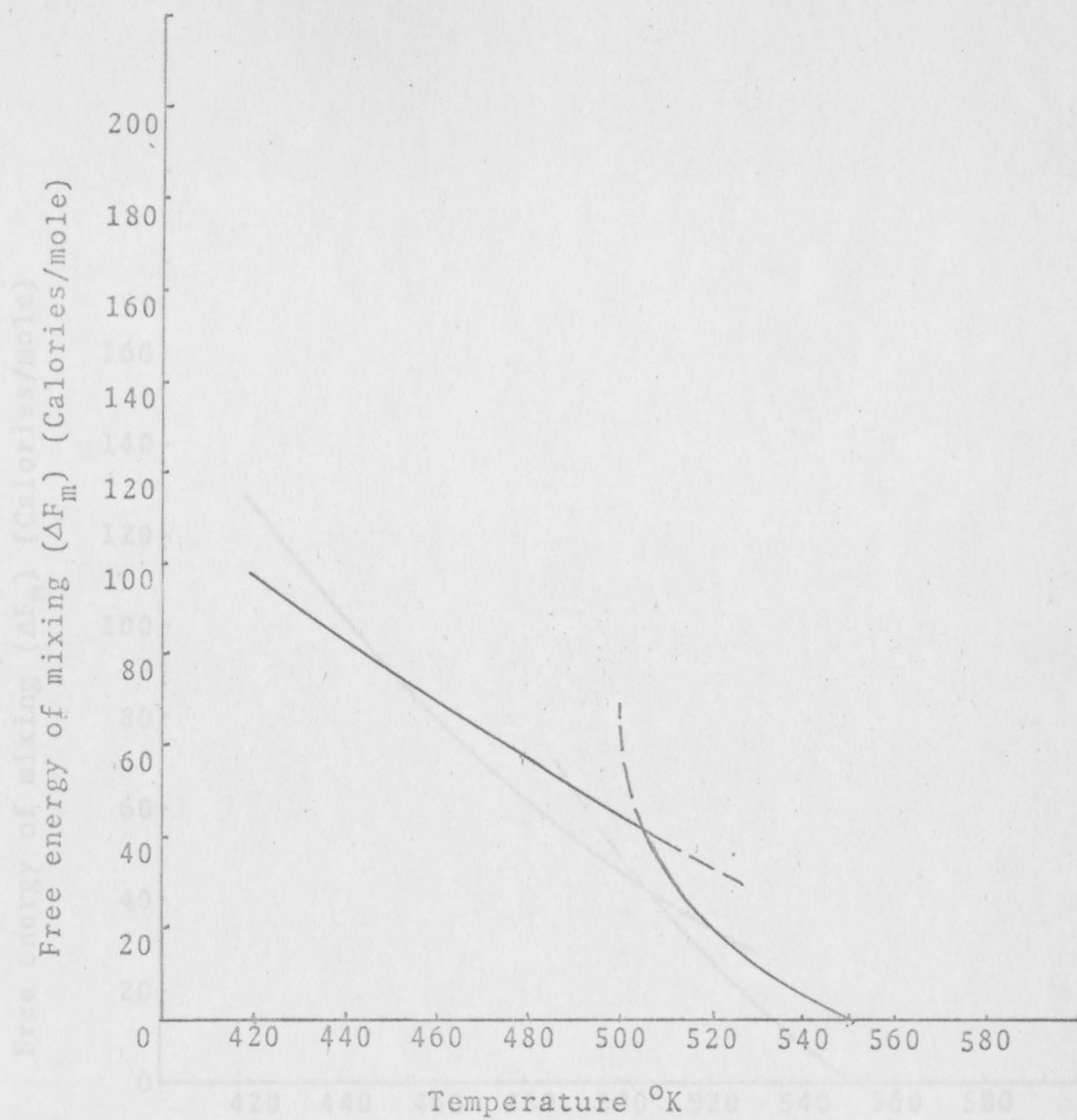


Fig. 92. Free energy of mixing as a function of temperature for Tl-Zn alloy (1.0 atom percent Zn)

Fig. 93. Free energy as a function of temperature for Tl-Zn alloy (1.20 atom percent Zn)

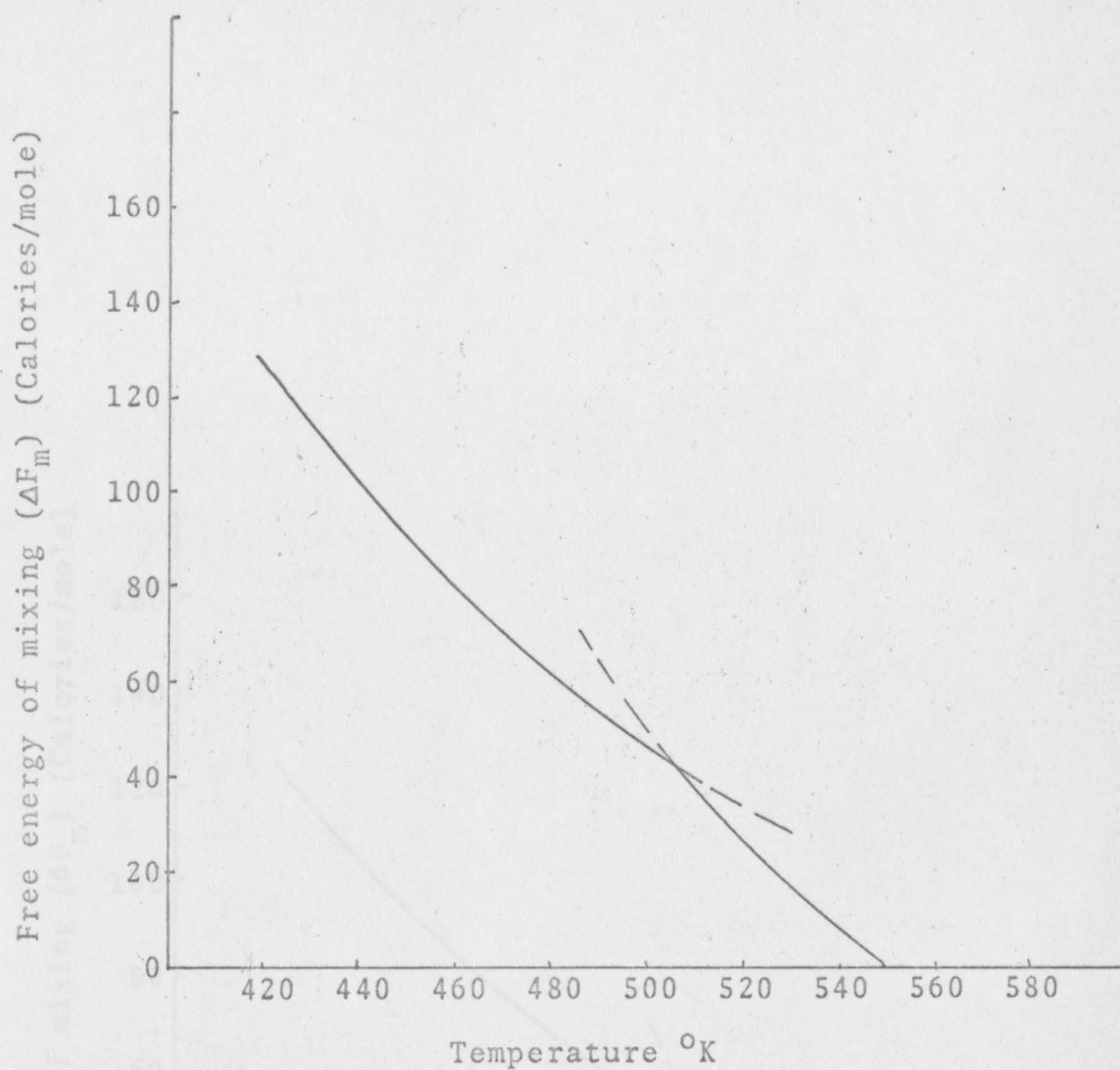


Fig. 93. Free energy as a function of temperature for Tl-Zn alloy (1.20 atom percent Zn)

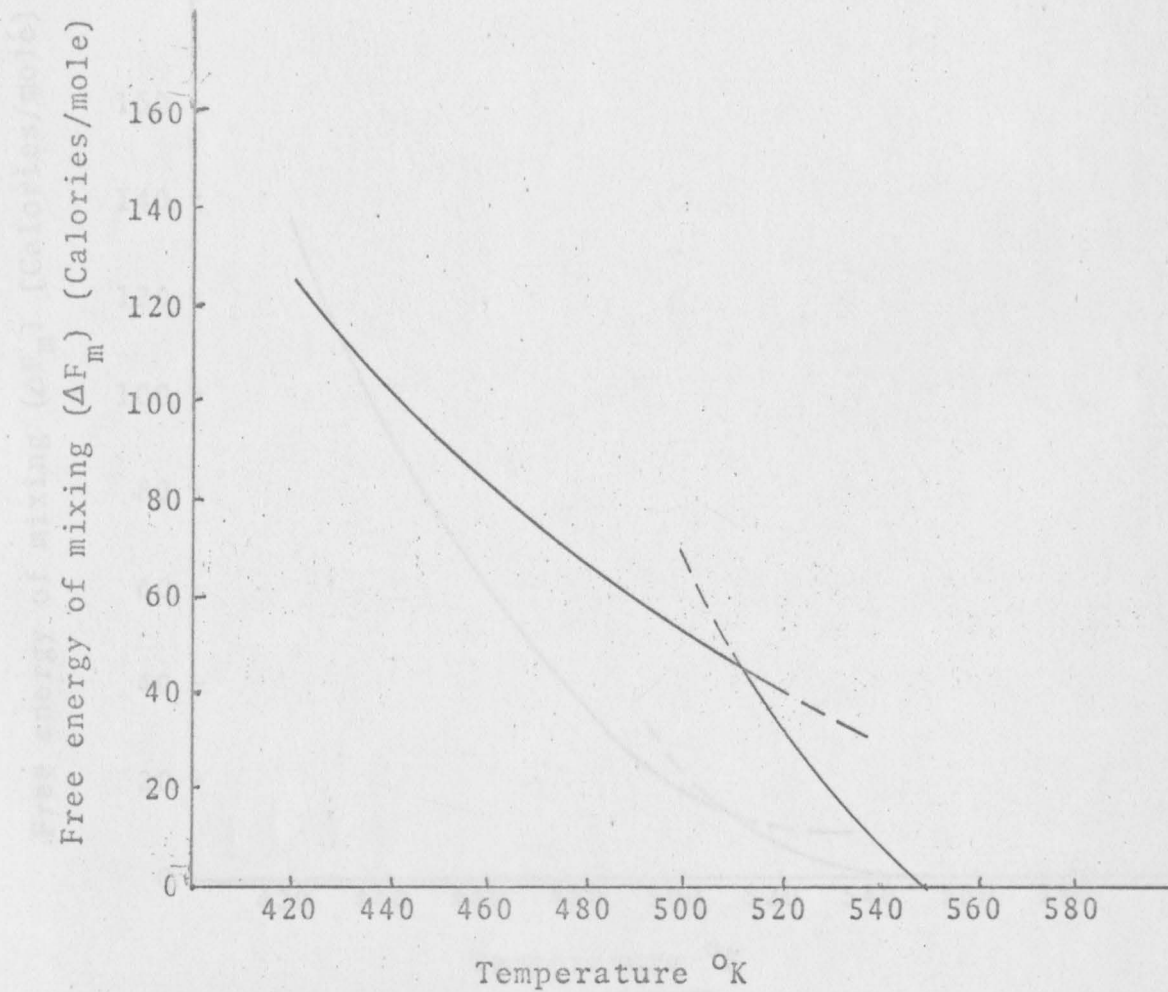


Fig. 94. Free energy as a function of temperature for Tl-Cd alloy (0.044 atom percent Cd)

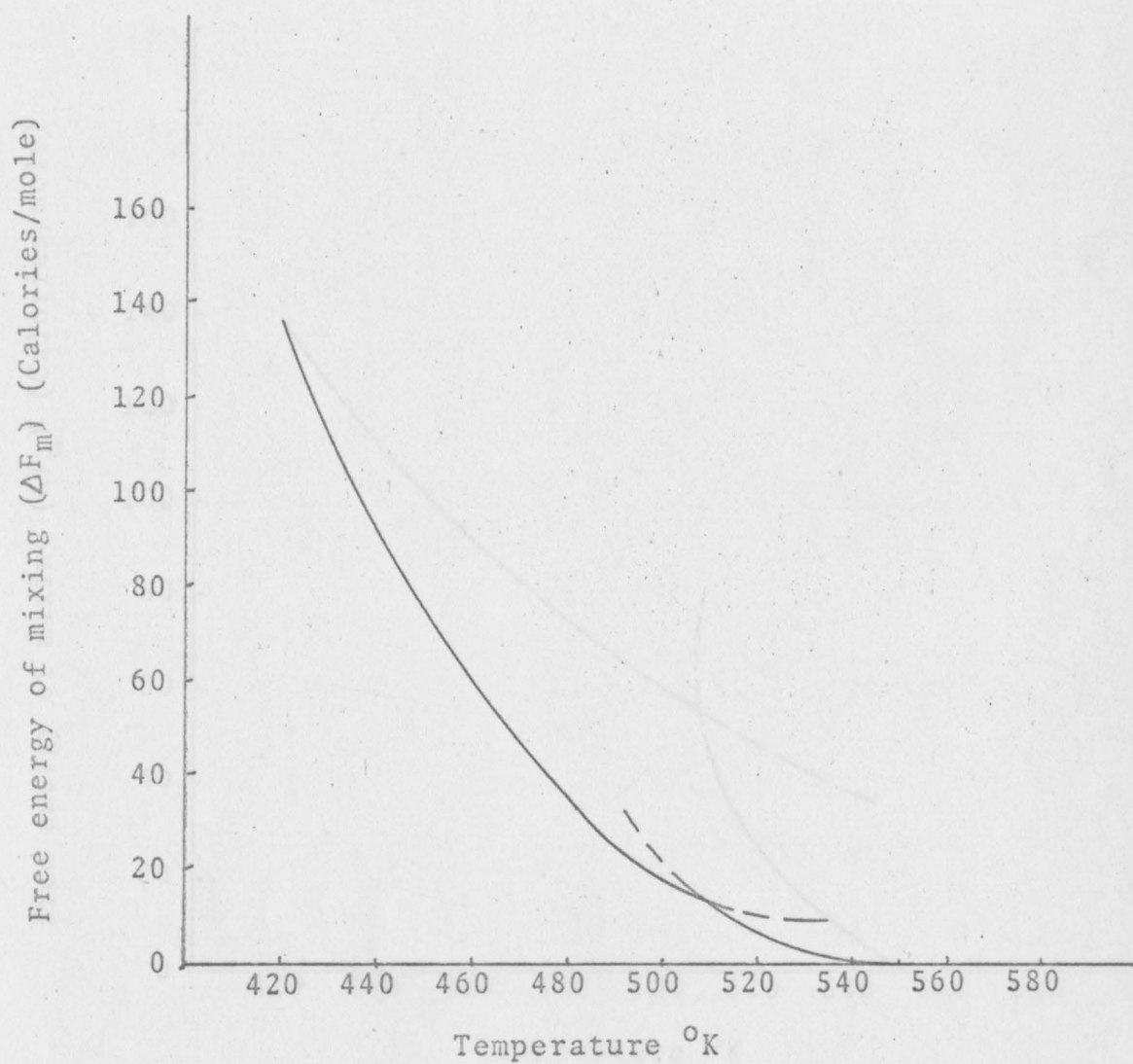


Fig. 95. Free energy <sup>of mixing</sup> as a function of temperature for Tl-Cd alloy (0.18 atom percent Cd)

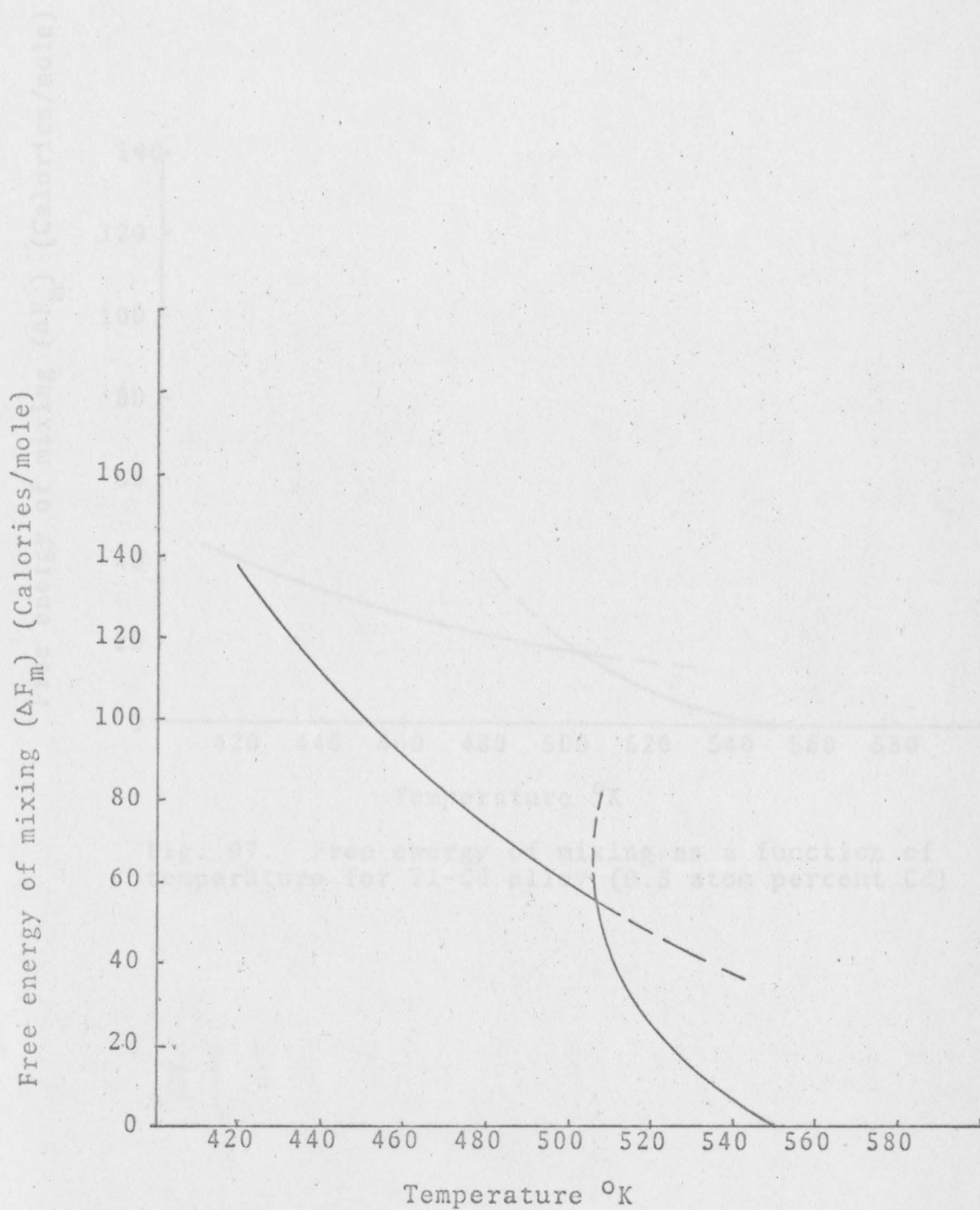


Fig. 96. Free energy of mixing as a function of temperature for Tl-Cd alloy (0.44 atom percent Cd)



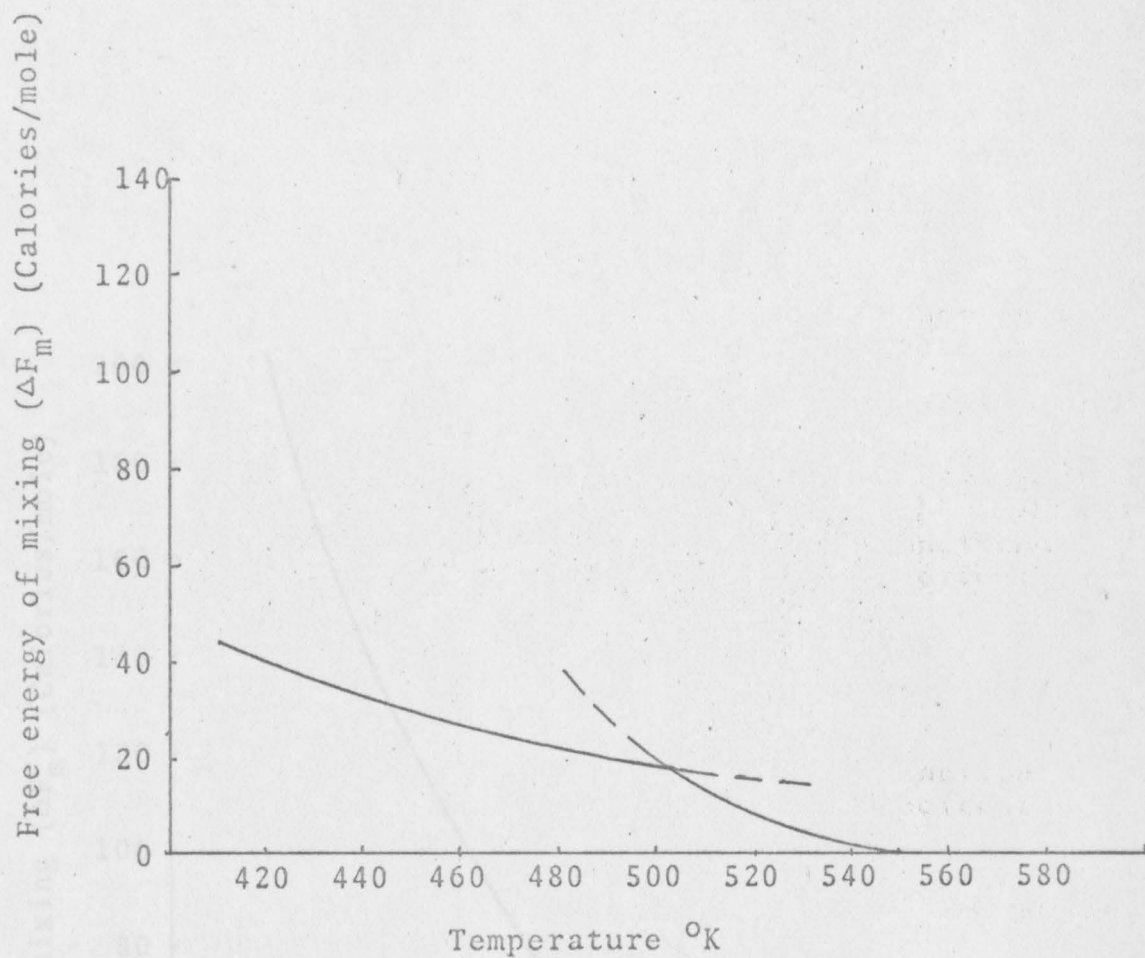


Fig. 97. Free energy of mixing as a function of temperature for Tl-Cd alloy (0.5 atom percent Cd)

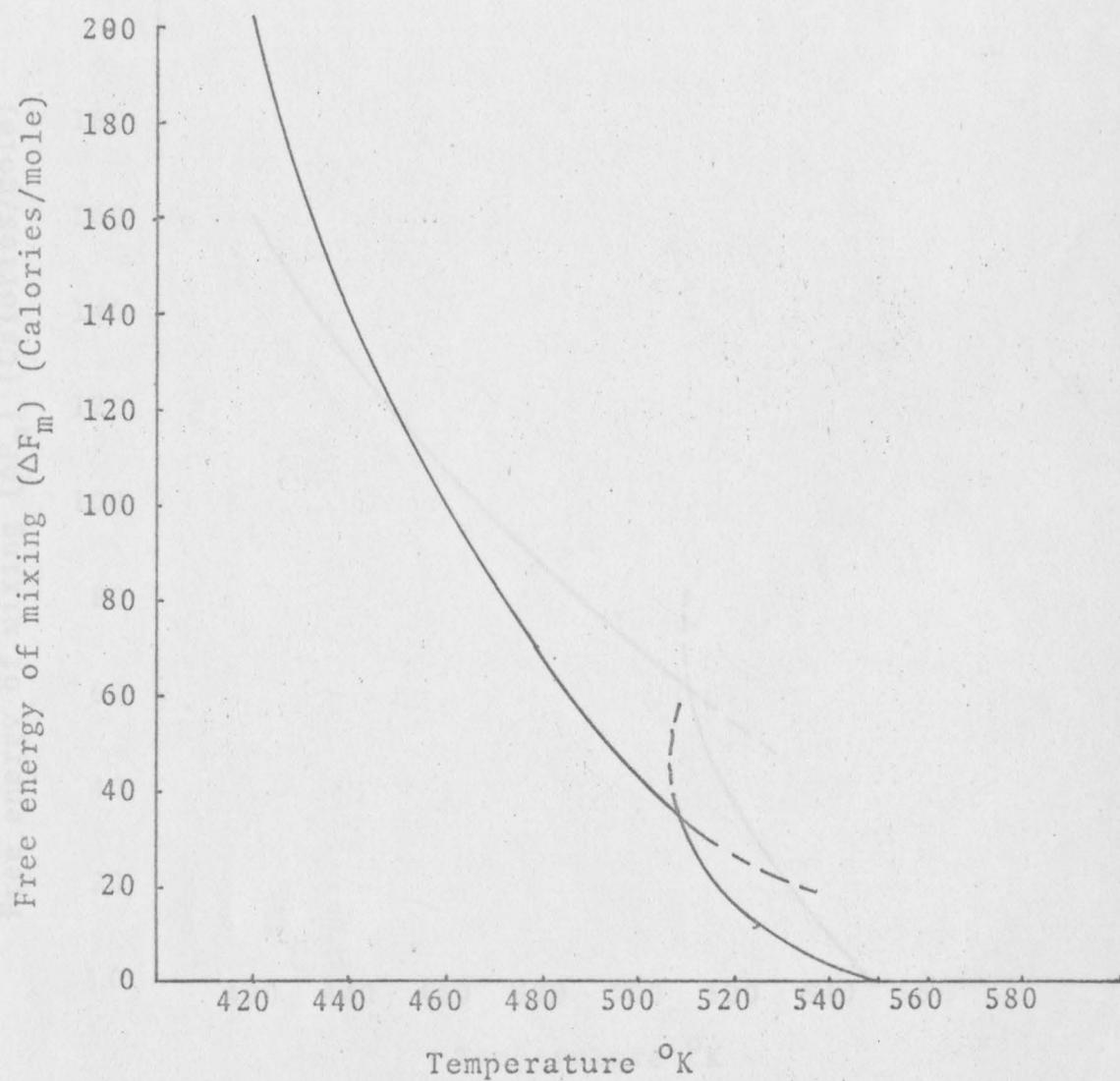


Fig. 98. Free energy of mixing as a function of temperature for Tl-Cd alloy (0.6 atom percent Cd)

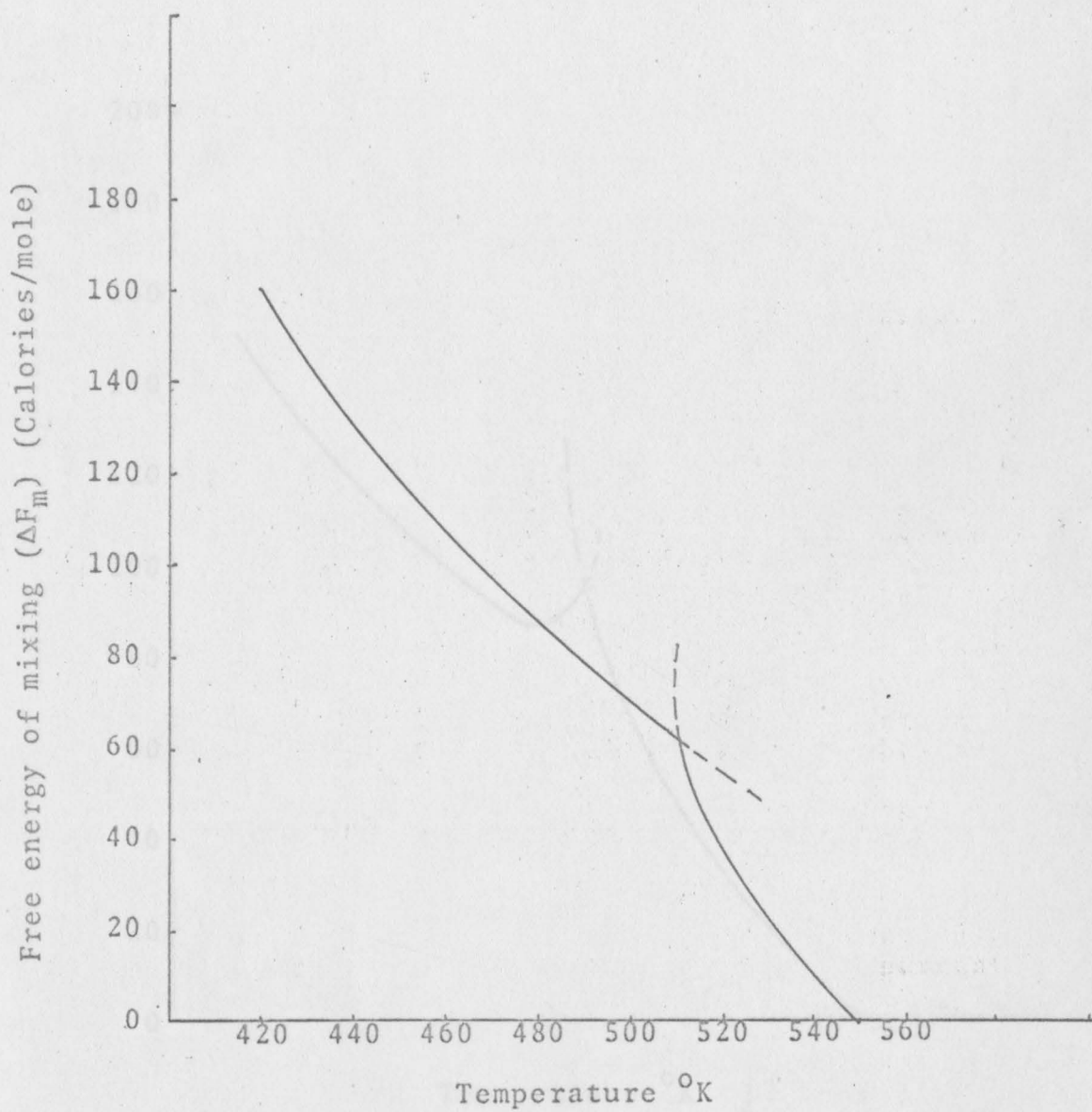


Fig.99. Free energy of mixing as a function of temperature for Tl-Cd alloy (0.88 atom percent Cd)

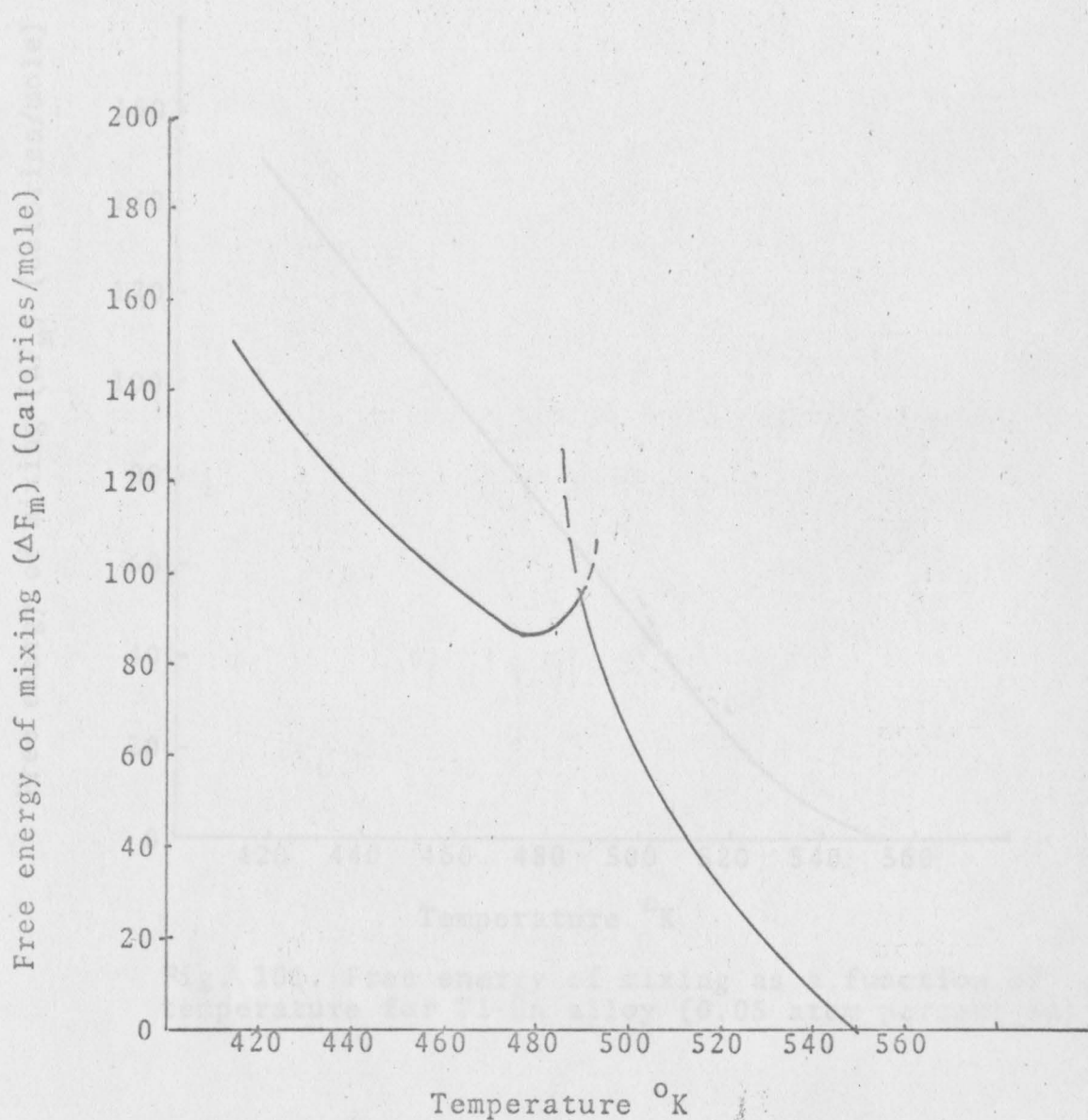


Fig. 100. Free energy of mixing as a function of temperature for Tl-Cd alloy (1.0 atom percent Cd)

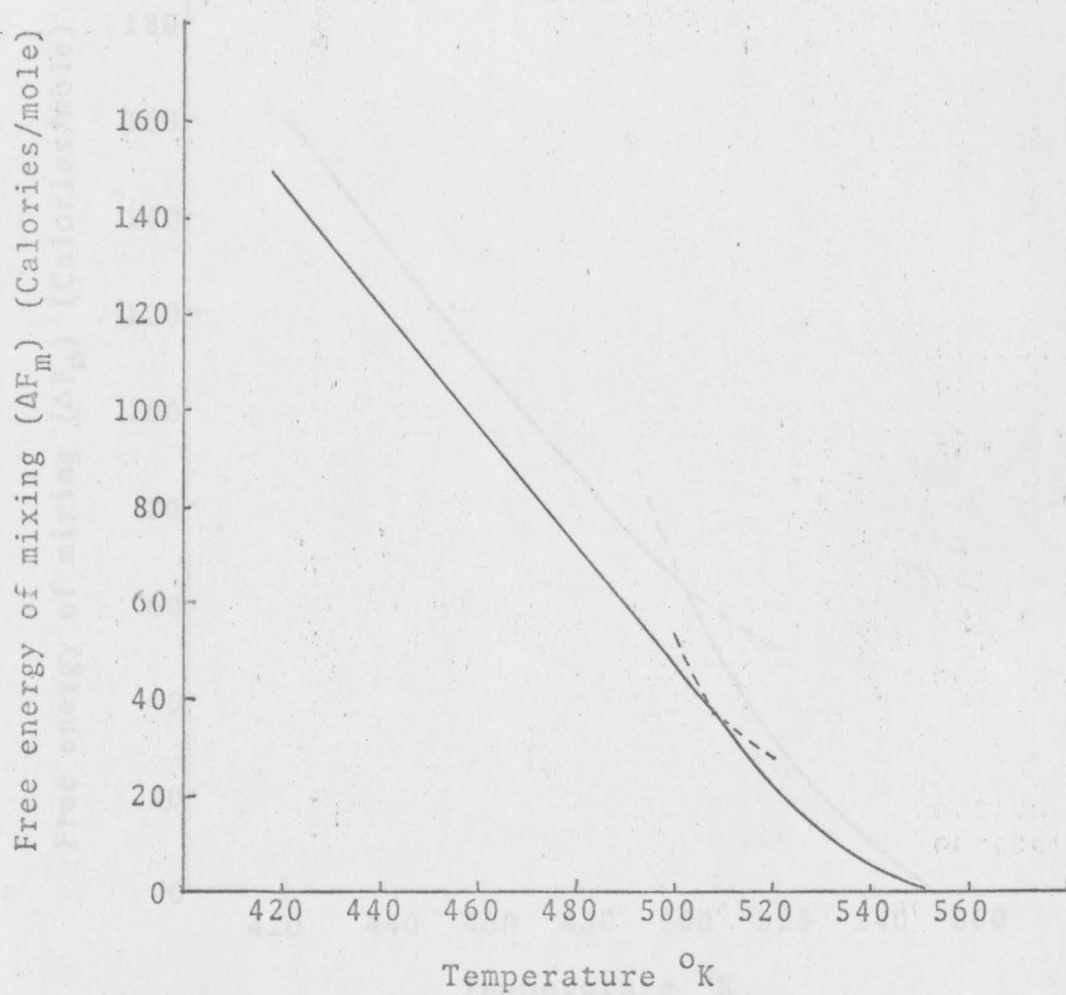


Fig. 101. Free energy of mixing as a function of temperature for Tl-Sn alloy (0.05 atom percent Sn)

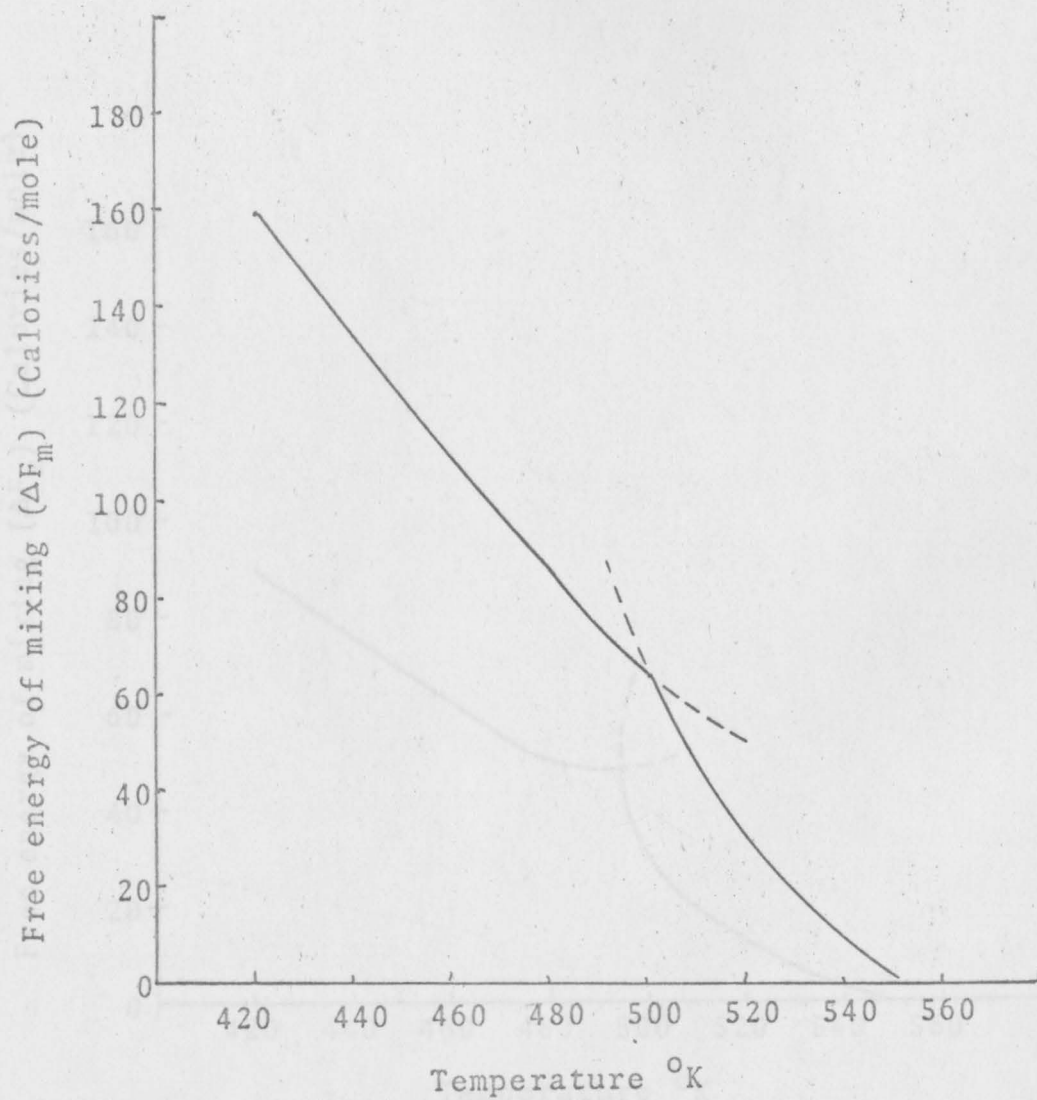


Fig. 102. Free energy of mixing as a function of temperature for Tl-Sn alloy (0.2 atom percent Sn)

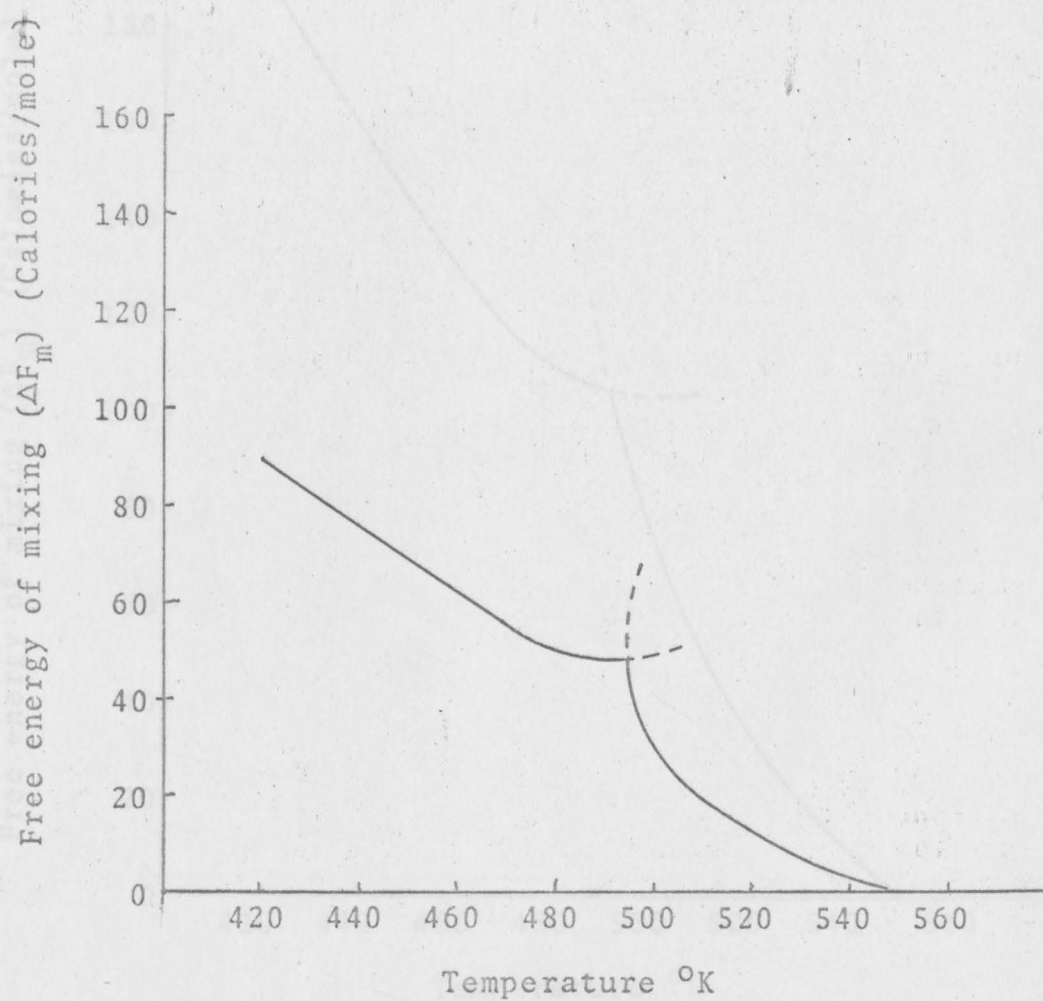


Fig. 103. Free energy of mixing as a function of temperature for Tl-Sn alloy (0.4 atom percent Sn)

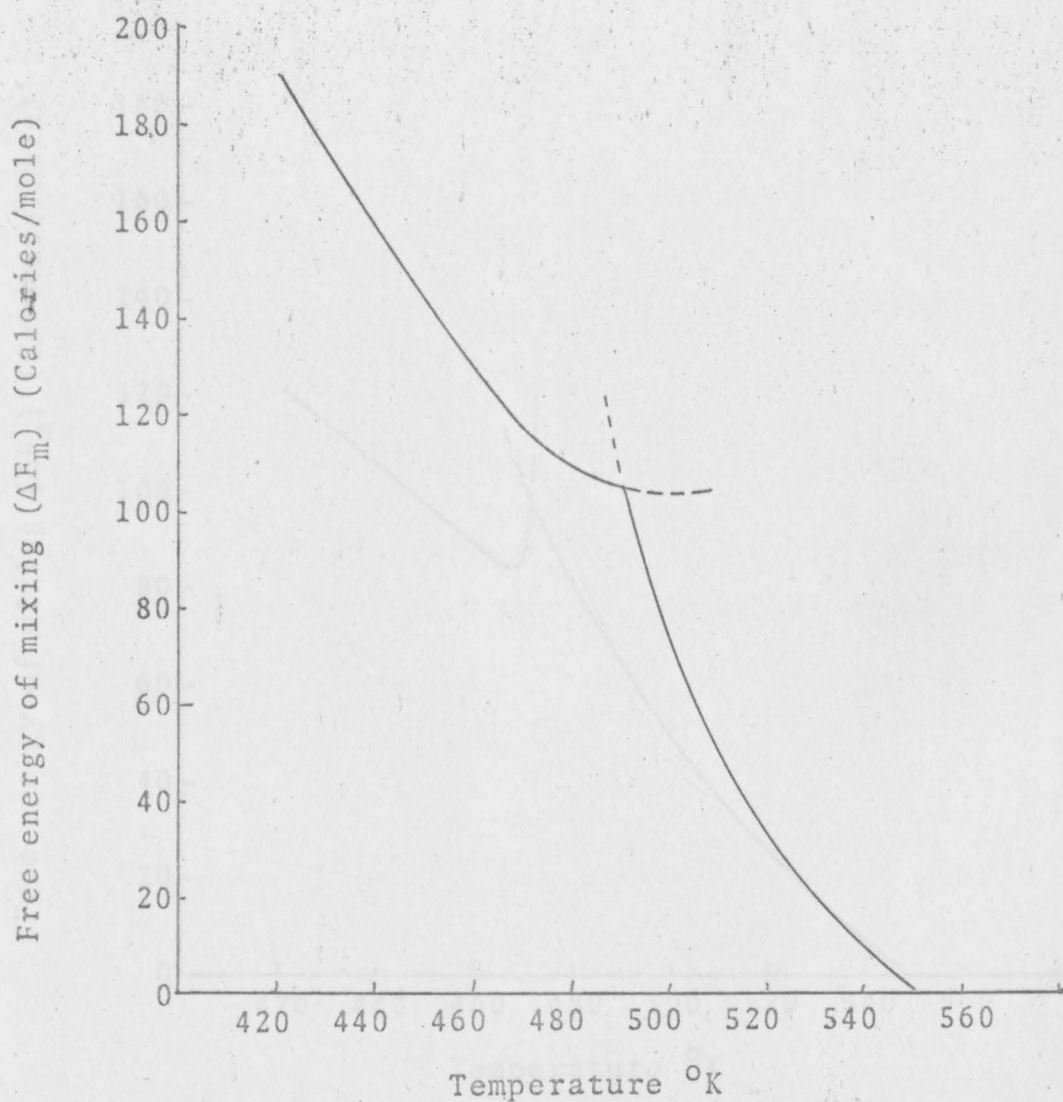


Fig. 104. Free energy of mixing as a function of temperature for Tl-Sn alloy (0.6 atom percent Sn)



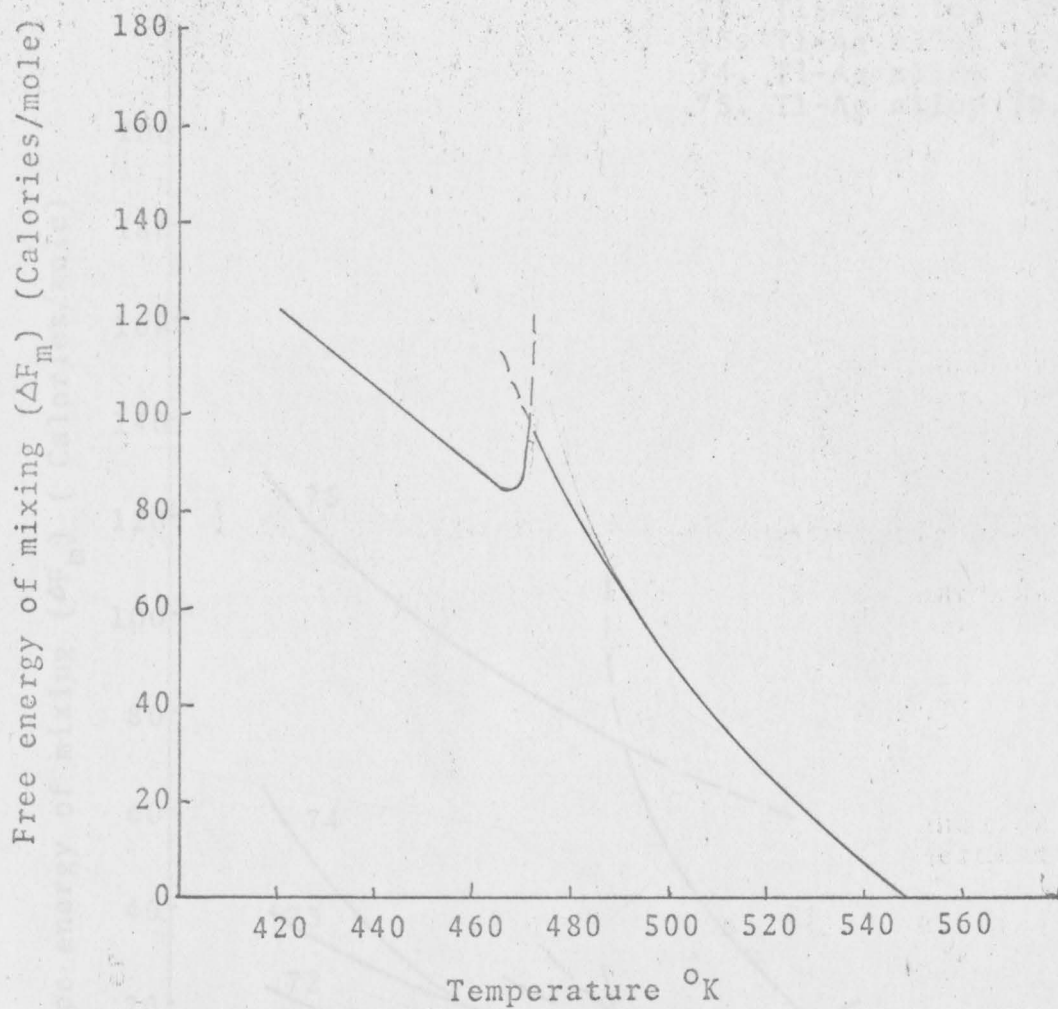


Fig. 105. Free energy of mixing as a function of temperature for Tl-Sn alloy (1.0 atom percent Sn)

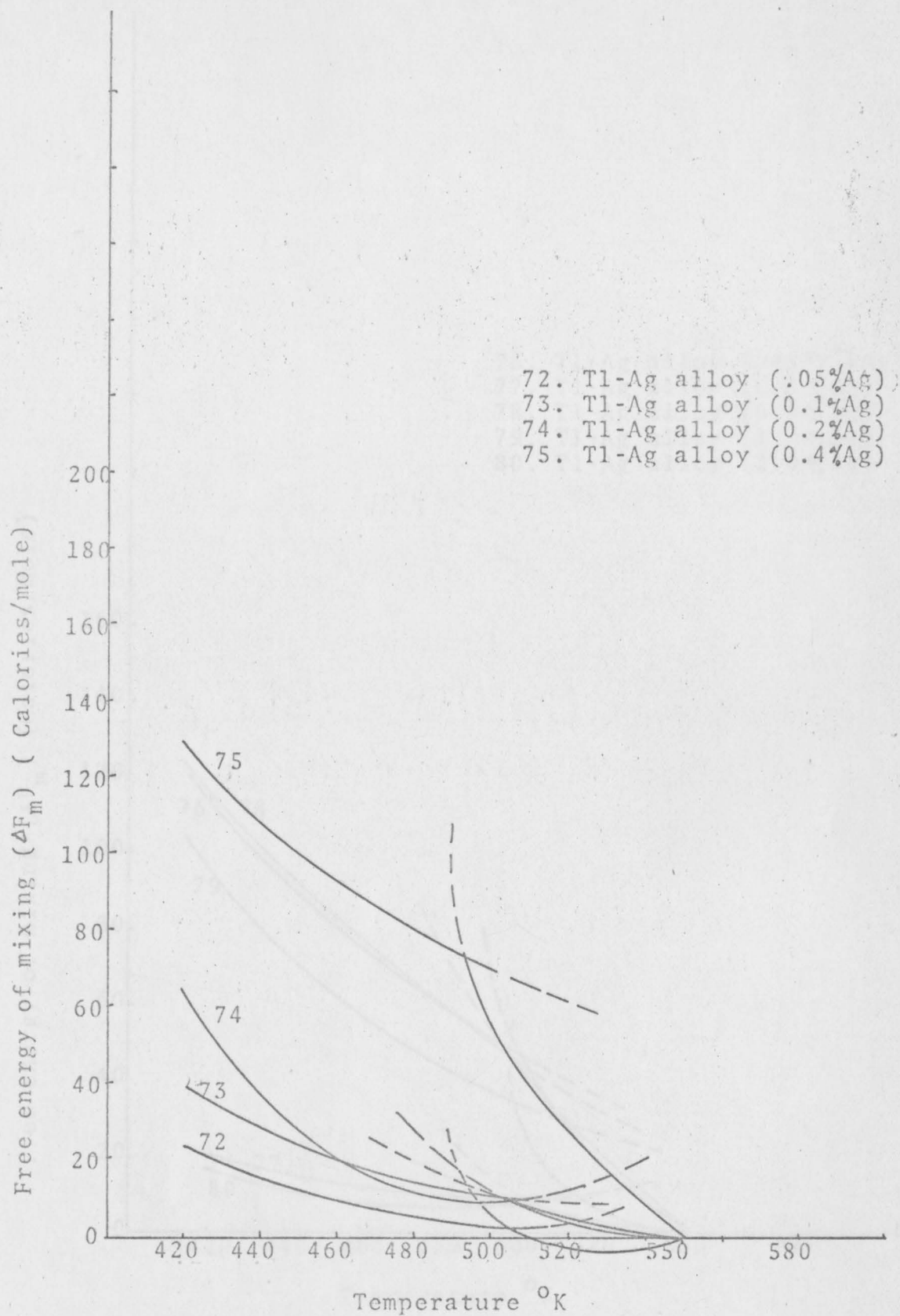


Fig. 106. The combined curves of free energy,  $\Delta F_m$ , as function of temperature for a group of alloys. m

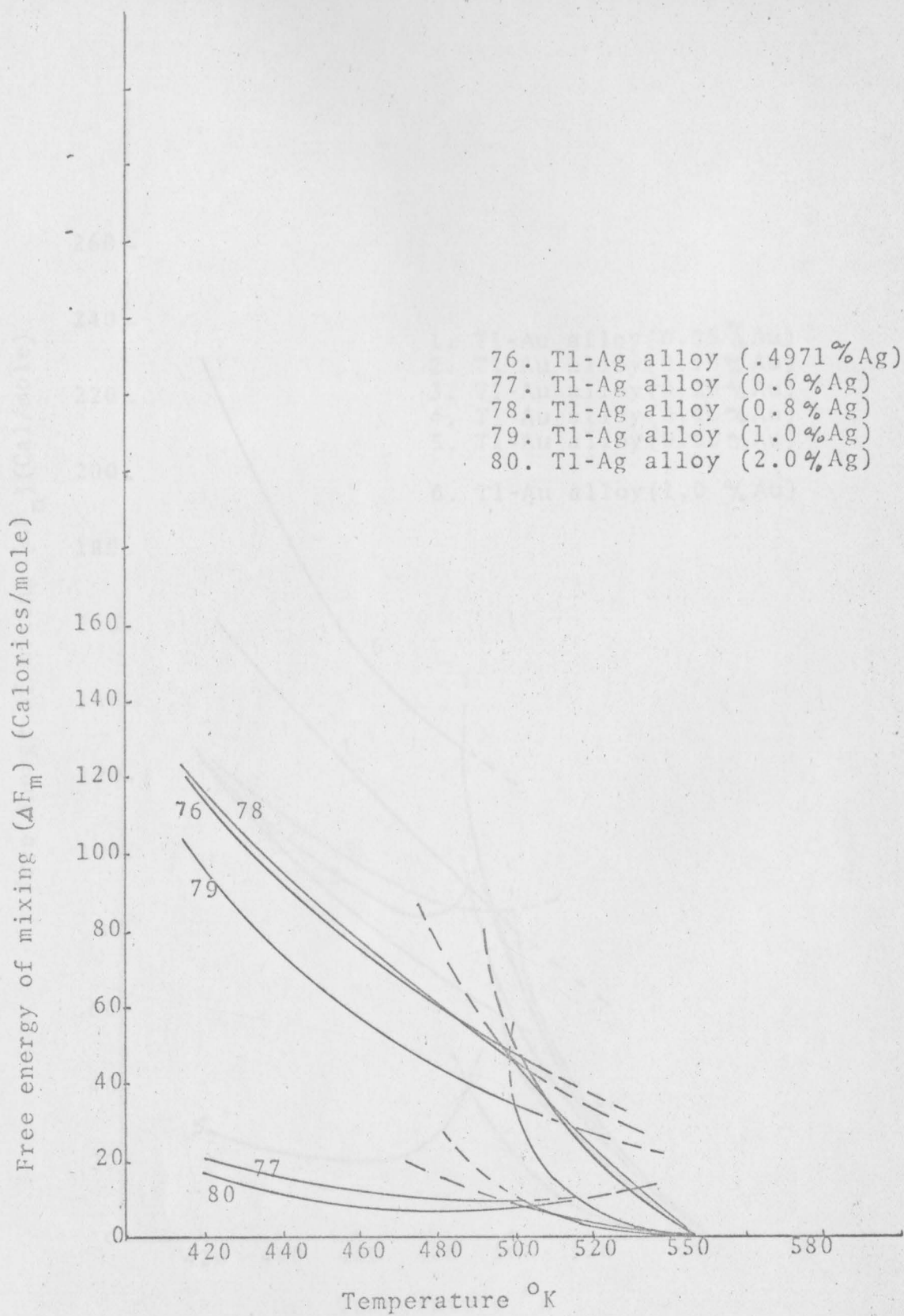


Fig. 167. The combined curves of free energy of mixing as a function of temperature for a group of alloys.

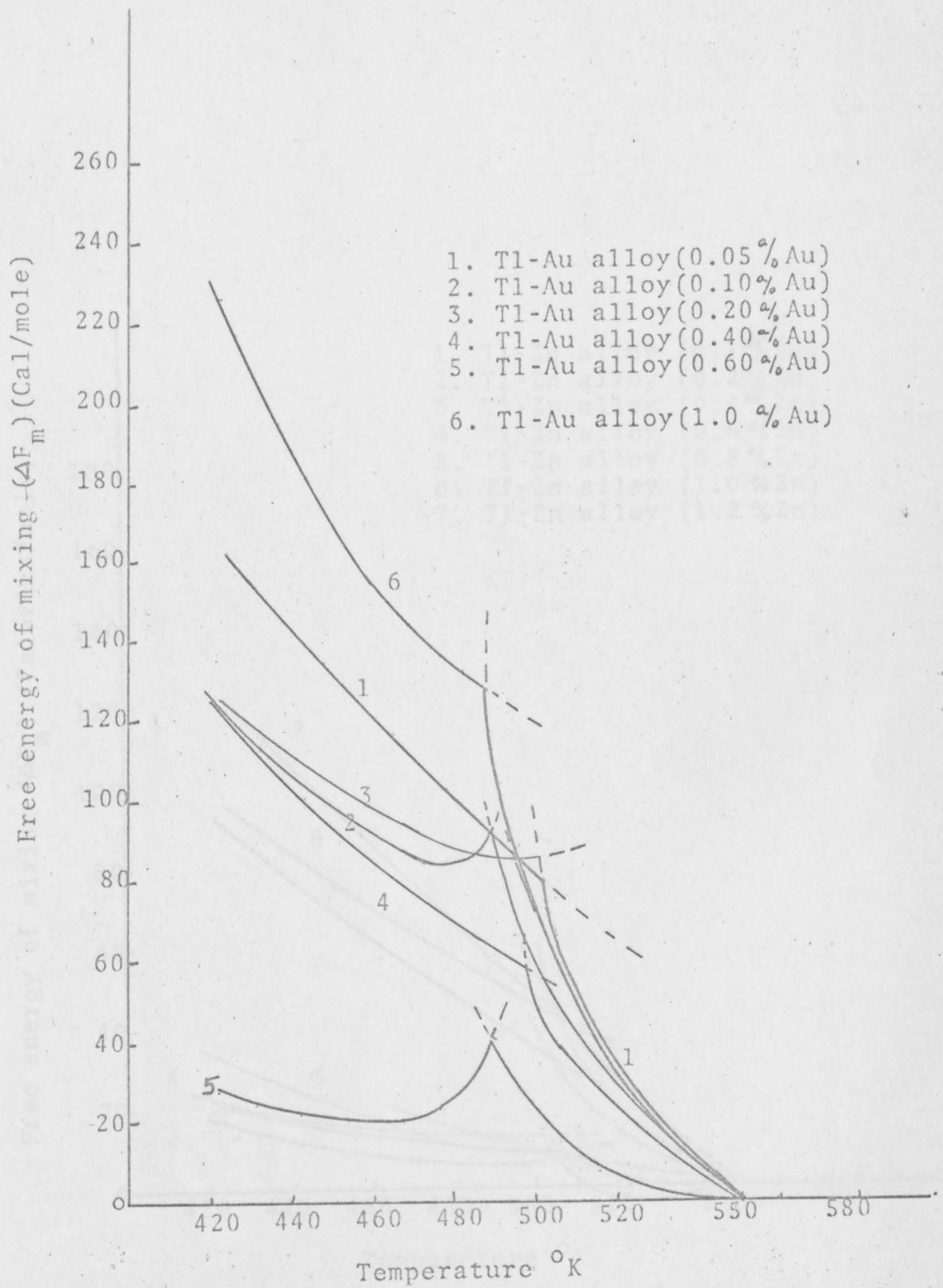


Fig. 108. The combined curves of free energy of mixing as a function of temperature for Tl-Au alloys.

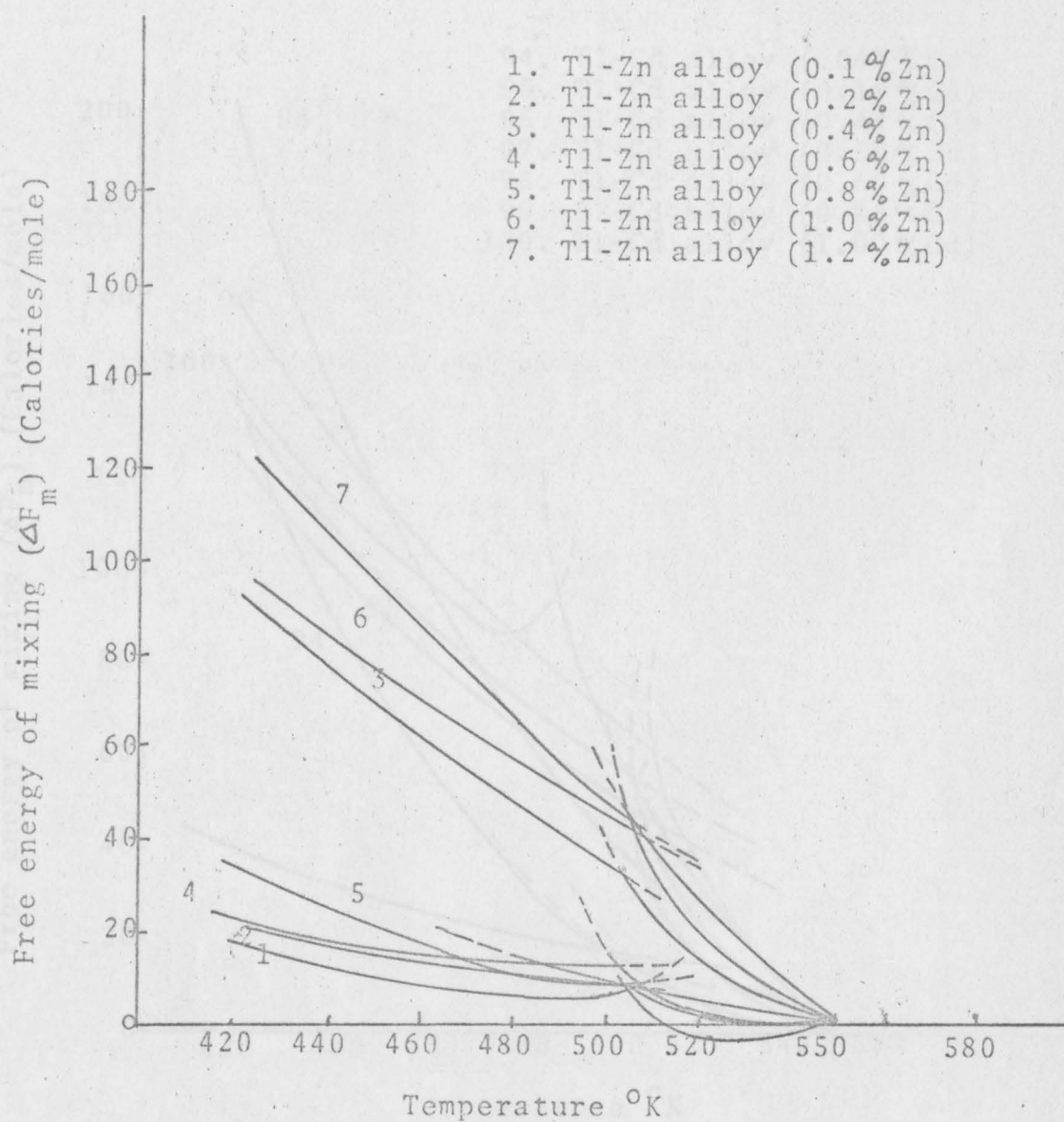


Fig. 109. The combined curves of free energy of mixing as a function of temperature for Tl-Zn alloys.

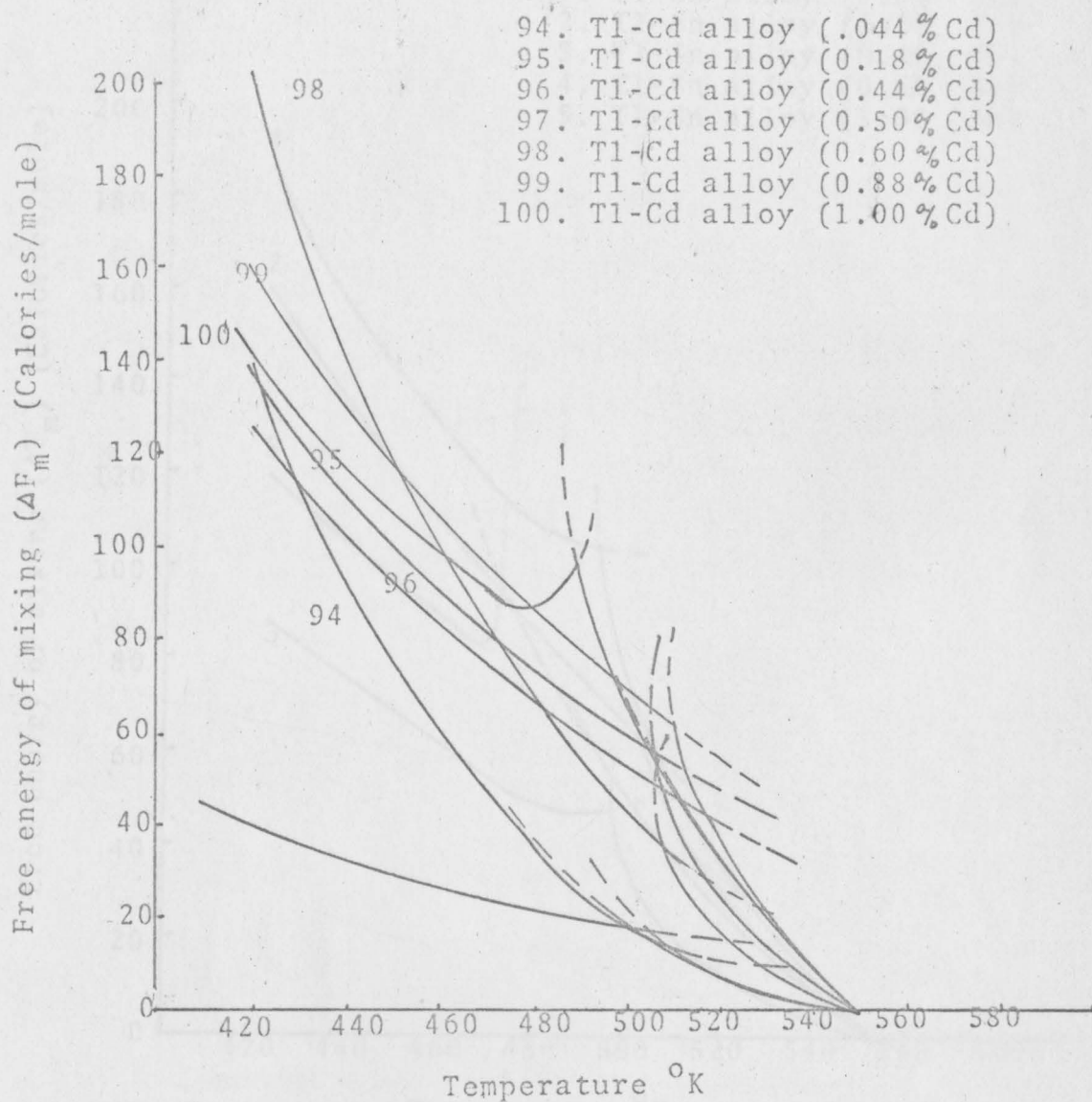


Fig. 110. The combined curves of free energy of mixing as a function of temperature, for Tl-Cd alloys.

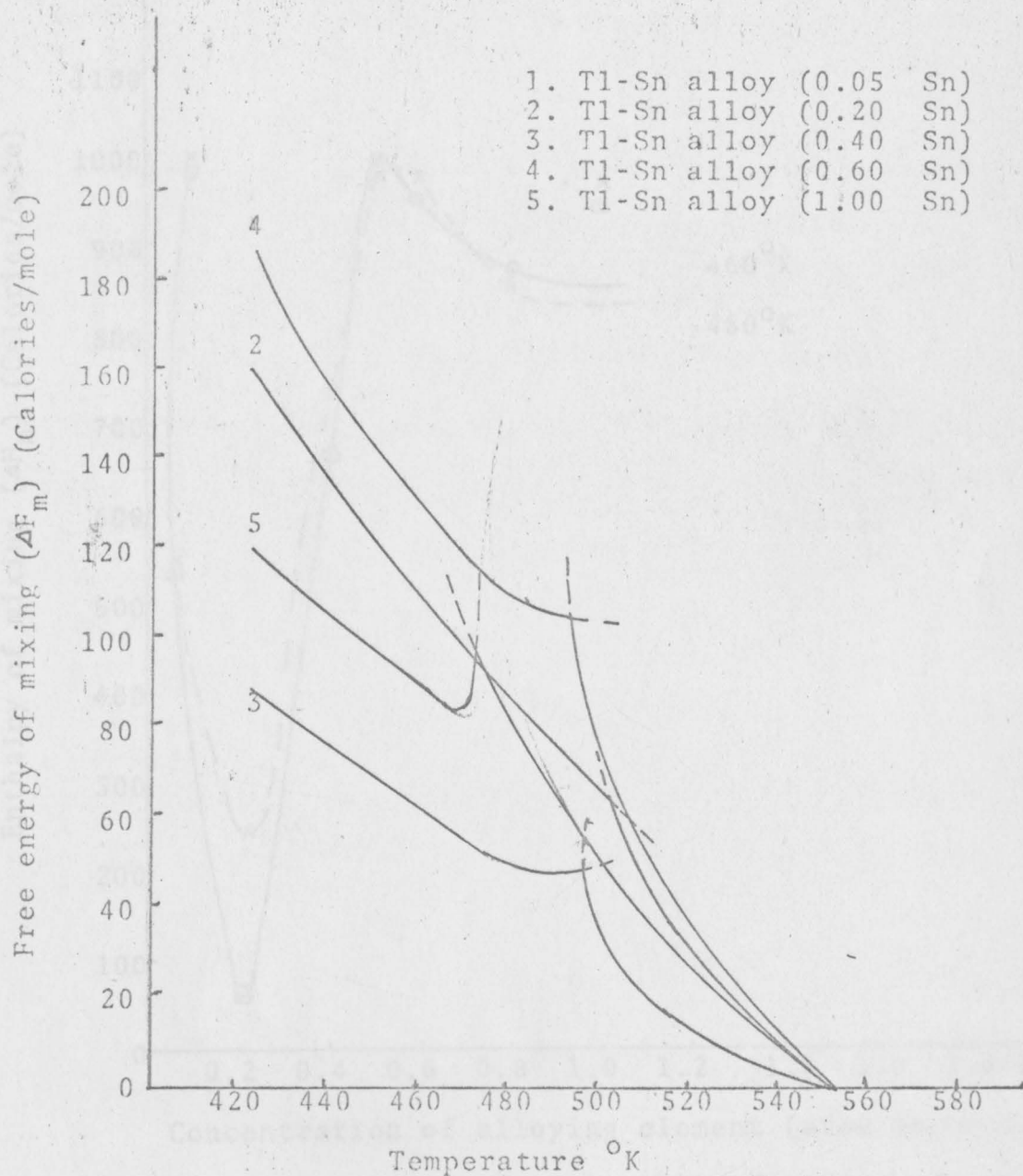


Fig. 111. The combined curves of free energy of mixing as a function of temperature, for Tl-Sn.

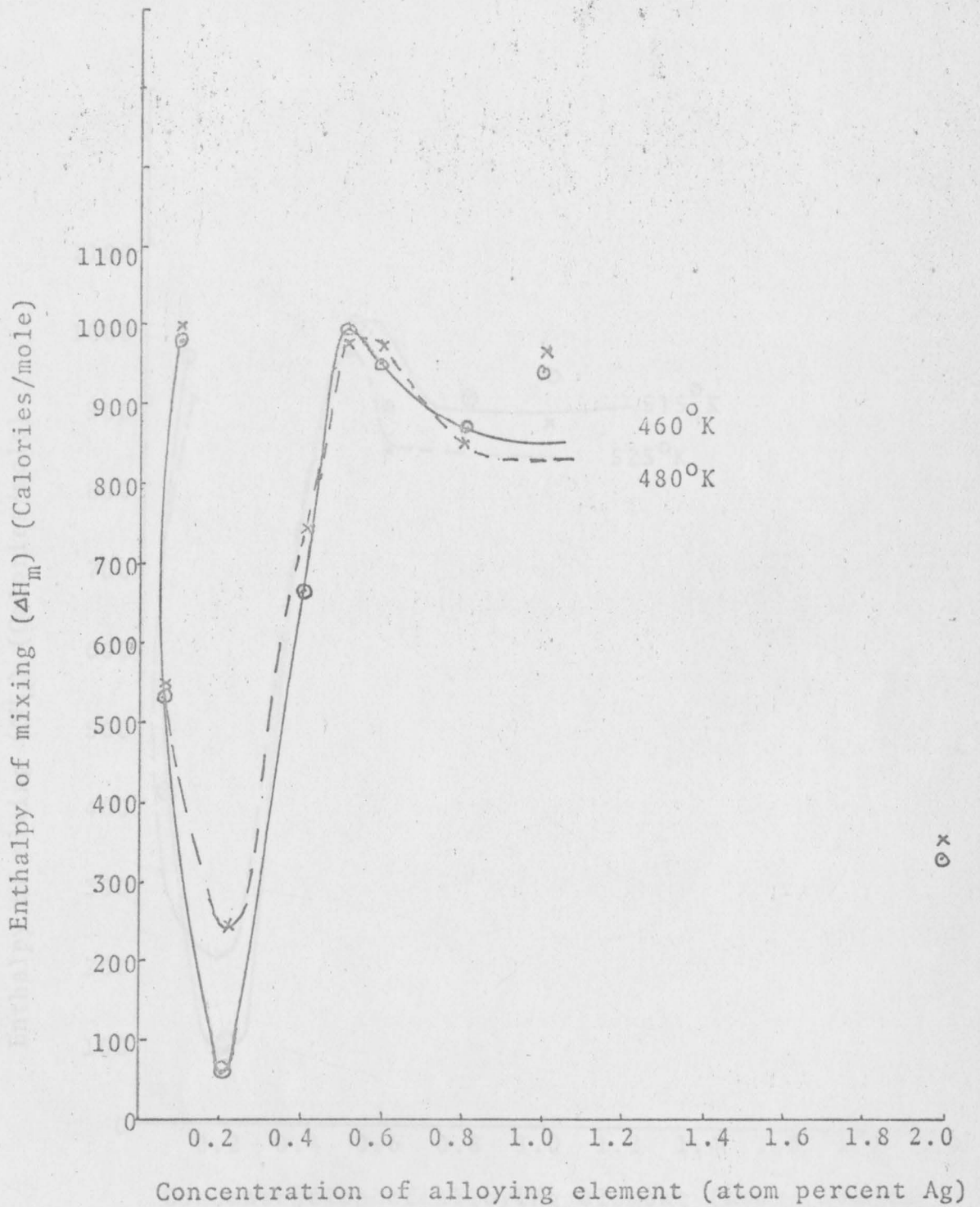


Fig. 112. Enthalpy of mixing as a function of atom percents of alloying element (Ag), for Tl-Ag alloys.



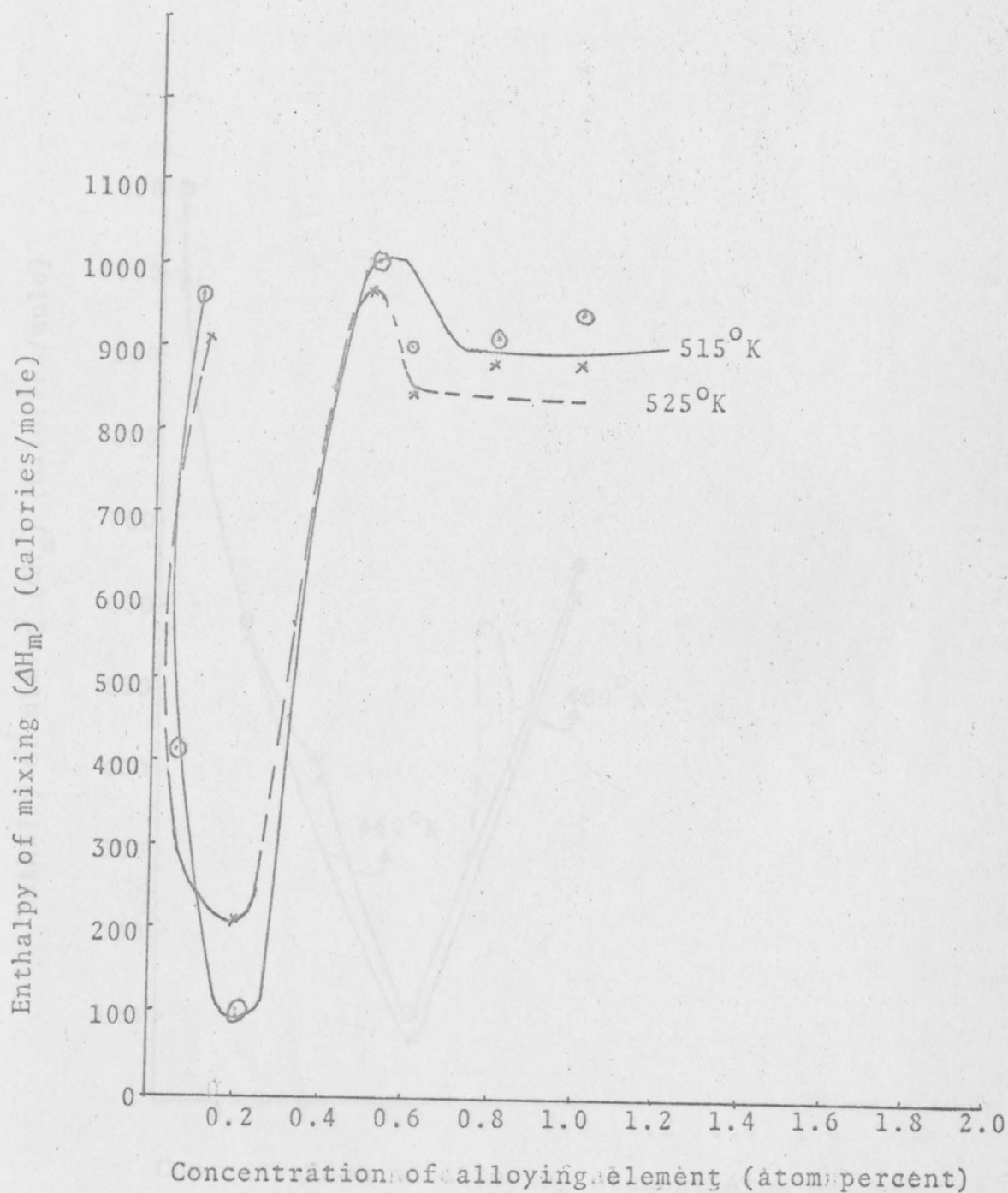


Fig. 113. Enthalpy of mixing as a function of atom percents of alloying element for Tl-Ag alloys.

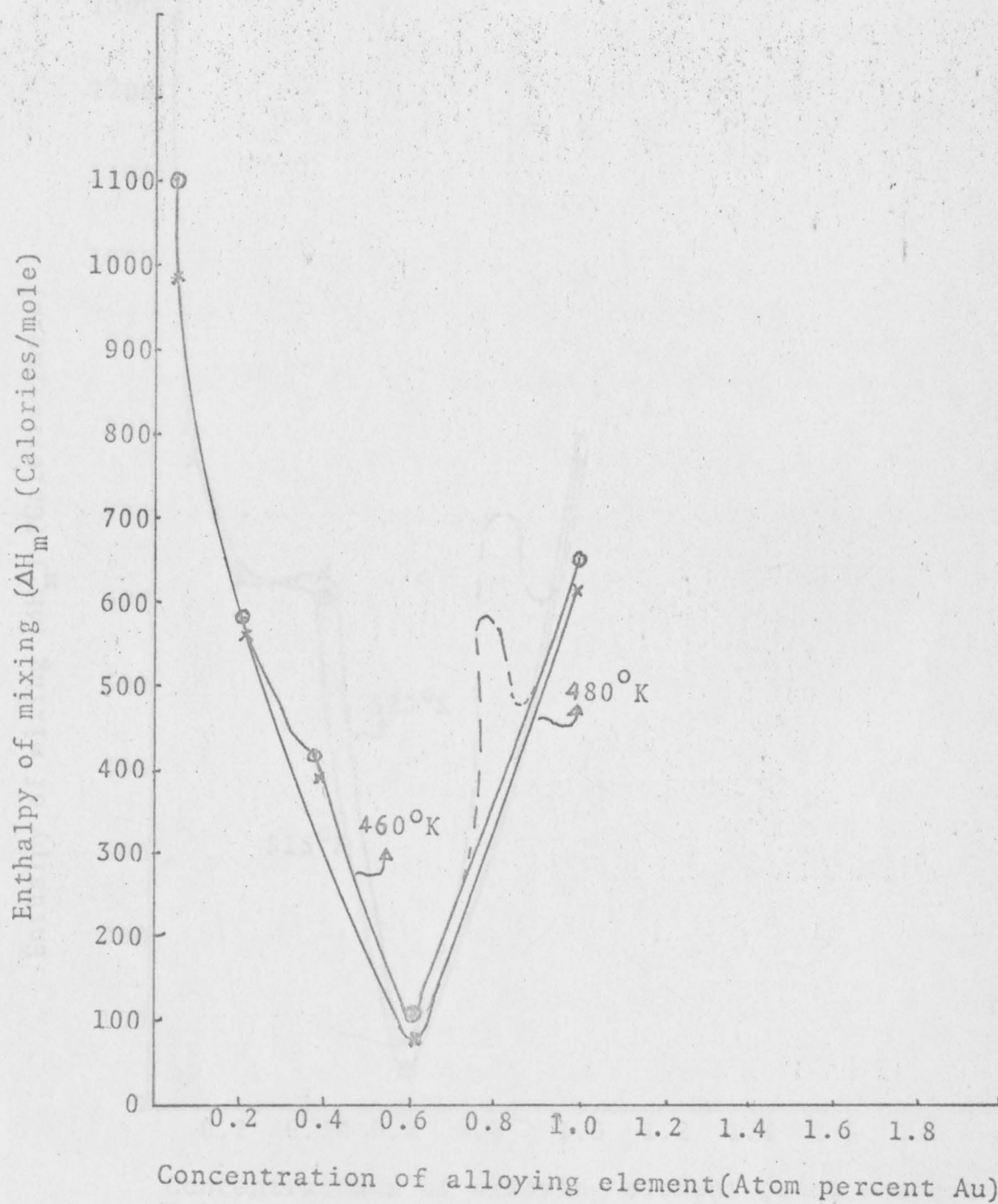


Fig. 114. Enthalpy of mixing as a function of atom percents of alloying element, Au, for Tl-Au alloys.

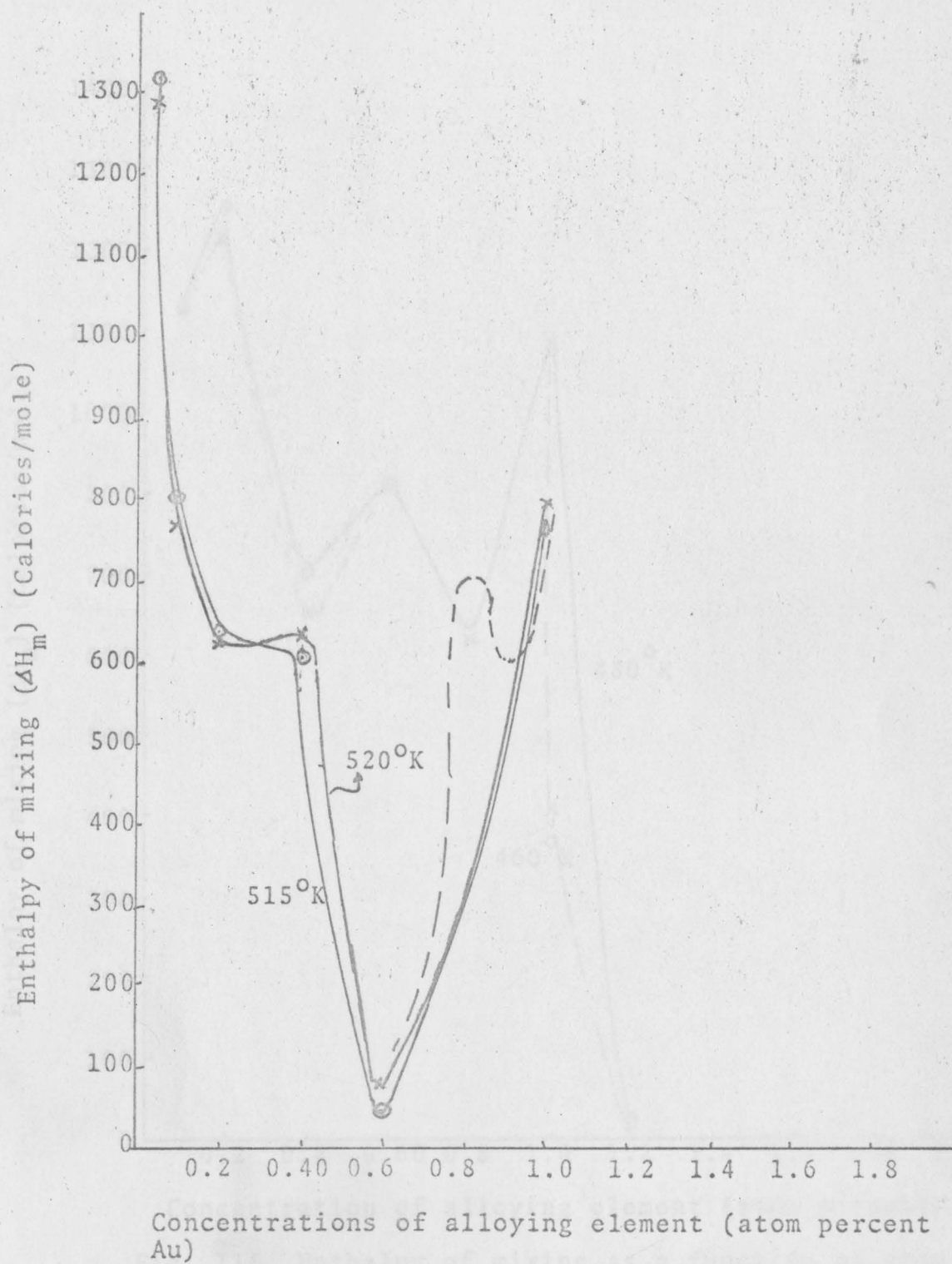


Fig. 115. Enthalpy of mixing as a function of concentration of alloying element, for Tl-Au alloys.

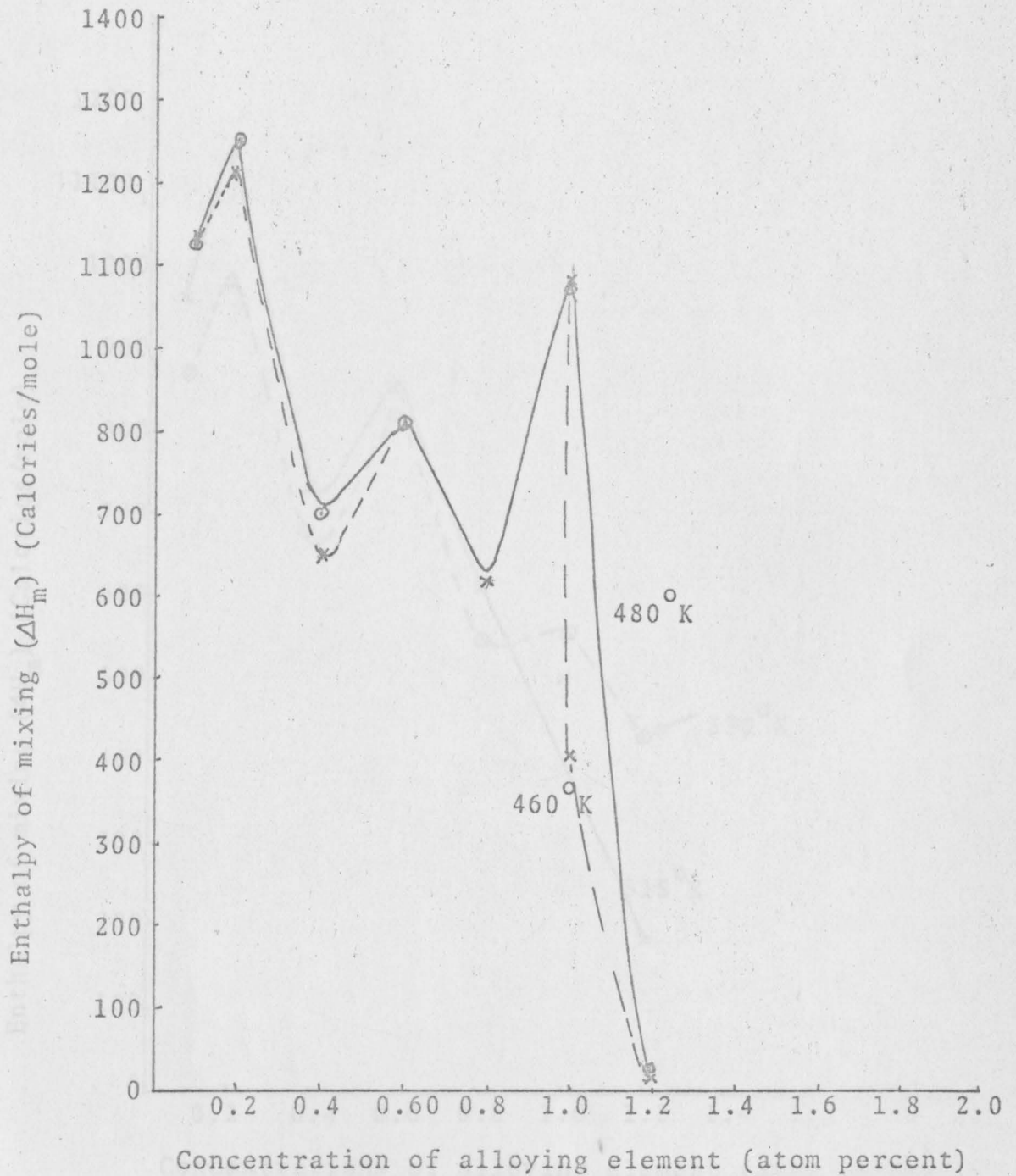
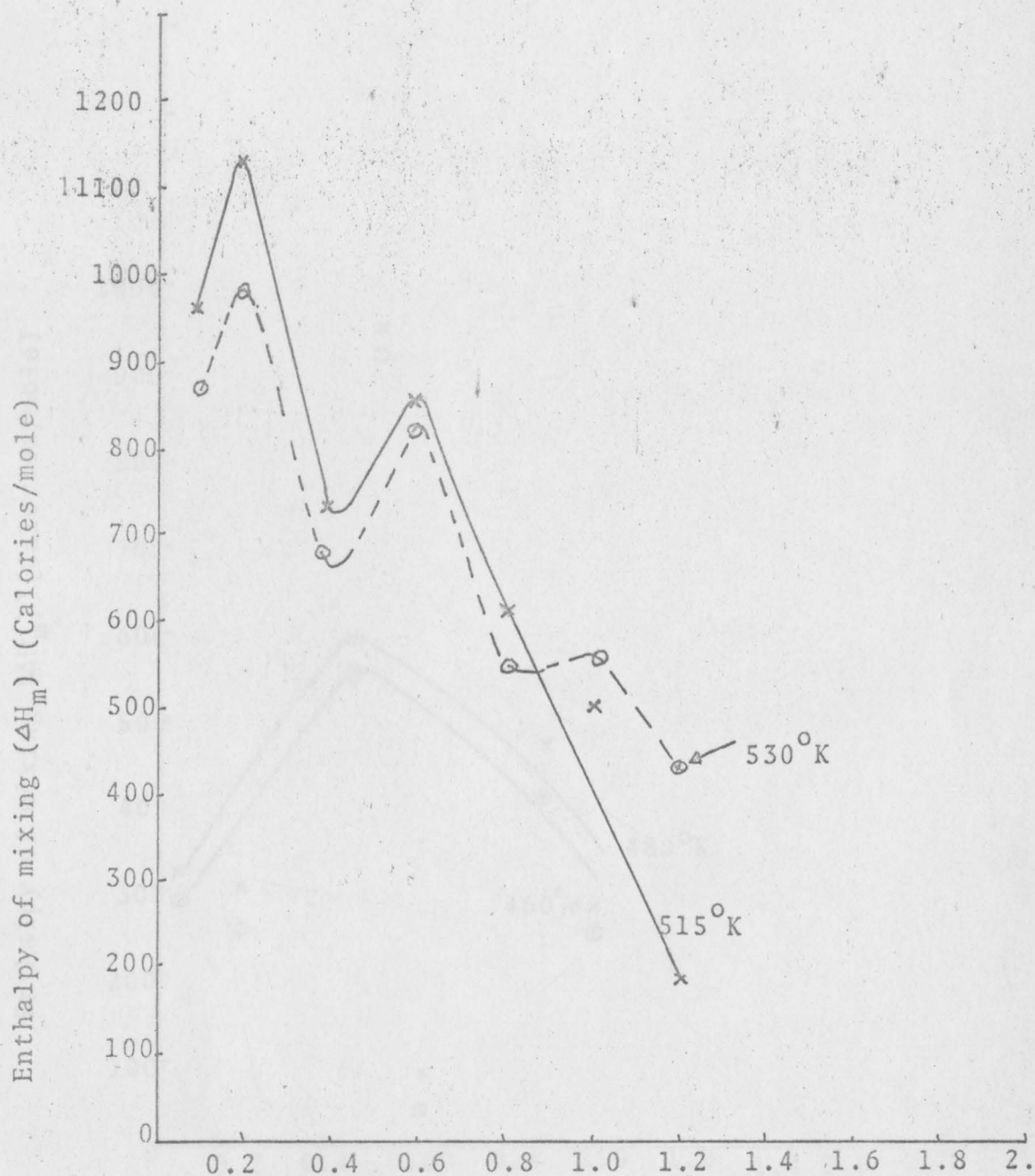


Fig. 116. Enthalpy of mixing as a function of atom percents of alloying element for Tl-Zn alloys.



Concentrations of alloying element (atom percent)  
 Concentrations of alloying element (atom percent) of  
 Fig. 117. Enthalpy of mixing as a function of atom  
 percents of alloying element, for Tl-Zn alloys.

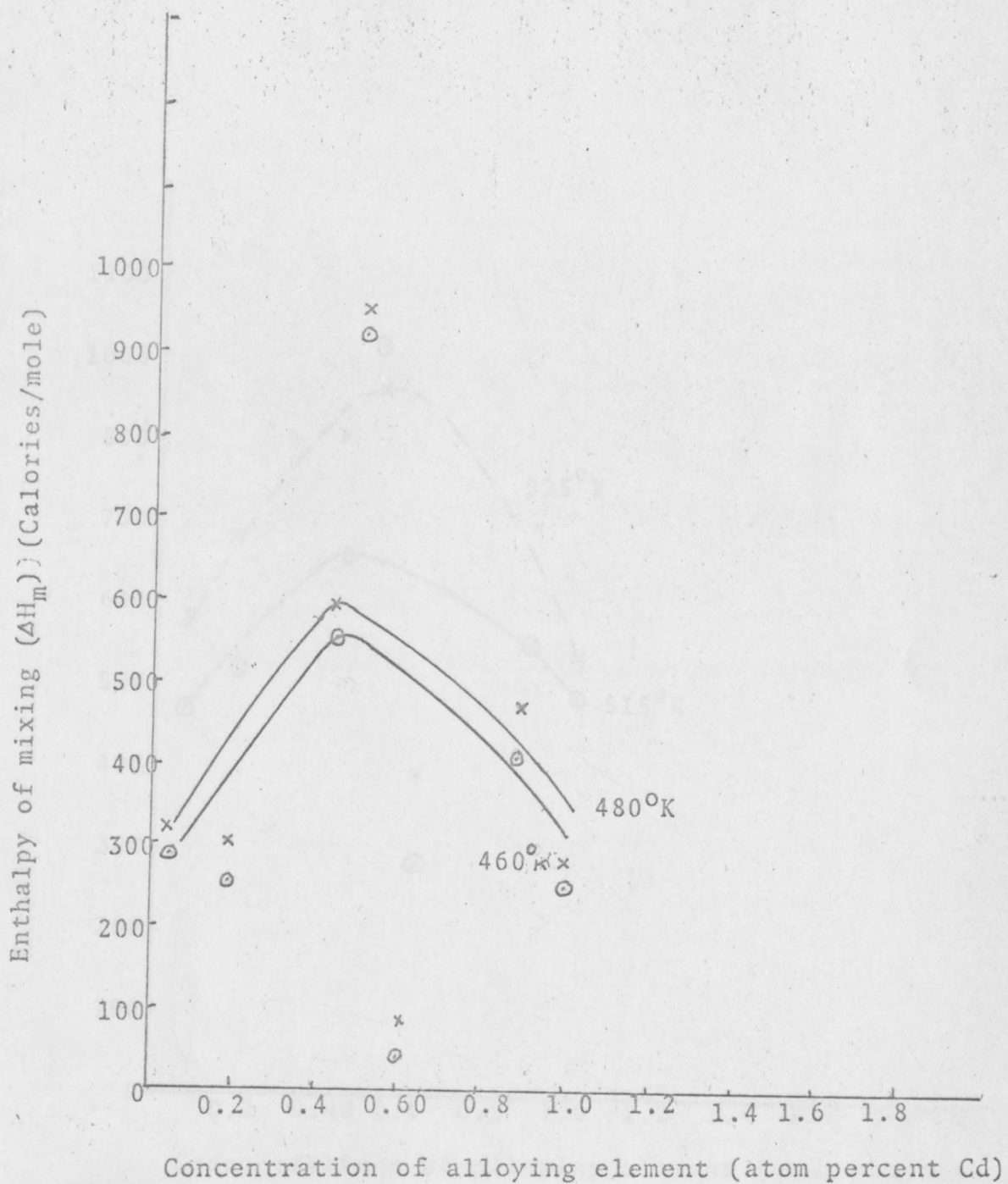


Fig. 118. Enthalpy of mixing as a function of concentration of alloying element, for Tl-Cd alloys.

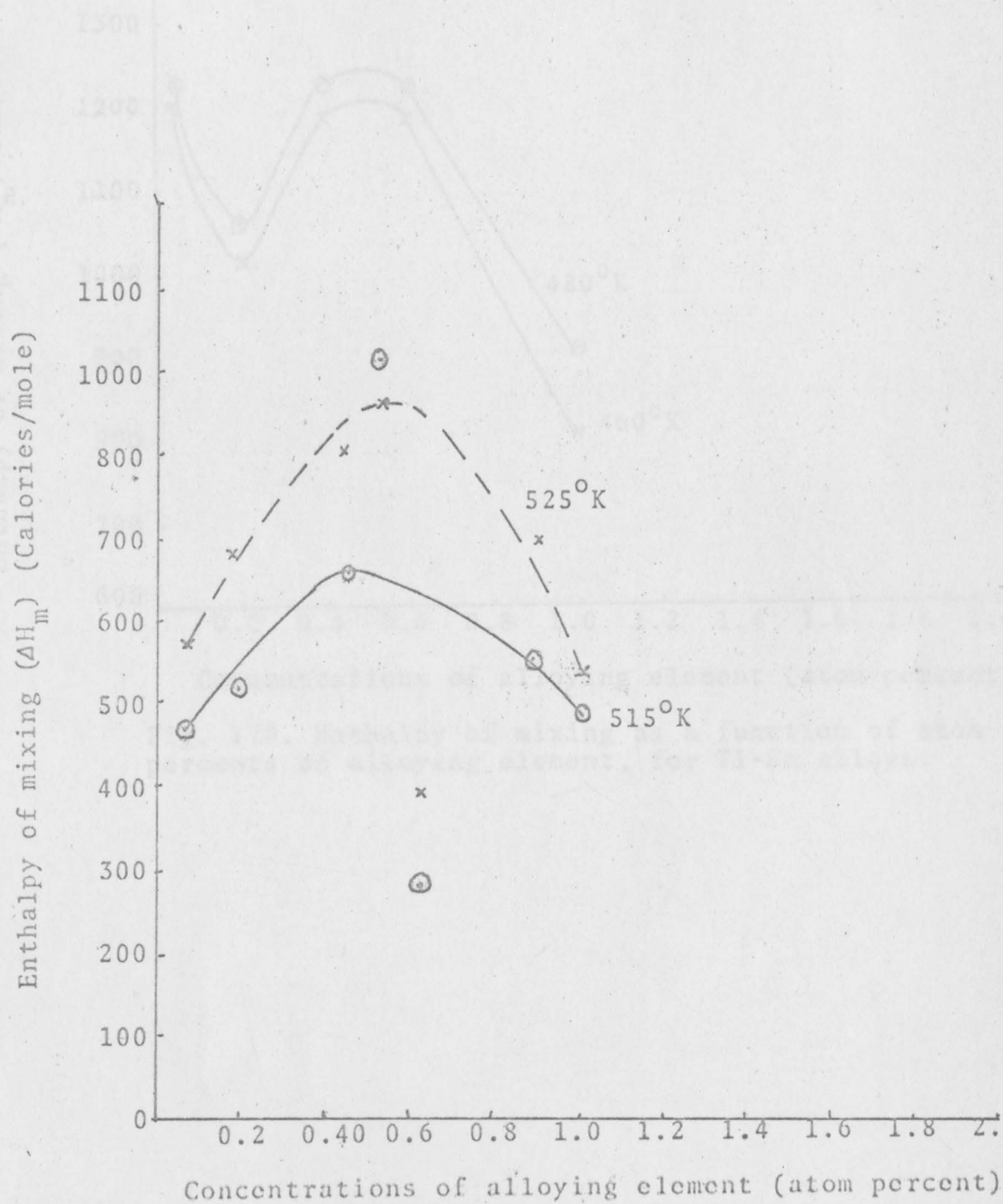


Fig. 119. Enthalpy of mixing as a function of atom percents of alloying element, for Tl-Cd alloys.

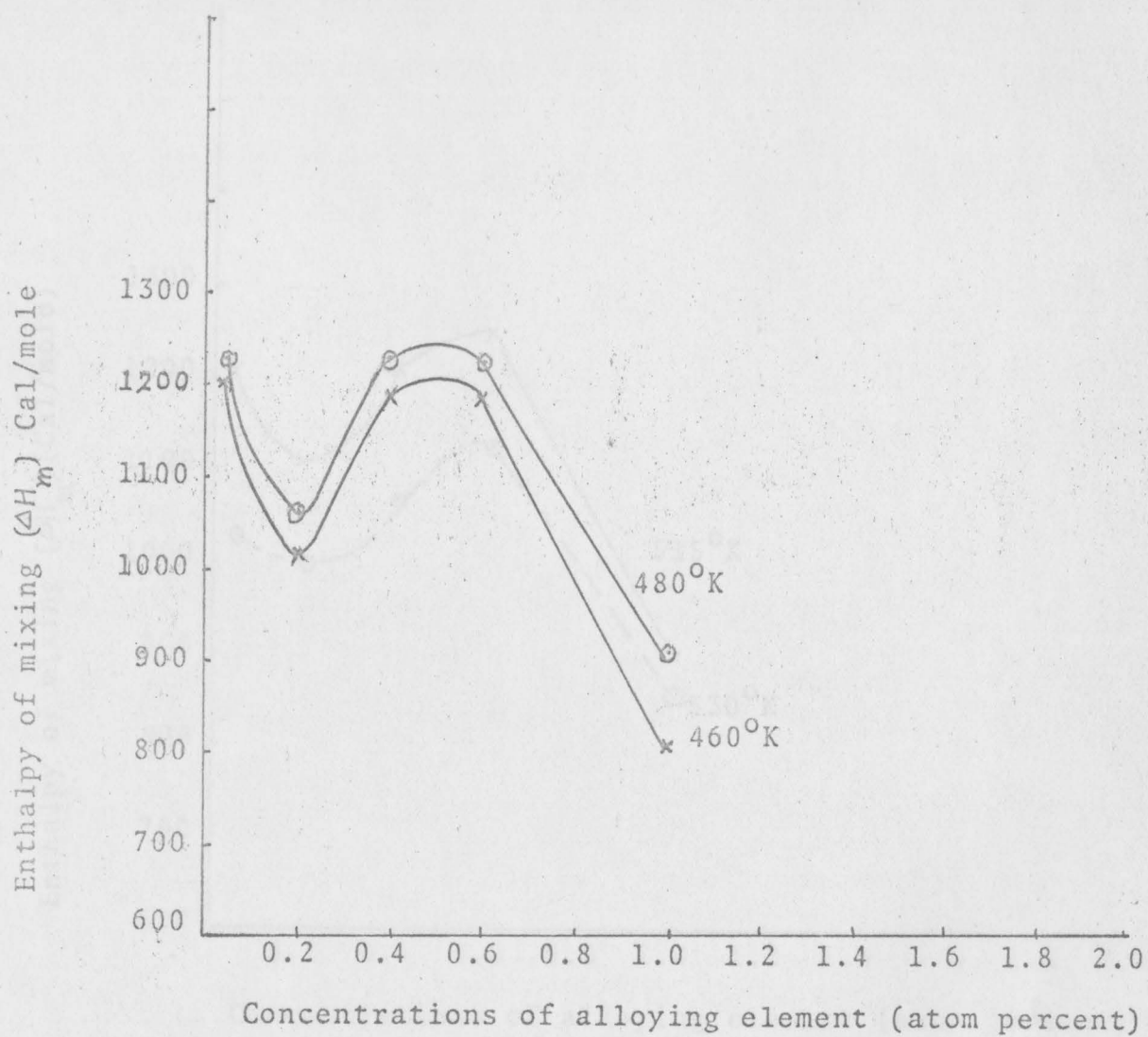


Fig. 120. Enthalpy of mixing as a function of atom percents of alloying element, for Tl-Sn alloys.



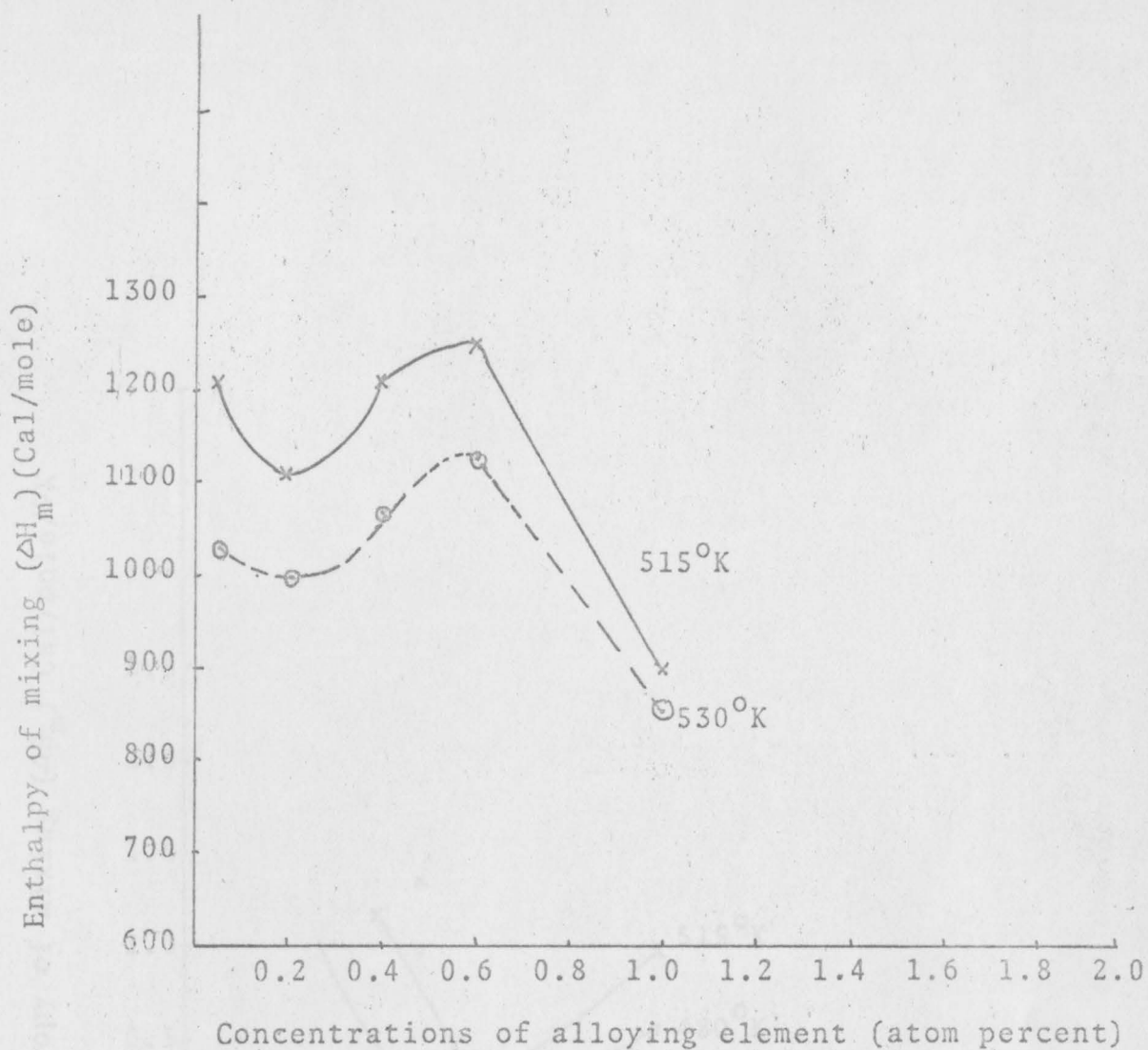


Fig. 121. Enthalpy of mixing as a function of atom percents of alloying element, for Tl-Sn alloys.

Fig. 122. Entropy of mixing as a function of atom percents of alloying element, for Tl-Sn alloys.

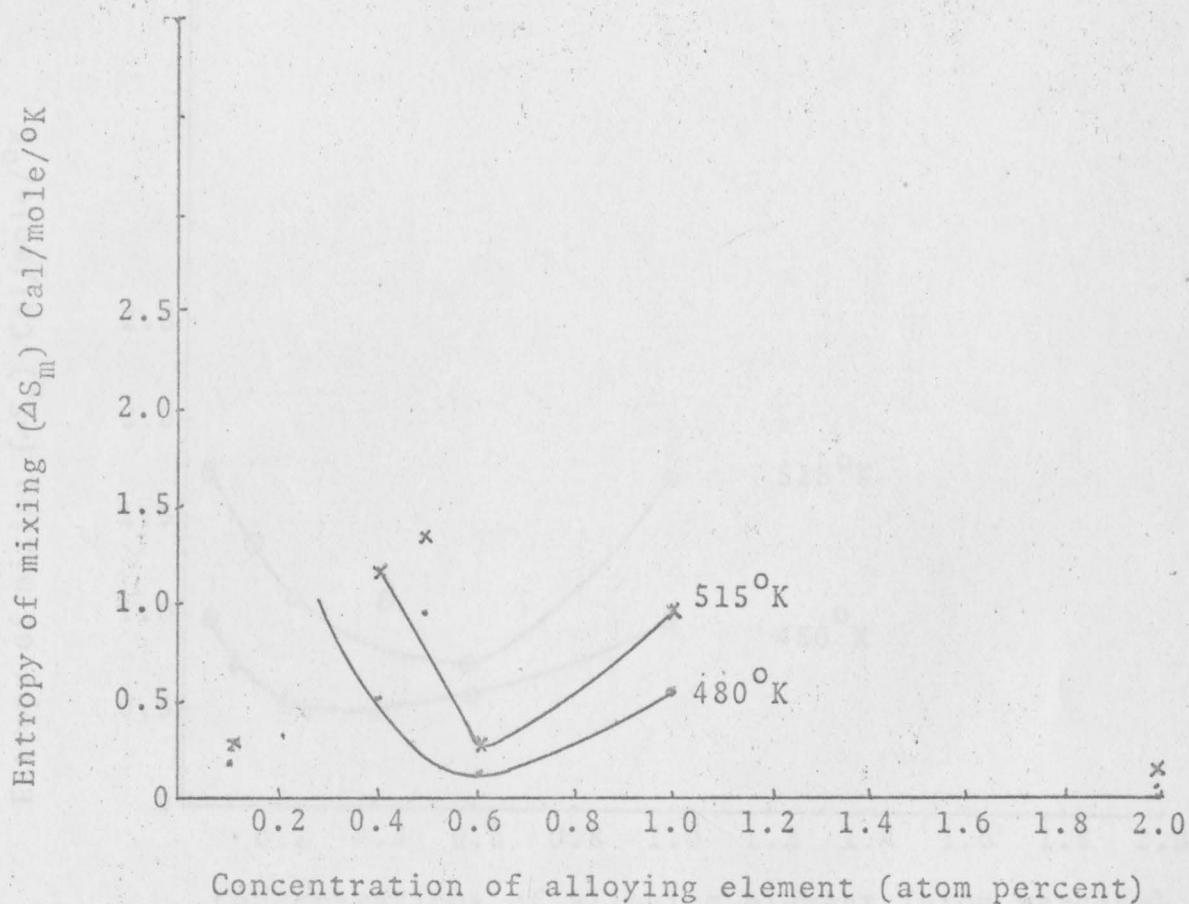


Fig. 122. Entropy of mixing as a function of atom percents of alloying element, for Tl-Ag alloys.

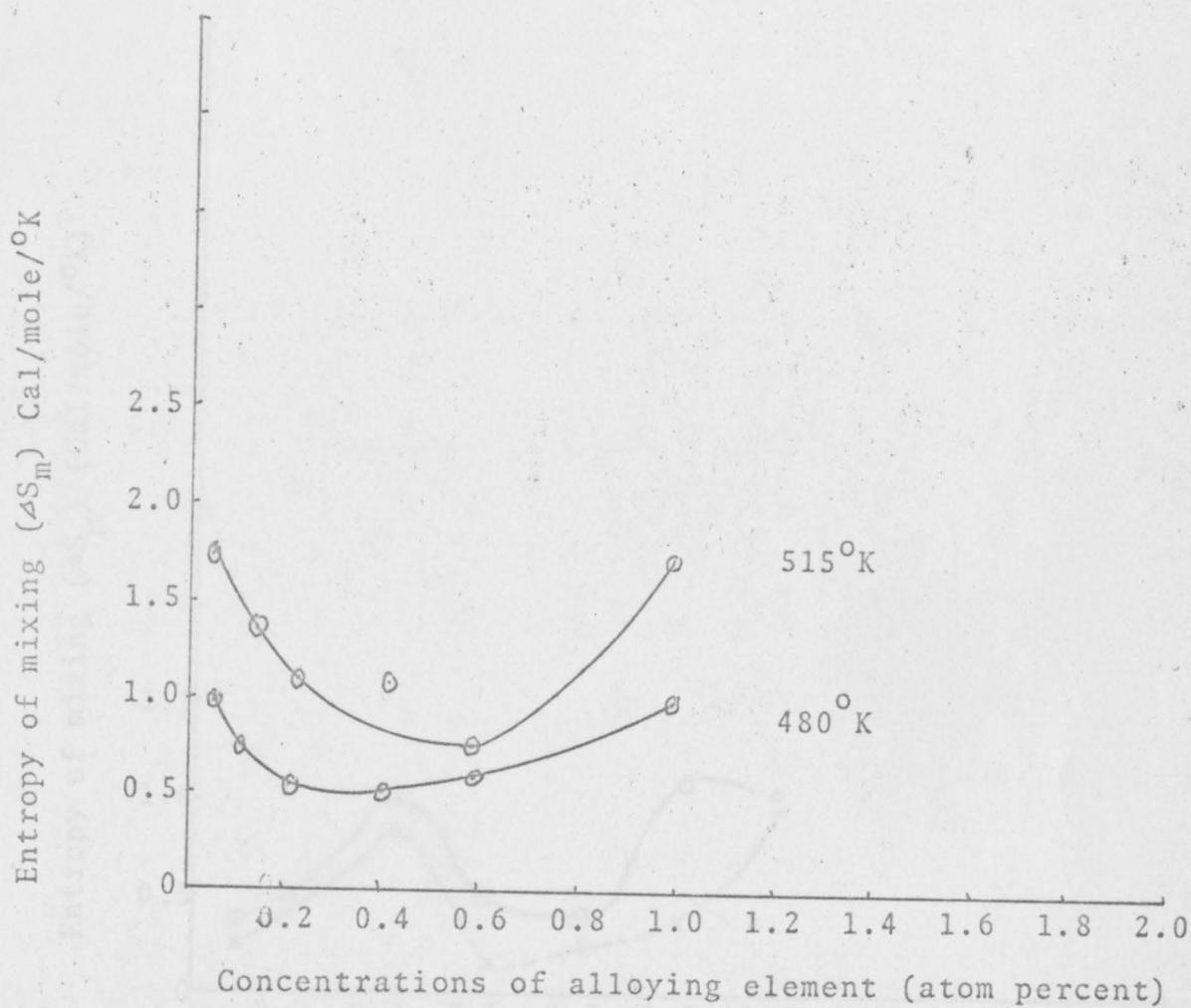


Fig. 123. Entropy of mixing as a function atom percents of alloying element, for Tl-Au alloys.

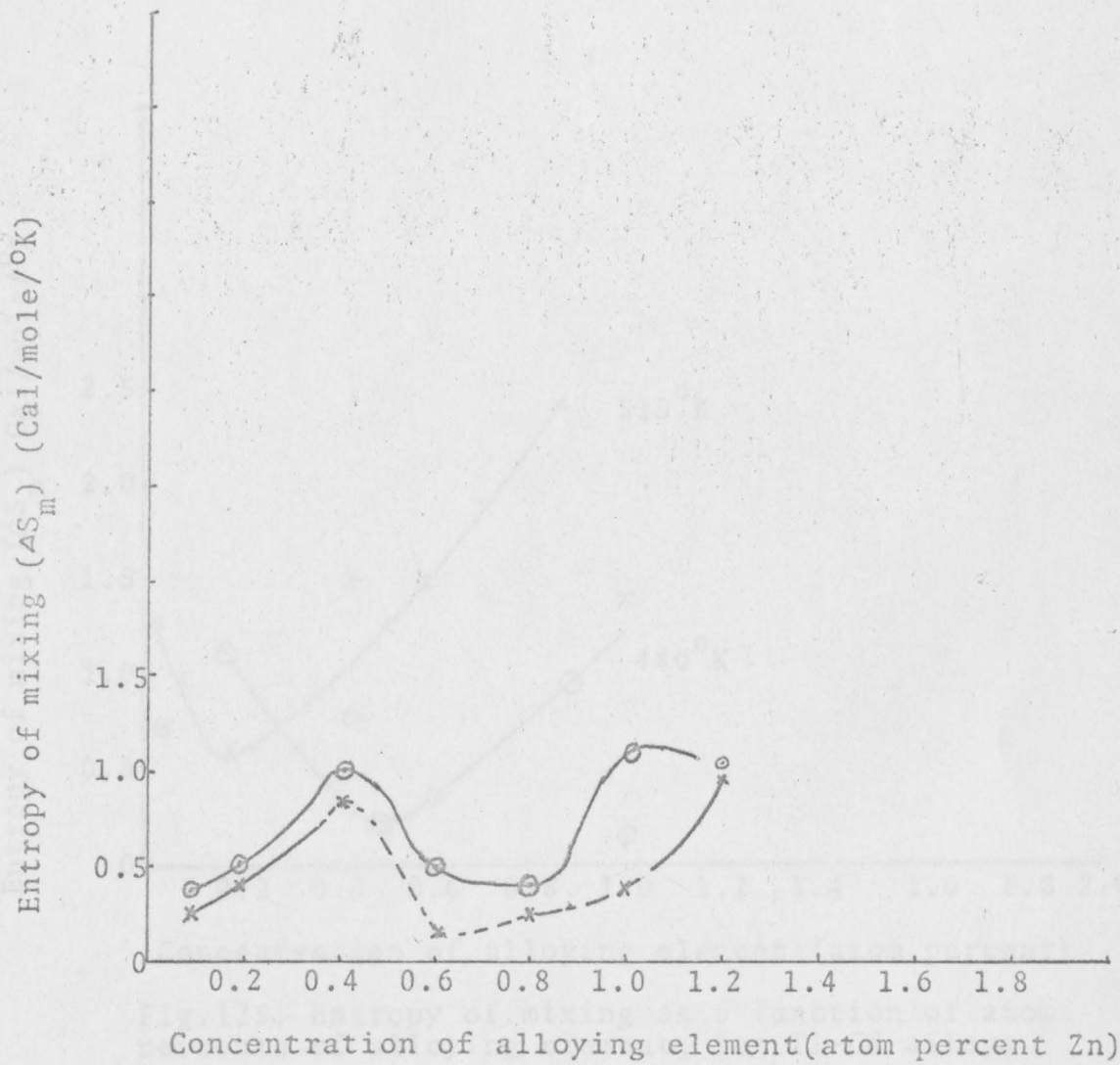


Fig. 124. Entropy of mixing as a function of the concentrations of alloying element, for Tl-Zn alloys.

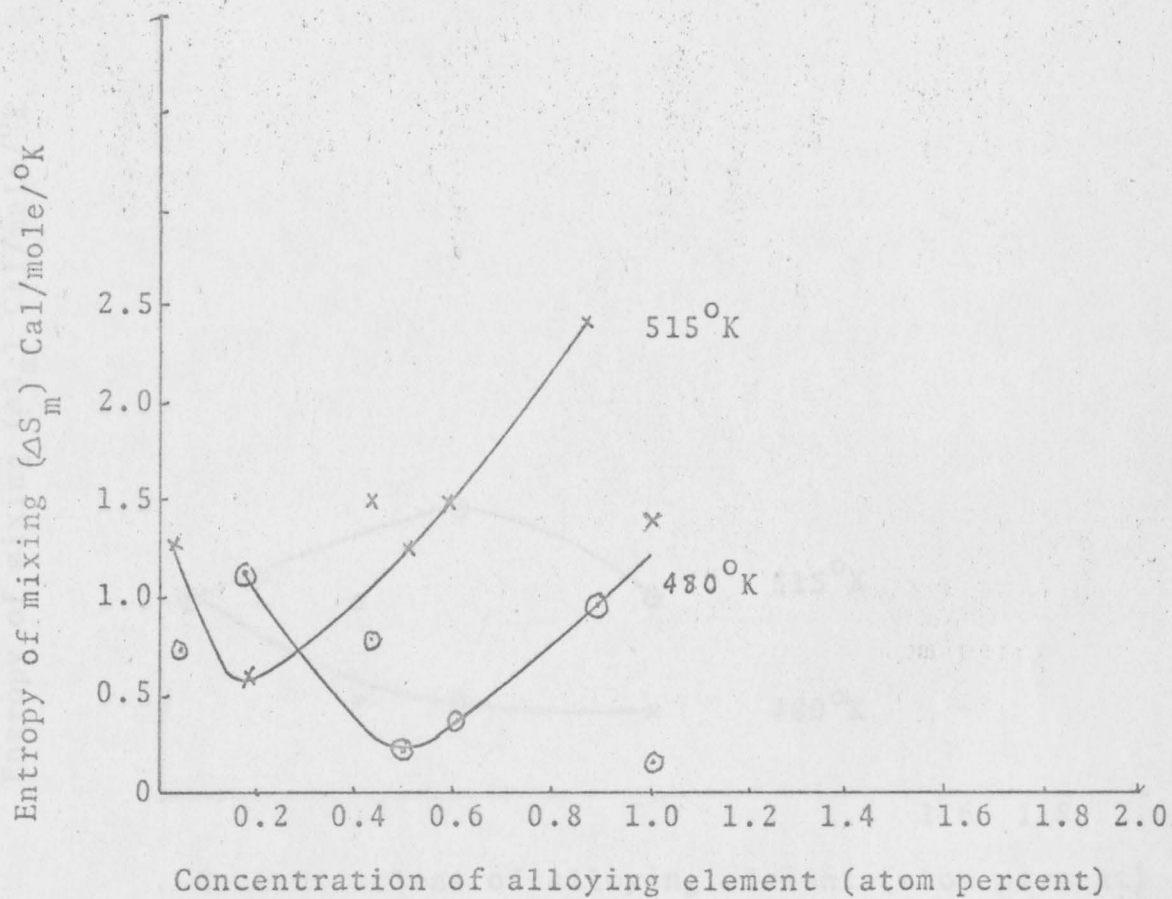


Fig.125. Entropy of mixing as a function of atom percents of alloying element, for Tl-Cd alloys.

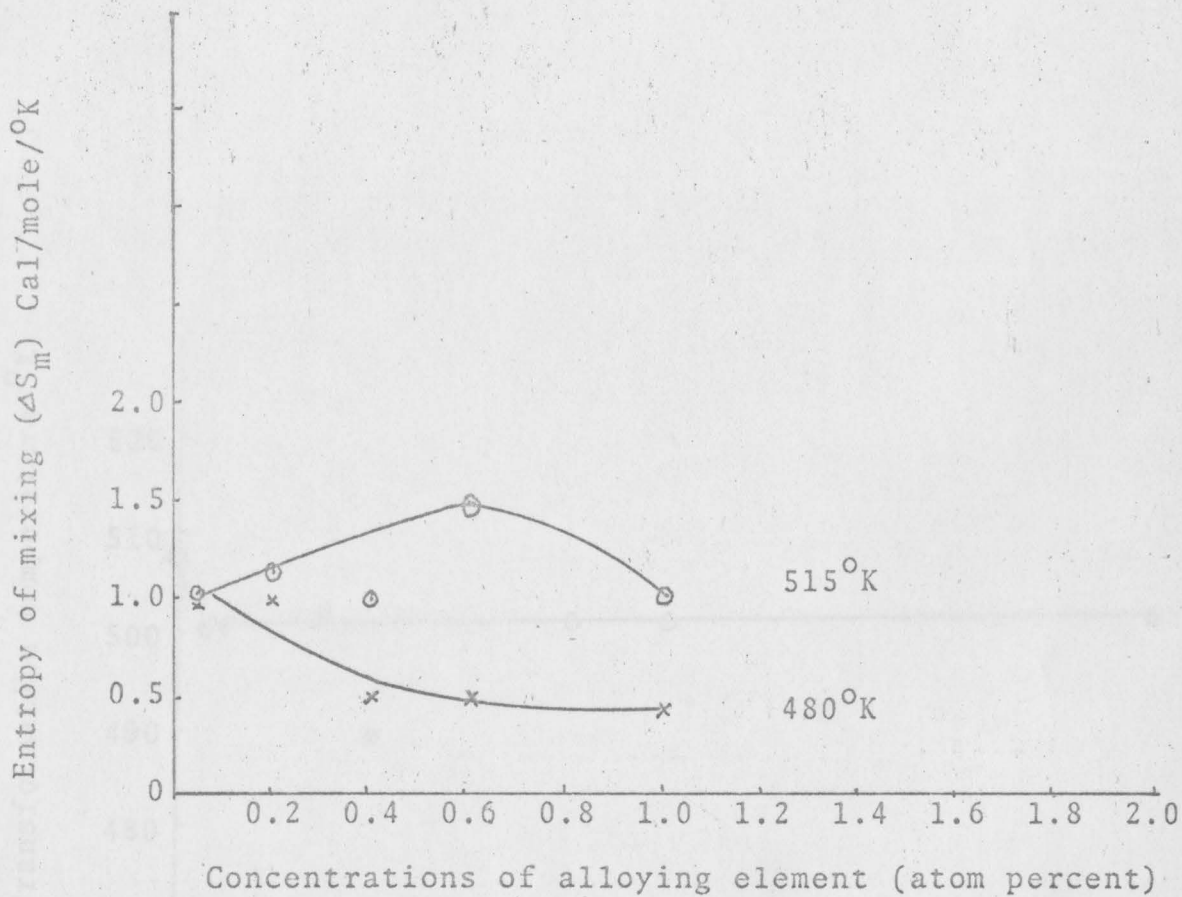


Fig. 126. Entropy of mixing as a function of atom percents of alloying element, for Tl-Sn alloys.

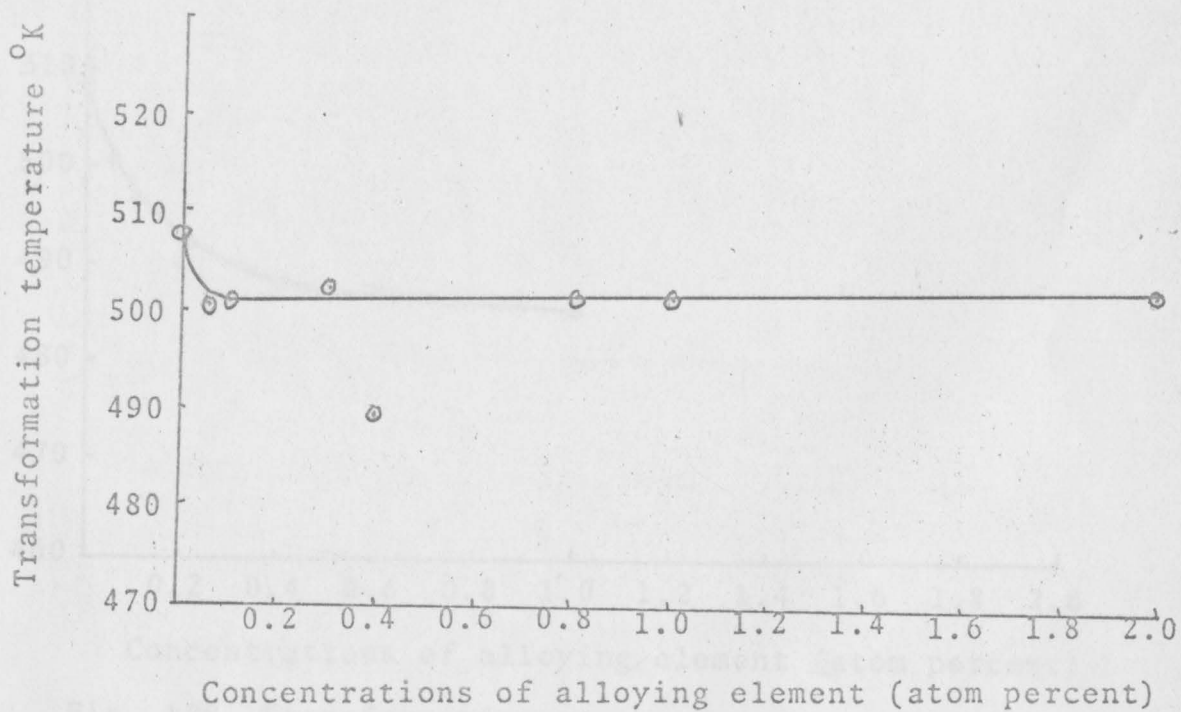


Fig. 127. Transformation temperature as a function of concentration of alloying element, for Tl-Ag alloys.

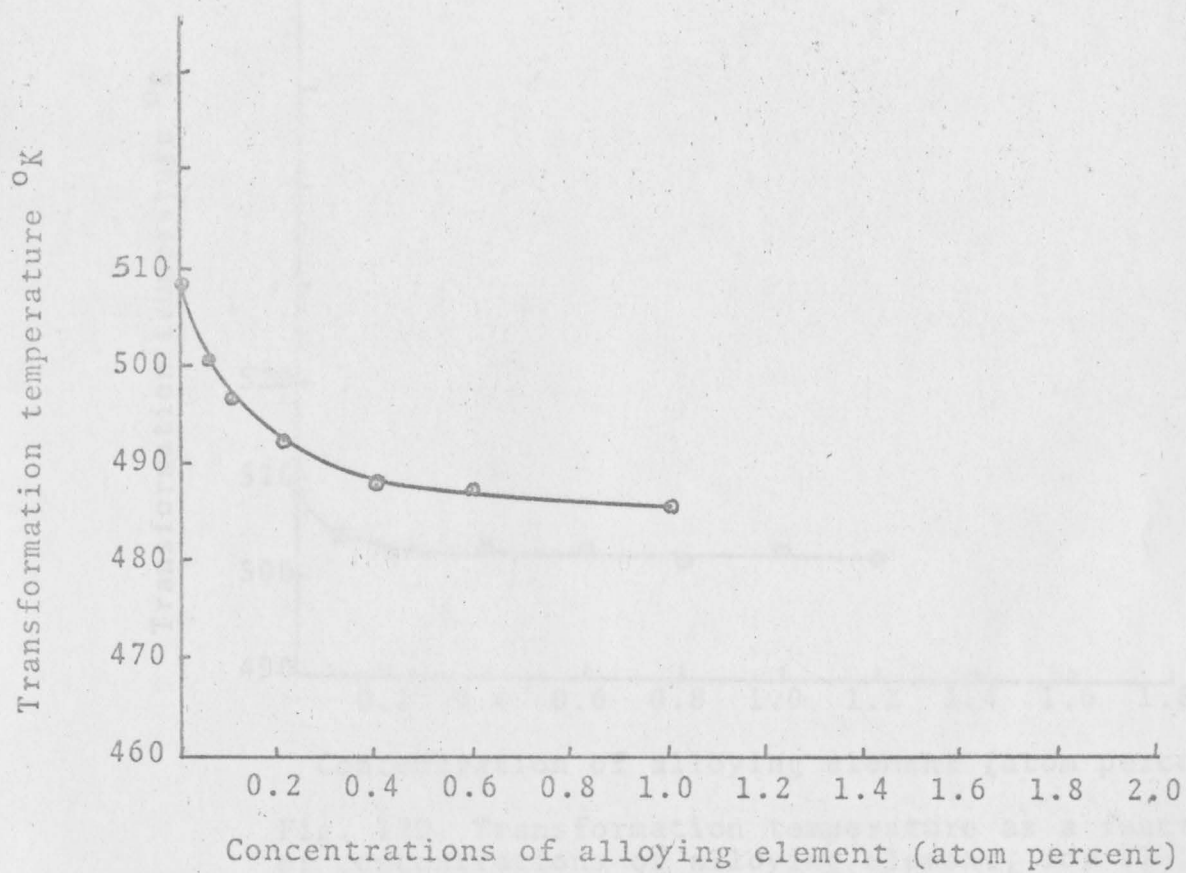


Fig. 128. Transformation temperature as a function of concentrations of alloying element, for Tl-Au alloy.



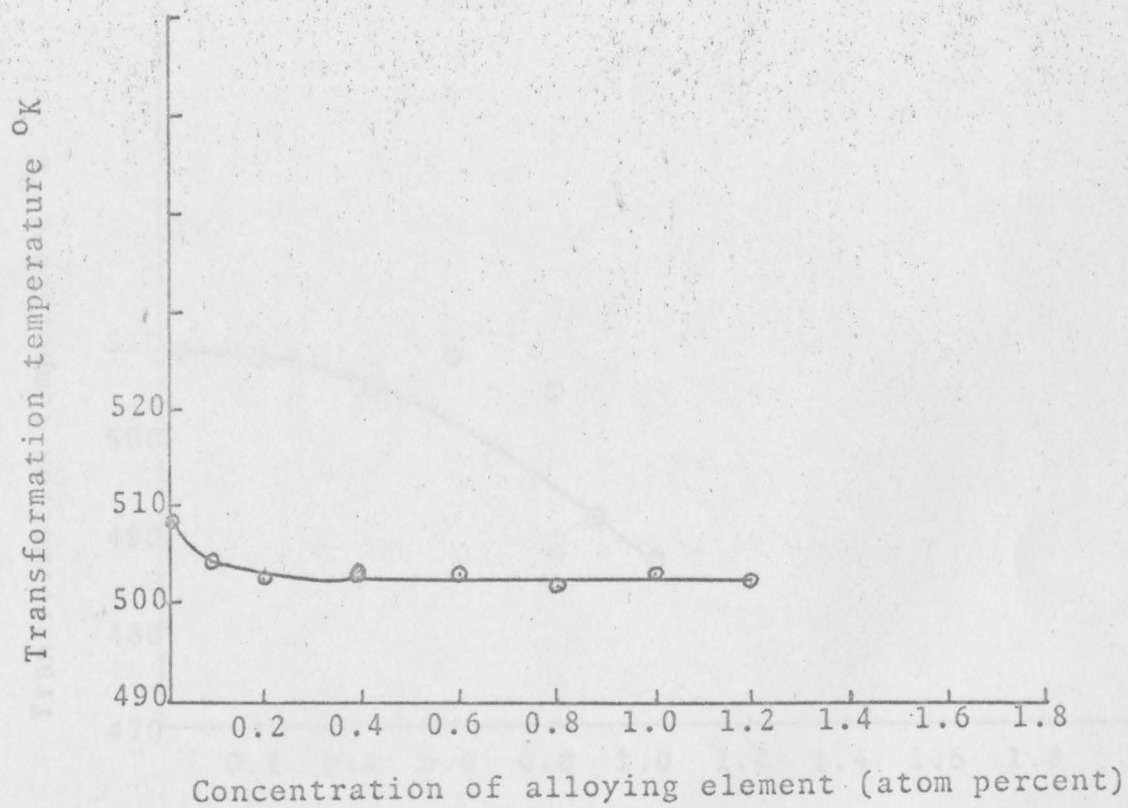


Fig. 129. Transformation temperature as a function of concentrations of alloying element, for Tl-Zn alloys.

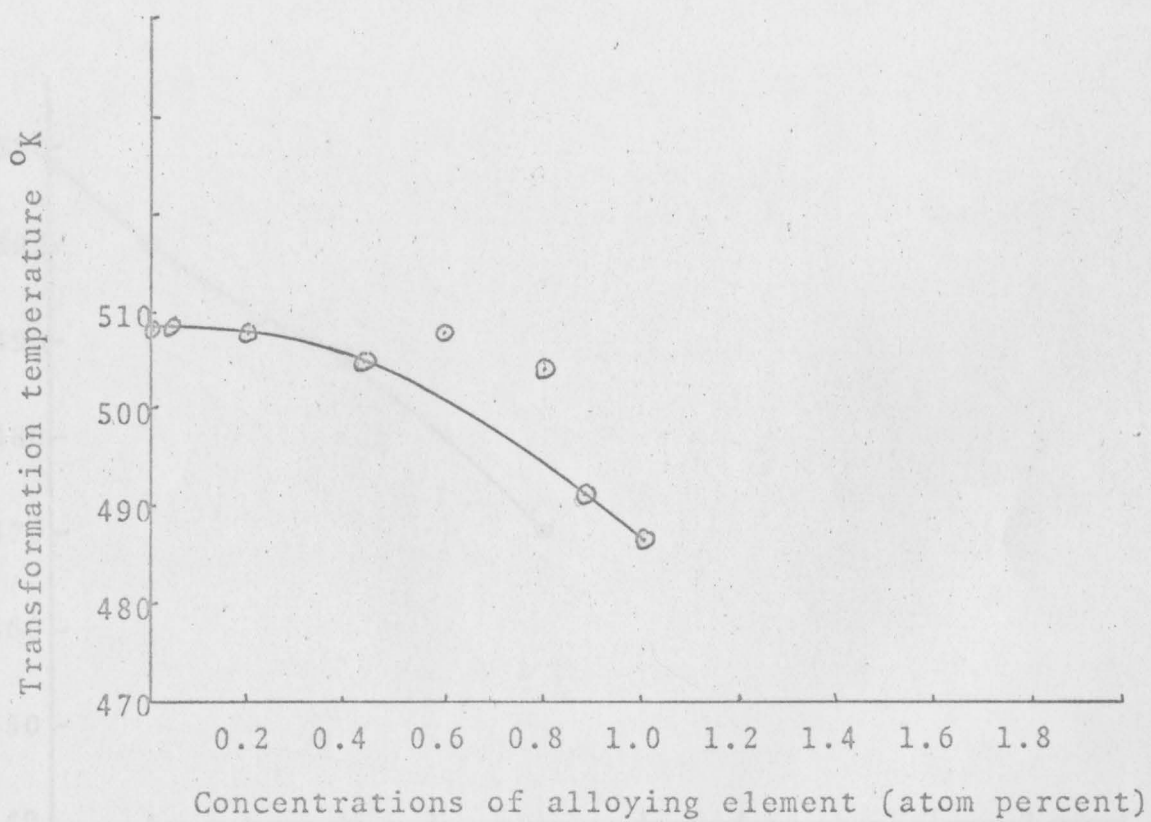


Fig. 130. Transformation temperature as a function of concentrations of alloying element, for Tl-Cd alloys.

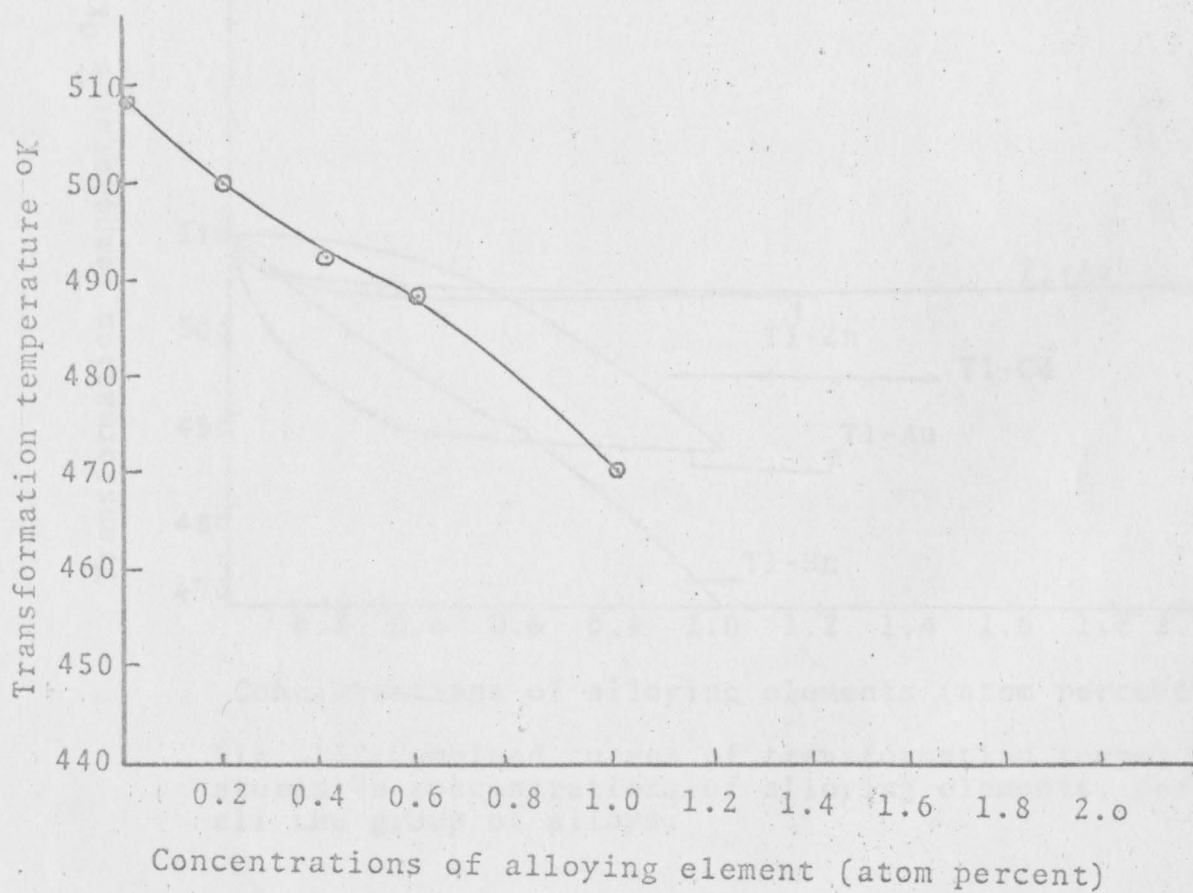


Fig. 131. Transformation temperature as a function of concentrations of alloying element, for Tl-Sn alloys.

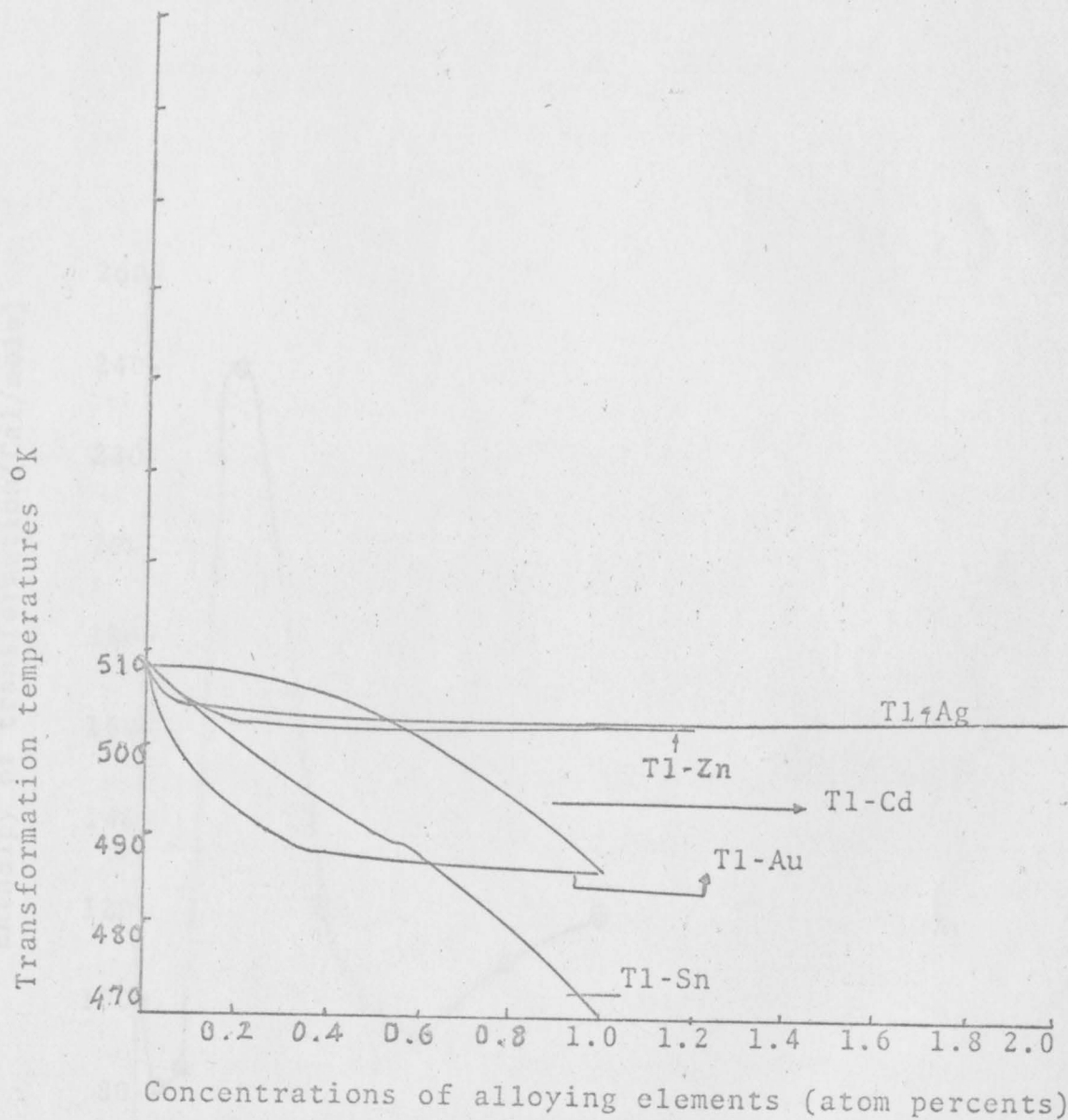


Fig. 132. Combined curves of transformation temperatures Vs concentrations of alloying elements, for all the group of alloys.

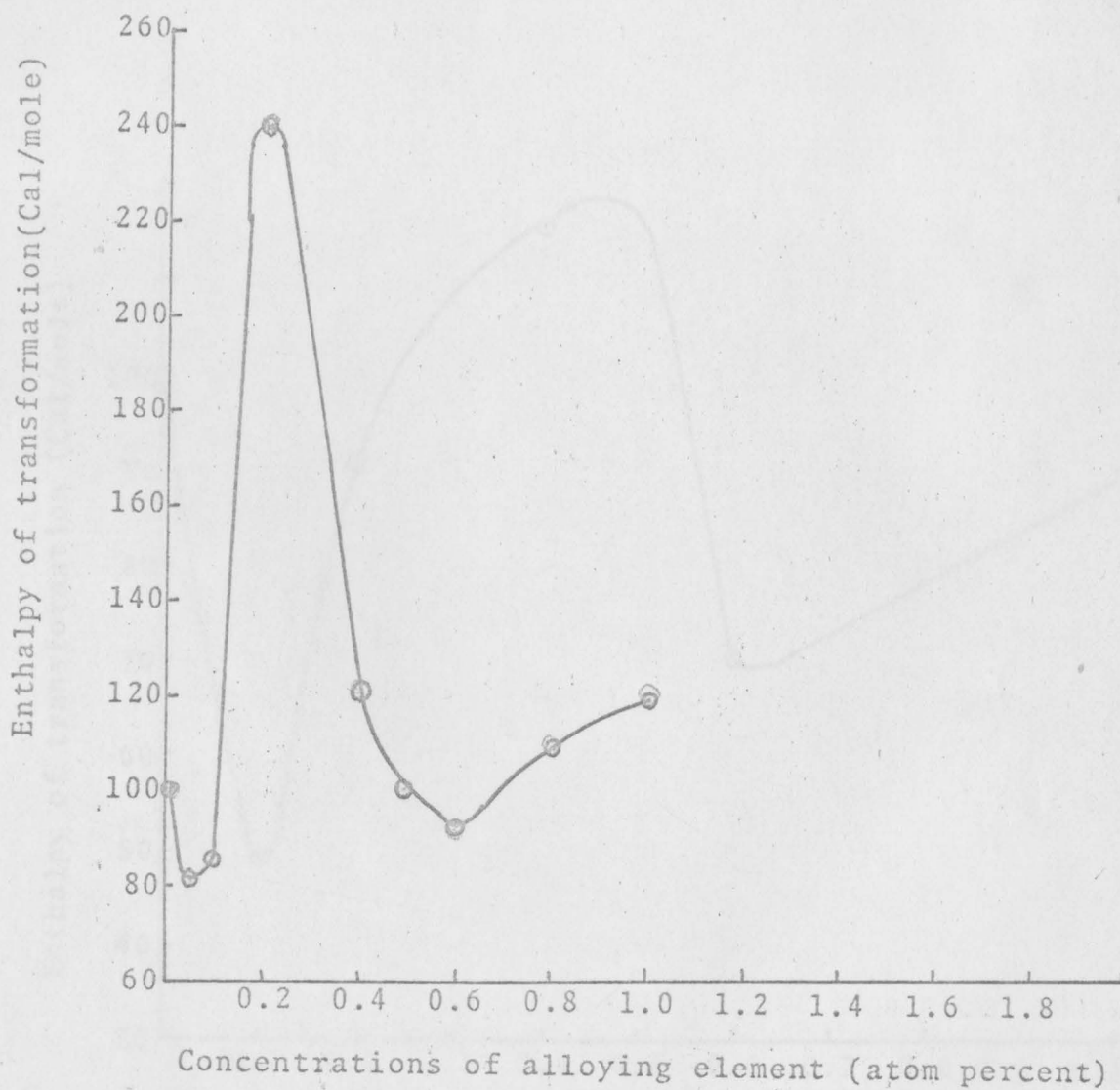


Fig. 133. Enthalpy of transformation as a function of concentrations of alloying element, for Tl-Ag alloy.

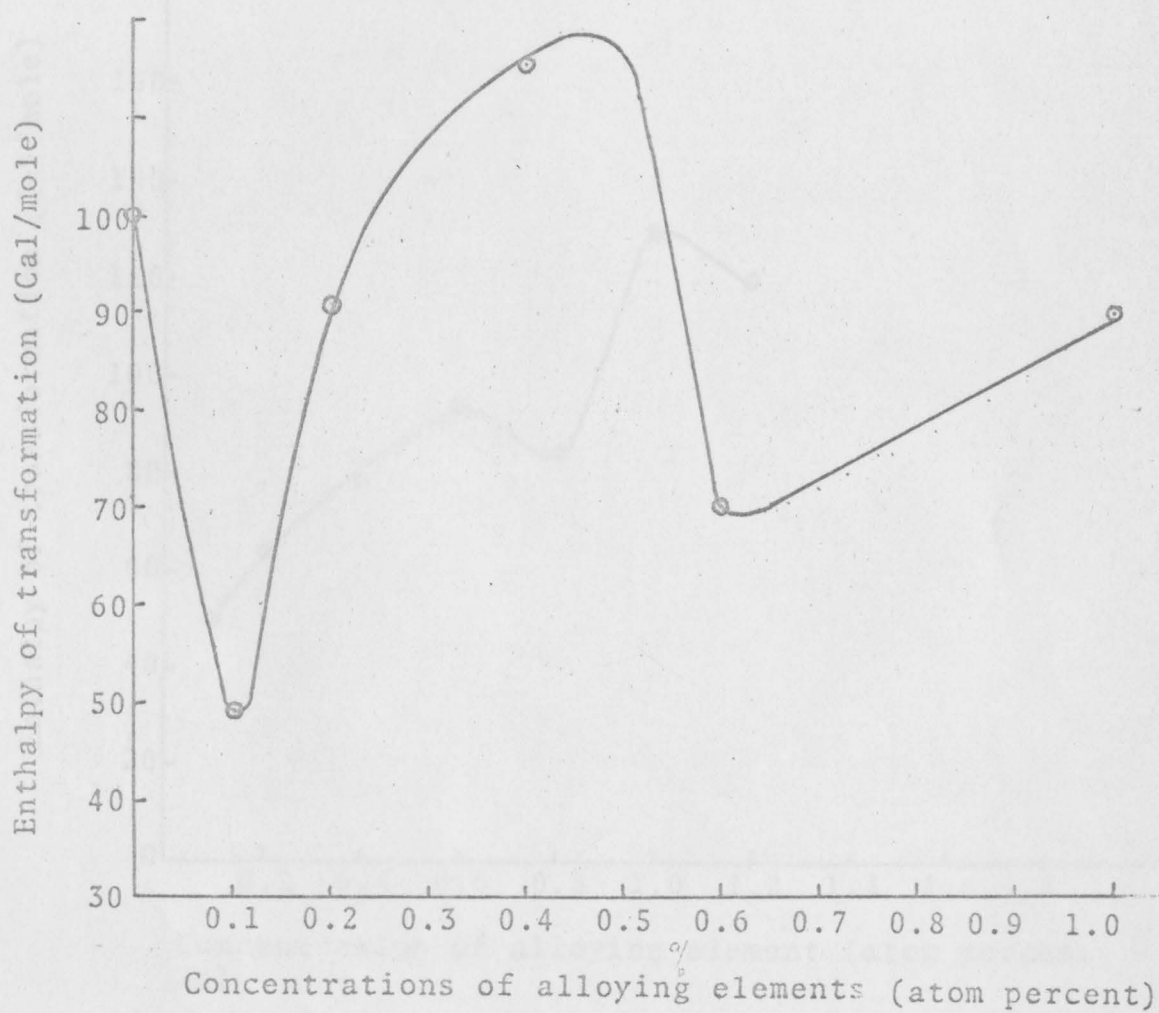


Fig. 134. Enthalpy of transformation as a function of concentrations of alloying element, for Tl-Au alloy.

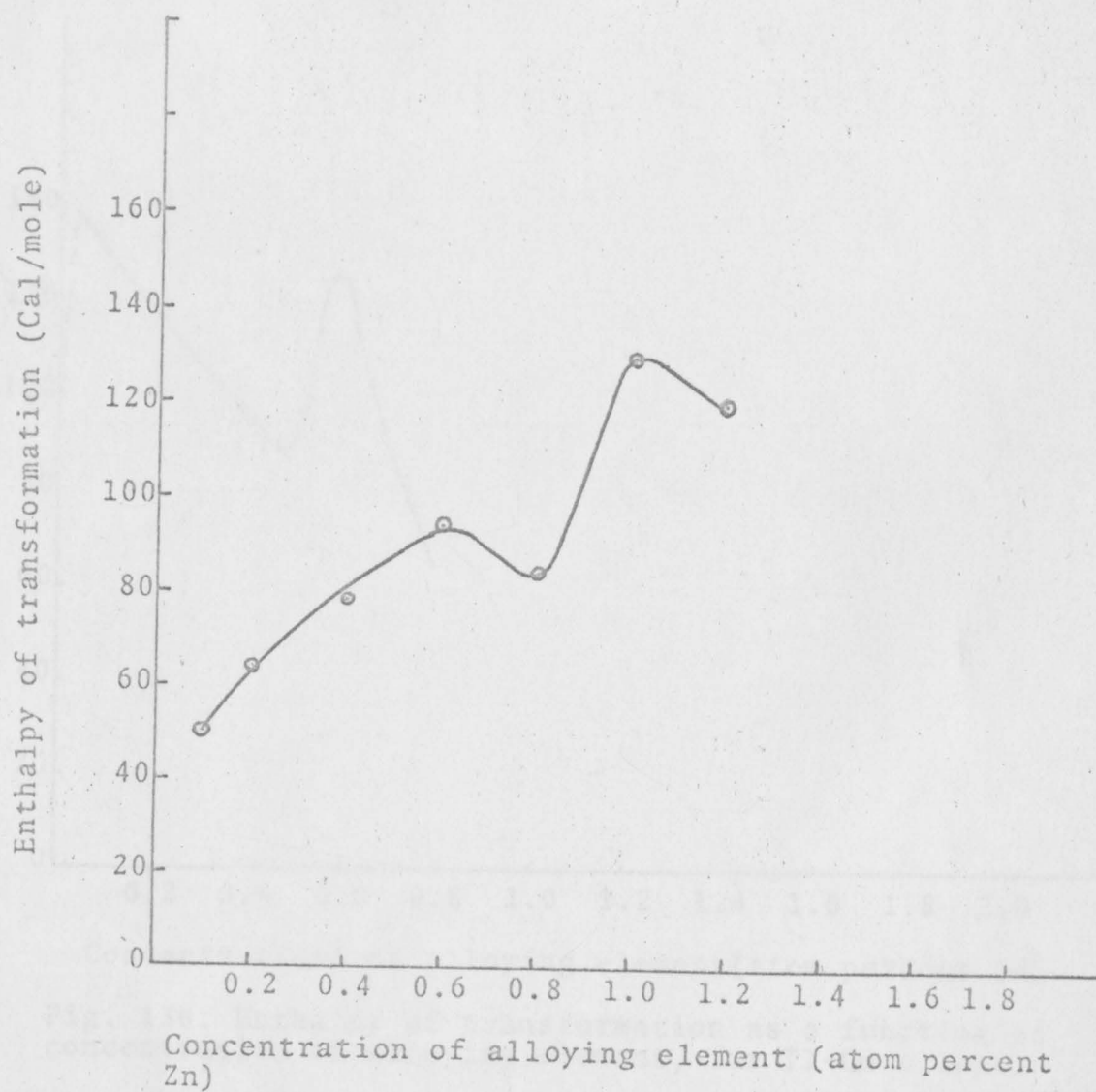


Fig. 135. Enthalpy of transformation as a function of concentrations of alloying element, for Tl-Zn alloys.

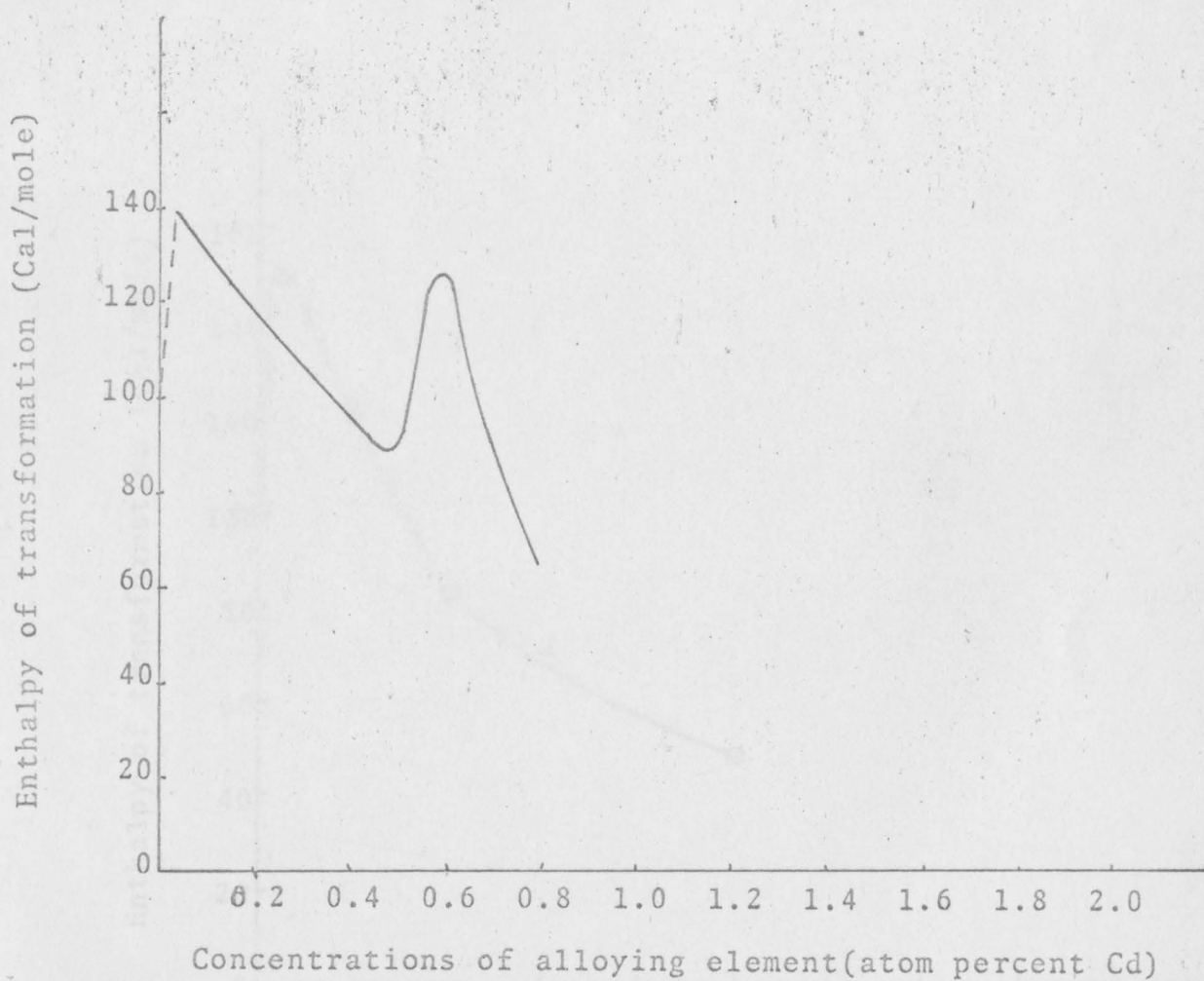


Fig. 136. Enthalpy of transformation as a function of concentration of alloying element, for Tl-Cd alloys.



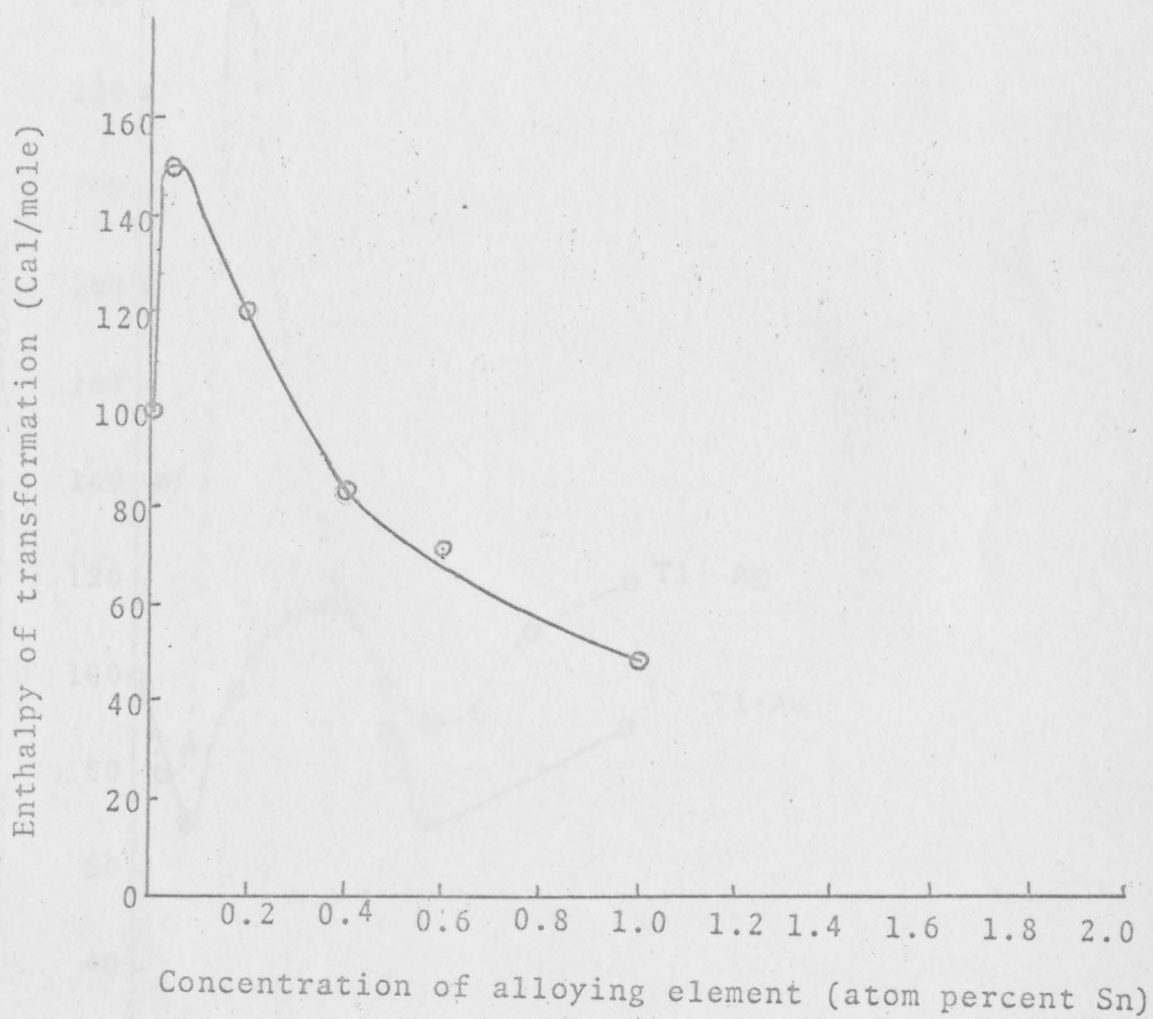


Fig. 137. Enthalpy of transformation as a function of concentrations of alloying element, for Tl-Sn alloys.

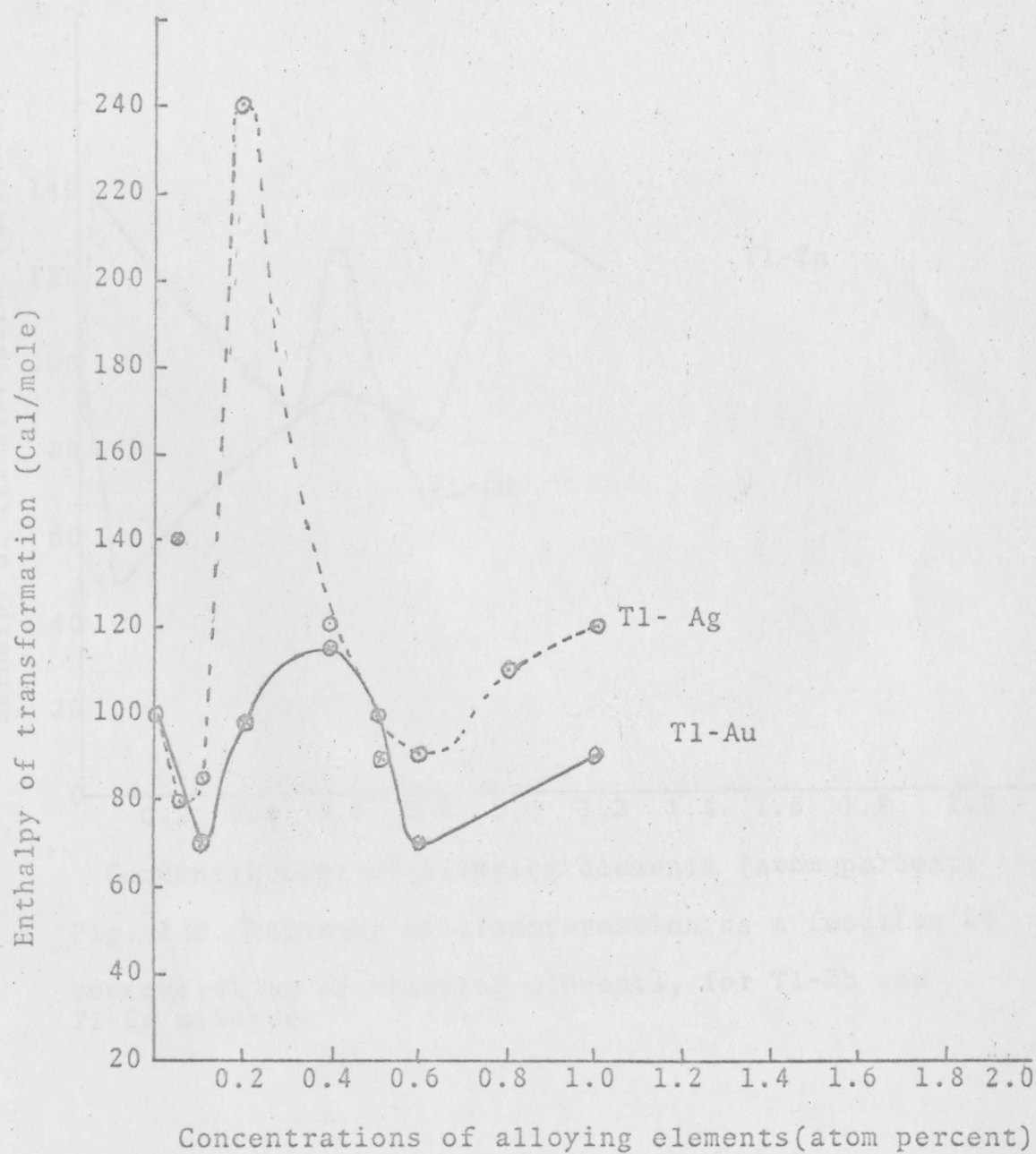


Fig. 138. Enthalpy of transformation as a function of concentrations of alloying elements, for Tl-Ag and Tl-Au alloys.

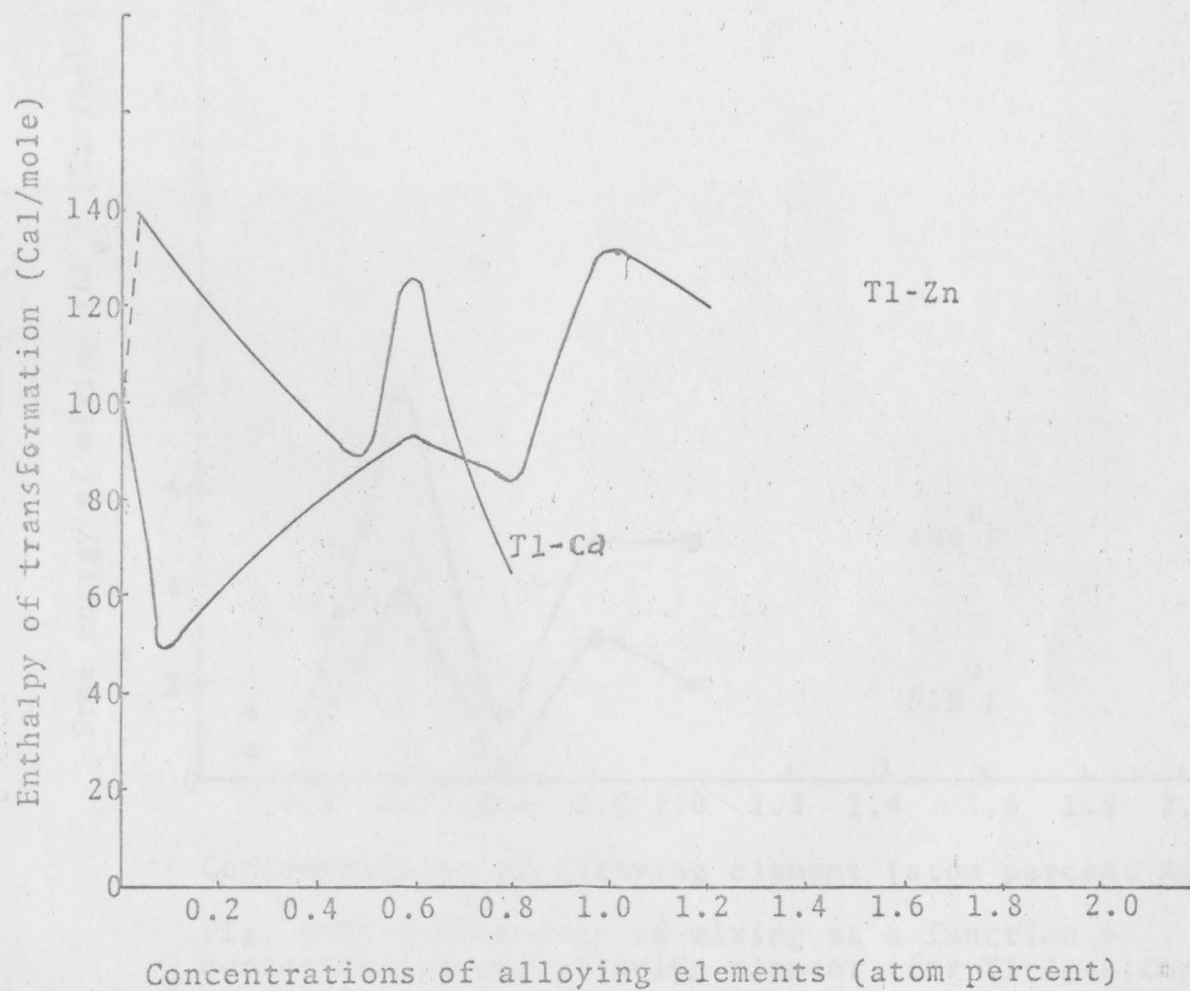


Fig. 139. Enthalpy of transformation as a function of concentration of alloying elements, for Tl-Zn and Tl-Cd alloys.

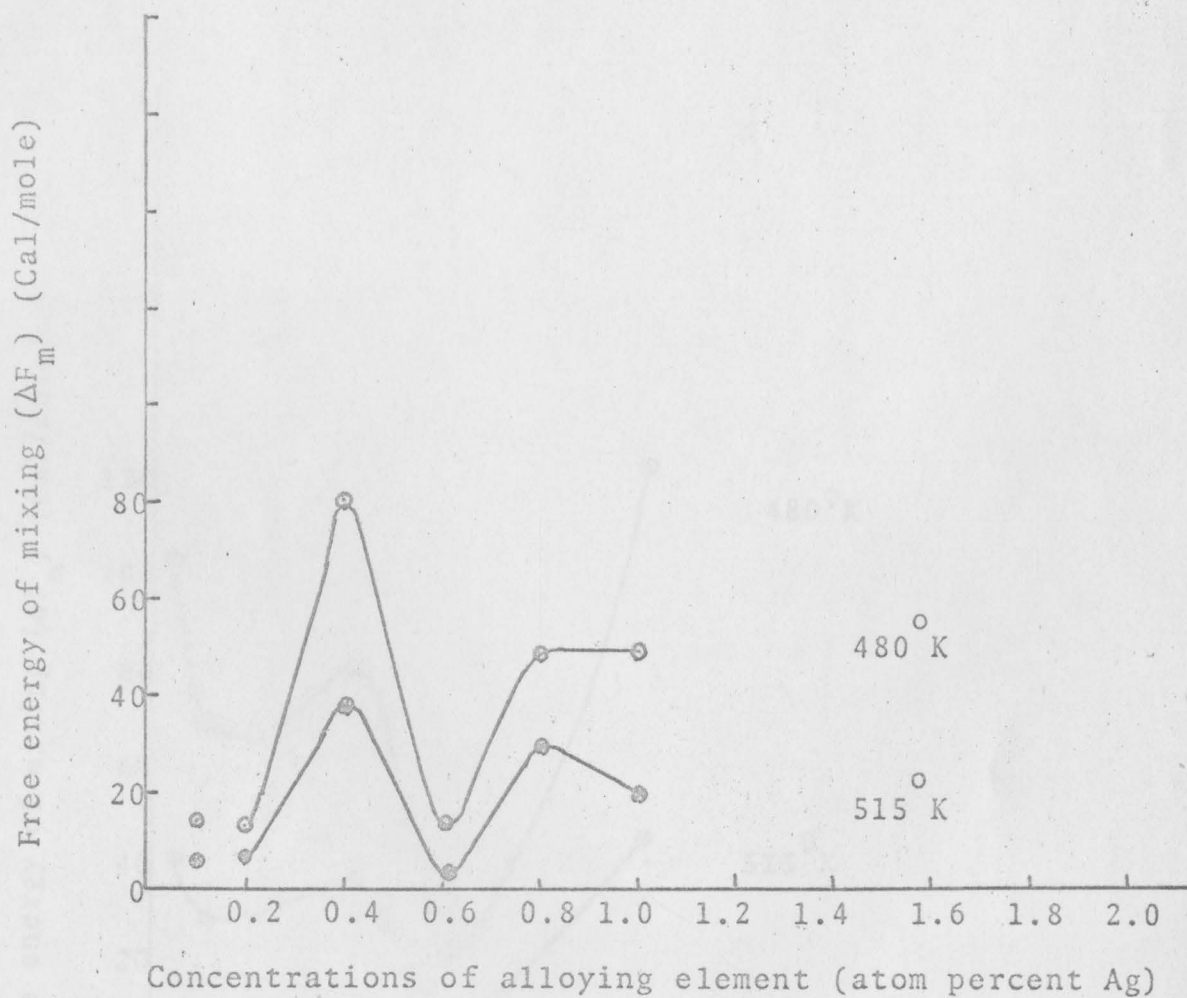


Fig. 140. Free energy of mixing as a function of concentrations of alloying element, for Tl-Ag alloy.

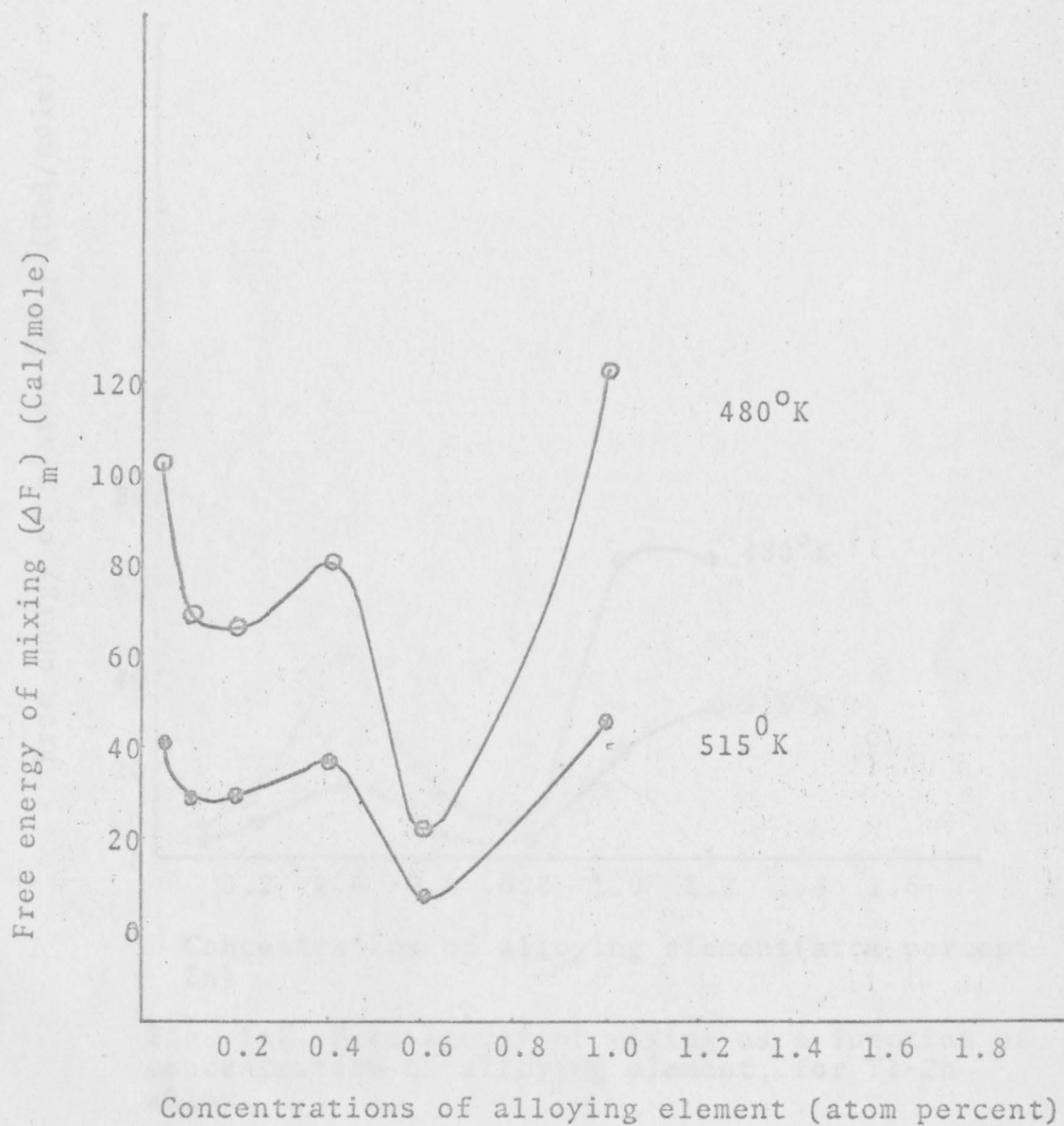


Fig. 141. Free energy of mixing as a function of concentration of alloying element, for Tl-Au alloy.

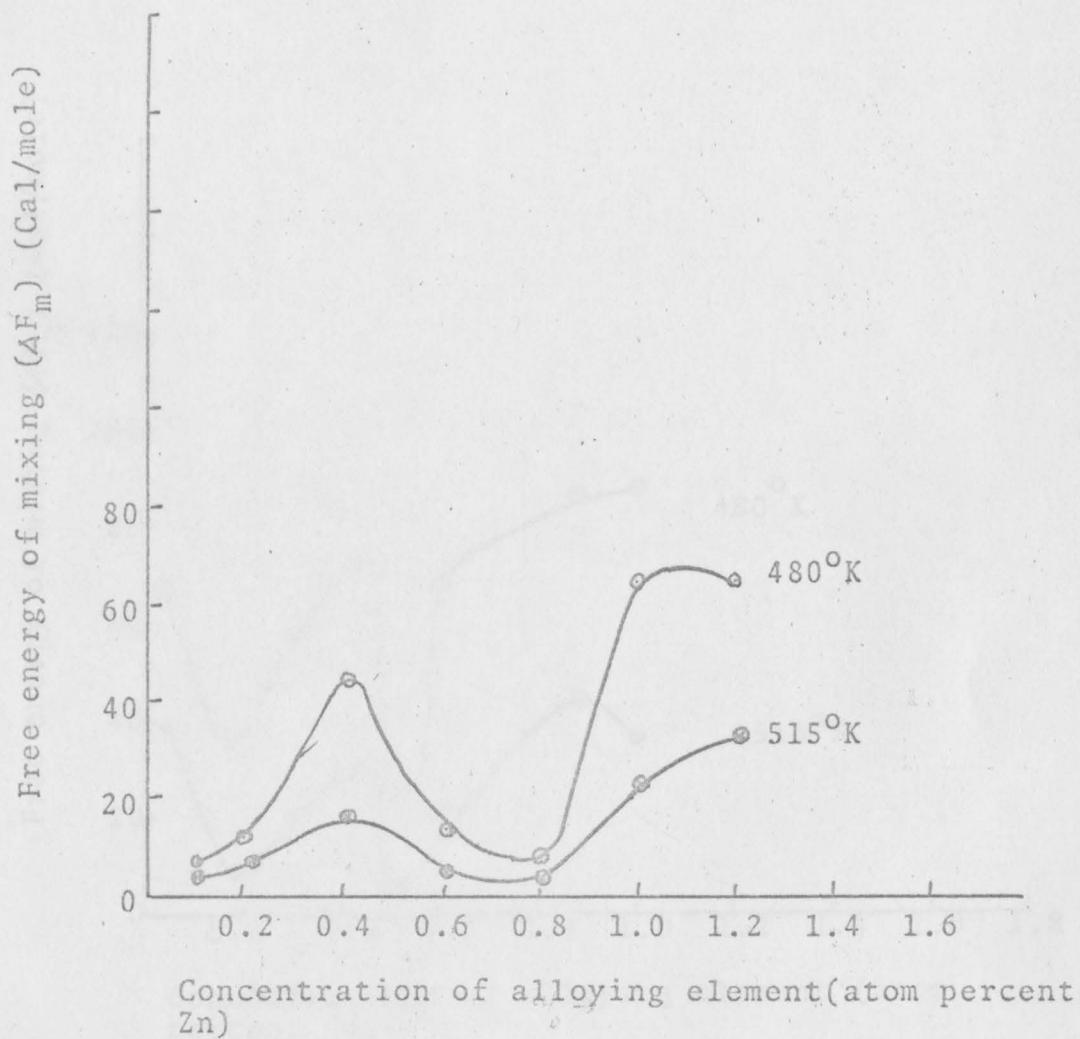


Fig. 142. Free energy of mixing as a function of concentration of alloying element, for Tl-Zn alloy.

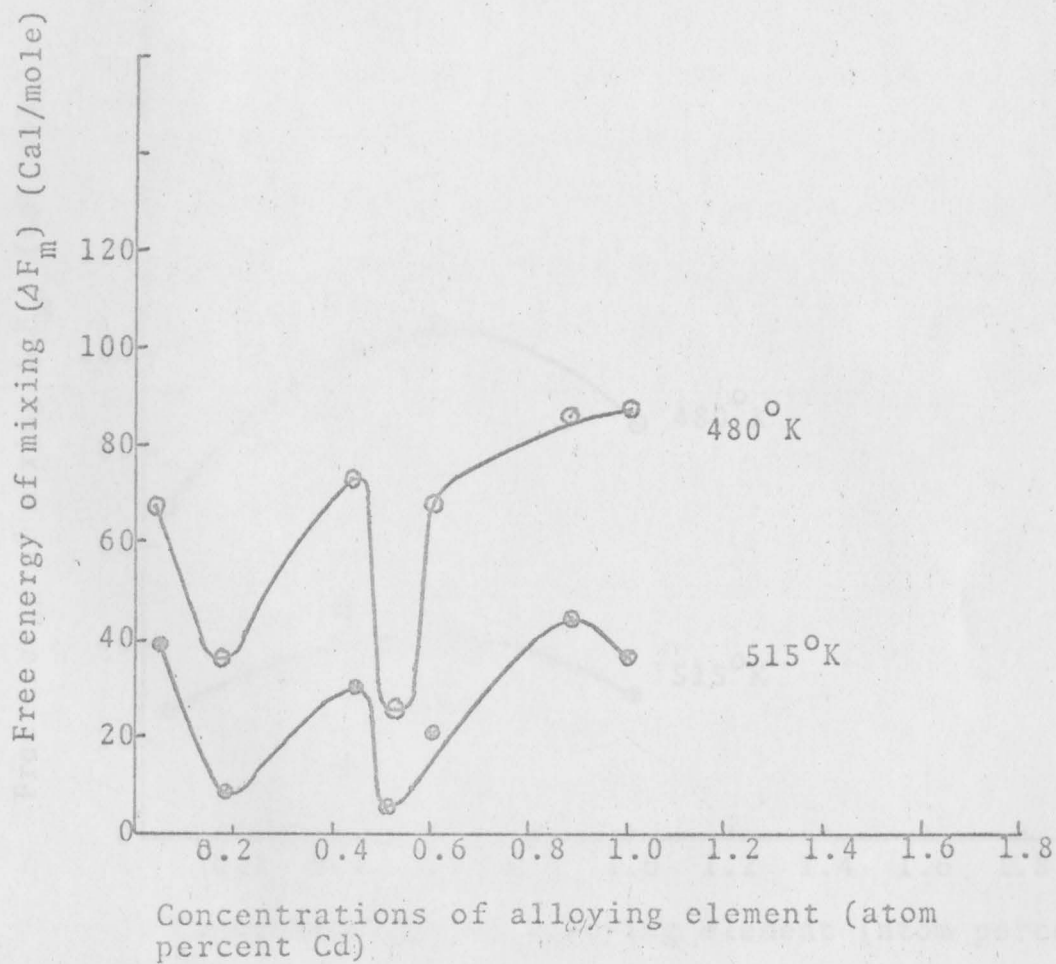


Fig. 143. Free energy of mixing as a function of concentrations of alloying element, for Tl-Cd alloy.

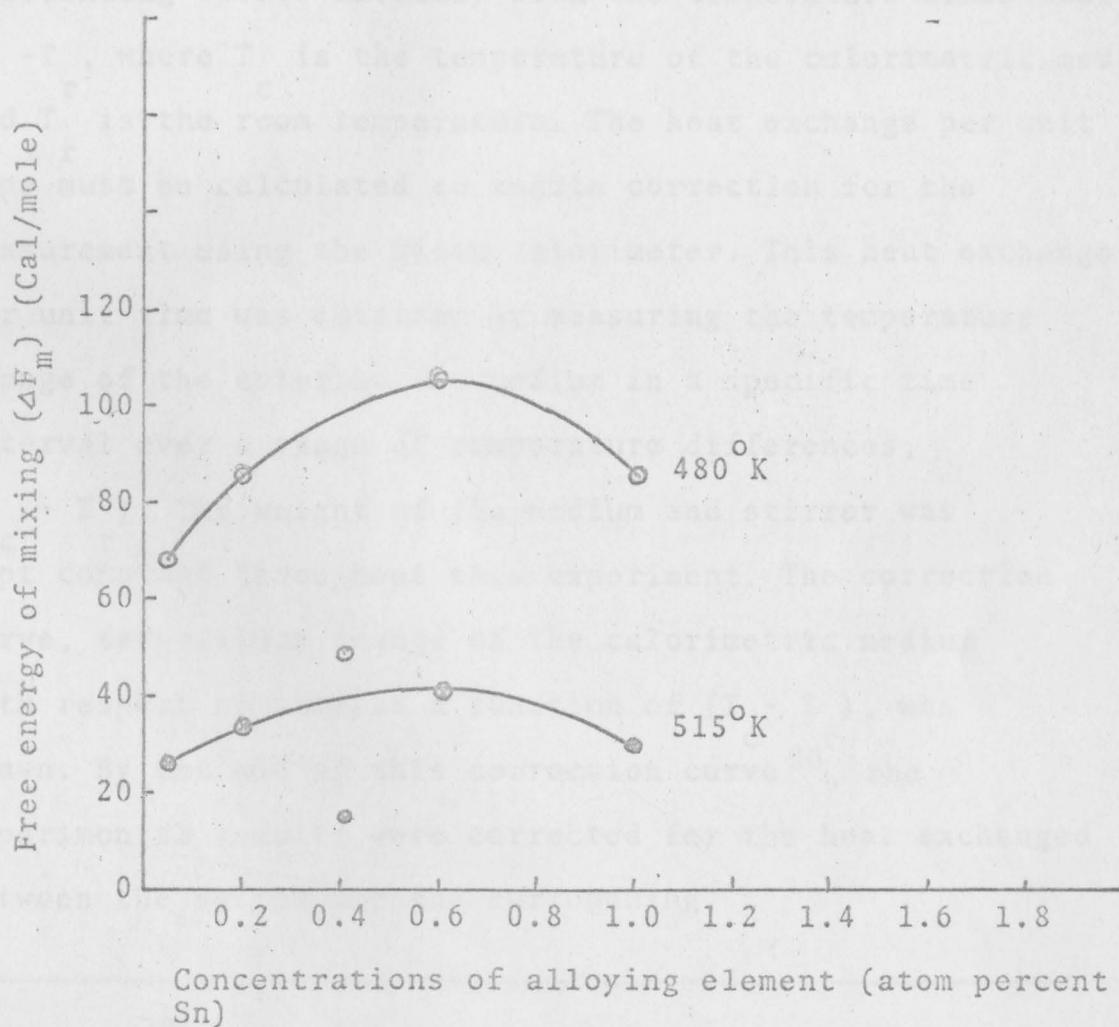


Fig. 144. Free energy of mixing as a function of concentrations of alloying element, for Tl-Sn alloys.



## APPENDIX A

The heat exchanged between the system and the surrounding varies directly with the temperature difference  $T_c - T_r$ , where  $T_c$  is the temperature of the calorimetric media and  $T_r$  is the room temperature. The heat exchange per unit time must be calculated to enable correction for the measurement using the Olsen calorimeter. This heat exchange per unit time was obtained by measuring the temperature change of the calorimetric medium in a specific time interval over a range of temperature differences,  $(T_c - T_r)$ . The weight of the medium and stirrer was kept constant throughout this experiment. The correction curve, temperature change of the calorimetric medium with respect to time, as a function of  $(T_c - T_r)$ , was drawn. By the use of this correction curve<sup>20</sup>, the experimental results were corrected for the heat exchanged between the system and the surrounding.

---

<sup>20</sup>Madden, Hugh F. and John A. Petras, The construction of a modified Olsen Calorimeter (Graduating Thesis submitted to Youngstown State Univ., 1967), p.16.

## BIBLIOGRAPHY

BOOKS

- Hultgren, Ralph, Raymond L. Orr, Philip D. Anderson, Kenneth K. Kelly. Selected Values of thermodynamic properties of metals and alloys. New York: John Wiley & Sons, 1963.
- Hansen, M. Constitution of Binary alloys. New York: McGraw Hill Book company, Inc., 1958.

ARTICLES

- Ewald, R. Ann. Physik. 1914 ed. Vol. 44.
- Levin, M. Z. anorg. Chem. 1905 ed. Vol. 45.
- Madden, Hugh F., John A. Petras, The construction of a modified Olsen calorimeter, -Graduating thesis submitted to Youngstown State University). 1967.
- Nishikawa & Ashara. Physic. Rev. 1920 ed. Vol. 15.
- Oelsen, W., O. Oelsen and D. Thiel. Z. Metallkunde. 1955 ed. Vol. 46.
- Oelsen, W., K. Rieskamp, and O. Oelsen. Arch. Eisenhütten w. 1955 ed. Vol. 26.
- Oelsen, W. Arch. Eisenhütten w. 1955 ed. Vol. 26.
- Orr, R.L., L.P. Warner and Hultgren, R. To be published.
- Roth, W.A., I. Meyer, and H. Zeumer. Z. anorg. chem. 1934 ed. Vol. 303.
- Schneider, A., and O. Hilmer. Z. anorg. u. allgem. chem. 1956 ed. Vol. 286.
- Seekamp, H. Z. anorg. u. allgem. chem. 1931 ed. vol. 195.
- Sinkiti Sekito. Z. krist. 1930 ed. Vol. 74.
- Umino, S. Science reports. 1927 ed. Vol. 16.
- Werner, M. Z. anorg. chem. 1913 ed. Vol. 83.